

Environmental geochemistry and acid mine drainage modelling of the Sabie River water system in the vicinity of abandoned gold mines

R Lusunzi

 orcid.org/0000-0002-1031-106X

Thesis accepted in fulfilment of the requirements for the degree Doctor of Philosophy in Engineering with Chemical Engineering at the North-West University

Promoter: Prof FB Waanders

Graduation: August 2023

Student number: 25497928

Declaration

I, **Rudzani Lusunzi** (student number: **25497928**), hereby declare that:

- That I have solely composed the thesis for the Philosophy of Doctorate in Chemical Engineering, hereby submitted by me, and that it has not been submitted, in full or in part, in previous application for a degree at this university or any other.

.....

Rudzani Lusunzi

.....14/02/2023.....

Date

Acknowledgement

I acknowledge North-West University and the Council for Geoscience for their financial assistance in completing this project.

My thanks go to my supervisors, Prof. F.B. Waanders and Prof. E. Fosso-Kankeu, for their constructive criticism and productive discussions throughout the study. This work would not have been possible without your significant contributions, constructive criticism, and fruitful discussions.

To Dr A. Tshibubudze and Ms. H.N. Mashale of the Council for Geoscience for technical assistance, as well as ArcGIS. Furthermore, Mr M. Kobola, Mr T.C Thiba, as well as Mr D. Nxumalo are thanked for the help with sampling. Finally, I'd like to thank everyone who helped me in any way during the dissertation's completion.

Abstract

The purpose of this research was to learn more about the release, transport, dispersal, and fate of metal species emitted by mine tailings storage facilities (MTSFs) on the Sabie River system. Analytical techniques and geochemical modelling were used to evaluate the chemical reactions that occur after metals are released from gold mine tailings in the Sabie Goldfield. MTSFs, a rainwater runoff pond and the Sabie River system were all considered as potential metal contaminants flow paths. Seasonal variation was taken into account to learn more about the effects on metal dispersion during the wet (summer) as well as dry (winter) seasons.

Very high concentrations of metal species were found in the tailings from the Nestor MTSF when compared to concentrations found in stream sediments. There was no substantial difference in metal (loid) distribution, specifically, cobalt (Co), nickel (Ni), lead (Pb), chromium (Cr), zinc (Zn), copper (Cu) and arsenic (As) between the summer and winter seasons. In addition, no indication of metal species dispersal was observed from the Nestor MTSF to the nearby water bodies, namely, the Klein Sabie and the Sabie River respectively. This is because the majority of the metal pollution is detached from the system over a short distance. When compared to concentrations found in stream sediments, the tailings from the Nestor MTSF had elevated concentrations of metal species. Acid producing minerals such as pyrite and secondary iron minerals, which are commonly found in mine wastes, were discovered to be possible pollutants to the Sabie River system. Furthermore, the mineral capable of neutralizing acid dolomite present in the sediments may function as a critical buffer.

Using traditional acid base accounting (ABA) criteria, gold mine tailings from the Nestor MTSF are classified as potential acid forming (PAF), whereas gold tailings from the Glynns Lydenburg MTSF are classified as non-acid forming (NAF) but may still produce alkaline drainage. Furthermore, tailings from these two sites were mixed, and ABA was performed to determine whether the alkaline tailings could neutralize the acid from the Nestor (MIX25 and MIX75). The results indicated that materials from the Glynns Lydenburg are capable of neutralizing the acid from the Nestor mine tailings. Therefore, materials from the Glynns Lydenburg MTSF can be an economically viable option to treat potential acid-generation from the Nestor MTSF by forming a base cover system in which vegetation will grow.

To characterize the solid phase speciation of metal species in the vicinity of the Sabie River system, a four-stage sequential extraction procedure was performed on mine waste, soil and

stream sediment samples. Organics and sulphides-bound fractions, as well as Fe and Mn-bound fractions were considered bioavailable, with metals in these phases being possibly remobilised under varying environmental settings. Aluminium and iron were discovered to achieve maximum bioavailability in mine waste, followed in decreasing order by manganese (Mn), As, Zn, Cr, Cu, Co, and Pb. Adsorption into Mn, Al, and Fe-hydroxide precipitates observable in the drainage path flowing towards the Klein Sabie River is the crucial process for this geochemical scavenging. The PHREEQC modelling code was used in conjunction with sequential extraction to characterize the chemical reactions that transform metals. According to the results of PHREEQC modelling, cation exchange played a substantial part in regulating the chemistry of surface water in the Sabie River system. The obtained results can be used to guide environmental management of gold mine tailings.

Keywords: Speciation, Toxicity, Stream Sediment, Mine Tailings Storage Facilities, Geochemical Modelling, Efflorescent Salts, Sabie River Catchment

List of papers appended

- (i) Lusunzi, R. and Waanders, F., 2022. Speciation of Metals in Sediments of the Sabie River System by Sequential Extraction. Presented in the IMWA2022 Conference, New Zealand. In: Proceedings of the IMWA2022 Conference-“Reconnect”, pp. 237-242; Pope, J.; Wolkersdorfer, C.; Rait, R.; Trumm, D.; Christenson, H.; Wolkersdorfer, K. (Editors).
- (ii) Lusunzi, R., Waanders, F., 2022. Hydrogeology, Mineralogy, and Chemical Fractionation of Mine Wastes Associated with Gold Mines: A Case Study from the Sabie Goldfield, South Africa. The 35th International Conference on Chemical, Biological and Environmental Engineering, ICCBEE-22). <https://doi.org/10.17758/IICBE4.C1122222>
- (iii) Lusunzi, R., Waanders, F., Netshitungulwana, K.R.T., 2021. Geochemical Variation of Sediments in the Sabie River, Mpumalanga, South Africa. In: Proceedings of the 14th IMWA Congress, “Mine Water Management for Future Generations” -In: Stanley, P.; Wolkersdorfer, Ch.; Wolkersdorfer, K. (Editors).
- (iv) Lusunzi, R., Fosso-Kankeu, E., Waanders, F., 2020. Seasonal Metal Speciation in the Sabie River Catchment, Mpumalanga, South Africa. 18th Johannesburg International Conference on Science, Engineering, Technology and Waste Management (SETWM-20) Proceedings, Volume 1. P 74-79, Johannesburg, South Africa.
- (v) Lusunzi, R., Novhe, N.O., Mashalane, T., 2019. Geochemical and Mineralogical Characterization of Precipitates from Sabie-Pilgrim’s Rest Goldfields for the Potential of Acid Mine Drainage. In: Proceedings of the IMWA 2019 Conference, “Mine water: Technological and Ecological Challenges”, Wolkersdorfer, Ch.; Khayrulina, E.; Polyakova, S.; Bogush, A. (Editors).

Book chapter

Buffering capacity of soils in mining areas and mitigation of acid mine drainage formation (Elvis Fosso-Kankeu and Bhekie Mamba (eds.) Hybridized Technologies for the Treatment of Mining Effluents, (119–146) © 2023 Scrivener Publishing LLC).

Aimee Steyn

Supplier Database No: MAAA0450241

*PostNet Suite #40
Private Bag X04
Menlo Park 0102*

Mobile: 060 530 1165

Email: noteworthy@myconnection.co.za /
honey@myconnection.co.za

18 August 2022

TO WHOM IT MAY CONCERN

This serves to confirm that the thesis for: *Doctor of Philosophy in Engineering with Chemical Engineering*

By: **R Lusunzi** – School of Chemicals and Minerals Engineering, North-West University.

Entitled: **Environmental geochemistry and acid mine drainage modelling of the Sabie River water system in the vicinity of abandoned gold mines**

has been edited by one of our accredited language editors, Dr MC Steyn. The accuracy of the content of the final work remains the student's responsibility.

A. Steyn

Contents

DECLARATION I

ACKNOWLEDGEMENT II

ABSTRACT III

LIST OF PAPERS APPENDED V

BOOK CHAPTER V

CONTENTS VII

LIST OF TABLES XIII

LIST OF ABBREVIATIONS XVIII

STUDY DESIGN 1

CHAPTER ONE 2

1. INTRODUCTION 2

1.1. Background 2

1.2. Problem statement 5

1.3. Research aims and objectives 5

Research aim 5

Research objectives 5

1.4.	The study area.....	5
1.4.1.	Location of the study area	5
1.4.2.	Geological setting of the Sabie River system	6
1.4.3.	Topographical and soil setting	9
1.4.4.	Climatic conditions	10
1.4.5.	Hydrological setting of the Sabie River system	10
CHAPTER TWO.....		14
2.	LITERATURE REVIEW	14
2.1.	Water pollution	14
2.1.1.	Sources of water pollution	15
2.2.	Bioavailability of metal species	16
2.3.	Metals in aquatic systems.....	20
2.3.1.	Aluminium	20
2.3.2.	Chromium	21
2.3.3.	Copper	22
2.3.4.	Iron.....	23
2.3.5.	Lead	24
2.3.6.	Nickel	25
2.3.7.	Zinc	25
2.4.	Basic biogeochemical processes in soils and sediments	26
2.4.1.	Adsorption.....	26
2.4.2.	Precipitation	28

2.4.3.	Complexation	29
2.5.	Acid mine drainage	30
2.5.1.	Management of AMD	31
2.6.	Waste management in South Africa.....	47
2.7.	Geochemical modelling	48
2.7.1.	Speciation-solubility models	49
2.7.2.	Inverse modelling.....	49
2.7.3.	Forward modelling	50
2.7.4.	Reaction path modelling	50
2.7.5.	Coupled transport and reaction modelling.....	50
CHAPTER THREE		52
3.	MATERIALS AND METHODS	52
3.1.	Sampling and site description	52
3.2.	Sampling procedure.....	53
3.2.1.	Tailing sampling	53
3.2.2.	Efflorescent crusts sampling.....	55
3.2.3.	Soil sampling.....	56
3.2.4.	Stream sediment sampling	56
3.2.5.	Water sampling.....	57
3.3.	Analytical methods	59
3.3.1.	Acid-Base Accounting.....	59

3.3.2.	X-ray fluorescence methods	60
3.3.3.	X-ray diffraction methods	61
3.3.4.	Sequential extraction procedure	61
3.3.5.	Ion Chromatography and Inductively Coupled Plasma-Mass Spectrometry	63
3.4.	Data treatment: statistics and geochemical modelling.....	64
3.4.1.	Data analysis	64
3.4.2.	Geochemical modelling	66
CHAPTER FOUR.....		67
4.	RESULTS AND DISCUSSION	67
4.1.	Mine tailings storage facilities geochemistry and mineralogy	67
4.1.1.	Acid base accounting results	67
4.1.2.	Geochemistry of sediments eroded from Nestor MTSF	69
4.1.3.	Mineralogy of sediments eroded from Nestor MTSF	74
4.2.	Efflorescent crust geochemistry and mineralogy	75
4.2.1.	Efflorescent crusts geochemistry	75
4.2.2.	Mineralogy of efflorescent crusts	77
4.3.	Soil geochemistry and mineralogy	78
4.3.1.	Soil surrounding mine tailings storage facilities	79
4.3.2.	Geochemistry and mineralogy of soils away from mining activities	83
4.4.	Stream sediment geochemistry and mineralogy	87
4.4.1.	Stream sediment and geochemistry	87
4.4.2.	Stream sediment mineralogy	100

4.4.3.	Speciation of metals in stream sediments	102
4.5.	Water Quality.....	105
4.5.1.	Spatial distribution of pollutants from mine effluent	105
4.5.2.	Spatial distribution of pollutants in surface water	107
4.5.3.	Metal speciation in water	112
CHAPTER FIVE.....		118
5.	MITIGATION MEASURES OF THE MINE TAILINGS STORAGE FACILITIES IN THE SABIE RIVER CATCHMENT.....	118
CHAPTER SIX.....		122
6.	CONCLUSION	122
6.1.	Recommendations.....	123
REFERENCES.....		125
APPENDICES.....		164
7.	ANNEXURE A: STREAM SEDIMENT AND SURFACE WATER SAMPLING SITES ALONG THE SABIE RIVER SYSTEM.....	164
8.	ANNEXURE B: SPECIATION PATTERN FOR METALS IN THE MINE WASTES OF NESTOR AND GLYNNS LYDENBURG MINES AND SURROUNDING SOILS.....	175
9.	ANNEXURE C: SPECIATION PATTERN FOR METALS IN THE MINE SOIL AWAY FROM MINING ACTIVITIES IN THE SABIE RIVER SYSTEM ..	177

**10. ANNEXURE D: SPECIATION PATTERN FOR METALS IN THE STREAM
SEDIMENTS OF THE SABIE RIVER SYSTEM..... 178**

List of Tables

Table 1 Trace metal relative mobility and bioavailability.	18
Table 2 Location of sampling sites	52
Table 3 Detection limits for some selected elements	63
Table 4 Results of acid base accounting.	67
Table 5 Comparison of ANC calculated and at a pH of 2.5 and 4.0.	69
Table 6 Final classification.	69
Table 7 Geochemistry of trace elements from sediments eroded from the Nestor MTSF.	70
Table 8 Geochemistry of bulk samples.....	73
Table 9 Mineralogical composition of tailings from the Nestor MTSF.....	74
Table 10 Mineralogy of tailings.....	74
Table 11 Geochemistry of efflorescent crusts from the Nestor and Glynns Lydenburg MTSF.....	75
Table 12 Distribution of metal species in efflorescent crusts (mg/kg) and soil screening values for metals (DEA, 2013).....	76
Table 13 Major elemental composition of soil near the Nestor MTSF.	79
Table 14 Geochemistry of soil near the Nestor MTSF.	80
Table 15 Mineralogical composition of soils near the Nestor MTSF.....	80
Table 16 Major elemental composition of soils around the Glynns Lydenburg MTSF.	81
Table 17: Geochemistry of trace elements near Glynns Lydenburg MTSF.	82
Table 18 Mineralogical composition of soil near Glynns Lydenburg MTSF.	83
Table 19 Geochemistry of soils in the Sabie area.....	84

Table 20 Mineralogy of soils away from mining activities.....	84
Table 21 Major elemental composition of stream sediment of the Sabie River system (wt. %).	87
Table 22 Chemical indices of weathering in the Sabie River catchment.	89
Table 23 Trace elements geochemistry of sediment from Sabie River catchment (mg/kg, dry weight).	91
Table 24 Values for enrichment factor.	95
Table 25 Trace metals enrichment factor.....	96
Table 26 Trace elements geo-accumulation in sediment from the Sabie River system.....	97
Table 27 Total REE concentrations in the stream sediment from Sabie River Catchment with descriptive statistics.	98
Table 28 The Pearson correlation coefficient of REEs in the Sabie River catchment.....	100
Table 29 Mineralogical composition of sediments from the Sabie River system.	100
Table 30 Physicochemical parameters of Nestor TSF seepage measured onsite.....	105
Table 31 Major cations, anions, and trace elements of seepage from Nestor TSF.	106
Table 32 Seasonal distinction of parameters measured in situ and alkalinity (mg/L CaCO ₃) measured in surface water of the Sabie catchment.	108
Table 33 Seasonal variation of cation and anions in the of Sabie catchment.....	109
Table 34 Seasonal variation of trace metals in the Sabie catchment.	111
Table 35 Maximum percentages of speciated metals measured in surface water in the Sabie River catchment.	113
Table 36 Range of highest speciated forms of metals from Nestor TSF seepage.....	115

List of Figures

Figure 1 The Sabie River system.	3
Figure 2 Study area location in the Sabie River system.....	6
Figure 3 Geological setting of the Sabie River system.....	8
Figure 4 Digital elevation map (DEM) in metres above sea level (MASL) representing the Sabie River system.	10
Figure 5 Hydrological setting of the Sabie River system.....	11
Figure 6 Photographs showing the sediments that are eroded from the Nestor MTSF.	54
Figure 7 Photograph showing the sediments that are eroded from the Nestor MTSF before the confluence with the Klein Sabie River.	54
Figure 8 Efflorescent crusts sampling in the Nestor and Glynn's Lydenburg MTSFs.	55
Figure 9 Soil sampling was conducted along the Sabie River system.....	56
Figure 10 Photographs showing where stream sediment sampling in the Sabie River system, was conducted.....	57
Figure 11 Sampling conducted on the seepage from the Nestor MTSF (A) and (B) photograph showing the water decanting from the Rietfontein mine adit.	58
Figure 12 Onsite water analysis was conducted in the Sabie River system.	59
Figure 13 Acid buffering characteristic curve (ABCC) curves of samples MIX25, MIX50 and AN.....	68
Figure 14 Photograph showing the sediments that are eroded from Nestor MTSF.	70
Figure 15 Metal species concentrations (mg/kg) in different fractions of mine wastes and surrounding soils.....	73
Figure 16 Trace elements geochemistry of efflorescent salts from the Nestor and Glynn's Lydenburg MTSF.	76

Figure 17 Mineralogical composition of efflorescent crusts from the Nestor (NS00) and Glynn's Lydenburg (GL00) MTSFs.....	78
Figure 18 Metal species concentrations (mg/kg) in different fractions of soils away from mining activities.....	86
Figure 19 Seasonal variation in arsenic and chromium concentrations in the Sabie River.....	93
Figure 20 Seasonal variation in arsenic and chromium concentrations in the Lone Creek River.	93
Figure 21 Metal species concentrations (mg/kg) in the different fractions in the stream sediments.	104
Figure 22 Chemical constituents distribution in Nestor TSF seepage.	107
Figure 23 Piper plot for Nestor MTSF seepage (red) and surface water for wet (blue) and dry (orange) seasons	117
Figure 24 SB01: Sabie River headwaters wet (A) and dry (B) seasons (R. Lusunzi).	164
Figure 25 SB 02: Sabie River wet (A) and dry (B) seasons (R. Lusunzi).	165
Figure 26 SB03: Sabie River wet (A) and dry (B) seasons (R. Lusunzi).	165
Figure 27 SB04: Sabie River wet (A) and dry (B) seasons (R. Lusunzi).	166
Figure 28 SB05: Sabie River wet (A) and dry (B) seasons (R. Lusunzi).	166
Figure 29 SB06: Sabie River wet (A) and dry (B) seasons (R. Lusunzi).	167
Figure 30 SB07: Sabie River wet (A) and dry (B) seasons (R. Lusunzi).	167
Figure 31 SB08: Sabie River wet (A) and dry (B) seasons (R. Lusunzi).	168
Figure 32 SB09: Sabie River inside Kruger National Park, wet (A) and dry (B) seasons (R. Lusunzi).	168
Figure 33 SB10: Lone Creek River, wet (A) and dry (B) seasons (R. Lusunzi).	169

Figure 34 SB11: Glynn's Drainage/Malieveld, wet (A) and dry (B) seasons River (R. Lusunzi).	169
Figure 35 SB12 Klein Sabie River, wet (A) and dry (B) seasons (R. Lusunzi).....	170
Figure 36 SB13: Klein Sabie River, wet (A) and dry (B) seasons (R. Lusunzi).....	170
Figure 37 SB14: Spitskop River, wet (A) and dry (B) seasons (R. Lusunzi).	171
Figure 38 SB15: Rietfontein Mine drainage, wet (A) and dry (B) seasons (R. Lusunzi).....	171
Figure 39 SB16: Goldstream, wet (A) and dry (B) seasons (R. Lusunzi).	172
Figure 40 SB17: Sabana River, wet (A) and dry (B) seasons (R. Lusunzi).	172
Figure 41 SB18: Mac-Mac River, wet (A) and dry (B) seasons (R. Lusunzi).	173
Figure 42 SB19: Sunlight River, wet (A) and dry (B) seasons (R. Lusunzi).....	173
Figure 43 SB20: Nkambeni/ Noord Sand River, wet (A) and dry (B) seasons (R. Lusunzi).	174
Figure 44 SB21: Bega River, wet (A) and dry (B) seasons (R. Lusunzi).	174

List of abbreviations

ABA	Acid Base Accounting
ALD	Anoxic Limestone Drain
AMD	Acid Mine Drainage
ANC	Acid Neutralizing Capacity
API	Acid Potential
CIA	Chemical Index of Alteration
CEC	Cation Exchange Capacity
EF	Enrichment Factor
HREE	Heavy Rare Earth Element
ICP-MS	Inductively Coupled Plasma Microscopy
IUWMA	Inkomati Usuthu Water Management Area
KNP	Kruger National Park
LREE	Light Rare Earth Element
MAMSL	Meters Above Mean Sea Level
MTSF	Mine Tailings Storage Facility
MPA	Maximum Potential Acidity
MPRDA	Mineral and Petroleum Resources Development Act
NAG	Net Acid Generating
NP	Neutralisation Potential
NAPP	Net Acid Production Potential
NNP	Net Neutralizing Potential
PAF	Potential Acid Forming
PTEs	Potential Toxic Elements
RAPS	Reducing Alkalinity Producing Systems
REE	Rare Earth Elements

SAPS	Successive Alkalinity Producing Systems
SQCs	Sediment Quality Guidelines
SRB	Sulphite Reducing Bacteria
UCC	Upper Continental Crust
WMA	Water Management Area
WWTP	Wastewater Treatment Plant
XRD	X-Ray Diffraction
XRF	X-Ray Fluorescence

STUDY DESIGN

This thesis is comprised of the following chapters:

- Chapter 1: Introduction

This chapter provides a history of gold mining on the Sabie goldfield, as well as a discussion of the major associated environmental issues. The problem statement, hypothesis, goals, and objectives, as well as a description of the research area, will be described in Chapter 1.

- Chapter 2: Literature review

This chapter presents a literature review relevant to the study area as well as a general overview of acid mine drainage (AMD) formation and mitigation measures.

- Chapter 3: Materials and methods

This chapter provides a description of sampling sites, sampling practices, sample preparation, and analytical techniques. This chapter goes into greater detail than the journal articles with respect to the analytical techniques.

- Chapter 4: Results and discussion

This chapter presents and discusses all of the study's findings.

- Chapter 5: Mitigation measures of the mine tailings storage facilities in the Sabie

In this chapter, all possible mitigation measures of AMD in the Sabie River system are presented.

- Chapter 6: Conclusions

Despite the fact that conclusions are presented in each journal article, this chapter describes the overall conclusions of the thesis and suggests areas where additional research is needed.

- References

There is a comprehensive list of references, including references in journal articles.

- Appendices

This section contains supplemental material.

CHAPTER ONE

1. Introduction

1.1. Background

Gold mining is a significant industry in South Africa, both in terms of economic importance and employment. Conversely, gold mining activities generate substantial quantities of waste in the form of waste rock, slimes, and tailings that in South Africa, are generally referred to as mine residue deposits. South Africa's gold discovery and mining history is fraught with ambiguity. According to Pretorius (1994), the first record of finding gold comes from the panning of a quartz vein as early as 1852 in the Witwatersrand Basin at the farm Paardekraal. However, the first significant gold concentrations were discovered in 1871 at the farm Eersteling in the Pietersburg Greenstone Belt, which is located south of the town of Polokwane in Limpopo Province. This was followed in 1872 by the discovery of the Sabie goldfield in Mpumalanga Province which prompted the first gold rush in South Africa. Although gold production commenced in 1888 during the Leydsdorp gold rush, initial finds in the Murchison and Giyani Greenstone Belts date back to 1871 and 1872 respectively. A huge discovery of a gold-rich Main Reef Leader in the Witwatersrand Basin was made during the year 1886 on the farm Langlaagte which subsequently shifted the focus away from the earlier discovered Sabie Goldfield (Pretorius, 1994). Bentley (1995) estimated that about 200 tons of gold have been recovered from the Sabie Goldfield. With its long history of gold mining, the Sabie Goldfield has resulted in abandoned mine tailings storage facilities (MTSFs). It is these mine wastes that pollute the environment, most commonly in the form of acid mine drainage (AMD).

Acid mine drainage, having low pH as well as elevated dissolved metal species concentrations, has the potential, in addition to other various types of pollution that also contribute to water quality degradation, to endanger South Africa's water resources. Overabstraction, habitat alteration, sewage effluents, toxic organic compounds, anthropogenic salinization, and invasive species of both flora and fauna are amongst known challenges (Davies et al., 1993; Simeonov et al., 2003; Dallas and Day, 2004; Fosso-Kankeu et al., 2011; Ma et al., 2016). Toxic trace metals from anthropogenic sources can also endanger marine creatures and affect human wellbeing (Patil and Paknikar, 2000). In South Africa, AMD has been reported in a number of mining areas, including the Witwatersrand Goldfields, KwaZulu-Natal and Mpumalanga Coalfields, as well as the O'Kiep Copper District (McCarthy, 2011).

The Sabie River basin is located in Mpumalanga, South Africa (Fig. 1), and along with those of the Komati and Crocodile, form part of the Inkomati River system. The Sabie River begins at an

altitude of 2207 metres above mean sea level (MAMSL) and flows eastward through the Kruger National Park (KNP) finally meeting the Inkomati River in Mozambique. The river courses through sawmills, waste treatment plants, fishery areas, trout farms, commercial forestry plantations, abandoned mines, and agricultural and industrial activities that dominate the upper Sabie River system (Roux et al., 2018). There are also illegal mining activities occurring in the upper stretches of the Sabie River system that are reprocessing old mine tailings storage facilities (MTSFs), especially the Nestor MTSF as well as the underground mining of old mining shafts (Nestor and Rietfontein mines). The water from the tailings processing was observed to be flowing downstream from the Nestor mine site towards the Klein Sabie River, about a kilometre before the confluence with the main Sabie River. In addition, water from material processing in the upper parts of the Spitskop River, which is less than 1 km from the main Sabie River, was also observed being washed downstream towards the main Sabie River.

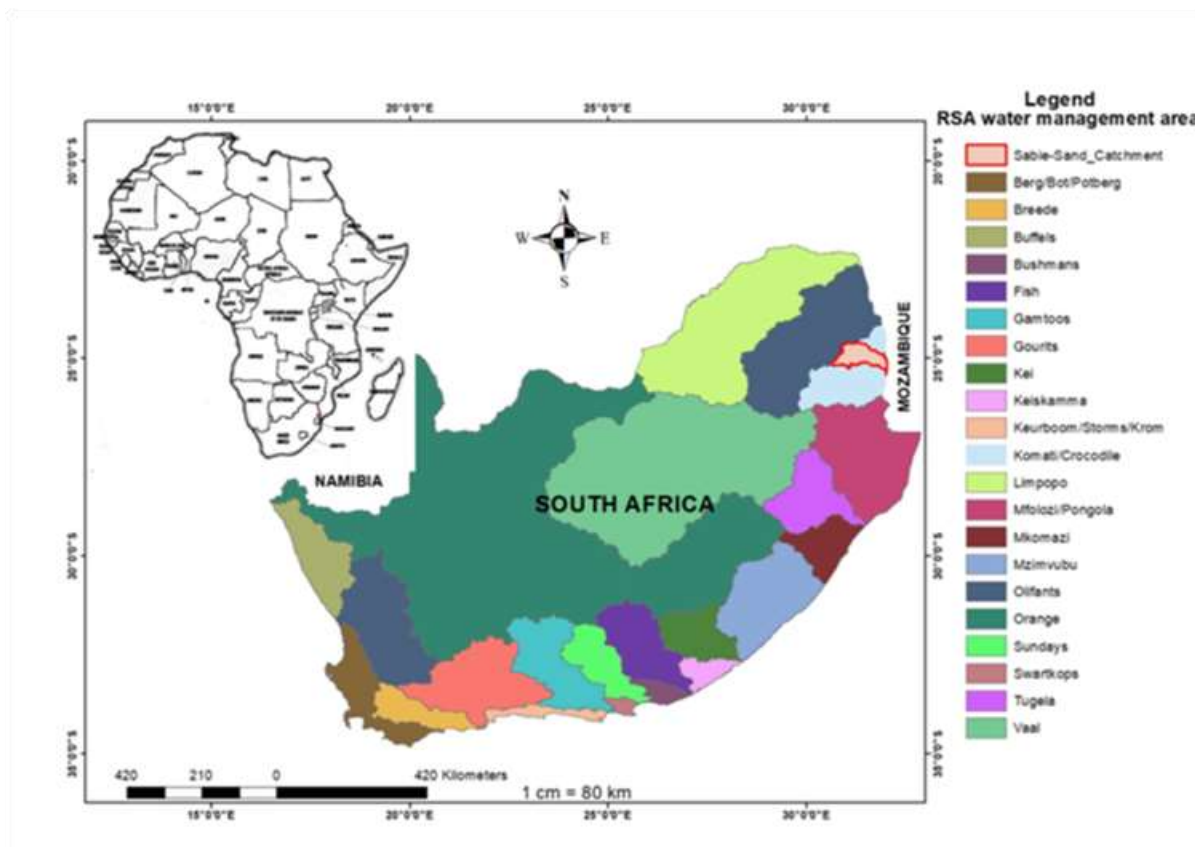


Figure 1 The Sabie River system.

Various studies have been undertaken in the Sabie goldfield and Novhe et al. (2014) assessed mine wastes along the Komati/Crocodile catchment on a regional scale and recommended further investigations in the Sabie mining area. Stolz (2018) however, investigated the quality of water of the Sabie River system in relation to adjacent land use, without considering the stream sediment

geochemistry. Recently, geochemical studies have been conducted on tailings of the Sabie goldfields to assess their potential for AMD formation by Lusunzi et al. (2017) as well as Lusunzi et al. (2018). Based on geochemical findings, metal species concentrations in mine wastes such as zinc (Zn), lead (Pb), vanadium (V), copper (Cu), chromium (Cr), and arsenic (As) were elevated. In addition, the samples from the Nestor MTSF were found to be potentially acid generating, in comparison to samples from the Glynn's Lydenburg MTSF, as per acid base accounting (ABA) experiments and mineralogical assessment (Lusunzi et al., 2018). Both the MTSFs are located on the bank of the Sabie River with the Nestor MTSF located less than 1 km northeast of the Klein Sabie River, a tributary of the Sabie River. Leachates from the Nestor MTSF having lower pH and elevated metal species concentrations were observed being washed downstream towards the Klein Sabie River (Lusunzi, 2018).

To date there has been no research conducted on the impact of abandoned mine tailings on water quality as well as stream sediment along the Sabie River catchment. Furthermore, no previous research has focused on the typical binding groups that contribute to metal retention in stream sediment near the Sabie River. It is therefore critical to explore the geochemical configuration of the sediment in Sabie Watercourse system. This data could be useful in assessing the risk and exposure of communities living in the vicinity of the mine sites.

A recent environmental investigation carried out in the Sabie mining area showed a need to develop a management plan for the Nestor MTSF (Lusunzi, 2018). This study will also formulate a management plan that could be used to rehabilitate the Nestor MTSF and mitigation of AMD further downstream to the Sabie River system.

The rehabilitation of polluted sediments and soil necessitates a thorough in situ classification of the speciation of potential toxic elements (PTEs) as well as their transformation over time and space. In this study, the speciation of nine metals, namely, aluminium (Al), cobalt (Co), copper (Cu), iron (Fe), zinc (Zn), manganese (Mn), nickel (Ni), chromium (Cr), and lead (Pb) as well as the metalloid As concentrations in the Sabie River system sediments and mine wastes have been characterized in order to evaluate the associated contaminant threat from the redistribution of metal species among the different phases of the sediment. In addition, the fractionation of these elements was used to assess bioavailability. This information, combined with site-specific environments may be applied to guide tailings storage facilities remediation and environmental management.

1.2. Problem statement

The ratio of primary sulphide to carbonate minerals and trace elements inherited from the ore deposits as well as any ore processing that have created new compounds determine the tendency of the mine wastes to generate acid or to produce a neutral drainage. Poor disposal of mine tailings in the Sabie Goldfield, especially the Nestor mine tailings storage facility (MTSF) represents substantial environmental concerns due to their potential influence on soils and river sediments of the Sabie River system, as well as surface and groundwater resources in the surrounding zones.

1.3. Research aims and objectives

Research aim

The primary goal of this research is to assess release of metal pollutants from mine tailings storage facilities (MTSFs), as well as to investigate their transport and dispersion within the Sabie River system. This will help in the development of suitable management plans for remediating the Nestor MTSF.

Research objectives

To achieve the main aim of the research, the following goals will be investigated:

- To determine the pyrite fractions and oxidation in the waste pile;
- To determine the mobility of trace elements and mineralogical constituents of the waste particles within the mines;
- To categorize any potential source of pollution (should they occur);
- To provide comprehensive data sets for further instigation such as mathematical modelling of AMD;
- To evaluate AMD generation and its environmental impact in the Sabie water system; and
- To formulate the AMD mitigation strategy for the Nestor MTSF.

1.4. The study area

1.4.1. Location of the study area

The Sabie River, which is located in South Africa's Mpumalanga Province, is one of the most biologically diverse rivers in the region. It flows through the Inkomati Water Management Area (WMA) and reaches the Kruger National Park (KNP) at a distance of 81.3 kilometres downstream from its headwaters (Fig. 2). The Inkomati primary drainage (X) region falls within the Inkomati

Usuthu Water Management Agency (IUWMA). There are three sub-basins within the Inkomati River system, namely, the Komati (X1), Crocodile (X2), and the Sabie (X3) (Roux et al., 2018). The Kruger National Park, the Sabie-Sand Game Reserve, and four smaller nature reserves protect more than half of the Sabie River. Commercial forestry, sawmills, the Sabie town area, trout farms and fishing areas, and to a lesser degree, agricultural as well as industrial activities dominate its upper reaches. There are also abandoned mines located in the upper Sabie River system, in which illegal mining activities are taking place as observed during site visits at the Nestor Mine.

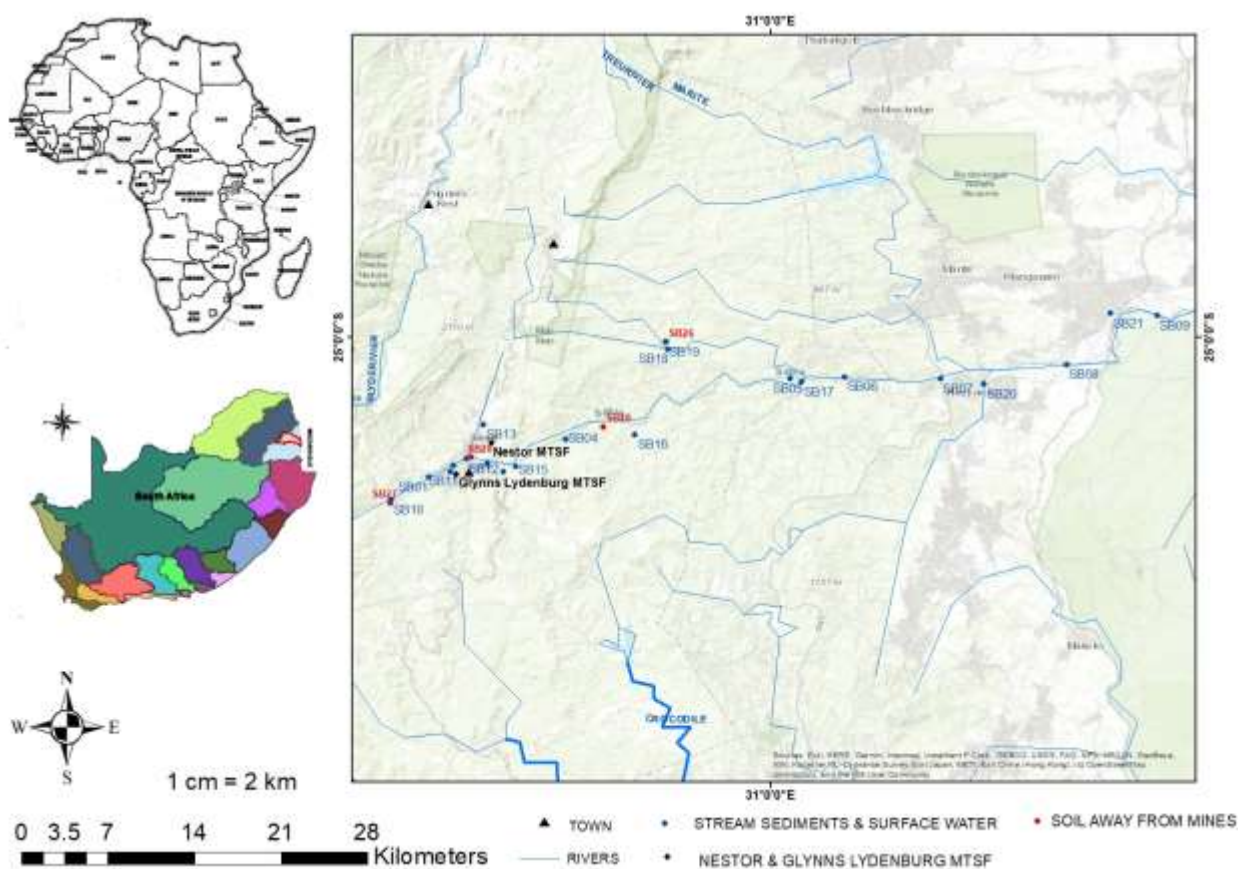


Figure 2 Study area location in the Sabie River system.

1.4.2. Geological setting of the Sabie River system

The region is geologically composed of rocks of different ages and groups (Fig. 3). The largest lithological unit in the study area is the 3105 Ma old Basement Complex consisting of the crystalline granite-gneiss of the Nelspruit Suite (Karno and Davis, 1991). Robb et al, (1983) and

Schutte (1986) defined the Nelspruit Granite Suite as a combination of banded gneiss, gneiss and porphyritic granite and rocks varying from granitic to tonalitic, comprised of minerals such as quartz, microcline, feldspar, biotite and accessory minerals. The Cunning Moor Tonalite, located northeast of Skukuza, which intruded the gneiss and migmatites of the Nelspruit Suite has a light grey colour with a medium-to coarse-grained texture (Robb, 1978, 1994c). In terms of mineralogy, the tonalite consists of quartz, plagioclase, microcline, biotite, and poikilitic crystals of sphene (Schutte, 1986). According to Barton, (1983), the tonalite had yielded an Rb-Sr whole-rock age of 2784 ± 53 Ma, having a preliminary $87\text{Sr}/86\text{Sr}$ ratio of 0.7034 ± 0.0003 . To the west, the 2600-2200 Ma old Transvaal Supergroup rocks underlie the study area. The protobasinal Wolkberg Group lies unconformably on the Nelspruit Suite and forms the lowermost fragment of the Transvaal Supergroup (Boer, 1995). Overlying the Wolkberg Group are the siliclastic sedimentary rocks of the Black Reef Formation that consist of felspathic quartzite, interlayered lenses of grit and conglomerate (Button, 1973). Conformably overlying the Black Reef Formation are the up to 2 km thick rocks of the Malmani Subgroup, mostly comprising of dolomites, which are part of the Chunuiespoort Group. Based on chert concentration and algal structures found in the dolomite, in ascending order, the Malmani Subgroup is divided into five formations, which are Oaktree, Monte Christo, Lyttelton, Eccles, and Frisco (Button, 1973; Clendanin, 1989; Tyler and Tyler, 1996). According to Martin et al. (1998), the Oaktree Formation is a transitional form of siliclastic sedimentation to platform carbonates comprised of 10-20 m thick carbonaceous shales, stromatolitic dolomites, and quartzites that have settled locally. The Monte Christo Formation consists of an erosive breccia as well as stromatolitic and oolitic platformal dolomites. Overlying the Monte Christo Formation is the Lyttelton Formation that is 100-200 m thick and is comprised of shales, quartzites and stromatolitic dolomites. Tyler and Tyler (1996), describe the Eccles Formation as cherty dolomites, which include a series of erosional breccias containing locally auriferous mineralization that can be attributed to the hydrothermal remobilisation of fluids by the Bushveld Complex. The Frisco Formation is the uppermost of the Malmani Subgroup, comprising mainly stromatolitic dolomites that are shale-rich towards the top, indicating deepening deposition conditions (Tyler and Tyler, 1996).

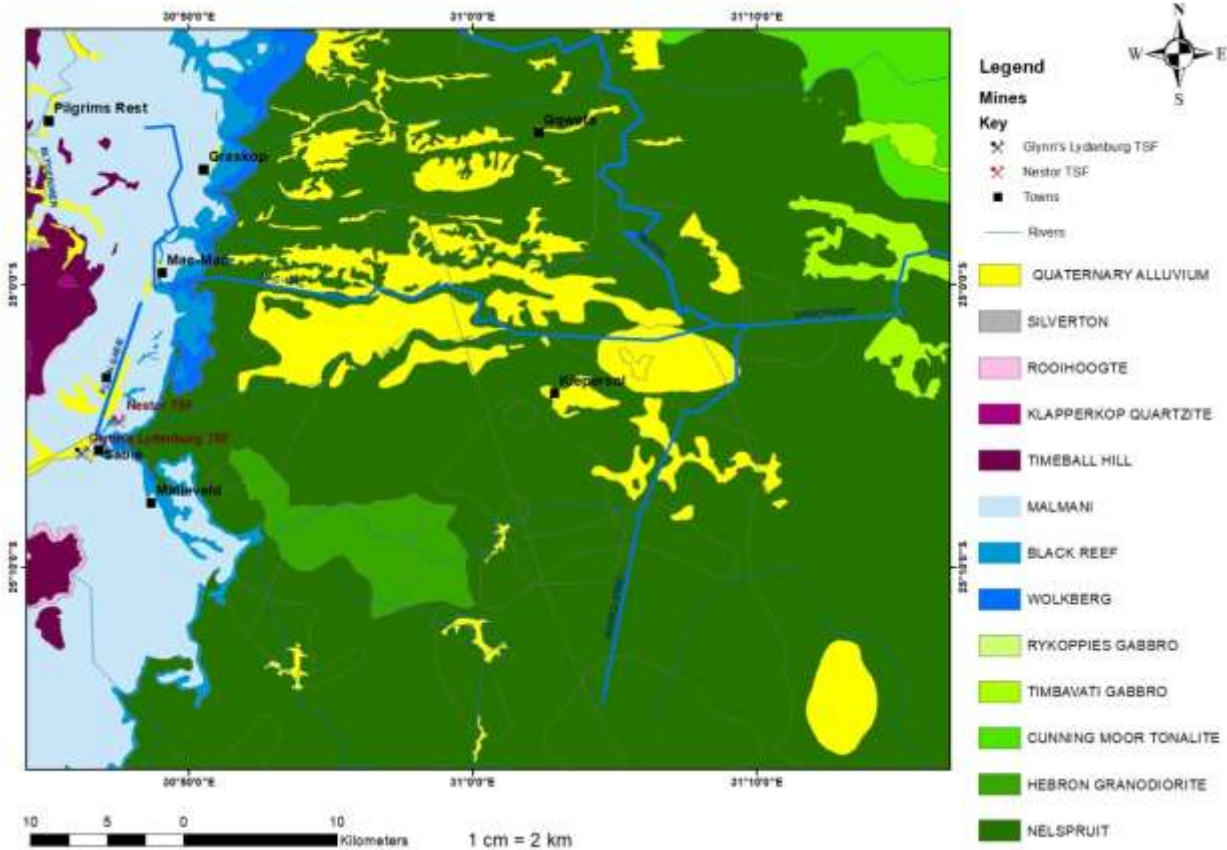


Figure 3 Geological setting of the Sabie River system.

The Nestor MTSF is located within the Black Reef Formation and the Glynns Lydenburg MTSF is located within the Oaktree Formation of the Malmani Dolomite of the Chunuiespoort Group that forms part of the Transvaal Supergroup (Lusunzi, 2018; Figure 2).

According to Boer et al. (1995), the Sabie goldfield can be classified as mesothermal and the Bushveld magmatism was responsible for the mineralization of gold within the Sabie-Pilgrim's Rest goldfields (Zietsman, 1964, 1967), which is also supported by isotopic and fluid inclusion data (Harley and Charlesworth, 1990, 1991, and 1992). Swiegers (1948) indicated that quartz veins with calcite are the key components of the stratiform ore bodies and both are saturated with several sulphides, silver, and gold, in various combinations within the goldfield. This includes the following dominant types:

- Considerable vein quartz-calcite saturated with occasional sulphide minerals;
- Vein quartz with thin sulphide groups;
- Calcite blows which are barren of mineralization;

- Quartz-calcite vein combinations with crystals and veinlets of sulphides;
- Crystalline pyrite masses;
- Considerable arsenopyrite, chalcopyrite, tetrahedrite and/or ores;
- Intertwining pyrite, arsenopyrite, and tetrahedrite masses; banded pyrite, tetrahedrite and/or arsenopyrite ores; and complex coated ores that frequently contain rafted trashes of parent rock, which include chert, dolomite, quartz arenite, or carbonaceous mudstones (Tyler and Tyler, 1996).

The ore in the discordant reefs is comprised of a variation of gold-quartz-sulphide mineralization, settled on various host rocks. The Rietfontein Reef is the most visible cross reef and the irregularly developed and refractory ore has been known for its high silver concentration with gold associated with pyrite, arsenopyrite and chalcopyrite. Meyer (1988) estimates that the Sabie-Rest Pilgrim's goldfield produced nearly 185 Mt of ore at a typical grade of approximately 8 g/t by 1988.

1.4.3. Topographical and soil setting

Topographically, the Sabie River system is divided into two regions: the Lowveld and the Middleveld (Fig. 4). The Middleveld region occupies the western portion of the catchment that is distinguished by a surging topography that becomes more rugged in the west. The Lowveld region, on the other hand, has a flat to gently undulant terrain, excluding in the east near the Lebombo Mountains (Deacon, 1996).

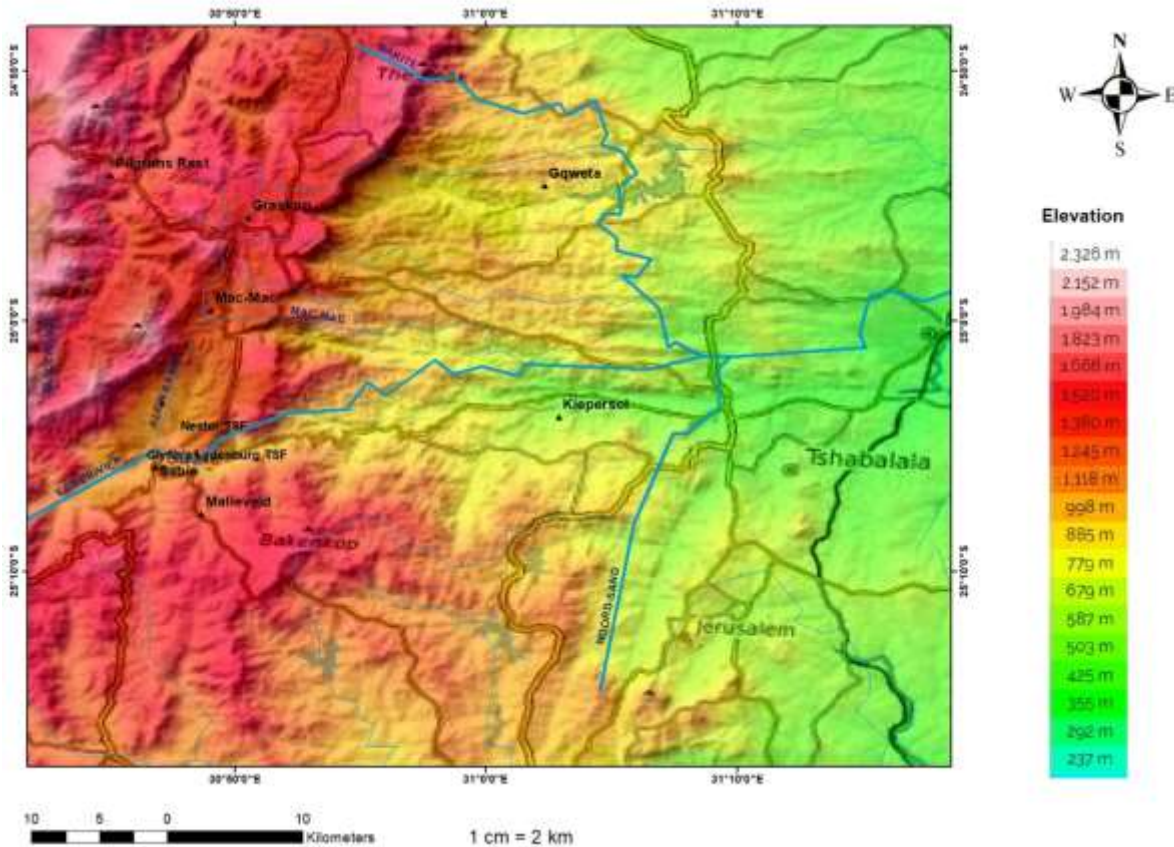


Figure 4 Digital elevation map (DEM) in metres above sea level (MASL) representing the Sabie River system.

1.4.4. Climatic conditions

Cooler temperatures in the Mpumalanga Highveld Plateau and hot, dry conditions in the eastern portion near the border with Mozambique generally define the climate of the Sabie River Basin. The whole River system is located in Southern Africa's summer rainfall region, having 80 percent of the rainfall falling between November and April. Rainfall in the Eastern Lowveld ranges from 600mm/year increasing to 1200mm/year in the Highveld. Evaporation rates are high, particularly during the summer, when the average evaporation rate is 1900mm/year.

1.4.5. Hydrological setting of the Sabie River system

Davies and Day (1998) defined a catchment as the area from which a river receives its water. The catchment of the Sabie River is a portion of the Inkomati drainage system (X Region), which is recognized as an international basin because it is shared by South Africa, Swaziland, as well as Mozambique (Fig. 5; Annexure A, Fig. 24-44). The Sabie River catchment, which begins in the north-eastern Drakensberg escarpment north of Long Tom Pass, shields an area of 7096

km², of which 6347 km² is located within South Africa and passes through the Kruger National Park. There are no distinctive large flood plains, wetlands, or swamps along the Sabie River (Deacon, 1996). However, due to variations in the distribution of sediment over the bedrock, the catchment contains a wide range of channel types (Van Niekerk and Heritage, 1993).

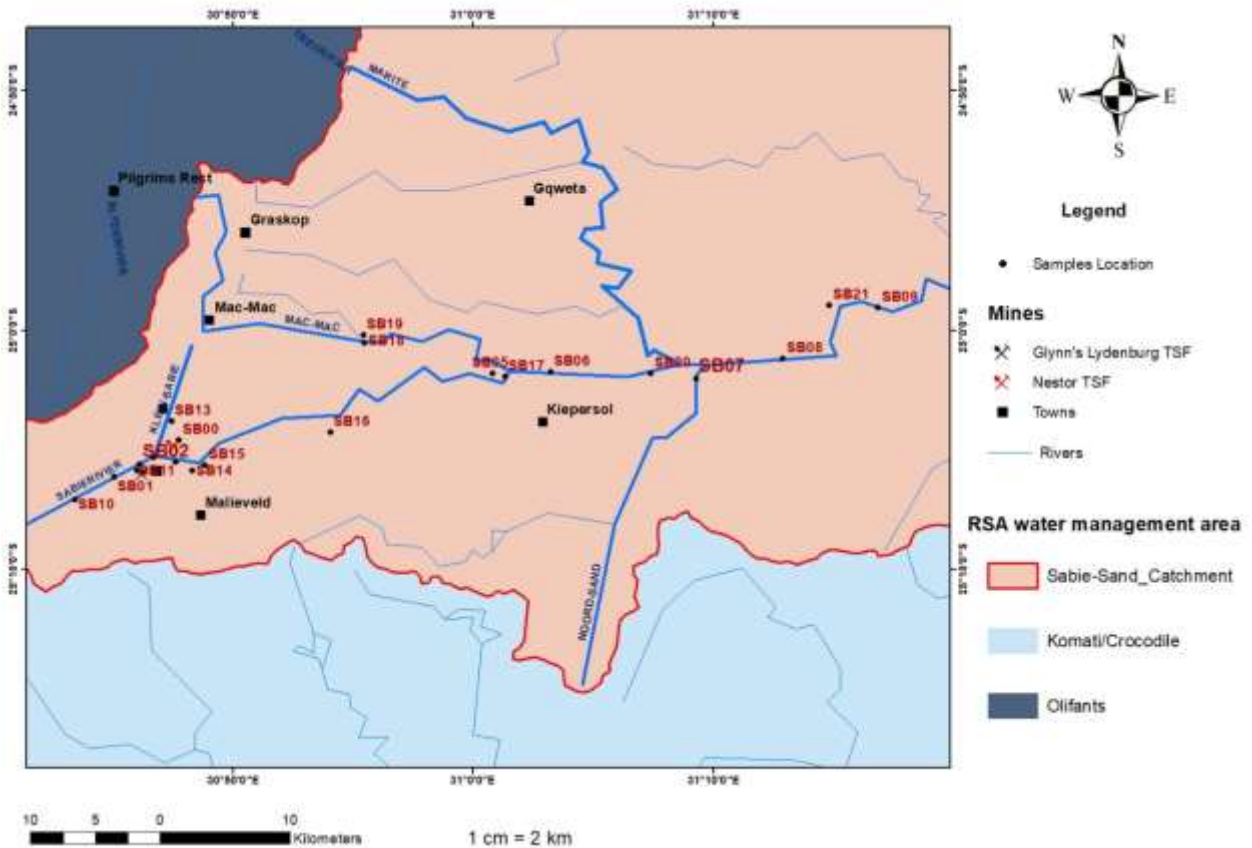


Figure 5 Hydrological setting of the Sabie River system.

Branches of the Sabie River include Lone Creek (SB10), Klein Sabie (SB12 and SB13), Spitskop (SB14), Sabaan (SB17), Mac-Mac River (SB18), Marite, White Waters, and North Sand River/Nkambeni (SB20). Some of the tributaries, focused on in this study, are the Bega River (SB21; Annexure A Fig. 44), which is part of the Sand River, a tributary of the Sabie River; Goldstream (SB16; Annexure A Fig. 39), and the Sunlight River (SB19 Annexure A; Fig. 42). In addition, a sample was collected in an unnamed stream that is flowing less than 50 m east of the Glynn's Lydenburg MTSF (SB11; Annexure A Fig. 34) and a drainage flowing east of the Rietfontein mine (SB15; Annexure A Fig. 38), which is probably water decanting from the old mine shaft (Annexure A).

1.4.5.1. *Lone Creek*

The Lone Creek begins at an elevation of 1921-MAMSL on a natural grassland area called the Hartebeesvlakte and flows southeast by easterly to merge with the Sabie River at an altitude of 1 062-MAMSL. The upper catchment is dominated by forestry plantations; nevertheless, there is also normal grassland and native forest (Annexure A; Fig. 33). The Lone Creek Waterfall, which is situated upstream from the sampling site, is a recognized feature in the landscape. The catchment is divided into two aquatic ecoregions: the Northern Escarpment Mountains and the North-eastern Highlands.

1.4.5.2. *Klein Sabie*

Beginning at an altitude of 1990-MAMSL (Annexure A; Fig. 35) the Klein Sabie flows southward to its convergence with the Sabie River at the Sabie Waterfall (Annexure A; Fig. 36). Upstream from the sampling point, commercial forestry is the dominant land-use, all though sawmills, the Sabie Waste Land-fill site, irrigated log-decks, dams, an industrial area, Simile and Tweefontein villages, and old abandoned mine tailings storage facilities (Nestor Mine) are other known features. The North-eastern Highland aquatic ecoregion encompasses the majority of the Klein Sabie catchment area. On the Klein Sabie River, there are two waterfalls.

1.4.5.3. *Spitskop River*

The Spitskop River begins at an elevation of 1474-MAMSL and flows north-by-north-easterly to the Sabie River, under Sabie town and the Sabie Wastewater Treatment Plants (Annexure A; Fig. 37). At an elevation of 956-MASL, the Spitskop River joins the Sabie River. The entire Spitskop catchment is part of the North-eastern Highlands aquatic ecoregion, and the upper catchment contains two dams and a waterfall. Commercial forestry is the dominant land use, with two sawmills, villages, and a holiday resort being secondary land uses. Illegal mining also takes place within the catchment area (Rietfontein Mine).

1.4.5.4. *Sabana River*

The Sabana River begins at an elevation of 1207-MAMSL and flows north-eastward to its convergence with the Sabie River at an elevation of 520-MAMSL. The entire catchment is part of the North-eastern Highlands aquatic ecoregion; agriculture and commercial forestry predominate in the upper reaches (Annexure A; Fig. 40). The catchment contains a large number of impoundments, with ten on the main channel.

1.4.5.5. *Mac-Mac River*

Beginning north of Graskop at an altitude of 1502-MAMSL and at an elevation of 518-MAMSL, the river flows south-eastern by southerly towards its convergence with the Sabie River (Annexure A; Fig 41). Commercial forestry dominates the catchment, which according to Midgley et al. (1994) accounts for nearly 90% of the river system. The upper parts, which are located above the Mac-Mac waterfalls, are part of the Northern Escarpment Mountains ecoregion, while the lower parts are part of the North-eastern Highlands aquatic ecoregion. York Timber's Driekop Sawmill is situated in the headwaters of the Mac-Mac River, where it flows through Graskop, through SAFCOL forestry areas, and then through the commercial plantations of Sappi and Mountain to Ocean forests to the Sabie convergence.

1.4.5.6. *Nkambeni River/Noord Sand*

Four villages, namely, Numbi, Shabalala, Mahushu and Sand River surround the Nkambeni River. This river flows through one of the villages (Sand River) and to the eastern side of Shabalala. It passes along the western boundary of the Kruger National Park finally joining the Sabie River (Annexure A; Fig. 43).

1.4.5.7. *Marite River*

The Marite River system includes the Maritsana, Ngwempisi, and Motitsi Rivers and is a branch of the Sabie River. The Maritsana River begins at an elevation of 1 752-MAMSL and flows easterly towards the Injaka Dam, where it enters the dam at an elevation of 800 m; commercial forestry is the prevailing land use. The Ngwempisi River, which originates at an altitude of 1497-MAMSL, flows eastward through the catchment towards Injaka Dam. The Motitsi River flows out of the Injaka Dam at an altitude of 738-MAMSL and flows east by southerly to the Maritsane River to form the Marite River. Rural settlement and the town of Hazyview dominate the catchment area that is located at about 2 km south of the sample point.

CHAPTER TWO

2. Literature Review

2.1. Water pollution

Water pollution is defined as the deterioration of water quality as determined by biological, chemical, or physical standards (Mateo-Sagasta et al., 2017).

Ahmad et al. (2014) and Silva et al. (2016), indicated that in the main, source rocks and their weathering intensity determine the composition of the resultant sediments. During the sedimentation cycle, sediments can be modified by parameters that include transport, deposition and diagenesis (Hurst and Morton, 2014). The geochemistry of major, trace, and rare earth elements (REE), as well as their elemental ratios, provides valuable information about sediment genesis as well as weathering settings at the source area. In most cases, the composition of the source rock is reflected by the major element geochemistry of the sediments (Armstrong-Altrin et al., 2012) and the concentration of weathering process (Shao and Yang, 2012; Shao et al., 2012; Šmuc et al., 2015).

Total elemental concentrations do not provide enough data about the bioavailability and toxicity of potentially toxic elements (PTEs) (Vetrimurugan et al., 2016). In several studies, the total concentrations of metal species in contaminated and uncontaminated soils in South Africa have been determined, for example, Netshitungulwana and Yibas (2012) assessed the geochemistry of stream sediment from the Olifants River catchment for AMD; Edokpayi et al. (2016) investigated trace metal contamination of surface water and stream sediment in the Mvudi River; Mugwabana (2018) investigated the sediment patterns and source areas within the Letaba River, Kruger National Park; and Nde and Mathuthu (2018) assessed the potential toxic elements (PTEs) as non-point sources of pollution in the Upper Crocodile River catchment. Furthermore worldwide, for example, Derviş, (2013) used the sediment quality triad to characterise toxic conditions in the Chisapeake Bay; Ibrhaim Adsani (2014) provided a detail study of sediments (mineralogy and geochemistry) of the Coastal Plain of the Arabian Gulf, Kuwait; Ali et al. (2016) assessed metal species in water and stream sediment of Karnaphuli River in Bangladesh using various indices; Hazermoshar et al. (2016) conducted a multidisciplinary study (geochemical, sedimentological and mineralogical) to characterise the sediments in Eynak Marsh, North Iran; Han et al. (2017) studied geochemical and eco-toxicological characteristics of stream water and sediments affected by AMD in the South Korea; and Liao et al. (2017) studied the distribution,

enrichment and source apportionment of metal species in river surface sediment affected with multiple pollution sources in Southern China.

2.1.1. Sources of water pollution

Pollutants are substances that are capable of causing physical, chemical, or biological changes in a body of water. Generally, pollution results from point and non-point sources (Spellman, 2009; Singh and Gupta, 2017). U.S. EPA (1996) defines point source pollution as any single distinguishable source of pollution from which contaminants are discharged. This includes air pollution from industrial sources and water pollution from factories.

A nonpoint source (NPS) can come from many sources, unlike point source pollution that discharges directly into surface waters from a pipe. Mostly, the nonpoint source results from runoff during rainfall or snow melt when precipitation flows over and through surfaces where it picks up pollutants and deposits them into nearby water bodies. Nonpoint source pollutants include nutrients, suspended sediments, pesticides, and toxic chemicals, as well as bacteria, viruses, and trash.

Agriculture, human settlement, and industry are the primary sources of water pollution (WWAP, 2017). Agriculture plays a significant role in water pollution, accounting for about 70 percent of water abstraction worldwide. According to UNEP (2016), large quantities of agrochemicals, chemical waste, sediments, and saline drainage are discharged into water bodies, posing risk to aquatic ecosystems, human health, and productive activities. The second major source of pollution is human settlement or urbanisation. Increased loading of nutrients, mainly phosphorus, in urban rivers results from increased imperviousness, increased runoff from urbanised surfaces and increased municipal and industrial discharges (Paul and Meyer, 2001). According to WWAP (2017), 80 percent of municipal wastewater is discharged untreated into water bodies worldwide. This means that each year, millions of tonnes of metal species, solvents, hazardous sludge, as well as other wastes are dumped into various bodies of water. Many industries such as timber and paper are frequently located on river banks simply because they require such large amounts of water for their manufacturing processes. As a result, their wastes, which contain acids, alkalis, dyes, and other chemicals, are deposited and poured into rivers as effluent (Singh and Gupta, 2017).

Further, water pollutants may be organic or inorganic in nature (Singh and Gupta, 2017). Organic pollutants are comprised of carbon, hydrogen, oxygen and sulphur compounds. These pollutants encompass diverse forms of chemicals; pesticides; volatile organic compounds; bacteria from livestock farming and sewage; food processing waste and pathogens. Inorganic pollutants may

also come from silt from runoff, metal species from acid mine drainage, logging, landfilling, and fertilizers from agricultural runoff that contain nitrates and phosphates, as well as chemical wastes from industrial effluents.

Mining is a significant contributor to water pollution as activities produce substantial wastes in the form of waste rock, tailings, and slimes (mining wastes). These mining wastes frequently contain high levels of toxic elements, whose mobility and dispersion pose an environmental risk to soils, water, ecosystems, and people. Devastating environmental impacts occur when mined sites are not rehabilitated, particularly when wastes containing sulphide minerals are exposed to water and weathering over time, releasing acid, metals, non-metals, and sulphate; resulting in acid mine drainage (AMD) (Akcil and Kudas, 2006; Dold, 2010). The pH of acid mine drainage is typically low (Gray, 1998), ranging from 2 to 8. (Skousen et al., 1999). Gold mine waste is thought to be South Africa's most significant single source of pollution (Oefetse, 2008). AMD has also been reported in South Africa's Witwatersrand region as a result of gold mining activities (Nengovhela et al., 2007). In the Witwatersrand Basin alone, there are over 270 mine tailings storage facilities (MTSFs), the majority of which are unlined and pose a serious threat to both groundwater and surface water quality (Rosner and Van Schalkwayk, 2000). AMD has been exacerbated by MTSFs that have been abandoned for more than a decade. The MTSFs have been in contact with oxygenated rain water (Naicker et al., 2003, McCarthy, 2011). As a result, the pyrite and other sulphide material in the MTSFs has oxidized. According to Naicker et al. (2003), the pyrite oxidation acidifies the water that percolates through the MTSFs and eventually enters the groundwater and streams along the Witwatersrand. Surface runoff from the MTSFs severely pollutes the watercourses in the Klip River's upper catchment (Chetty et al., 2021).

There was no evidence of acid mine drainage from the tailings of the Louis Moore Mine in the Giyani Greenstone Belt, Limpopo, according to Singo and Kamers (2021). Arsenic, on the other hand, posed a potential health risk because it could be mobilized under mildly alkaline conditions and contaminate soils and water.

2.2. Bioavailability of metal species

The bioavailability of elements is dependent on the type of element present in the environment. Parish (1977) defined metal as an element that exhibits cationic behaviour or is soluble in acids in an aqueous solution; thus, elements that are non-metals include hydrogen (H), oxygen (O₂), sulphur (S), selenium (Se), iodine (I), astatine (At), arsenic (As), phosphorus (P), nitrogen (N), silicon (Si), polonium, tellurium (Te), carbon (C), boron (B), and the rare gases radon (Rd), helium (He), krypton (Kr), neon (Ne), argon (Ar) and xenon (Xe). Except for mercury (Hg), most pure metals are solid at room temperature and are excellent conductors of heat and electricity, as well

as having a high lustre and malleability (Newman, 2015). Some elements C, O, H, and N, are recognized to be critical for a sustainable lifespan, with the major essential elements being magnesium (Mg), potassium (K), sodium (Na), phosphorus (P), calcium (Ca), and chlorine (Cl), trace elements being iron (Fe), iodine (I), arsenic (As), copper (Cu), manganese (Mn), zinc (Zn), cobalt (Co), molybdenum (Mo), chromium (Cr), vanadium (V), silicon (Si), selenium (Se), and boron (B), and some , aluminium (Al), lithium (Li), fluorine (F), and tin (Sn), supporting physiological functions at the ultra-trace level, (Walker et al., 2012). In bioavailability studies, the United States Environmental Protection Agency (EPA) identified metals of interest based on their potential for human exposure and increased health risks. These include antimony (Sb), lead (Pb), selenium (Se), aluminium (Al), arsenic (As), copper (Cu), mercury (Hg), chromium (Cr), nickel (Ni), cadmium (Cd), and beryllium (Be) (McKinney and Rodgers, 1992). Metal species like Zn, Na, V, Ti, Mn, Co, Mo, Mn, V, and silver (Ag) are currently considered less important (Dussel, 1994). Bioavailability, as defined by Newman and Jagoe (1994), is the extent to which a contaminant in a probable cause is available for commitment by an organism. Many factors influence bioavailability in surface water, groundwater, sediment, and air. Physical and chemical forms of metal species, pH, mineral assemblages, oxidation-reduction potential, temperature, total organic concentration, suspended particulate concentrations, water volume, velocity of water, and extent of water availability, mainly in arid and semi-arid environments, wind transport, as well as removal from the atmosphere by rainfall are all factors to consider (Luoma, 1985).

Metals exist in a variety of physical and chemical forms in nature. These include the elemental state (extremely rare in nature), as a mineral combination, as a free cation dissolved in water, or bound to organic or inorganic molecules in either solid or dissolved phases (Allen, 1993), and this distribution of metals is referred to as metal speciation. The term speciation has been defined as the presence of an element in distinct and distinguishable forms, such as chemical, physical, or morphological state (Nieboer and Fletcher, 1996). In order to understand the biogeochemical cycling of trace elements in seawater, Goldberg (1954) introduced the concept of speciation. According to Caruso et al. (2000), during speciation the transition metals, lanthanides and actinides exist in different oxidation states and form different chemical species. Various factors affect metal speciation and these include pH, redox conditions, the oxidation state of an element, the solubility of solid compounds, biochemical processes, the accessibility and nature of complexing agents, complex and ion-pair development. Speciation studies focus on the determination of concentrations of different chemical species of an element as well as its physical exhibitions. The four main chemical reactions that determine metal speciation (Bourg, 1995) are ion exchange and dissolution reactions; adsorption and desorption processes; precipitation and co-precipitation; as well as complexation to inorganic and organic ligands. A number of chemical

reactions determine metal speciation in the environment, namely, sorption, precipitation, and complexation. These reactions influence metal partitioning across solid and liquid phases, thereby influencing mobility and bioavailability.

With the application of sequential extraction, it has become possible to determine the speciation of metals, their bio-mobility and toxicity, as well as to assess the degree of pollution of bottom sediments (Sahuquillo et al., 2003). It is possible to differentiate between oxidised and reduced, complexed or chelated and free metal ion in dissolved form through the application of kinetic and thermodynamic data (Gupta et al., 2013).

According to Elder (1989) and Salmons (1995) metals may be subdivided into six different fractions in solid phases in soils, sediments and surface water particulates. These include dissolved; exchangeable; carbonate; iron and manganese oxides; organic; and crystalline (Table 1; modified from Salmons, 1995). Variation in factors such as pH, redox state, organic matter concentrations, as well as environmental settings affect the segregation of fractions.

Table 1 Trace metal relative mobility and bioavailability.

Metal species and association	Mobility
Exchangeable	High
Iron-Manganese oxides	Medium
Organic matter	Medium/High
Sulphide minerals	Strongly dependent of the environmental conditions
Crystalline	Low

Potential toxic elements (PTEs) of concern, depending on deposit size, include Pb, Fe, Cu, As, Cd, and, in some cases, Tl or Se. Furthermore, besides PTEs, AMD may encompass rare earth elements (REEs) (Verplanck et al., 2004). These released PTEs have the potential to contaminate soils, sediments, surface water, and groundwater (Bain et al., 2001; Jung, 2001; Armienta and Segovia, 2008). McCloskey et al. (2005) indicated that mine tailings storage facilities are the primary source of AMD, but open pit underground workings, highwalls, and ore stockpiles also add to the volume of AMD formed. While pH-buffering reactions are frequently sufficient to neutralize AMD, attenuating the concentration of dissolved PTE requires a series of reactions

(sorption and precipitation). Secondary minerals precipitating during oxidation-neutralization reactions may be replaced PTEs, either temporarily or permanently (Levy et al., 1997a; Gleisner, 2005; Sánchez et al., 2005). Secondary minerals precipitated in AMD surroundings can be more effective than engineered designs at removing PTEs in AMD. In this way, secondary minerals add to the natural decline of PTEs in AMD environments (Levy et al., 1997b).

Bioavailability as well as toxicity of a particular element are dependent on the chemical forms in which that element occurs in various fragments of the sample (Vetrimurugan et al., 2016). Comprehensive data applicable to environmental studies can be obtained using a toxicity characteristic leaching procedure (TCLP) or sequential leaching. The data includes trace metal origin, occurrence mode, biological and physicochemical availability, mobilization, as well as transportation (Nemati et al., 2009).

In South Africa, several studies on sequential extraction have been carried out for example Gouws and Coetzee (1996) assessed metal speciation in the sediments of the Vaal River system, Gauteng; the quality of sediment from the Nyl River system in Limpopo was determined using sequential extraction (Greenfield et al. (2007); Benamer (2014), used measured the mobility and bioavailability of elements in the Berg River, Western Cape; the mobility of elements in sediments from the Highveld coalfield acid mine drainage area in Mpumalanga Province was investigated (Fosso-Kankeu et al. 2017); Manyatshe et al. (2017), studied metal retaining potential of sediments of the Mooi River, North West; and Matabane et al. (2021), measured the potentially toxic elements (PTEs) in sediments from the Blood River, Limpopo. In addition, sequential leaching has been performed worldwide to assess the binding forms of elements including for example Sracek et al. 2012, investigated mining-related contamination of the Kefue River drainage system in Zambia's copper district; Nemati et al. (2011), investigated metal speciation in sediments from Sungai Buloh, Selangor, Malaysia at various depths; Khorasanipour et al. (2012), investigated trace elements in the sediments from Sarcheshmeh copper mining area, Iran; metal pollution in river sediments from the abandoned Boccheggiano pyrite mining area in Italy were investigated (Pagnanelli et al. 2004); Sarmiento et al. (2009), evaluated the toxicity and potential risk of an AMD-polluted river in the Iberian Belt, which is located southwest of Spain; Delgado et al. (2011), assessed estuarine sediments from the Guadiana saltmarshes affected by multiple anthropogenic pollution sources, Spain; Torres et al. (2013), investigated the metal transfer between Sancho Reservoir water and sediment (Iberian Belt, SW Spain); and Arenus-Lago et al. (2014), investigated metal contamination in soils from the Touro copper mine in NW Spain; and Ranville et al. (2004), investigated metal attenuation at the abandoned Spenceville copper mine, Nevada County (United State of America).

2.3. Metals in aquatic systems

Various factors are involved in the configuration of water flowing on the surface of the earth. These comprise the geological setting of the river system as well as the extent of the soil sorption complex, according to Florinsky (2000) and Walker et al. (2005). Other factors include:

- Physical progressions such as sedimentation and sorption; and
- The watershed system's topography.
- The dissolution and weathering of minerals that formed the catchment area;
- The mixing of different types of water;
- Chemical processes that occur in the marine environment; hydrolysis, redox, precipitation, and complexing reactions;
- The means as well as extent of land use in the catchment area, as well as water use;
- The weather (including temperature and precipitation);
- The depth of river systems and their proximity to the basis of contamination.

Metal species can occur in three different forms in the marine environment, subject to the physicochemical parameters in the water, namely as free ions, which are the most toxic towards living organisms, complex compounds, and precipitated molecules of a compound (Manahan, 2003). As a result, metal speciation is affected by numerous elements, including water pH, temperature, concentration of dissolved oxygen, organism biotic action (Horng et al., 2009; Vicente-Martorell, 2009), and bedrock composition, which will be discussed in the following sections.

2.3.1. Aluminium

Aluminium (Al) occurs in the form of various alumina-silicates and is one of the most common elements making up 7.8% of the earth's outer layer. It exists in almost all rocks and in both primary and secondary minerals (in excess of 270 different minerals), with orthoclase $K(AlSi_3O_8)$, albite $Na(AlSi_3O_8)$, anorthite $Ca(Al_2Si_2O_8)$, sillimanite Al_2SiO_5 and kaolinite $(Al_2O_3 \cdot 2SiO_2 \cdot 2H_2O)$ being the most important ones. Biotite is the most common mica mineral and marls and clays are results of aluminosilicates weathering (Kabata-Pendias, 2000).

The aluminium sources are classified into two types: natural and anthropogenic. Aluminium naturally exists in the atmosphere as a result of weathering processes and volcanic eruptions (Al-Thai et al., 2018b; Mold et al., 2019b). Aluminium is transferred from soil particulates to the aqueous environment during natural weathering (Mohammed et al., 2014). Aluminium's ability to form organic and mineral complexes with varying degrees of hydration aids in its transition from

solid to liquid phase (soil-water) (Mohammed et al., 2014). Furthermore, because aluminium is highly soluble in acidic environments, acid rain can increase the amount of dissolved aluminium in the surrounding water (Barabasz et al., 2002; Mold et al., 2019b). In fact, aluminium can exist in several forms in water and is influenced by various parameters such as pH, which determines which forms of aluminium are available in an aqueous environment (World Health Organisation, 2003).

Aluminium salts are used in a variety of industries including paper, dyeing and tanning, water and sewage decontamination, wherein aluminium sulphate $[Al_2(SO_4)_3 \cdot 18H_2O]$ is used as a coagulant. Aluminium is only soluble at high or low pH and is not affected by weathering in terms of dissolution. Therefore, Al is insoluble at pH 5.0 to 9.0, which is typical in most natural waters. There are three types of aluminium species identified under different conditions, namely, the soluble Al^{3+} that predominates acidic environments, aluminium hydroxide $Al(OH)_3$ that is insoluble and predominates neutral environment as well as $Al(OH)_4^-$ which is dominant in alkaline environments (Habs et al., 1997).

Aluminium may be present in mine water in concentrations ranging from near zero to more than 4 g/L (Moncur et al., 2005), but researchers are rarely interested in recovering this element due to the high cost of using the impure recovered product for metallurgy. However, alternative methods of valorising aluminium were discovered. For example, precipitation of Fe^{3+} and Al^{3+} followed by dissolution in sulphuric acid can produce a poly-alumino-iron sulphate coagulant useful for the removal of suspended solids and colour (Menezes et al., 2010). On the other hand, aluminium recovery and reuse for advanced mine water treatment via sulphate removal as ettringite is possible (Dinu et al., 2016). The recovered aluminium in hydroxylated form can be used directly for further processing of the source mine water or transferred to another mine water site, primarily when the aluminium quantity exceeds the water source treatment requirements. This will happen depending on the discharge limits and the amount of aluminium in the mine water (Dinu et al., 2016).

2.3.2. Chromium

Chromium (Cr) occurs almost entirely in nature in the form of oxygen-containing compounds, with chromite ($FeCr_2O_4$), crocoite ($PbCrO_4$), and chrome ochre (Cr_2O_3) being the most important ones. Other anthropogenic sources of Cr include the manufacture of metallic Cr and its complexes, refractory materials, factories producing mineral and synthetic dyes and anticorrosion paints, welding gases and tanned leather, oils, spent lubricants, cement, industrial wastewater, the tanning and printing industries, and municipal sewage (U.S. EPA, 1999).

Chromium comes into the environment in two forms, dependent on its source of release, namely Cr(III) and Cr(VI) compounds (U.S. EPA, 1999). Chromium exists in a variety of oxidation states, but two of them are particularly important in the environment: Cr(III) as cationic Cr^{3+} and Cr(VI) as an anion (CrO_4^{2-} or HCrO_4^-) with distinct chemical properties. Under reducing environments, Cr(III) is the prevailing form in most minerals and water, whereas Cr(VI) is stable under oxidising conditions. Cr(VI) is highly soluble, mobile, and toxic in chromate, whereas Cr(III), which exists as a cation, is largely insoluble and immobile (Puzon et al, 2005; 2008).

In aqueous solutions, Cr^{3+} , $\text{Cr}(\text{OH})^{2+}$, $\text{Cr}(\text{OH})_3$, $\text{Cr}(\text{OH})_4^-$, $\text{Cr}_2(\text{OH})_2^{4+}$, $\text{Cr}_3(\text{OH})_4^{5+}$ hydroxyl complexes can exist thermodynamically. At high chloride and sulphate concentrations, mixed complexes like $\text{Cr}(\text{SO}_4)^+$ and $\text{Cr}(\text{OH})\text{Cl}^+$ can form, especially in acidic environments (Swietlik, 1998; Barakat and Giusti, 2003). The inorganic species bound to Cr(III) in the aquatic environment are determined by the pH. $\text{Cr}(\text{OH})_2^+$ is the dominant species at pH 4.5 to 5.5; $\text{Cr}(\text{OH})_3$ is dominant at pH 5.5 to 7.0, and $\text{Cr}(\text{OH})_3$ is dominant at pH 7.5 to 9.0. (Swietlik, 1998). Cr(VI) appears in aqueous solutions as chromates, dichromates, and hydrogen dichromates, which are only found in strong acid solutions. According to Sperling et al. (1992), HCrO_4^- and CrO_4^{2-} ions occur in typical surface water with dissolved Cr concentrations less than 5 g/dm^3 , where chromate ions predominate at a pH above 7 and hydrogen chromate at pH 6. While Cr(III) compounds are dominant in water with a pH of 5.0 to 7.0, Cr(VI) compounds predominate well-oxygenated water having a pH close to 8. In natural aquatic environments, chromium precipitates as a suspension, mostly as hydroxides, and it does not remain dissolved for long (Pettine et al., 1990). Cr is a siderophile and is found in ultrabasic rocks. It substitutes in micas, garnets, pyroxene, and magnetite. In soils, it is persistent in chromite, limonite, magnetite, and clays (Levinson, 1974).

2.3.3. Copper

The outer layer of the earth contains approximately 0.02 percent copper (Cu). Bornite (Cu_5FeS_4), tetrahedrite (3CuSSbS_3), enargite (Cu_3AsS_4), chalcocite (Cu_2S), chalcopyrite (CuFeS_2), cuprite (Cu_2O), malachite [$\text{CuCO}_2\text{Cu}(\text{OH})_2$], as well as azurite [$2\text{CuCO}_3\text{Cu}(\text{OH})_2$] are the most common ores containing Cu (Yang and Ni, 2007).

Copper concentrations in water are caused by anthropogenic activities. In water it comes from smelter effluent, the Cu/Cu-compound processing, and the electroplating industries. Fungicides, pigments, insecticides, catalysts, algicides, and piping and other corrodible apparatus made of Cu, brass, or bronze that have been exposed to water, particularly at high temperatures, are other ways Cu enters water (Kabata-Pendias and Pendias, 2000). Free Cu^{2+} ions, which can easily

pass through biological membranes are important factors controlling Cu bioavailability, according to Brown and Markich (2000). While both insoluble and soluble Cu species exist in water, the presence of nitrates and dissolved oxygen promotes Cu dissolution. Cu^{2+} ions as well as the complexes such as CuCO_3 (aq), $\text{Cu}(\text{HCO}_3)_2$, $\text{Cu}(\text{OH})_4^{2-}$ and $\text{Cu}(\text{OH})_3^-$ are the most common species in water with a high hydrogen carbonate concentration (Drogowska et al., 1994).

Copper poisoning can cause cancer, hemochromatosis, gastrointestinal problems, and accumulation in the kidneys, brain, skin, and heart.

Copper forms complexes with a variety of nitrates, sulphates, silicates, and phosphates. Cu insoluble complexes account for 40-90 percent of its total amount in water; 99 percent of Cu is transported as adsorbed on the silty segment as well as hydroxides (Moore et al., 1996). Direct electrowinning, copper reduction on iron metal, and copper precipitation using biogenic produced hydrogen sulphide, as in the Paquesor BioteQ systems (Menezes et al., 2009), are all options for copper recovery.

2.3.4. Iron

Iron (Fe) is one of the most abundant elements in nature, accounting for 5.08 % of the earth's outer layer (Greenwood and Earnshaw, 1998), and is found in almost all rocks, soils, and natural water as ferrous or ferric iron compounds. Fe enters water systems through weathering of rocks and soil, as well as leaching and infiltration. It can also be found in mineral oxides such as magnetite (Fe_2O_3), siderite (FeCO_3), limonite ($2\text{FeO}\cdot 3\text{H}_2\text{O}$), and goethite ($\text{Fe}_2\text{O}_3\cdot \text{H}_2\text{O}$), as well as such sulphides as pyrite (FeS_2) and chalcopyrite (CuFeS_2). These minerals dissolve in water and react with aggressive CO_2 to form $\text{Fe}(\text{HCO}_3)_2$ (Kabata-Pendias and Pendias, 2000).

Where there is oxygen existent, Fe^{2+} rapidly oxidizes to Fe^{3+} , which is then precipitated as a hydrated iron oxide. Oxidation is likely driven by ferro bacteria such as *Ferrobacillus* and *Gallionella* in areas with low oxygen levels (subterranean waters) (Coupland et al., 2004).

Mining, engineering industries, rock and mineral dissolution, and sewage systems are all sources of iron pollution in water. Haemochromatosis (an inherited condition in which iron levels in the body gradually increase over time) and laundry stains are two potential consequences of iron poisoning (Holnor, 2015). Iron is the most abundant metal in mine drainage, and several recovery methods have been investigated, including direct use of ochre deposits as brick components (Dudeney, 1997; Hedin, 2002), as pigment (Cornell and Schwertmann, 2003; Sapsford et al., 2015), or as reactive substrate for trace element and nutrient removal (Sapsford et al., 2015), or

acid dissolution conversion of ochre and mine water treatment sludges for use as coagulants (Rao et al., 2002).

2.3.5. Lead

According to many scientists, lead (Pb) is the 36th most common element in the outer layer of the earth, having concentrations ranging between 12.5 and 16 ppm (Levinson, 1974; Kabata-Pendias and Pendias, 2000). According to Taylor and McLennan (1985), Pb constitutes 8 ppm of the continental crust and 0.8 ppm of the oceanic crust. Lead commonly occurs in three oxidation states in nature, namely, Pb, Pb²⁺ and more rarely as Pb³⁺ and Pb⁴⁺. Galena (PbS) is the most common lead (Pb) mineral and less common Pb minerals include cerussite (PbCO₃), anglesite (PbSO₄), crocoite (PbCrO₄), wulfenite (PbMoO₄) and pyromorphite (Pb(PO₄)₃Cl) (Greenwood and Earnshaw, 1997). All these minerals have poor solubility, which implies that Pb migrates less intensively than other elements considered toxic such as Cd or Zn.

Lead contamination is common, because it can come in contact with normal waters through the corrosion of tanks, industrial wastewaters, pipes, and materials containing Pb or admixtures of Pb. Concentrations of Pb in water draining areas with traces of PbS or other deposits encompassing admixed Pb may reach 1,000 g/dm³ (Kabata-Pendias and Pendias, 2000). Furthermore, Pb can enter water from the atmosphere with Pb concentrations in gasoline additives contributing to approximately 60% of air pollution (Tukker et al., 2001). Pb precipitates (carbonates, phosphates, and sulphates) are poorly soluble in water, implying that Pb concentrations in water sources are low. Pb exists primarily in soluble form as Pb²⁺ and [PbCO₃(aq)]⁰, as well as in a basic medium as [Pb(CO₃)₂]²⁻, [Pb(OH)₂(aq)]⁰ as well as [Pb(OH)]⁺ (Badawy et al., 2002). The very low concentrations of Pb found in water with a pH of 9.0 to 10.0 and sufficient hydrogen carbonate concentrations are due to the former's low solubility. [Pb₄(OH)₄]⁴⁺, [Pb₆(OH)₈]⁴⁺, and [Pb(OH)₃]⁻ are some other soluble forms of Pb (Yusupov et al., 2000). Pb complexes that may occur in high pH and salinity waters include [Pb₂(H₂O)₅OH(NO₃)²⁺], [NO₃⁻], [Pb(H₂O)₂(OH)₂], [Pb(OH)₃H₂], [Pb(OH)₃H₂]⁻, [Pb₂(H₂O)₅OH](NO₃)⁺, [Pb(H₂O)₄NO₃]⁺, and [Pb(H₂O)₃OH]⁺ are some examples (Yusupov et al., 2000). Lead poisoning can have the following consequences: anaemia, headache, kidney, reproductive system, liver, brain, and central nervous system destruction (Kannan and Sarojini, 2010).

Lead sorption on bottom sediment particles is influenced by organic matter concentration as well as sediment granulometry. Pb is strongly partitioned on humic substances in acidic conditions and at pH>6 is completely adsorbed to sediments with no dissolved compounds (Sauvé et al., 1998).

2.3.6. Nickel

Nickel (Ni) is a transition metal that is widely distributed in various environmental settings, including air, water, as well as soil. It can come from either natural or anthropogenic sources. As the 24th most common element in the outer layer of the earth, it accounts for approximately 3% of the outer layer of the earth. In addition, it is the 5th most prevalent element as far as weight is concerned after iron, cobalt, palladium, and platinum. Under environmental conditions, Ni²⁺ is the most dominant oxidation state of Ni; other oxidation states, although found less frequently, include Ni¹⁻, Ni¹⁺, Ni³⁺ and Ni⁴⁺ (Clayton and Clayton, 1994; Young, 1995; Kitaura et al., 2003).

Anthropogenic and natural nickel sources exist in the environment. Silver refineries, the electroplating industry, metal finishing and forging, battery manufacturing, and mining industries are all potential sources of nickel pollution in aquatic systems (Patil et al., 2008). Processes such as precipitation, adsorption, and complexation are responsible for the deposition of nickel in sediment (WHO, 1991; Ngrigu and Pacyna, 1998). Associated with organic matter, Ni is transported in the rivers as precipitated coatings on particles (Diagomalinolin et al., 2004).

Dependent on the dose and level of exposure, health effects such as respiratory tract infections, cancer, asthma, contact dermatitis, lung fibrosis, and cardiovascular disease may occur (Chen et al., 2017).

2.3.7. Zinc

Zinc (Zn) is one of the most abundant elements in nature, accounting for 4×10^{-3} percent of the outer layer of the earth. It occurs in sulphide, silicate and carbonate ores primarily as zincite (ZnO), sphalerite (ZnS), smithsonite (ZnCO₃), and calamine (ZnSiO₄H₂O). Zn and its complexes are utilized in the production of pigments, cosmetics, alloys, crop protection products, paints, pharmaceuticals, wood preservatives, as well as metal surface galvanization (Mattielli et al., 2009). The main sources of Zn, according to Simon-Hettich et al. (2001), are metal processing plants, chemical factories, and wastewaters from Zn smelters, particularly viscose producing ones.

In surface water, zinc is of secondary sources and readily liquefies in water with high levels of CO₂ and DO, forming hydrogen carbonate ([Zn(HCO₃)₂], (ZnOH)⁺, (ZnHCO₃)⁺, [Zn(OH)₃]⁻, [Zn(OH)₄]²⁻ complex ions and (ZnO₂)⁻ forms in soils under hypergenic conditions (Masliy et al., 2000). Zinc species exist only in pH-dependent environments. Zn salts hydrolyse at pH 7-7.5, whereas at pH >8, the hydroxide Zn(OH)₂ precipitates out and is amphoteric, whereas further increases in pH may cause it to dissolve, resulting in the tetrahydroxy zincate(II) [Zn(OH)₄]²⁻

(Masliy et al., 2000). Zn exists as a divalent ion at pH 7 and readily forms complexes with inorganic and organic complexes. Zn is quickly absorbed in bottom sediments as well as the surface of suspended particulate matter (Bertling et al., 2006). In the presence of sulphide ions, zinc precipitates and is adsorbed onto organic substances, a process regulated by the pH of the water. Sorption stops at pH 5.8, and humic acids bind 60% of zinc's cationic concentration at pH 5.8. Given the high solubility of the compounds containing Zn, its assimilation and the associated risks of it entering the food chain are significant. An acidic pH encourages Zn migration in the environment as well as binding by plants and other soil creatures (Simon-Hettich et al., 2001).

According to speciation studies, the main forms of Zn found in bottom sediments are sulphides and carbonates; though it can be found partitioned to Mn and Fe oxides. Organo-zinc compound concentrations are lower, and the proportion of exchangeable and adsorbed forms reflected as bioavailable is minimal (Bourg and Darmendrail, 1992; Bertling et al., 2006).

2.4. Basic biogeochemical processes in soils and sediments

Trace elements interact with sediment and soil once they are deposited in these mediums. These interactions are based on soil-sediment characteristics and environmental influences such as pH and redox potential. Reactions such as (ad)sorption, precipitation, and complexation can keep metal species in soil and sediment.

Metals species mostly found in industrial effluents include arsenic silver (Ag) (As), iron (Fe), copper (Cu), chromium, cobalt (Co), manganese, lead (Pb), nickel (Ni), selenium (Se), zinc (Zn) and cadmium (Cd). Mining, tanning, paint, paper, printing, plating, fertilizer, electronic industries insecticides and pesticides, and photographic are the most common (Holnor, 2015). Various conventional technologies are routinely used to treat metal polluted wastewater, but their application is frequently limited due to technical and economic challenges. To treat industrial wastewater containing metals, chemical precipitation, ion exchange, chemical oxidation and reduction, filtration, electrochemical treatment, and membrane technologies are commonly used (Potgieter et al., 2006).

2.4.1. Adsorption

According to Stumm and Morgan (1996) adsorption refers to the attachment of molecules onto surfaces. An adsorption process involves the contact of solids with liquids or gases in which mass transfer is towards solids and desorption is the reverse of this process. This is because some solids preferentially adsorb other solutes from the solution onto their surfaces. The main objective of this process is either waste treatment or purification of the valuable component of a feed stream. Certain solids have the ability to concentrate some substances from fluids onto their

surfaces. In this process, the adsorbed substance (solute) is referred to as the adsorbate, and the solid substance is referred to as the adsorbent, which determines the mobility and bioavailability of metal species in the sediment in aquatic environments.

Physical adsorption and chemical adsorption/chemisorption are the two types of adsorptions. The forces of attraction between adsorbate and adsorbent particles in physical adsorption are weak Van der Waals forces. Because Van der Waals forces are weak, physical adsorption is limited. Chemical bonds serve as the forces of attraction between the adsorbate and the adsorbent in chemical adsorption. It is a lengthy procedure. . The physical adsorption is a freely reversible phenomenon that results from intermolecular forces of attraction between the solid and the adsorbed substance. On the other hand, chemical sorption is an irreversible process resulting from chemical interaction between the solid and the absorbed substance (Halnor, 2015).

The adsorption process is suitable even when the metal ions are present in concentrations as low as 1mg/L due to adsorbent regeneration, minimization of chemical and/or biological sludge, high efficiency, metal recovery (Ahalya et al., 2003), flexibility, and simplicity of design. Adsorption has been found to be a superior technique for removing metal species from wastewater due to its insensitivity to toxic pollutants, low cost, and ease of operation (Holnor, 2015). Holnor and Ubale (2013) were the first to propose the use of activated carbon for heavy metal adsorption.

Several chemical, biological, and waste vegetable matters or substances have been used as adsorbents for the removal of heavy metals from wastewater by various researchers. However, in order to make the adsorption process cost effective, the adsorbent must be readily available, inexpensive, and environmentally friendly. As a result, most researchers used low-cost adsorbents that were abundant in nature, or materials that required little processing or were by-products or waste materials from another industry, or that had lost their economic or further processing values. Seaweed, orange peel, peanut skins, bamboo-pulp, dyed sawdust, algae, clay, zeolite, sawdust, flyash, maize or corn cob, modified cotton and wool, tea waste, dyed jute, groundnut shells are examples of adsorbents (Holnor and Ubale, 2013), cassia siamea, coffee, green tea, date tree leaves, jambhool, potato husk, ashoka leaf powder, syzygium cumini, Jute and sun hemp, prosopis spicegera, ratrani leaf powder, jute stick, cashew nut shells, coconut husk, feathers, hairs, bagasse, apple pomace, and almond husk (Holnor, 2015).

Various factors influence the adsorption process and these include the pH, temperature, surface area, adsorption isotherms, and the nature of adsorbate. Metal removal from wastewater, softening hard water and drying gases, decolourisation and purification are some of applications of the adsorption process (Singh and Singh, 2005).

2.4.2. Precipitation

Precipitation is the process that occurs in a chemical reaction when the solubility of a salt is exceeded, implying that the solution is supersaturated in terms of the precipitating compound. As a result, the solute concentration will be greater than the rate of solid-liquid equilibrium. Precipitation processes are characterized by the solubility of the metals to be removed. The driving force behind the process of precipitation is the degree of supersaturation required for effective precipitation. The addition of another reagent to the system alters the equilibrium conditions in the process of precipitation (Ullmann and Gerhartz, 1998).

The precipitation process occurs in three mechanisms in the order: nucleation, growth, and agglomeration. According to Jones et al. (2004), nucleation is the preliminary development of a solid phase solution that occurs when the clusters and aggregates of molecules or ions in a supersaturated solution reach a critical size where entities grow rather than dissolve. Primary and secondary nucleation can occur. The birth of a solid phase naturally from the solution is referred to as primary homogeneous nucleation, which is induced by foreign particles. It is caused by the presence of existing crystals. Contact nucleation, such as crystal-crystal contact or crystal-crystalliser contact is one type of secondary nucleation. Furthermore, shear nucleation influenced by fluid, fracture nucleation influenced by particle impact, attrition nucleation resulting from particle impact from fluid flow, and needle nucleation influenced by particle disruption are all possible (Jones et al., 2004). Nucleation rate is a function of supersaturation. Crystals enlarge during the growth process as a result of crystalline material deposition on the existing crystalline surface. This process is also a function of supersaturation occurring at lower supersaturation levels than the nucleation process. The final particle size distribution is determined by the rate of nucleation and growth. The level of supersaturation influences the type of growth that occurs. Rough growth is preferred at high supersaturation levels, birth and spread growth is preferred at intermediate supersaturation levels, and spiral or smooth growth is preferred at low supersaturation levels. When the rate of nucleation exceeds the rate of growth, the resulting crystals are small and numerous (Kroschwitz and Seidel, 2006). Agglomeration is the process by which two or more particles are brought together and remain in contact for a sufficiently long enough period for a crystalline bridge or a stable particle/agglomerate to form. This is a collision-driven process with direct relationship to the nucleation process. As a result, the rate of agglomeration depends on supersaturation and the square of the number of particles present. Furthermore, because of the large number of particles involved, agglomeration plays an important role in the formation of larger particles and crystallisation processes (Lewis et al., 2015).

Generally, precipitation is utilized to remove metals from several types of wastewaters, including AMD and hydrometallurgical effluents (U.S. EPA, 2000). Chemical precipitation is used in approximately 90 percent of industrial wastewater treatment plants (Grijalva, 2009). However, metal recovery by precipitation is not yet common practice and there are several possible chemical precipitations for removing metals from wastewater, including hydroxide (OH^-), sulphide (S^{2-}), carbonate (CO_3^{2-}), and phosphate (PO_4^{3-}) (Grijalva, 2009). Depending on the geochemical and biogeochemical conditions, oxidation and hydrolysis reactions can lead to the precipitation of a variety of hydroxides (e.g., goethite, gibbsite, and hydrous ferric iron), sulphates (e.g., gypsum, anglesite, melanterite), and hydroxy sulphates (e.g., jarosite, alunite, and schwertmannite) (Nordstrom and Alpers, 1999). Secondary minerals are important in reducing pollutants in mine seepages (Lee et al., 2002; Sánchez-España et al., 2005).

2.4.3. Complexation

The complexes are compounds that result from donor-acceptor mechanisms between two or more chemical species. Complex ions are formed by combining simple cations and anions together with other molecules that can act as binding agents (ligands).

Complexes are categorized into three types depending on the nature of acceptor substance, namely, metal ions complexes, inorganic molecular complexes, and inclusion complexes. Generally, the metal ion complex consists of a transition metal (e.g., Cu, Fe, Ni) coordinated with one or more counter ions or molecules to form a complex. The cation (typically a metal) serves as a central atom and the anion (which serves as a ligand) may be an inorganic species including bromine (Br^-), chlorine (Cl^-), fluorine (F^-), carbonate ion (CO_3^{2-}), and phosphate (PO_4^{3-}). The interaction of solutes with metals results in both inorganic and organic complexes. Metal species such as Cd and Cr can be dissolved and transported more easily thanks to complexation reactions (Langmuir, 1978).

Chelation is one of the most important complexation reactions that occurs between a central cation as well as a specific ligand known as a chelating agent resulting in very stable complexes. The formation of two or more coordinate bonds between a multidentate ligand (chelating agent) and a single central atom is referred to as chelation (Ringbom, 1967). Complex formation is subjective to factors like pH, temperature, species concentration, as well as competitive reactions (Chauhan et al., 2015). Chelating agents are commonly used in soil decontamination (Peters, 1999; Dermont et al., 2008; Leštan et al., 2008; Zhang et al., 2013). Several factors should be considered when selecting a chelating agent. These advantages include: (i) the ability to form very stable complexes; (ii) discernment for some metal species; (iii) lower sorption attraction on

soil surfaces; (iv) lower cost; (v) environmental friendliness combined with low toxicity; (vi) the ability to be recycled or reused; and (vii) low biodegradability if reuse is required (Peters, 1999; Dermont et al., 2008; Leštan et al., 2008). Because of its ability to form stable complexes and low biodegradability, polyaminocarboxylic acid and nediarninetetraacetic acid (EDTA) are the most commonly used chelating agents (Nowack and Vanbriesen, 2005). Citric acid (CA), on the other hand, can be used in some cases (Wasley et al., 2001).

Disadvantages of biogeochemical process

When metals in solution in the range of 1-100 mg/L are present, these processes may be ineffective or extremely expensive, and they frequently necessitate a high level of skill for operation and use of hazardous chemicals (Ahluwalia and Goyal, 2007). Another disadvantage of traditional treatment technologies is the generation of toxic sludge as a result of the chemicals used (Gupta et al., 2000), which is often difficult to dewater and must be disposed of with extreme caution (Kapoor et al., 1999). Metal ion removal is unpredictable, and the reagent requirements are high (Barros, et al., 2003).

2.5. Acid mine drainage

Acid mine drainage (AMD) occurs in mining environments as a consequence of sulphide minerals such as pyrite (FeS_2) being exposed to water as well as oxygen resulting in the oxidation of sulphides (Blowes et al, 2003). To oxidize pyrite, water and oxygen must be present where water serves as a reaction medium, reactant, as well as product transport in this process. Mine residue deposits typically contain pyritic minerals such as pyrrhotite and pyrite, which can oxidize when exposed to oxygen and water, resulting in AMD. AMD is distinguished by a low pH and elevated concentrations of contaminants such as metal species and sulphate ions (Sracek et al, 2010).

The detrimental effects of AMD have been documented by various researches in Africa for example, Naicker et al. 2003 and McCarthy, 2011, in Asia for example, Naoto et al. 2021, in Canada for example, Neculita et al. 2007 and Sracek et al. 2004 in Europe, for example, Galán et al. 2003 and Gomes and Favas, 2006, and in the USA for example, Alpers et al. 1994b.

It is also worth noting that mine drainage can either be acidic or alkaline; thus, the word AMD refers to drainage waters with high concentrations of potential contaminants throughout.

2.5.1. Management of AMD

2.5.1.1. Control of AMD

There are numerous approaches that can be taken for mine waste segregation and avoiding oxidizing environments to keep sulphides isolated from oxygen.

2.5.1.1.1. Water covers

In humid climates, preventing AMD usually entails controlling oxygen fluctuation with water or approximately saturated porous media (Pabst et al., 2018). Water covers are typically used to dispose of reactive mine tailings under water (Pabst et al., 2018).

The tailing materials that have a potential to produce acid can be prepared and stored under water in order to avoid contact between the minerals and dissolved oxygen (Pabst et al., 2018). In the past, the practice of disposing of mine wastes into the ocean took place without any environmental concerns or considerations. Recently, most countries have excluded this practice for AMD control (Edinger, 2012); however, few countries still use it cautiously (Edinger, 2012), including Canada (Samad and Yanful, 2005).

A changing water table in reactive waste rock has been identified as the ultimate environment for acid formation as well as relocation (Bell, 1988; Jones, 1990). Because of the very low diffusivity of oxygen in water, disposing of reactive waste rock underneath the water table limits oxidation to almost zero. Underwater disposal of reactive waste rock provides a lasting solution to the problem of acid generation. Under saturated conditions, oxygen diffusion is limited; nevertheless, a small volume of oxygen transfer occurs (List, 1989).

The oxygen supply to tailings under water is small, being approximately 1000 times lower than in air, making AMD generation negligible. This approach may be more expensive to implement for older simulated tailings storage facilities. The method, however, is effective in inhibiting the oxidation of reactive tailings. Another significant challenge is constructing dikes that will last the lifetime of the tailing pools (Pabst et al., 2018). As an alternative, elevated water tables (EWT) can be used as water covers. The EWT approach is based on regulating the reactive tailings' water table level and degree of saturation (Pabst et al., 2018). When well premeditated and employed, the EWT approach can be quite effective in limiting AMD generation (Pabst et al., 2018).

2.5.1.1.2. Mine land reclamation

Mine land reclamation was previously defined as either restoring mine property to its pre-mining condition before modifying it to mark it accessible for another dynamic use (Sweeting and Clark, 2000). Heavy equipment used to clear vegetation and eradicate both soil and waste rock during mining operations disrupting landscape aesthetics and soil mechanisms (Sweeting and Clark, 2000; NYSDEC, 2005). Inadequate management and the absence of regulations can result in severe disruption of soil and water resources, landscape, vegetation, and habitats, or even total destruction in the worst-case scenario (Nsiah and Schaaf, 2019; Salmiati et al., 2012). Mine land reclamation helps nature restore itself from such disturbances and destructions within short periods, as natural processes alone may take many years to rehabilitate such damages. However, there is a need to test long-term ecosystem recovery because the restoration science has grown rapidly in recent years (Prach et al., 2001; Roubířková, 2013).

Compaction and amalgamation during storage can also weaken soil structure (Strohmayer, 1999). Reduced nutrient cycling and availability may result from topsoil stockpiling (NYSDEC, 2005; Rai et al., 2014), which can jeopardize reclamation and overall revegetation success (Salmiati et al., 2012).

Following instabilities like mining, organic modification has been shown to encompass elevated amounts of major plant nutrients and can also be a valuable source of organic matter (Larney and Angers, 2012; Nsiah and Schaaf, 2019), which can improve the biological, chemical, and physical properties of the soil. Soil organic matter (SOM) concentration, nutrient supply, and pH are the most important determinants of a disturbed site's suitability for reestablishment (Nsiah and Schaaf, 2019). The use of organic amendment in conjunction with stockpiled topsoil (TSP) is a thriving management exercise for improving nutrient supply as well as the soil's physical and chemical characteristics (NYSDEC, 2005; Nsiah and Schaaf, 2019). Salmiati et al. (2012) also described the use of organic amendment for reclamation as interdependent, with waste products from agriculture, forestry, and urban areas helping to meet land reclamation goals.

Backfilling and revegetation work well together to reduce acid loads from disturbed land areas (Skousen et al., 2019) However, according to Kuipers et al. (2006), these methods work best when used in tandem and tailored to specific site conditions. Systematic modelling studies of the site's unique condition (biological, hydrologic, and geochemical characteristics) are a prerequisite to laying a foundation for durable monitoring as well as providing an understanding into the mechanistic processes involved in AMD progression (Edwards et al., 2000). Alternatively, gold mine tailings have the potential to be used for building and construction (Mashifana et al., 2019)

or as a prospective site for profitable artisanal gold mining employing straightforward methods like a centrifugal separation system (Munganyinka et al., 2022).

2.5.1.1.3 Biocidal AMD control

An abandoned mine that has already begun producing AMD can be considered a perpetual polluter. Because both oxygen and water are required to generate AMD, excluding either (or both) of these should be possible to prevent or reduce AMD production (Johnson and Hallberg, 2005). Furthermore, bacterial activity regulation prevents the contamination process from being catalysed (Obreque-Contreras et al., 2015). The bacterial component of AMD formation was first recognized in the early 1950s by Leathen et al. (1953) and subsequent research that appears to peak in the 1980s and 1990s revealed that many common surfactants such as sodium lauryl sulphate (SLS), sodium dodecylbenzene sulfonate (SDS), alkyl benzene sulfonate (ABS), biosolids, and other organic materials significantly inhibited bacterial activity with respect to *Thiobacillus ferrooxidans* (Gusek, 2005). According to Kleinmann and Erickson (1983), *Thiobacillus ferrooxidans* is crucial in determining the rate of pyrite oxidation.

The bacteria organism thrives in aqueous environments with pH values of 2.0 (Baker and Banfield, 2003). To survive in this hostile environment, the microbes encase themselves in a thick oily protein membrane that employs several protective mechanisms, including proton "pump" mechanisms that allow the cells to maintain a circumneutral cytoplasmic pH (Goulbourne, et al., 1998). The microbe, in effect, "stews in its own juices" and is destroyed. Because of the simple destruction mechanism involved, developing a surfactant resistance strategy for a *Thiobacillus ferrooxidans* cell may be difficult (but not impossible). The AMD, on the other hand, could be viewed as a de facto *Thiobacillus ferrooxidans* defensive strategy: the acidity in the AMD tends to destabilize the long-chain carbon bonds in surfactants, making them less potent (Gusek, 2022).

Bacterial populations related to acid production have been successfully controlled with anionic surfactants, primarily in coal mines such as North Fork Coal Mine (Jones, 1990; Duggan et al., 1992) and Fisher Coal Mine (Gusek and Plocus, 2016) in the United States of America. Anionic surfactants inhibit bacterial activity, slowing acid production. Because anionic surfactant compounds are highly soluble and easily degradable, especially under acidic environments, their effectiveness as a control technique may be limited in time, despite their being proven as biocidal agents (Kleinmann and Erickson, 1983; Johnson and Hallberg, 2005). For maximum benefit, surfactant application should be repeated three times per year (Gusek, 2022).

In the mid- to late-1980s and the decade that followed, bactericide use was centred on promoting revegetation of pyritic coal mine wastes such as coarse coal refuse (e.g. Branchton Coal Refuse

Disposal Area, Butler County in the USA, Parish et al., 1994) and reducing acidic drainage from pyritic shale partings in surface mine backfill. One significant advancement in *Thiobacillus ferrooxidans* bactericide technology was the development of controlled release pellets containing SLS. The revegetation step appeared to be critical to the success of the bacteria suppression process; otherwise, SLS reapplications as frequently as three times per year were suggested (Kleinmann, op cit.). Verburg et al. (2003) found that using a 1% LS solution to suppress ARD formation in a metal mine tailing containing 60% pyritic sulphur yielded positive results.

Other non-surfactant organic amendments that have been found to be effective in suppressing *Thiobacillus ferrooxidans* include: composted sewage sludge, composted paper mill sludge, pyruvic acid, a water-soluble extract from composted sewage sludge (Pichtel and Dick, 1990), spent brewery grain (Lindsay et al., 2010; Gusek et al., 2021) and waste milk/dairy products (Jin et al., 2008).

2.5.1.1.4 Alternative dump construction

A reactive waste managing technique that suggests settlement of reactive as well as nonreactive waste material during the construction or restoration of the mine storage facility. The goal of this storage facility design is to compress reactive waste in a non-reactive material, thereby preventing or controlling acid generation (Jones, 1990). For this method to be successful, it is very important to attain the correct degree of thoroughness by mixing alkaline and acid-generating materials. This type of mine storage facility construction is only reasonable if there is an abundant bulk of impermeable neutralizing material available and an equitable hauling distance. The model of selective mine storage facility was used at Equity Silver Mine (Jones, 1990).

2.5.1.2. Treatment of AMD

To be appealing, this process must be cost effective, simple to set up and preserve, and produce a limited quantity of solid by-products. The efficiency and viability of water treatment varies greatly subject to the treatment used and the unique characteristics of the site. There are active and innovative (passive) management systems for AMD, and the choice depends on site-specific conditions. The following sections summarize some of the available technologies.

2.5.1.2.1. Active Treatment

In cases where AMD is already taking place a commonly established treatment measure is to treat the already polluted water to remove elevated metal levels and acidity. Active treatment is the process of improving water quality through techniques that necessitate continuous inputs of artificial energy and/or (bio)chemical reagents (Younger and Sapsford, 2006). There are several

active methods, with ODAS, which stands for -oxidation, alkali dosing, and sedimentation, being the well-known active technique (Younger and Sapsford, 2006). The method is comparable to the one used in a wastewater treatment plant. Traditional wastewater treatment methods include desulphurisation, sorption, sedimentation, ion exchange, as well as membrane practices such as reverse osmosis and filtration. The water is diverted from the course, treated, and then discharged in these treatment systems (Younger and Sapsford, 2006).

The six most commonly used chemicals in AMD treatment include, but not limited to, are limestone, hydrated lime, quicklime, soda ash, caustic soda, as well as ammonia (Trumm, 2010).

2.5.1.2.1.1. Limestone

For decades, limestone has been used to increase the pH and metal precipitation in AMD. This is because it is less expensive and easier and safer to handle than any of the other AMD chemicals. Nonetheless, limestone has a low solubility and a tendency to armour the iron hydroxides when added to AMD, limiting its use. To increase limestone dissolution and reaction, fine-ground sand-sized limestone can be dumped directly into streams (Simmons et al., 2006), or the limestone can be pulverized by water-powder rotating drums and metered into the stream (Skousen et al., 2019). Limestone has been studied for its use in AMD treatment in both aerobic and anaerobic environments, such as open limestone channels and anoxic limestone drains. According to Barnhisel et al. (2000) and Skousen et al. (2019), limestone is of limited use in routine chemical treatments as it reacts slowly and dissolves, whereas other more reactive and effective liming materials are available.

Several studies have used limestone to treat AMD from coal and metal mines, for example, Maree et al. 2004 and 2005.

2.5.1.2.1.2. Hydrated lime

According to Skousen et al. (2019), hydrated lime is frequently used for AMD treatment. It is hydrophobic due to the finely ground powder and in general, mechanical mixing is required for dissolution. According to Barnhisel et al. (2000a), hydrated lime performs well and is cheaper in high acidity as well as high volume flow situations where a lime treatment plant with large storage bins and an aerator/mixer is used to help dispense and mix the chemical with water. However, hydrated lime is ineffective when a very high pH (>10) is essential to remove ions like Mn.

2.5.1.2.1.3. Quicklime

According to Skousen *et al.* (2019) quicklime (CaO) is used with lime dozers and portable quicklime dispensing machines, which may have controlled dispensers or a water-wheel concept. The water wheel rotates in response to the flow of water, causing the screw feeder to dispense the chemical. Due to the fact that CaO is highly reactive, this system (water wheel) was initially used for small and/or periodic high acidity flows, but recently, controlled automated dispensers have been attached to large silos for high-flow/high-acidity situations (Barnhisel *et al.*, 2000; Trumm, 2010).

Tests comparing a portable water wheel dispensing system to caustic soda (NaOH) systems revealed an average cost savings of 75% and savings of 20-40% over NH₃ schemes (Skousen *et al.*, 2019).

2.5.1.2.1.4. Soda ash

Soda ash is commonly used in remote areas for AMD treatment due to its low flow rate of less than 750 L/min as well as low levels of acidity and metal species (Skousen *et al.*, 2019). In most cases, the use of soda ash is motivated by convenience rather than cost. Skousen *et al.* (2019) reported that soda ash is delivered in briquettes and gravitationally fed into water via storage bins. Water quality and flow rate determine the number of briquette bags that can be used per day.

One disadvantage of soda ash is that it cannot be utilized in high flow situations such as those exceeding 750 L/min as it becomes too expensive, the briquettes adsorb moisture and then expand to the corners of the bin, preventing them from contacting water (Skousen *et al.*, 2019).

2.5.1.2.1.5. Caustic soda

Caustic soda (NaOH) is the best option in remote areas having low flow (100 L/min or 30 gpm) high acidity situations or high concentration of Mn in AMD (Skousen *et al.*, 2019). Caustic soda requires special care when handling (Skousen, 2002). According to (Johnson and Hallberg, 2005), NaOH is nearly nine times more expensive than lime despite being approximately 1.5 times more effective.

2.5.1.2.1.6. Ammonia

Even though ammonia complexes (NH₃ or NH₄OH) are useful in the treatment of AMD, anhydrous ammonia is extremely dangerous. Ammonia has the ability to increase the pH of receiving water to 9.2, is extremely soluble, reacts quickly, and forms gas when released from the tank (Barnhisel

et al., 2000). To go beyond pH 9.2, a large amount of NH_3 must be added because at this value the buffering capacity of the solution is reached and no further pH increases will occur. Injecting NH_3 into the AMD is one of the quickest ways to increase the pH of the water. Because NH_3 has a lower density than water it should be injected near the bottom of the pond or water inlet. According to (Barnhisel et al., 2000), NH_3 is cheap, with a cost reduction of 50-70 percent possible when NH_3 is replaced with NaOH.

Advantages of AMD active treatment technology 2005 (Johnson and Hallberg):

- There is no need for additional space or construction;
- Quick and efficient removal of acidity and metals; and

Active treatment technology disadvantages (Hilton, 1990; Barnhisel et al., 2000; Skousen, 2002; Skousen et al., 2017):

- There must be an uninterrupted supply of energy and chemical energy to function properly;
- The overall cost is increased by the use of expensive chemicals and the engagement of sufficient manpower to maintain the system;
- They should be regularly maintained as well as supplying chemicals for proper functioning, which is not easy to control; especially for most remote previously mined sites; and
- System costs and efficiency vary depending on the type of neutralizing means used.

2.5.1.2.2. Passive Treatment

Also known as innovative treatment systems, passive treatments require little maintenance to treat water or solids using improved natural processes onsite (Gazea et al., 1996; Younger and Sapsford, 2006; Skousen et al., 2017; Skousen et al., 2019). These systems of AMD treatment were originally developed in the USA's Appalachia coalfield where many coal seams are associated with pyritic strata, especially in the northern Appalachians (Skousen et al., 1998; Skousen et al., 2017).

These treatment systems increase the quality of the influent water through naturally occurring geochemical and biological processes while requiring little operation and upkeep. The pH of mine water will rise when it mixes with alkaline water or comes into direct contact with carbonate rocks. The precipitation of hydroxides, oxyhydroxides, and sulphides influence metal contaminant removal and these reactions are influenced by prevailing local conditions such as oxygen

concentration, water chemistry, and soil chemistry. The reactions can take place in either aerobic (oxidizing) or anaerobic (reducing) environments (Skousen et al., 1998, 2017; Skousen, 2002). Site-specific passive treatment technologies exist. Before evaluating and selecting the type of appropriate passive treatment, factors such as discharge chemistry (pH, dissolved oxygen concentration, ferric/ferrous Fe ratio, and Al concentration), flow rate, site characteristics, and local topography should be taken into account (Hedin and Nairn, 1993; Hedin et al., 1994; Skousen et al., 1999 Skousen et al., 2000). In many cases, passive treatment systems are made up of a series of treatment stages, each of which are designed to target and remove a specific contaminant. The first treatment stage in most passive treatment systems occurs in a sedimentation pond to remove sediment that has the potential to clog subsequent treatment stages (McCauley, 2011).

The different types of passive treatment technologies range from proven technologies operating at full scale to technologies that appear promising but have yet to be confirmed at full scale and newer technologies that have been explored at laboratory-scale only. These technologies have been applied worldwide to treat polluted water and have been proven to treat a few hundred kilolitres per day (DWA, 2013; Skousen et al., 2017). Two different types of passive treatment exist, namely, biological (e.g., wetlands and vertical flow systems) and geochemical (open limestone channels, permeable reactive barriers, limestone leach beds) (McCauley, 2011).

2.5.1.2.2.1. Biological Passive Treatment Systems

2.5.1.2.2.1.1. Aerobic Wetlands

The system makes use of wetland vegetation such as *Typha (Cattails)* planted in shallow sediments (30cm) beneath a limestone base. The limestone is mixed with an organic substrate, and the system is designed to collect water while also providing residence period for metal oxidation, hydrolysis, and metal hydroxide settling (White, 2000; Skousen and Ziemkiewicz, 2005; Skousen et al., 2017; Skousen et al., 2019). Plants in the system help to achieve uniform flow, stabilize the substrate, and maintain microbial activity, whereas limestone aids in the creation of net alkaline conditions (Skousen and Ziemkiewicz, 2005; Skousen et al., 2019).

Metal removal from an aerobic wetland is accomplished by reducing the flow and allowing oxidation, which is frequently catalysed by bacteria. If the pH is 3.5 or higher the resulting Fe^{3+} from Fe^{2+} oxidation precipitates as iron hydroxide in these configurations. Other metals that coprecipitate with Fe may settle on these structures as well.

2.5.1.2.2.1.2. Anaerobic Wetlands

Anaerobic wetlands are composed of wetland vegetation such as *Typha* established in shallow (>30 cm) porous substrates made of soil that, according to Skousen et al. (2019), can be mixed with organic materials such as sawdust, bales, manure/straw, peat moss, hay, and spent mushroom compost. The dissolution of carbonate and reduction in microbial sulphate generates alkalinity. AeWs are the best-suited technology for handling net-acidic drainage, having low pH, elevated Fe concentration, as well dissolved oxygen of above 2 mg/L AMD because they produce an alkaline environment. The mechanism and efficacy of AMD treatment varies according to season and wetland age (Barnhisel et al., 2000). Some wetland plant species accumulate metals differently, with some accumulating high concentrations on their tissues and others accumulating little (Barnhisel et al., 2000).

The alkalinity produced in an AeWs by certain bacteria; *Desulfovibro* and *Desulfotomaculum* consumes acid as a source of metabolism between organic substrate and sulphate. Bacteria can only degrade a portion of organic matter because it requires simple organic compounds or action by fermenting or other bacteria to degrade complex compounds. The bacterial conversion of sulphate to hydrogen produces bicarbonate alkalinity in water:



The sulphate reducing bacteria work best at pH levels between 6 and 9, but can function at pH levels as low as 5. (Skousen et al., 1998). Skousen et al. (1998) discovered that bacteria control their microenvironment even when the influent pH is lower than 3. If the degree of acidity input exceeds the system's neutralization capability, there will be a decrease in pH as well as a reduction in sulphate (Skousen et al., 1998). Seeding of the wetland system with specially designed and selected microorganisms is crucial to present or re-establish microbial activity (Skousen et al., 1998). Experiments with appropriate controls have not been conducted to determine the efficacy of this approach (Barnhisel et al., 2000).

Another source of alkalinity in an anaerobic wetland is when limestone under organic material reacts with acid:



Anaerobic wetlands work best when treating low AMD flows with adequate acidity (Hedin et al., 1994; Skousen et al., 1998).

2.5.1.2.2.1.3. Vertical Flow Wetlands

Developed for contaminated water treatment in the 1980s, vertical flow wetlands (VFWs) were described by Skousen et al. (2017). Burns et al. (2012) and Skousen et al. (2017) coined the word successive alkalinity producing systems (SAPS), but other researchers have referred to them as reducing and alkalinity producing systems (RAPS) (Skousen et al., 2017), or vertical flow ponds.

Vertical flow wetlands have three basic components: a layer of organic substrate, a layer of limestone, and a drainage system, which in most cases, may include a flushing system (Skousen et al., 2017). In the VFWs, low pH and metal-rich water is deposited to a depth of 1 to 2 m over 0.2 to 0.6 m of organic substrate resting on 0.5 to 1 m layer of limestone. When the hydraulic head of the water drives it through the organic substrate, oxygen is consumed and anoxic conditions occur. The main function of the organic layer is to convert all iron (Fe) to ferric iron (Fe^{2+}), thus preventing ferric hydroxide from coating the underlying limestone. Sulphate reduction neutralizes acid in the organic layer and in the limestone base (Skousen et al., 2019). Mine drainage flows into the cell's top, forming a layer of water that prevents oxygen from infiltrating the bottom layers. The organic layer in the water will remove dissolved oxygen, while anaerobic conditions deeper in the water will promote the growth of sulphate-reducing bacteria. The reducing anaerobic environment reduces the likelihood of hydroxide precipitation by converting ferric iron to ferrous iron.

Because iron (Fe) and aluminium (Al) oxidation and reduction produce precipitates capable of clogging the cell, many SAPS systems now incorporate flushing systems (Rees and Bowell, 2001b). In general, flushing systems work by creating head alterations that move water quickly through the system (Skousen et al., 2017). Other organic materials have plugging issues, whereas mushroom compost performed well in SAPS. Composted municipal waste and a variety of other organic materials contributed to acceptable levels of sulphate reduction (Eger, 1994).

SAPS requires little material for the provision of similar treatment as aerobic wetlands are more proficient (Skousen et al., 2017). SAPS requires some maintenance in addition to periodic flushing (Rees and Bowell, 2001a; Costello, 2003; Skousen et al., 2017).

2.5.1.2.2.1.4. Bioreactors

Bioreactors, also known as sulphate-reducing bioreactors, were modified from anaerobic wetlands (SRB). They are similar to VFWs except that the main reactant is organic matter, which is commonly mixed with limestone (Gusek, 2004). SRBs are anoxic chambers consisting of

organic matter and sulphate reducing bacteria such as *Desulfovibrio*, where the bacteria facilitates chemical reactions that promote alkalinity, sulphate reduction and metal precipitation (Gusek, 2005; Christenson et al., 2017). The setup of the system consists of a mixture of limestone and organic substrates (Gusek, 2005; Moreira, 2018).

Bioreactors are typically injected with particular microbial populations intended for specific water or may include specified substrates (Neculita, et al., 2007b; Lefticariu et al., 2015; Skousen et al., 2017). Microbial sulphate lessening is the crucial method of treatment (Neculita et al., 2007b). Bioreactors handle highly acidic and elevated metal water, such as AMD containing transition metals like Fe. Because of their slow flow rate and the ability to operate multiple units in parallel, SRBs can be used to treat either low flows or comparatively large systems. Skousen et al. (2017) stated that most bioreactors are useful in treating metal mine drainage, but Sandy and DiSante (2010) reported few bioreactors built to treat acidic effluent from coal mining to remove selenium.

The microbial system must first adapt to the AMD chemical composition and substrate which slows bioreactor start-up. To speed up treatment the bioreactor may be injected with microbial communities from other operational systems. Iron sulphide (FeS) is a bioreactor by-product that removes both iron and sulphur from the solution (Skousen et al., 2019). In the organic layer, iron sulphide (FeS) precipitates. However, in some cases, FeS can be found in the effluent and settling pond, probably in conjunction with intrinsic sulphur.

The system is cost effective and has low operational and maintenance requirements; burial of the system minimizes vandalism and it can be constructed in remote areas (Gusek, 2005; Kousi et al., 2015; Figueroa et al., 2016). It can regulate and accommodate differing flow rates and retention time (Gusek, 2004). However, there are also disadvantages associated with SBSs. Cold climates can compromise the efficiency of the system because it decreases the rate of bacterial growth and degrades the quality of organic matter in the system (Karabelnik et al., 2008; Langergraber, 2008; dos Reis et al., 2018; Ben Ali et al., 2019;). Acidic conditions reduce sulphate-reducing bacteria, which has a negative impact on metal removal in the system (Karabelnik et al., 2008; Langergraber, 2008; dos Reis et al., 2018). Long-term efficiency of these systems is frequently reported to be limited by hydraulic failures such as clogging and preferential flow-paths (Gusek, 2005; Uster, 2013).

Few bioreactor methods rely on adding organic supplements on a regular basis to provide microorganisms with nutrients and carbon (Zamzow, et al., 2006; Sobolewski, 2010; Skousen et al., 2017). The addition of ethanol to the influent improves system performance in cold

temperatures, while the addition of limestone buffers the pH of influent water to a neutral range (Gusek, 2005; Moreira, 2018).

2.5.1.2.2.2. Geochemical Passive Treatment Systems

Anoxic limestone drains (ALDs), open limestone channels (OLCs), limestone leach beds (LLBs), steel slag leach beds (SLBs), diversion wells, limestone sand, and low pH iron oxidation channels are examples of geochemical passive treatment techniques.

2.5.1.2.2.2.1. Anoxic Limestone Drains

Kilborn (1999) and Seervi *et al.* (2017) defined anoxic limestone drains (ALDs) as layers of coarse limestone aggregate buried in carefully constructed drainage lines along gently graded slopes through which contaminated water will pass. ALDs are covered with clay or compacted soil to retain carbon dioxide (CO₂), exclude oxygen (O₂), and promote metal hydrolysis (Cravotta *et al.*, 2004). Before the water is released into the environment, the effluent is contained in a settling pond, where metal precipitation occurs (Hedin *et al.*, 1994).

ALDs are intended to raise the alkalinity of the acid mine drainage (AMD) while retaining the iron (Fe) in its reduced state. This avoids oxidation of ferrous iron (Fe²⁺) and precipitation of Fe(III) oxide-hydroxide on the limestone or armouring, which would significantly reduce the neutralising agent's effectiveness. When compared to an open system, which will produce 50-60 mg alkalinity/L in equilibrium, the partial pressure of carbon dioxide (CO₂) in the drain is increased, accelerating the rate of limestone dissolution and, as a result, increasing the concentration of alkalinity, which can reach up to 275 mg/L. (Hedin *et al.*, 1994). The mining industry has taken note of the concept of producing alkalinity using anaerobic limestone treatment systems. In acid drainage, buffering is introduced in the form of alkalinity (Barnhisel *et al.*, 2000b; Santomartino and Webb, 2007; Skousen *et al.*, 2017).

Once constructed, the use of ALDs to mine water requires little maintenance. Mine water is held in a drain that is impervious to both oxygen and water and is allowed to course through a bed of limestone gravel. Plastic bottom liners and a clay cover are typically used to construct the bed. The drain's dimensions range from narrow (0.6 to 1.0 m) to wide (up to 20 m diameter, usually about a metre deeper, with the length of about 30 m) (Hedin *et al.*, 1994).

The Tennessee Department of Health and Environment was the first to propose ALD for coal mine water treatment. This has recently been established at various sites for the treatment of both coal and metal sulphide mine water (Gusek, 1995; Gazea *et al.*, 1996; Barnhisel *et al.*, 2000b; Santomartino and Webb, 2007). ALDs are typically used as stand-alone passive treatment

systems, or together with aerobic wetlands and/or compost wetlands for subsequent metal removal. ALDs have been reported to enhance the performance of constructed wetlands that previously had performed poorly (Hedin et al., 1994).

2.5.1.2.2.2. Open Limestone Channels

According to Santomartino and Webb (2007), open limestone channels (OLCs), also known as oxic limestone drains (OLDs), are open channels containing coarse limestone for treatment of contaminated water. These systems are more useful when AMD must be transported over a long distance before or during treatment via an open channel lined with calcium-rich limestone (Cravotta and Trahan, 1999). OLCs can be built in two ways. The first method involves a drainage trench packed with limestone and polluted mine drainage (Ford, 2003). The limestone raises the alkalinity of the system and promotes precipitation of ferric as well as aluminium hydroxides. The second method involves directly dumping limestone fragments into a contaminated stream. The limestone dissolves, adding alkalinity to the polluted mine water and raising the pH (Rose and Lourenso, 2000).

OLCs are most effective for AMD remediation when the concentrations of iron (Fe) and aluminium (Al) are between 10 and 20 mg/L and the acidity is less than 90 mg/L as calcium carbonate (CaCO_3). Furthermore, studies have shown that the generation of alkalinity is directly proportional to the acidity of the influent. This means that the higher the acidity of the influent, the greater the alkalinity generation. A steep topography is required in OLC systems to generate the required aeration and to prevent metal hydroxide coating of limestone (Skousen et al., 2019). Taylor et al. (2005) reported field results from a variety of locations, demonstrating that OLCs are capable of removing approximately 70% of Fe, 40%-50% Al, and 10%-20% Mn from solution.

In practice, increasing channel length/residence time compensates for the slow reaction rate of armoured limestone. OLCs are used for long-term treatment in appropriate cases. (Skousen et al., 2017). These systems require continuous maintenance in order to ensure a maximum lifecycle and efficiency. This is because their performance is reduced with Fe-armouring. Therefore, the OLCs perform best when incorporated with other passive treatment systems (Cravotta and Trahan, 1999).

2.5.1.2.2.3. Limestone Leaching Beds

Limestone Leaching Beds (LLBs) are typically small basins laden with coarse limestone, with 2-10 cm diameter sized lumps. The systems are constructed in such a way that water can have a residence time of at least 30 minutes in the LLB (Skousen et al., 2017, 2019). These beds are

also utilized in the pre-treatment of AMD with a pH of less than 3.0 and dissolved oxygen (DO) of less than 1mg/L in both upward and downward flow strategies (Skousen et al., 2017).

2.5.1.2.2.3. Emerging Passive Treatment Systems

2.5.1.2.2.3.1. Phytoremediation

Environmental contaminants are removed, contained, or rendered harmless using florae and the microbiota associated with them, and agronomic and techniques soil modifications, according to Wong (2003). This technology has recently gained attention as a novel, cost-effective alternative to more traditional treatment methods used at hazardous waste sites (Salt et al., 1995, 1998; Chaney et al., 1997; Chaudhry et al., 1998; Meagher, 2000; Prasad and Freitas, 2003; Pulford and Watson, 2003; Alkorta et al., 2004; Gardea-Torresdey et al., 2005a). The branch of phytoremediation used to treat contaminated soil includes subcategories such as phytoextraction/phytomining, phytostabilization, rhizofiltration, and phytovolatilization.

Phytoremediation is most effective when combined with other treatment methods for low and moderate concentrations of contamination, or as a final polishing step in site remediation. This is because high levels of contamination can be lethal to plants and inhibit their growth (U.S. EPA, 2006).

Before implementing phytoremediation technology, the following factors must be considered (U.S. EPA, 2006):

- Depth of the contamination requiring treatment that must be within the range of depth of plant root growth;
- To be treated, the root zone must be in contact with contaminants;
- Possible bioconcentration of contaminants up the food chain; and
- Monitoring of the fate of contaminants within the plants.

A number of sites have fully implemented phytoremediation (U.S. EPA, 2006).

2.5.1.2.2.3.2. Phytoextraction/Phytomining

If metal must be recovered, phytoextraction or phytomining, as defined by the ITRC (2009), is the uptake of pollutants by plant roots and translocation within the plants. The notion of using plants to clean up polluted areas is not new, and there is no specific source to which it can be traced (Blaylock and Huang, 2000). Metals can accumulate in plants via two methods: continuous/natural and chemically improved phytoextraction (Salt et al., 1998). Continuous

phytoextraction is dependent on certain plants' natural capability to gather, translocate, and resist high metal concentrations throughout the growth cycle. Chemically enhanced phytoextraction is based on the use of chelating agents in the soil to stimulate metal uptake by the plants (Garbisu and Alkorta, 2001). The use of fast-growing trees such as *Salix* or *Populus* species has recently been proposed as a third method for metal extraction (McGrath et al., 2001).

Various plants were suggested for use in water treatment about 300 years ago, according to Hartman (1975). *Thlaspi caerulescens* (pennycress) and *Viola calaminaria* (viola) were the first plant species documented at the end of the nineteenth century as accumulating high levels of metals in leaves and containing elevated concentrations of zinc when growing on soils enriched in this element (Salt et al., 1998).

If there are only a few plants that can do this, climate, soil conditions, and ground/surface water are all a detriment to species selection. This tool is typically used to treat inorganic contaminants such as metals like zinc (Zn), lead (Pb), manganese (Mn), copper (Cu), mercury (Hg), molybdenum (Mo), cadmium (Cd), silver (Ag), cobalt (Co), chromium (Cr), and nickel (Ni), metalloids selenium (Se), arsenic (As), radionuclides uranium (²³⁴U, ²³⁸U) plutonium (²³⁹Pu), caesium (¹³⁷Cs) strontium (⁹⁰Sr), and nonmetals boron (B). For phytomining, plants must be hyperaccumulators. More than 300 species hyperaccumulate Ni, including 26 species of Co, 24 species of Cu, 19 species of Se, 16 species of Zn, 11 species of Mn, one species of Tl, and one species of Cd (Barceló and Poschennieder, 2003). Consideration should be given to if the resulting vegetation will be detrimental to local faunas.

Plants like Indian mustard, hybrid poplars, pennycress, and alyssum sunflower can be used in phytoextraction. Because they have shallow root systems and grow slowly, these plants are most effective in the top 30 cm of soil. However, Indian mustard can be genetically modified to grow in contaminated soil with more biomass, allowing it to hyperaccumulate selenium in less time than unmodified Indian mustard (Adams et al., 2000)

Phytoextraction is more cost effective than other remediation techniques (Glass, 2000; U.S. EPA, 2000). Furthermore, there may be an economic benefit from metal recovery from the ashes of some hyperaccumulators' burned material (Chaney et al., 1997).

The main disadvantage of this technique is that it can only be applied to remediate low to moderately contaminated sites and requires a long duration (Robinson et al., 1998; Blaylock and Huang, 2000; Vassilev et al., 2004).

2.5.1.2.2.3.3. Phytostabilization

The ITCR (2009) defined phytostabilization as "the immobilization of contaminants in soil via adsorption and accumulation by roots, adsorption into roots, or precipitation within the root zone plants, and the use of plants and plant roots to prevent contaminant migration via wind and erosion, leaching, and soil dispersion." The advantages associated with this technique include low cost, no soil removal requirements, enhances ecosystem restoration, and does not require any disposal of hazardous materials or biomass (ITCR, 2009). Nonetheless, there are drawbacks to phytostabilization; the contaminants will persist. Additionally, fertilization or soil modification may be required (ITCR, 2009). The phytostabilization technique supplies fertilizing agents and aids in the establishment of microorganisms.

2.5.1.2.2.3.4. Rhizofiltration

Rhizofiltration is the process of removing contaminants via plant roots from solutions through biogeochemical processes, namely, adsorption or precipitation or absorption (ITCR, 2009), which is accomplished by rhizosphere microorganisms (Wong, 2003). Because this technique is used in water, plants on a floating platform are either aquatic or terrestrial (Phytoremediation Team, 2009). The presence of plant roots improves conditions for bioremediation by increasing soil aeration and regulating soil moisture. By physically removing the plants, the contaminants can also be physically removed. This technique has been shown to be very effective in the remediation of extracted groundwater, surface water, and wastewater with low pollutant concentrations (Salt et al., 1995).

Rhizodegradation is advantageous because contaminants are actually broken down rather than transported, eliminating the need for harvesting. This technology has some drawbacks, such as the fact that pH control is required. In addition, influent concentrations and flow rate regulation are required. Plants, particularly terrestrial plants, may need to be grown and relocated to their new location (ITCR, 2009).

According to Salt et al. (1995), plants used in rhizofiltration can remove up to 60% of their dry weight in toxic metals. This technology is useful for removing metals such as lead (Pb), zinc (Zn), cadmium (Cd), copper (Cu), nickel (Ni), and chromium (Cr), as well as radionuclides such as cesium (Ce), strontium (Sr), and uranium (U) (U.S. EPA, 2000; ITCR, 2009). Many large root plant species, including sunflower (*Helianthus sp.*), rye (*Elymus sp.*), corn (*Zea mays*), and Indian mustard (*Brassica juncea*), have shown success in rhizofiltration process (Salt et al., 1995). Many aquatic species are capable of removing metals from water. Water hyacinth (*Eichhornia*

crassipes; Kay et al., 1984; Zhu et al., 1999), pennywort (*Hydrocotyle umbellata*; Dierberg et al., 1987), and duckweed (*Lemna minor spp.*; Mo et al., 1989) are examples.

2.5.1.2.2.3.5. Phytodegradation

Phytodegradation comprises the uptake of contaminants and breaking them down through metabolic processes within the plant (ITCR, 2009). Aside from the plant roots, contaminants can also be broken down in the soil by enzymes and other compounds produced by plant tissues. Phytodegradation is applicable to organic contaminants and their uptake is influenced by their hydrophobicity, solubility, and polarity (U.S. EPA, 2006). After absorption by the plant roots, moderately hydrophobic and polar compounds are more likely to be taken up (Adams et al., 2000). Contaminants such as chlorinated solvents, insecticides, PCP, PCBs, and munitions may be removed through phytodegradation (U.S. EPA, 2006).

2.6. Waste management in South Africa

South Africa has developed a wide range of legislative measures aimed at improving the quality of the environment. These are some examples:

- Act 85 of 1993 on Occupational Health and Safety; To provide for the health and safety of persons at work, as well as the health and safety of persons in connection with the use of plant and machinery; to protect persons other than persons at work from hazards to health and safety arising from or in connection with the activities of persons at work; to establish an advisory council for occupational health and safety; and to provide for matters related thereto.
- Act 108 of 1996, South African Constitution; According to Chapter 2 section 24 of the south African Constitution, Everyone has the right to an environment that is not harmful to their health or wellbeing; and to have the environment protected, for the benefit of present and future generations, through reasonable legislative and other measures that prevent pollution and ecological degradation; promote conservation; and secure ecologically sustainable development and use of natural resources while promoting justifiable economic and social development.
- Act 36 of 1998, National Water Act; The National Water Act 36 of 1998 seeks to fundamentally reform the law governing water resources, repeal certain laws, and address related issues.
- Act 107 of 1998, National Environmental Management Act; The National Environmental Management Act 107 of 1998 intends to provide for cooperative, environmental governance by establishing principles for environmental decision-making, institutions that

will promote cooperative governance, and procedures for co-ordinating environmental functions exercised by state organs; and to provide for matters related thereto.

- Act 28 of 2002 on Mineral and Petroleum Resource Development; The Mineral and Petroleum Resources Development Act 28 of 2002 aims to provide for equitable access to and sustainable development of the nation's mineral and petroleum resources, as well as to address related issues.
- The Act on Air Quality (Act 39 of 2004); Intends to do the following: to reform the law governing air quality in order to protect the environment by providing reasonable measures for the prevention of pollution and ecological degradation, as well as for securing ecologically sustainable development while promoting justifiable economic and social development; to provide for national norms and standards governing air quality monitoring, management, and control by all spheres of government; to provide for specific air quality measures; and to provide for matters incidental to air quality monitoring, management, and control.
- The Waste Act of 2008, National Environmental Management (Act 59 of 2008); An Act to reform the waste management law in order to protect health and the environment by providing reasonable measures for the prevention of pollution and ecological degradation and for ensuring ecologically sustainable development; to provide for institutional arrangements and planning issues; to provide for national norms and standards for regulating waste management by all spheres of government; and to provide for specific waste management measures.

2.7. Geochemical modelling

Many studies involving geochemical modelling have been conducted since the 1960s. Environmental reactions that affect water quality frequently occur at temperatures ranging from 0 to 100 °C. Evaporation, dissolution and precipitation of minerals, dilution or mixing of water bodies, speciation and complexation of organic and inorganic matter, ion exchange, adsorption or desorption of solute, oxidation-reduction of constituents, reaction with or production of gases, and reactions catalysed by light or biological organisms are examples of processes of interest (Nordstrom, 2007). Geochemical modelling attempts to simulate all of the aforementioned processes have been undertaken by employing either mass action or mass balance equations. Geochemical modelling, on the other hand, does not account for transport and can be conceptualized as a stirred tank reactor in which the distribution of chemically reactive species is calculated mathematically. Modelling of the transport of chemical constituents down a flow path is included in coupled transport and reaction models (Crawford, 1999).

Inverse models and reactive path models are two types of geochemical modelling. Geochemical reaction models include speciation-solubility reactions.

2.7.1. Speciation-solubility models

The speciation-solubility models define the distribution of a stable species in the system as well as calculating mineral saturation states (Zhu and Anderson, 2002). To determine the species spectrum and solve the equations involved, most of these models assume local equilibrium (van der Lee and De Windt, 2001). Chemical equilibrium can be solved by minimizing a system's Gibb's free energy or using mass action equations and equilibrium constants (Crawford, 1999).

The Mixed-Solvent Electrolyte model, a comprehensive thermodynamic model, has been used to calculate phase equilibria and chemical speciation in selected aqueous actinide systems (Wang et al., 2017). Jimenez et al. (2022) investigated the speciation and solubility of sodium molybdate (Na_2MoO_4) in water of temperature ranging between zero and 110 °C. Metals originating from active gold mining tailings storage facilities (TSFs) in the Witwatersrand Basin's evolution and transport were assessed using this technique (Camden-Smith et al., 2014) and Drapeau et al. (2021), investigated the extraction of lead from waste at two typical mining sites, namely, Zeida and Mibladen, two non-operational former Pb-Zn mines in Morocco's Moulouya region.

2.7.2. Inverse modelling

Inverse modelling or mass balance modelling, can provide a list of possible reactions that occurred during the transformation of a combination of initial water samples into a final composition if the composition of water samples along the same flow path and the mineral assemblages of the rock through which the water flows are known (Nordstrom, 2007). Inverse modelling does not take into account thermodynamic properties or kinetic constraints, instead relying on mass balance equations (Zhu and Anderson, 2002).

This technique is primarily used in groundwater modelling (e.g. Slimani et al., 2016) but it can also be used for surface water modelling (e.g. Peikam and Jalali, 2016). Ibrahim and El-Naqa (2018), used inverse geochemical modelling to define the chemical reactions responsible for the salinization of the Azraq basin along the groundwater flow path. Stour et al. (2022) used inverse geochemical modelling to investigate the hydro-geochemical processes that govern the evolution of surface and groundwater resources in Egypt's El Fayoum depression. Camden-Smith and Tutu (2014) investigated the release mechanisms of pollutants from an abandoned mine tailings storage facility near Johannesburg, Witwatersrand goldfield, using inverse geochemical

modelling. Inverse geochemical modelling was also used to assess the rainwater leachability of metals from gold mine tailings (Grover et al., 2016).

2.7.3. Forward modelling

Forward modelling is especially useful in performance testing or design studies, where the composition of a solution is calculated after a reaction or equilibrium is reached (Crawford, 1999).

Thermodynamic models use equilibrium constraints and are assumed valid for homogeneous reactions with sufficient residence time to reach equilibrium. Heterogeneous reactions, on the other hand, such as mineral dissolution and precipitation, as well as their adsorptive properties, are frequently kinetically controlled, and models should ideally be accustomed accordingly. The geochemical modelling had been applied for characterization of gold mine tailings in the Central Rand Goldfield (Netshiongolwe, 2018). Wu (2021), used geochemical modelling to study gold tailings storage facilities of the West Rand Basin, Witwatersrand goldfield.

2.7.4. Reaction path modelling

In this modelling type, the reaction progress is monitored in small increments. The species distribution and saturation indices are calculated at each step and equilibrium is maintained by the dissolution or precipitation of defined minerals (Crawford, 1999). These reactions are used to describe forward reactions in a water system, such as the addition of gas or minerals. (Zhu and Anderson, 2002).

The quantitative assessment of uranium distribution and modeling of its geochemical speciation in gold mine polluted land in South Africa was carried out by Tutu et al. (2003). Marini (2013) discussed the theoretical aspects and applications of reaction path modelling in predicting water-rock interactions. Apallaro et al. (2011) used reaction path modelling to investigate the release and fate of elements in the metabasalt-serpentine shallow aquifer.

2.7.5. Coupled transport and reaction modelling

A reactive transport model is a hybrid of a forward geochemical reaction and a hydrologic model that is used to depict geochemical changes over time along various dimensional flow paths (Crawford, 1999). According to Charlton and Parkhurst (2002), reactive transport modelling can be used to study the migration of contaminants such as metals, radionuclides, and organic compounds, as well as to simulate natural and artificial processes for aquifer remediation and laboratory column experiments.

To account for the transport of chemical species produced by microbial processes, a coupled transport/reaction model for copper was developed (Liu and Neretnieks, 2009). A simplified solid mechanics model was developed for the local variation of permeability and porosity as a function of local bed deformation (Salloway et al., 2013). To better understand the transport and reactions of trace metals as they move through a catchment from upland sources to downstream areas and water bodies, a spatially distributed trace metal transport and transformation model was developed (Suie et al., 2021).

CHAPTER THREE

3. Materials and Methods

3.1. Sampling and site description

The research was carried out at specific sampling points along the Sabie River catchment in Mpumalanga Province.

There are abandoned mines situated in the upstream of Sabie River basin that include the Nestor, Glynn's Lydenburg, and Rietfontein Mines. In order to assess the probability of the metal species dispersion from mine tailings storage facilities (MTSFs) into the Sabie River catchment, various sample mediums were used. The samples were classified as follows: (i) sediments eroded from (MTSFs), (ii) efflorescent crusts developed on the surfaces of the MTSFs, (iii) seepage from MTSFs, (iv) soils surrounding MTSFs, (v) soils away from mining activities, (vi) stream sediments from the Sabie River and connected streams and (vii) surface water. In addition, sediments and water samples were taken along the mine watercourse (Nestor and Rietfontein). These samples were considered the most representative of the surface environment and are generally used in environmental geochemical surveys. Sampling was done seasonally, commenced in November-December 2019 (wet season), and was repeated in July-August 2020 (dry season); December 2020 (wet season); May-June 2021 (dry season); September-October 2021 (wet season); June-July 2021 (dry season); February-March 2022 (wet season).

All the sample sites were located by GPS and geo-referenced to UTM coordinates (Table 2).

Table 2 Location of sampling sites

Sample ID	Latitude	Longitude	Name
NS01	-25.07640	30.79641	Nestor MTSF
GLO1	-25.09921	30,77105	Glynn's Lydenburg MTSF
SB01	-25.10180	30.75148	Sabie River
SB02	-25.09328	30.76915	Sabie River
SB03	-25.09139	30.79383	Sabie River
SB04	-25.07399	30.85084	Sabie River
SB05	-25.02999	31.01396	Sabie River
SB06	-25.02865	31.05386	Sabie River

SB07	-25.03009	31.12361	Sabie River
SB08	-25.01968	31.21520	Sabie River
SB09	-24.98432	31.28106	Sabie River
SB10	-25.11795	30.72392	Lone Creek River
SB11	-25.09743	30.76707	Malieveld
SB12	-25.08810	30.77848	Klein Sabie River
SB13	-25.06341	30.79114	Klein Sabie River
SB14	-25.09753	30.80553	Spitskop River
SB15	-25.09382	30.81434	Rietfontein drainage
SB16	-25.07068	30.90130	Goldstream
SB17	-25.03235	31.02239	Sabana River
SB18	-25.00851	30.92504	Mac-Mac River
SB19	-25.00318	30.92422	Sunlight River
SB20	-25.03386	31.15503	Nkambeni/Noord Sand
SB21	-24.98270	31.24733	Bega River
SB26	-25.00336	30.92363	Soil away from mines
SB27	-25.12038	30.72363	Soil away from mines
SB28	-25.08709	30.78212	Soil away from mines
SB29	-25.06496	30.87818	Soil away from mines

3.2. Sampling procedure

3.2.1. Tailing sampling

Data generated from Lusunzi (2018) formed the baseline to this study. The two MTSFs in the Sabie Goldfield, namely, Nestor and Glynn's Lydenburg were mapped and characterised, based on their acid-base accounting, geochemistry and mineralogy. In addition, three samples were collected seasonally from tailings eroded from the Nestor MTSF (NS01; Fig. 6A). These tailings were traced downstream of the MTSF and five additional samples were collected in the middle (NS02; Fig. 6B) and before the confluence with the Klein Sabie River (NS03; Fig. 7). Grab sampling was done using a scoop and the samples were placed in polythene plastic bags that

were tightly sealed with cable ties. Additional tailings were also taken from the adjacent Glynn's Lydenburg MTSF (GL00 and GL01).



Figure 6 Photographs showing the sediments that are eroded from the Nestor MTSF.



Figure 7 Photograph showing the sediments that are eroded from the Nestor MTSF before the confluence with the Klein Sabie River.

Two bulk samples were collected from the Nestor MTSF (AG) and the Glynns Lydenburg MTSF (AN) respectively. About 20 kg composite tailings samples were collected from the base of the MTSFs and placed in plastic buckets that were tightly closed and transported to the North-West University laboratory for analyses. The samples were dried in a drying stove at 40°C for 24 hours and were stored in airtight containers to limit the degree of pre-oxidation as proposed by the ASTM D5744-18 standard. The samples were sieved using a 200-mesh sieve to obtain samples of less than 75 µm particle size distribution to be able to conduct the following tests (Stewart *et al.*, 2006). Two mixtures were prepared using the samples from the Nestor MTSF (AG) and the Glynns Lydenburg MTSF (AN). The mixtures contained 25 wt. % AN and 75 wt. % AG was prepared and is referred to as MIX25. The second mixture contained 50 wt. % AN and 50 wt. % AG was prepared and is referred to as MIX50. MIX25 and MIX50 were subjected to the same static test (ABA, NAG and ABCC) that was used to estimate the acid-generating probabilities of samples AG as well as AN.

3.2.2. Efflorescent crusts sampling

Two samples were collected from each mine tailings storage facility seasonally, namely, Nestor (Fig. 8A; EN01) and Glynns Lydenburg (Fig. 8B; EG01) in the wet season (February 2018) and during the dry period (August 2020). The efflorescent crusts developed on the sides of MTSFs were carefully collected and tightly sealed in polyethylene plastic bags using cable ties (Fig. 9).



Figure 8 Efflorescent crusts sampling in the Nestor and Glynns Lydenburg MTSFs.

3.2.3. Soil sampling

The soil samples were taken near the Nestor and Glynns Lydenburg mine tailings storage facilities in February 2019 as well as November 2021 in order to assess potential of metal species dispersion. In addition, four samples were collected in the dry season in areas not influenced by mining activities (June 2021) and they were used as background reference samples.

Generally, soils contain various layers that are referred to as soil horizons. There is variation in terms of properties and elemental distributions together with thickness, which can range from few millimetres to sometimes meters. It is crucial to be consistent in terms of the soil horizon being considered when comparing the composition of different soils. Therefore, the B-horizon was considered for this study. Soil samples of approximately 5 kg were randomly collected near the mine tailings storage facilities as well as away from these mine impoundments (Fig. 9). Organic debris was removed from the surface samples prior to collection, and placed in double plastic bags with duplicate labels of the sample number. After collection of the samples, precise coordinates (WGS84) of the localities were saved with the sample number. All information, sample number, coordinates and general site description, was updated and saved daily on spreadsheets for future use.



Figure 9 Soil sampling was conducted along the Sabie River system.

3.2.4. Stream sediment sampling

In total, 21 composite stream sediment samples (SB01 to SB21) were randomly collected at various distances from the mine tailings storage facilities (MTSFs), agricultural area, industrial area, and commercial/urban areas. Sampling took place in November and December 2019 to

represent the summer season, as well as in July and August 2021 to represent the winter season. Samples of stream sediment were taken along the Sabie River system, upstream, middle, and downstream, to evaluate their potential influence on metal distribution in receiving water. The top part of the sediments (0 to 10 cm) were collected using a shovel and plastic bucket to homogenize the samples collected, and then placed in sample bags that were tightly sealed to prevent the infiltration of oxygen as well as preservation of biological or chemical equilibria (Fig. 10).



Figure 10 Photographs showing where stream sediment sampling in the Sabie River system, was conducted.

A handheld GPS was used to define the position of the predetermined sample locations. Metal concentrations in sediments are not uniformly distributed across grain sizes, so the finer-grained clay-size fraction (<75 μm) with high metal concentrations due to large surface areas present, as well as the existence of metal oxide and organic layers on mineral surfaces that tend to sorb metals, was chosen for analysis.

3.2.5. Water sampling

Water samples were also taken before the stream sediment at the same sites and drainage along the mine sites to assess the prominence of AMD from the MTSF. Two mine sites were considered for this study, namely, Nestor Mine (seepage from the mine storage facility; Fig. 11A) and the Rietfontein Mine (water decanting from the mine adit; Fig. 11B). There was no seepage/leachate observed near/around the Glynn's Lydenburg mine tailings storage facility.

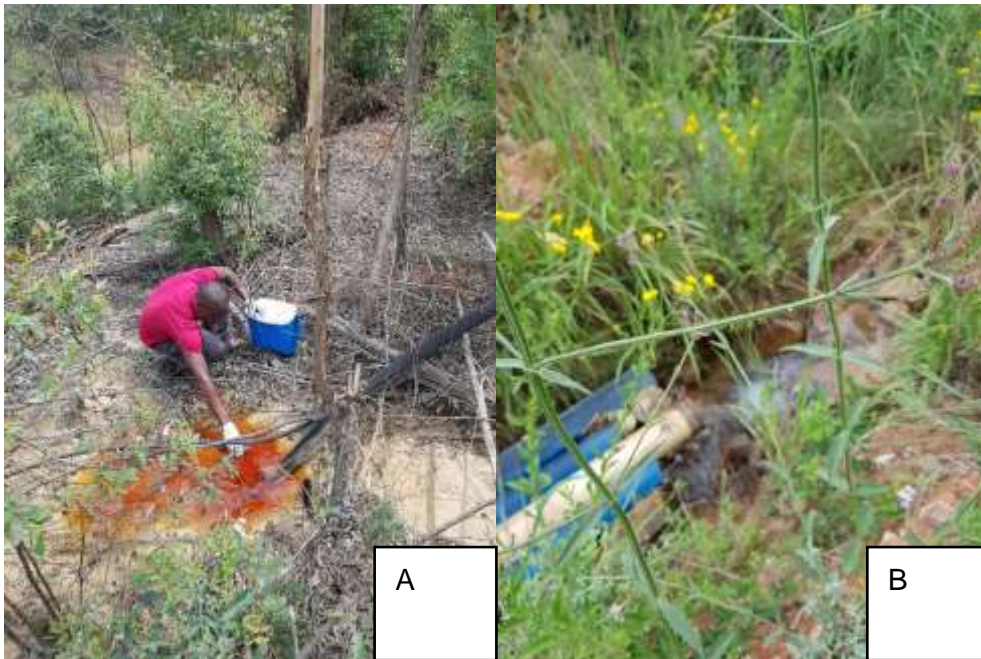


Figure 11 Sampling conducted on the seepage from the Nestor MTSF (A) and (B) photograph showing the water decanting from the Rietfontein mine adit.

Physico-chemical parameters of the collected samples were analysed to determine the speciation of pollutants and impact of dispersion potential due to tailings storage facilities. Onsite analysis of physico-chemical parameters, namely, temperature ($^{\circ}\text{C}$), redox potential (Eh), electrical conductivity (EC), and pH were done using a Wissenschaftlich-Technische-Werkstätten (WTW) multi 3430 measurement meter in accordance to the South African National Standard (SANS) 5011 method (Fig. 12). Sampling was done according to standard procedures (APHA, 1998). Before field analysis, the probes were calibrated with reference buffer solutions. Water samples were taken in 500 mL polyethylene bottles that had been pre-cleaned. The samples had been filtered through 0.45 μm filters to eliminate all microorganisms as well as suspended sediments before being prepared for elemental (major, minor, and trace element) and anion studies. The alkalinity and acidity levels of the water samples was also tested, with the samples for alkalinity testing not being filtered. The elemental analysis samples were collected in acidified plastic bottles and preserved with nitric acid (in order to prevent oxidation or reduction of redox-sensitive species). Samples were immediately placed in a cooler (at 4°C) for transportation and storage.



Figure 12 Onsite water analysis was conducted in the Sabie River system.

3.3. Analytical methods

X-ray fluorescence (XRF), X-ray diffraction (XRD), as well as four-stage sequential extraction was used to analyse the collected tailings and stream sediment samples. Analytical techniques such as inductive coupled plasma-mass spectrometry (ICP-MS) and ion chromatography (IC) were used to analyse water samples. All experiments were carried out in triplicate, with the results reported as mean values.

3.3.1. Acid-Base Accounting

Established in 1974 to assess coal wastes, the acid-base accounting (ABA) of a waste material is the balance between its acid production and acid consumption properties. In 1978 these test procedures were modified (Sobek et al., 1978). This concept is very important in terms of decision making regarding the storage and treatment of mine wastes. The acid production potential (APP) is calculated as $APP = 31.25 \times \text{percent sulphur}$, with the assumption that two moles of acid are produced for every mole of sulphur. In modified ABA, the APP is calculated from the sulphide sulphur concentration (Lawrence, 1990).

By first determining the acid strength to be used in the next step, a simple fizz test is used to determine the neutralization potential (NP). Based on this data, hydrochloric (HCl) acid is added to the sample and boiled until the reaction ends. The subsequent solution is then back titrated to pH 7 with sodium hydroxide (NaOH) to define the quantity of acid used up in the reaction between the sample and HCl. Modified ABA determines NP by performing a 24-hour acid digestion at room

temperature and back titrating using NaOH to determine the acid consumed to an end point of 8.3. The net neutralizing potential (NNP) is a measurement of the difference between the neutralizing and acid forming potentials. It is calculated by subtracting the APP from the NP and can be positive or negative. NNP values less than 20 (kg CaCO₃/ton) are likely to form acid, NNP values greater than 20 are unlikely to form acid, and NNP values between -20 and 20 are uncertain in terms of acid potential (Lapakko, 1993b).

The ABA test assumes that all of the sulphur in the sample is reactive, which does not account for the occurrence of non-reactive sulphur minerals such as gypsum. Modified ABA assumes that sulphur present as sulphate does not produce acid. If acid-producing sulphate minerals such as jarosite are present, this may underestimate available APP.

3.3.2. X-ray fluorescence methods

Generally, X-ray fluorescence (XRF) is the emission of characteristic or secondary X-rays from a material that has been excited by bombardment with high energy electrons or other X-ray or -ray photons. If the incident particle has enough energy, it can knock an orbital electron out of the inner shell of the target atom. Environmental analysis has grown dramatically in the last decade, owing primarily to the need to assess the quality of our environment, which necessitates the availability of reliable analytical data (Khalid et al., 2015).

The solid samples (mine tailings, soil, and stream sediment) were geochemically analysed for elemental composition by XRF at the Council for Geoscience using a PANanalytical Zetium XRF spectrometer. Major oxides, namely, aluminium oxide (Al₂O₃), magnesium oxide (MgO), iron(III) oxide (Fe₂O₃), manganese oxide (MnO), silica (Si₂O), calcium oxide (CaO), sodium oxide (Na₂O), titanium oxide (Ti₂O), potassium oxide (K₂O), chromium(III) oxide (Cr₂O₃) as well as phosphorus pentoxide (P₂O₅) were analysed on glass disks while trace elements, nickel (Ni), copper (Cu), cobalt (Co), arsenic (As), uranium (U), zinc (Zn), lead (Pb), cerium (Ce), lanthanum (La), gallium (Ga), chromium (Cr), barium (Ba), strontium (Sr), vanadium (V), thorium (Th), Yttrium (Y), scandium (Sc), zirconium (Zr), and Ytterbium (Yb), were analysed on pressed powder pellets.

Milled samples were heated at 1000 degrees Celsius for a minimum of three hours to oxidize the Fe²⁺ and S and to define the loss of ignition (LOI) gravimetrically. One gram of heated sample and 10 g of Claisse flux (49.5% LiBO₂, 49.5% Li₂B₄O₇, and 1% LiBr) were fused at 980 °C to produce homogeneous glass disks. Twelve grams of milled sample and three grams of Licowax were combined, poured into an aluminium cap, and pressed using hydraulic press with a pressure of about 25 tons to produce a stable powder briquette.

The major and trace element calibrations on the XRF spectrometer were set up using optimum optical combinations for each selected element and corrected for background, matrix and inter-element interferences where applicable. Reference materials were used to set up regression lines between measurements and certified concentration and to verify the calibrations.

3.3.3. X-ray diffraction methods

The XRD measurements were carried out on BRUKER D8ADVANCE instrument equipped with 2.2kW Cu long fine focus tube(Cu K α , $\lambda=1.54060$) and a sample changer with 90 positions. The instrument is outfitted with a 3.7° active area LynxEye detector. Samples were scanned from 2 to 70° 2 θ CuK α radiation with step size of 0.02° 2 θ steps size/0.5 sec and generator settings of 40 kV and 40mA. A representative sample of the soil material was crushed and pulverized to fine powder of about 20 μ m in size for bulk analysis. To ensure random orientation, a sub-sample was pressed into a shallow plastic sample holder against rough filter paper. The phase identification was performed using the BRUKER DIFFRACPlus evaluation program. Semi-quantitative approximations were used to determine phase concentrations (with a 5% accuracy) using the RIR (Reference Intensity Ratio) method and relative peak heights/areas proportions (Brime, 1985).

3.3.4. Sequential extraction procedure

To estimate binding forms of metal species in solid samples, the European Standard, Measurement and Testing (SM&T), formerly the BCR (Community Bureau of Reference of the European Commission), proposed sequential extraction. All extractions were performed using a mechanical shaker for 16 hours (overnight) at room temperature (25 °C). The extract was then separated from the solid residue by centrifugation at 3000 rpm for 20 minutes, and the supernatant liquid was transferred into a polyethylene volumetric flask. The residue was washed with 20 mL of deionized water, shaken for 15 minutes on the end-over-end shaker, and centrifuged at 3000 rpm for 20 minutes. As a result, the supernatant was decanted.

A four-stage sequential extraction was done following the procedures described by Nemati et al. (2011) and Takalio et al. (2001). The sequential extraction procedure was as follows:

- The first step (exchangeable metals) is as follows: 1 g of dry sediment was treated with 40 mL of 0.11 M acetic acid. The mixture was shaken at 22°C for 16 hours at a speed of

250 rpm. Centrifugation at 3800 rpm for 20 minutes separated the extract from the solid phase. Prior to analysis, the supernatant liquid was decanted into a 50 mL polypropylene centrifuge tube and stored in a refrigerator at 4 °C. The residue was washed with 20 mL of double-distilled water, shaken for 15 minutes, and centrifuged for 20 minutes at 3800 rpm. The second supernatant liquid was discarded with no residue loss (Nemati et al., 2011).

- Second step (metals bound to iron and manganese oxides): Metals bound to iron and manganese oxides were extracted by adding 40 mL of 0.1 M hydroxyl ammonium chloride ($\text{NH}_2\text{OH}\cdot\text{HCl}$) to the first step residue (adjusted to pH 2 with 2 M nitric acid). After shaking the mixture for 16 hours at 22 °C at a speed of 250 revolutions per minute, it was centrifuged for 15 minutes and decanted as described in step 1. Before proceeding to the next step, the residue was washed with 20 mL distilled water, centrifuged, and the supernatant discarded as described in the first step (Nemati et al., 2011).
- Third step (metals bound to organic matter and sulphides): small aliquots of 10 mL of 8.8 M hydrogen peroxide (pH 2 to 3) were carefully added to the centrifuge tube residue. The tube was loosely covered (to avoid significant hydrogen peroxide loss), and the residue was digested at room temperature for 1 hour with occasional shaking. The contents of the tube were digested continuously for 1 hour at 85 °C in a water bath with occasional shaking for the first 30 minutes, and the volume was reduced to 2 to 3 mL by further heating the uncovered tube. After adding 10 mL of hydrogen peroxide (pH 2-3) to the tube, it was heated to 85 °C and digested for 1 hour before the volume in the uncovered tube was reduced almost to dryness. After cooling, 50 mL of 1 M ammonium acetate (pH 2 adjusted with concentrated nitric acid) was added to the residue and shaken for 16 hours at 22 C at 250 rpm. The extract was separated from the solid phase using centrifugation and decantation, as previously described, and stored at 4 degrees Celsius (Nemati et al., 2011).
- For metals that were insoluble in the previous steps, the residue from the third step was digested with aqua regia ($\text{HNO}_3 + 3\text{HCl}$). To accomplish this, 6 mL of distilled water was added to the same residue, followed by 15 and 10 mL of aqua regia solution. The residue was evaporated to near dryness in a water bath after each aqua regia solution was added. The extract was filtered through filter paper after a small amount of 1 M nitric acid solution was added to the last residue in the centrifuge tube (Tokalio et al., 2001).

3.3.5. Ion Chromatography and Inductively Coupled Plasma-Mass Spectrometry

The IC technique is frequently employed to determine the concentrations of common anionic components (U.S. EPA, 1986). A sequence of columns were filled with ion-exchange resins separate anions from solution and combine them with hydrogen to form acids. Using a conductivity detector, the electrical conductivities of various acids, which are varyingly strong electrolytes from which anions concentrations can be calculated, were measured.

An inductively coupled plasma (ICP) is a type of plasma source that gets its energy from electric currents generated by electromagnetic induction, or time-varying magnetic fields. Inductively Coupled Plasma Mass Spectrometry (ICP-MS) is an elemental analysis technique. The resulting instrument is capable of detecting trace multi-element analysis, often at the part per billion or part per trillion or Nano grams level. ICP-MS has been widely used over the years, with applications in a variety of fields including drinking water, wastewater, natural water systems/hydrogeology, geology and soil science, mining/metallurgy, and food sciences (U.S. EPA, 1986; Ammann, 2017).

The ICP-MS analysis was done using the Agilent 7500ce with Octopole Reaction System. Based on calibration curves with standard solutions made from a commercial stock solution, element concentrations were quantified. The ICPMS method was validated by analyzing the water reference material NIST 1643e before the analysis of unidentified samples. Every ten samples were run through the control material throughout the study to guarantee analytical precision.

ICP-MS has a number of significant advantages, including extremely low detection limits for a wide range of elements. Some elements can be detected at part per trillion levels, while the majority can be detected at part per quadrillion levels. Table 3 below lists some of the most common detection limits for each element. The ICP-MS can determine elements with atomic masses ranging from 7 to 250. This ranges from lithium (Li) to uranium (U). Because of the abundance of argon in the sample, some masses, such as 40, are prohibited. Other regions that may be blocked include mass 80 (due to the argon dimer) and mass 56 (due to ArO), the latter of which greatly hinders Fe analysis unless the instrumentation is equipped with a reaction chamber (Batsala et al., 2012).

Table 3 Detection limits for some selected elements

Element	Detection limit (ppt)
U	<10
Cd, Au, Sb	10-50
Pb, Se, Co	50-100

Cr, Cu, Mn	100-200
Zn, As, Ti	400-500
Li, P	1-3 ppb
Ca	<20 ppb

ICP-MS spectrometers can analyse both solid and liquid samples. In this study, triplicate aqueous samples were analysed for metals and anions using ICP-MS and Ion IC. The element concentrations were compared to the South African SANS241 (2015) and the World Health Organization (WHO, 2011) water quality guidelines. ICP-MS was used to determine the elements manganese (Mn), arsenic (As), chromium (Cr), cobalt (Co), copper (Cu), aluminium (Al), nickel (Ni), lead (Pb), and iron (Fe) while IC was used for measuring fluorine (F), chlorine (Cl), nitrate (NO₃) and sulphate (SO₄).

3.4. Data treatment: statistics and geochemical modelling

3.4.1. Data analysis

3.4.1.1. Assessment of metal pollution in sediment

Metal concentration in sediments is the result of an addition of metal species originating from natural sources and anthropogenic activities. Therefore, the choice of background values plays a major contribution in the interpretation of geochemical data. In many studies, the average crustal abundance data was used as a reference baseline. The enrichment factor (EF), pollution load index (PLI), and geo-accumulation index (I_{geo}) were used to evaluate the grade of pollution along the Sabie River system because of metal species dispersion. A similar approach was used to characterise sediment pollution (e.g., Han et al., 2017; Muzerengi, 2017). In addition, the chemical index of alteration as described by Nesbit and Young (1982) and Taylor and McLennan (1995) was employed to calculate the degree of weathering in the Sabie River system.

Enrichment factor

The enrichment factor (EF) is an index/indicator that measures the level of contamination in the environment (Barbier, 2016). In this study, EF was calculated to assess the potential anthropogenic input of metal species to the Sabie River catchment. It was calculated as follows:

$$EF = \left[\left(\frac{C_n}{LV} \right)_{sample} - \left(\frac{C_n}{LV} \right)_{background} \right]$$

Where (Cn/LV) sample is the concentration of analysed metal species and one of the following metals: Al/Ca/Fe/Sc/Ti/Rb and (GB/LV) background-reference concentration of analysed metal species (Cn) and one of the following metals: Al/Ca/Fe/Sc/Ti/Rb.

Rb was used as a reference element in this study, and SB18 (Mac Mac River) was chosen as a background because there are no mining activities and little anthropogenic input. Islam et al. (2015c) proposed the ratio of measured concentration to natural abundance as a contamination factor (CF) and classified it into four grades for long-term pollution monitoring of a single metal: low degree (CF<1), moderate degree (1≤CF<3), significant degree (3≤CF≤6), and very high degree (CF≥6).

Geo-accumulation

The geo-accumulation index was used to assess the degree of metal pollution in sediment by comparing it to the baseline metal concentration in the surrounding area. Geo-accumulation index can be defined as follows: $I(geo) = \log_2\left(\frac{C_n}{1.5B_n}\right)$; where Cn is the potential toxic element (PTE) concentration and Bn is the measured concentration of the element in unpolluted sediments (Barbier, 2016).

Other studies, such as (Sarmiento et al., 2011), used a similar approach to characterize sediment pollution (Han et al., 2017). The samples were categorized as unpolluted (Igeo <1) or highly polluted (Igeo > 5).

Chemical index of alteration

The chemical index of alteration (CIA) was used to assess the extent of feldspar weathering in comparison to unaltered rocks from the Sabie catchment area. The CIA is defined as follows: $CIA = (Al_2O_3 / (Al_2O_3 + CaO^* + Na_2O + K_2O)) \times 100$ (Nesbit and Young, 1982), where CaO* is the amount of CaO incorporated in the silicate fraction of rocks. Taylor and McLennan (1995) determined that the average upper continental crust had a CIA value of 47. This means that CIA values between 45 and 55 indicate weak weathering conditions, while values above 100 indicate extreme weathering, which is supported by the presence of typical weathering minerals like kaolinite and gibbsite.

3.4.2. Geochemical modelling

PHREEQC is a computer program that simulates chemical reactions and transport processes in unpolluted or polluted water. In addition, PHREEQC has all of the geochemical model's capabilities, including speciation, batch-reaction, one-dimensional reactive transport, and inverse modelling (Parkhurst and Appelo, 1999).

PHREEQC is frequently used as a geochemical calculation module (server) in other software programs due to its general geochemical speciation and reaction capabilities, as well as its modular input organization. PHREEQC has been used to calculate saturation indices, activities, and pH in water-quality data management software (Scientific Software Group, 2010, AquaChem), to generate predominance diagrams and estimate parameters (Kinniburgh and Cooper, 2010, PhreePlot), and to consider geochemical effects in watershed processes (Hartman et al., 2007, DayCentChem). PHREEQC is most commonly used as a geochemical module for reactive transport models. The unsaturated zone (Jacques and Šimůnek, 2004, HP1; Szegedi et al., 2008, RhizoMath; Wissmeier and Barry, 2010a, 2010b) is a reactive-transport environment (Mao et al., 2006, PHWAT; Parkhurst et al., 2004, 2010, PHAST; Prommer et al., 1999, PHT3D), acid mine drainage (Malmström et al., 2004, LaSARPHREEQC) and radionuclide isolation (Källvenius and Ekberg, 2003, TACK).

The PHREEQC geochemical modelling software was used to forecast metal speciation in water. The MINTEQ.V4.DAT was used for the ion interaction method because it could incorporate all of the parameters that were chosen. pH, temperature, redox (pE), and determined concentrations of calcium (Ca), magnesium (Mg), iron (Fe), arsenic (As), calcium (Ca), manganese (Mn), copper (Cu), chlorine (Cl), sulphate (SO₄), and nitrate (NO₃) were used as input data for the modelling program.

CHAPTER FOUR

4. Results and discussion

4.1. Mine tailings storage facilities geochemistry and mineralogy

During the sampling period of July 2020, two bulk samples were taken from each MTSF; namely, Nestor and Glynns Lydenburg and their acid-base accounting, geochemistry, and mineralogy are discussed below.

4.1.1. Acid base accounting results

In Table 4, the ABA of the samples collected from the Nestor and Glynns Lydenburg MTSFs respectively, are summarised. The Nestor MTSF sample (AG) is characterised by a low paste pH of 2.5, which is a strong indication that the sample is acid generating and may contain high concentrations of stored acidity. In addition, the sample AG has no acid neutralizing capabilities (ANC). On the other hand, the Glynns Lydenburg MTSF (AN) has a relatively high paste pH of 7.7, indicating that it may be most likely be a non-acid generating sample. It also has an extremely high acid neutralising capacity (ANC) of 184 kg H₂SO₄/t, which indicates a high concentration of acid-neutralizing minerals. MIX25 and MIX50 have a paste pH of 5.1 and 6.1 respectively, which indicates that both mixtures may generate alkalinity. The mixtures may be suitable to treat or prevent AMD generated by the tailings from the Nestor Mine. These two mixed samples also have ANC values of 56 and 96 kg H₂SO₄/t respectively, which are relatively high when compared with their maximum potential acidity (MPA) values.

Table 4 Results of acid base accounting.

Sample ID	Paste pH	ANC (kg H ₂ SO ₄ /t)	S _(Total)	MPA (kg H ₂ SO ₄ /t)	NAPP (kg H ₂ SO ₄ /t)	R _{ANC/MPA}
AG	2.5	0	0.43	13	13	0
AN	7.7	184	0.07	2	-182	86
MIX25	5.1	56	0.34	10	-46	5
MIX50	6.1	96	0.25	8	-89	13

AG, MIX25, MIX50 and AN have net acid generation capacity (NAG) pH values of 2.7, 4.9, 5 and 5.9 and NAG values of 6.9, 0, 0 and 0 kg H₂SO₄/t, respectively. The NAG results thus indicate that AG is a potential acid-forming sample and could release up to 6.9 kilograms of sulphuric acid

per ton of material. MIX25, MIX50, AN were categorized as non-acid forming (NAF) using the NAG classification criteria summarised in Table 4.

The acid buffering characteristic curve (ABCC) curves of MIX25, MIX50 and AN are illustrated in Figure 13. The sample from the Nestor MTSF (AG) does not have an ABCC as it has no acid-neutralizing capabilities. The mixed sample, MIX25, MIX50 together with the Glynn's Lydenburg MTSF sample (AN) have the ability to neutralise 50 and 90 kg H₂SO₄/t respectively, before the pH of the solution drops substantially below 2,5, which corresponds closely to the ANC results determined using the ABA method (Table 4).

When the pH of mine tailings falls below 4 due to sulphide mineral oxidation by Fe²⁺, rate as well as amount of acid produced increases dramatically. Thus, the effective or freely available acid-neutralising capacities refer to the quantity of acid neutralized prior to drop in pH of solution to a value of 4. Samples MIX25, MIX50 and sample AN neutralize 35, 77 and 155 kg H₂SO₄/t respectively before the pH of the solution drops to a value of 4 (Fig. 12). A large portion of the ANC determined using the ABA method is freely accessible for acid neutralization.

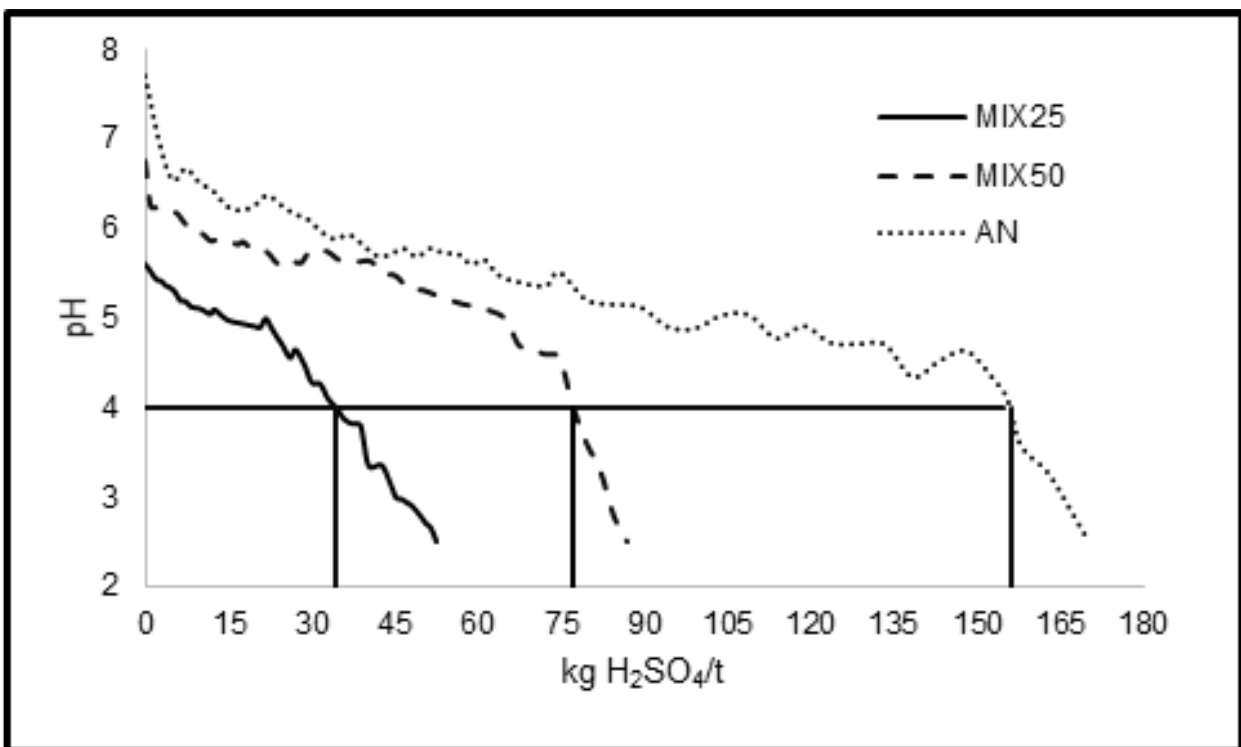


Figure 13 Acid buffering characteristic curve (ABCC) curves of samples MIX25, MIX50 and AN.

Comparing the ANC of each sample using the ABCC and the ABA method (Table 5), a substantially large portion of the ANC measured using the ABA method is freely accessible for

acid neutralisation. A high concentration of highly reactive carbonate minerals such as calcite or dolomite will most likely be the cause of the high availability of acid neutralization. It can be concluded that the ANC of MIX25, MIX50 and AN are not overestimated and will be readily available for acid neutralisation.

Table 5 Comparison of ANC calculated and at a pH of 2.5 and 4.0.

Sample	ANC (ABA)	ANC (ABCC _{pH=2.5})	ANC (ABCC _{pH=4})
	(kg H ₂ SO ₄ /t)	(kg H ₂ SO ₄ /t)	(kg H ₂ SO ₄ /t)
MIX25	56	53	35
MIX50	96	87	77
AN	184	170	155

Using the net acid production potential (NAPP), NAG pH as well as the classification criteria summarized in Table 6, the acid-generating capabilities of the Nestor MTSF (AG), MIX25, MIX50 and the Glynn's Lydenburg MTSF (AN) can be classified as PAF, NAF, NAF and NAF to a high degree of confidence as seen in Table 5.

Table 6 Final classification.

Sample	NAPP	NAGpH	Classification
	(kg H ₂ SO ₄ /t)		
AG	13	2.7	PAF
MIX25	-46	4.9	NAF
MIX50	-89	5	NAF
AN	-182	5.9	NAF

4.1.2. Geochemistry of sediments eroded from Nestor MTSF

Generally, the tailings from the Nestor MTSF display a yellow-ochre colour, all though areas of grey-greenish traces can be observed (Fig. 14). The lowest levels of the MTSF exhibits slightly cemented layers (crusts) of brown-reddish colour. The tailings have a sandy-clayey appearance and a variation of sand and very fine (silt and clay) fractions. These small sizes of grains (silt and clay) suggest that the waste is susceptible to airborne transport during the dry seasons, a possible cause for metal dispersion. However, this mechanism of environmental contamination might only be limited to dry seasons as the MTSF remains wet for most of the wet season. In addition, the

upper levels of the MTSF are crossed by numerous erosion gullies that point to the removal of the tailings through mechanical transport by water, followed by a discharge of the waste outside the MTSF boundary.



Figure 14 Photograph showing the sediments that are eroded from Nestor MTSF.

There is a big variation in terms of metal species on sediments eroded from the Nestor MTSF expresses as milligram per kilogram dry weight (mg/kg DW; Table 7). These concentrations vary significantly from the sample collected near MTSF (NS01) to the sample collected before the confluence with the Klein-Sabie River (NS03). In all the samples, the concentrations of the metal species As, Cr, Cu and Pb occur above upper continental crust values as per Rudnick and Gao, especially during the wet season (2003). In addition, the concentrations of metal species As, Cr, Cu, Ni and Pb occur above TEL guidelines (MacDonald *et al.*, 2000), and are likely to impact nearby aquatic organisms. In addition, the concentrations of the metal species As and Cr occur above the consensus-based PEC guideline of 33 ppm and 111 ppm respectively (MacDonald *et al.*, 2000).

Table 7 Geochemistry of trace elements from sediments eroded from the Nestor MTSF.

Sample number	As (mg/kg)		Co (mg/kg)		Cr (mg/kg)		Cu (mg/kg)		Ni (mg/kg)		Pb (mg/kg)		Zn (mg/kg)	
	WT	DR	WT	DR	WT	DR	WT	DR	WT	DR	WT	DR	WT	DR
NS01	366	363	11	17	135	58	77	37	32	24	38	14	27	8.8
NS02	782	552	29	7.7	247	147	70	74	53	31	27	60	15	14
NS03	224	89	30	45	127	238	99	74	51	49	13	17	90	42
UCC	4.8		26		92		28		47		17		67	

TEL	9.79	43.4	31.6	22.7	35.8	121
PEC	33	111	149	48.6	149	459

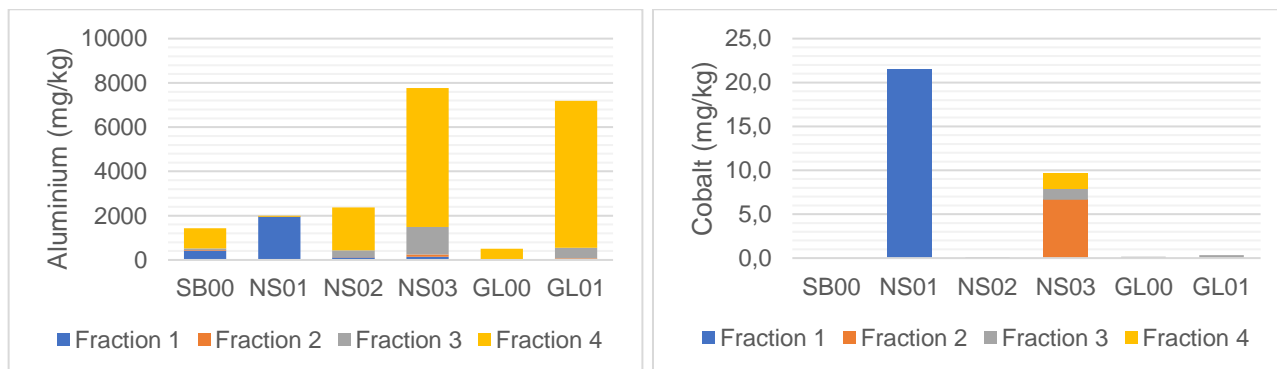
WT, wet season; DR, dry season

Based on the geochemistry of the sediments eroded from the Nestor MTSF, the pollution to the Sabie River system might be limited to As and Cr. This is because the concentrations of these two metal species are extremely high, occurring above the consensus-based PEC guideline.

4.1.2.1. Metal distribution in sediments and soils around the Nestor and Glynns Lydenburg MTSFs

A sequential chemical extraction was performed in order to define the distribution of metal species in various geochemical portions of tailings and sediments from Nestor MTSF. The samples were collected near the MTSF (SB00 and NS01), traced downstream under the Klein Sabie bridge (NS02) and before the confluence with the Klein Sabie River (NS03; Annexure B). In addition, two samples from the adjacent Glynns Lydenburg MTSF (GL00 and GL01) were also assessed. Because mobility and bioavailability of metal species are associated with solubility, bioavailability declines in the order exchangeable>reducible>oxidizable>residual. Figure 15 depicts concentrations of selected metal species associated with each soil fraction.

With the exception of Mn at samples NS01, NS03, and SB00, all metal species in the Nestor MTSF are found to be highly partitioned to the crystalline structure of the tailings material (F4 fraction). This implies that these metals are geogenic in origin. The mobility and bioavailability of metal species extracted from the tailings samples investigated declined in the following order: Fe>Al>As>Mn>Zn>Cu>Ni>Cr>Pb>Co. The residual fraction has the highest concentration of Fe in the tailings material, followed by the Fe-Mn bound, exchangeable, and less oxidizable fraction (F3). Mn is released from the exchangeable, residual, oxidizable and reducible fractions and will be bioavailable. Therefore, the concentration of Mn can have negative impact to the ecosystem.



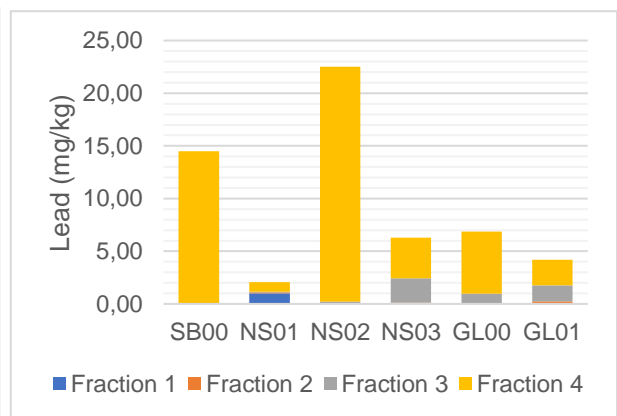
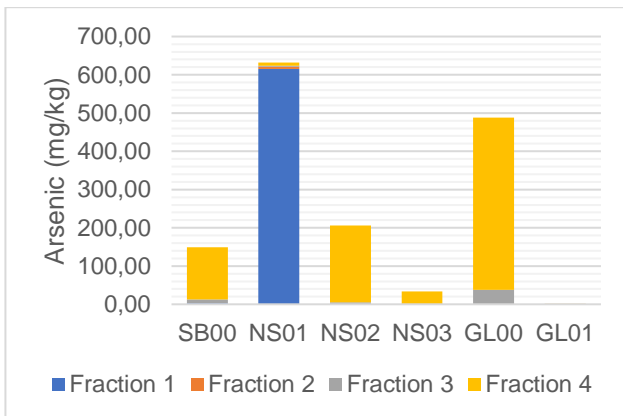
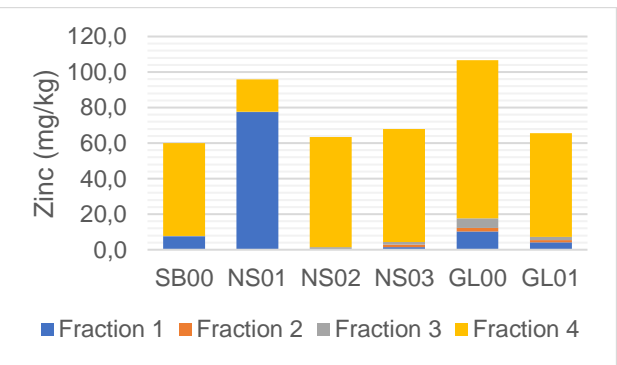
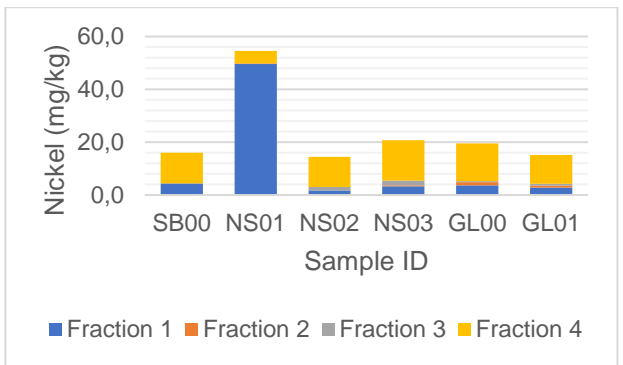
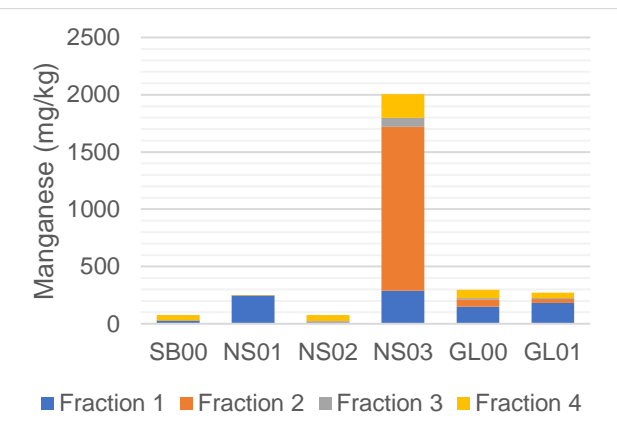
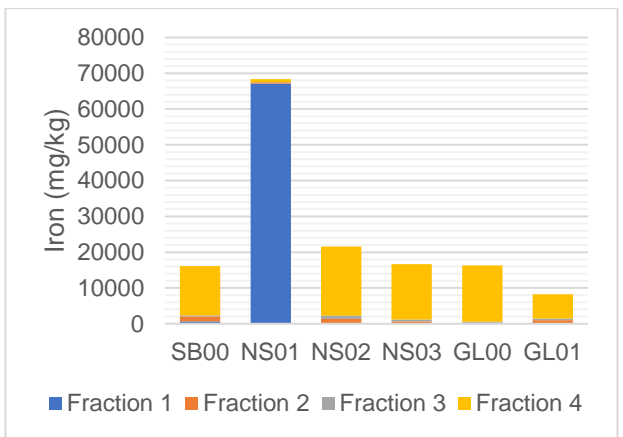
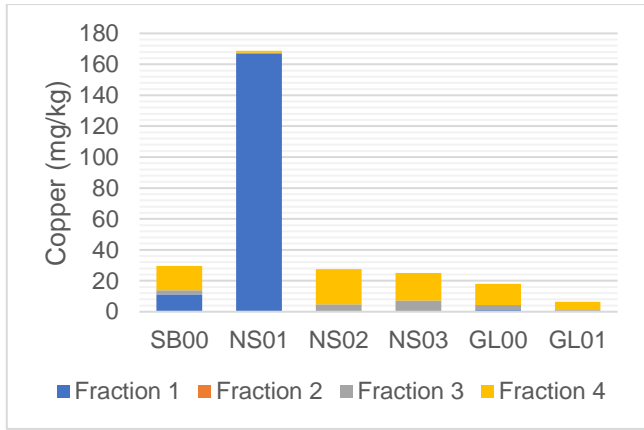
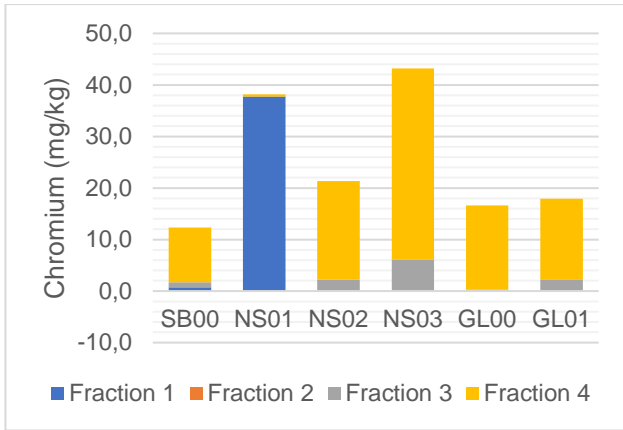


Figure 15 Metal species concentrations (mg/kg) in different fractions of mine wastes and surrounding soils.

In the Glynns Lydenburg MTSF, all the metal species are partitioned on the fourth fraction. However, in the sample site GL01, elevated Mn partitioned on the fourth fraction can be attributed to the dolomitic nature of the tailings stored in that facility. This is of no concern since substantial concentrations of Mn can co-precipitate with the carbonates in the MTSF like dolomite. In the studies samples from the Glynns Lydenburg MTSF, the mobility and bioavailability of metal species decreased in the order Fe>Al>As>Mn>Zn>Cr>Cu>Ni>Pb>Co.

In addition to Fe, also found in all the four fractions, except at NS01 (F3), the majority of Al occurrences in the mine wastes is partitioned on the first and the fourth fractions, that is, they are bound to the fractions containing exchangeable metals and the residual fraction. This indicates that the Al and Fe in the mine wastes are not very bioavailable (4th fraction) and will only be released with changes in ionic composition (1st fraction). In both the Nestor and Glynns Lydenburg MTSFs, the total Zn, Cr, As, Cu, Ni, and Pb were highly partitioned in residual fraction. This suggest that there is relatively low mobility and availability of these metal species from the MTSFs to the surrounding environment.

4.1.2.2. Geochemistry of bulk samples

The geochemistry of the bulk samples is shown in Table 8. The dominant oxide is silica in both bulk samples occurring at 71.7 wt. % and 54.5 wt. % at the Nestor (AG) and Glynns Lydenburg (AN) MTSFs respectively. The Nestor MTSF sample has a low concentration of CaO, F₂O₃ and MgO respectively compared to that found at the Glynns Lydenburg site, but the Fe₂O₃ value is still 3 times higher than the UCC value. This can be attributed to the dolomitic nature of the mine tailings from the Glynns Lydenburg Mine. All concentrations of CaO, Fe₂O₃, and MgO occur above upper continental values for the Glynns Lydenburg MTSF (Wedepohl, 1995).

Table 8 Geochemistry of bulk samples.

Sample ID	SiO ₂ (wt. %)	Al ₂ O ₃ (wt. %)	Fe ₂ O ₃ (wt. %)	CaO (wt. %)	MgO (wt. %)	K ₂ O (wt. %)	TiO ₂ (wt. %)	Cr ₂ O ₃ (wt. %)	MnO (wt. %)	V ₂ O ₅ (wt. %)	P ₂ O ₅ (wt. %)
AG	71.7	6.7	12.8	0.1	0.3	3.5	0.2	0.03	0.04	0.02	0.07
AN	54.5	3.8	22.1	11.7	3.9	1.5	2.4	0.05	0.1	0.03	0.09
UCC	66.8	15.1	4.09	4.24	2.3	3.19	—	—	0.07	—	0.18

UCC, upper continental crust (Wedepohl, 1995); —, no values

4.1.3. Mineralogy of sediments eroded from Nestor MTSF

The Nestor MTSF samples contain quartz and mica as the main primary minerals (Table 9). In addition, two secondary minerals hematite (2 wt. %) and jarosite (4 wt. %) are present at sampling site NS01. The primary acid-producing mineral pyrite is present in the sample collected before the confluence with the Sabie River (NS03). In addition, the secondary mineral, gibbsite, is present together with a clay mineral kaolinite; implying that there is weathering of pyrite taking place.

Table 9 Mineralogical composition of tailings from the Nestor MTSF.

Sample Id	Quartz (wt. %)	Mica (wt. %)	Plagioclase (wt. %)	Pyrite (wt. %)	Gibbsite (wt. %)	Hematite (wt. %)	Jarosite (wt. %)	Kaolinite (wt. %)
NS01	84	6	3	ND	ND	2	4	ND
NS02	93	7	ND	ND	ND	ND	ND	ND
NS03	83	5	ND	3	7	ND	ND	2

ND, not detected

4.1.3.1. Mineralogy of tailings (bulk samples)

Table 10 shows the mineralogy of the tailings collected from the Nestor (AG) and Glynns Lydenburg (AN) MTSFs. The acid-generating sample (AG) is mainly composed of quartz and mica, with low concentrations of goethite and magnetite respectively. On the other hand, the Glynns Lydenburg MTSF sample (AN) is composed of quartz as the principal mineral and acid-neutralizing mineral dolomite as well as mica. In addition, the secondary mineral goethite is present in higher concentration than in the Nestor MTSF, consistent with geochemical data that detected higher concentration of Fe₂O₃ in the Glynns Lydenburg MTSF.

Table 10 Mineralogy of tailings.

Sample ID	Quartz (wt. %)	Dolomite (wt. %)	Goethite (wt. %)	Mica (wt. %)	Magnetite (wt. %)
AG(B)	80.5	ND	1.5	17.9	0.1
AN	59.7	29.4	2.9	8	ND

Based on the findings from Lusunzi (2018), the Glynns Lydenburg MTSF had no potential to produce AMD and it was suggested to use these tailings to rehabilitate the Nestor MTSF. Based on the mineralogical composition of the bulk tailings sample (Table 9), the Glynns Lydenburg

mine tailings have an acid neutralising potential as it contains high concentration of dolomite. Therefore, soil samples surrounding the MTSF were also collected in order to assess the suitability of their geochemical properties for rehabilitation of the Nestor MTSF.

4.2. Efflorescent crust geochemistry and mineralogy

The efflorescent crusts developed on the Nestor and Glynns Lydenburg MTSFs were seasonally collected to assess their possible impact onto the surrounding environmental settings. Their geochemical and mineralogical compositions are discussed below.

4.2.1. Efflorescent crusts geochemistry

There was a wide seasonal variation shown in terms of major elements geochemistry in the Nestor (NS00) and Glynns Lydenburg (GS00) MTSFs. From XRF results, the dominant oxides silica and Fe₂O₃, showed a wide seasonal variation (Table 11). In both sites, silica dominated the wet season while during the dry season, Fe₂O₃ was the dominant oxide at Nestor MTSF (32.0 wt. %). The concentrations of CaO occurred in high concentrations in the Glynns Lydenburg efflorescent in both seasons' crusts (10.9 and 8.3 wt. %) and this can be attributed to the dolomitic nature of the tailings. This is confirmed by high concentration of MgO at Glynns Lydenburg MTSF that was 4.40 wt. % in wet and 9.6 wt. % during the dry season. Also occurring in minor concentrations in samples from both sites is MnO, while concentrations of TiO₂, Na₂O, K₂O, P₂O₅ and Cr₂O₃ were below zero.

Table 11 Geochemistry of efflorescent crusts from the Nestor and Glynns Lydenburg MTSF.

Sample ID	SiO ₂ (wt. %)		TiO ₂ (wt. %)		Al ₂ O ₃ (wt. %)		Fe ₂ O ₃ (t) wt. %		MnO (wt. %)		MgO (wt. %)		CaO (wt. %)	
	WT	DR	WT	DR	WT	DR	WT	DR	WT	DR	WT	DR	WT	DR
NS00	72.56	13.12	0.17	0.1	2.1	2.34	1.22	31.99	0.006	0.14	0.02	0.19	12.62	0.18
GL00	78.57	48.4	0.19	0.09	3.29	2.69	7.99	8.32	0.024	0.1	4.4	9.58	2.05	8.34

WT, wet season, DR, dry season

Figure 16 presents the trace elements composition of the efflorescent crusts from the Nestor and Glynns Lydenburg MTSFs expressed in mg/kg. Arsenic is the dominant trace element found at both sites at 1904-2371 mg/kg at Nestor and 1202-1575 mg/kg at the Glynns Lydenburg efflorescent crusts. This is consistent with the tailings geochemistry that found As equally a probable basis of metal contamination to the surrounding locations (Table 4). In addition, the concentrations of Cu and Pb are elevated at the Nestor MTSF more especially during the dry

season. These results indicate that the efflorescent crusts from this MTSF have an ability to store pollutants.

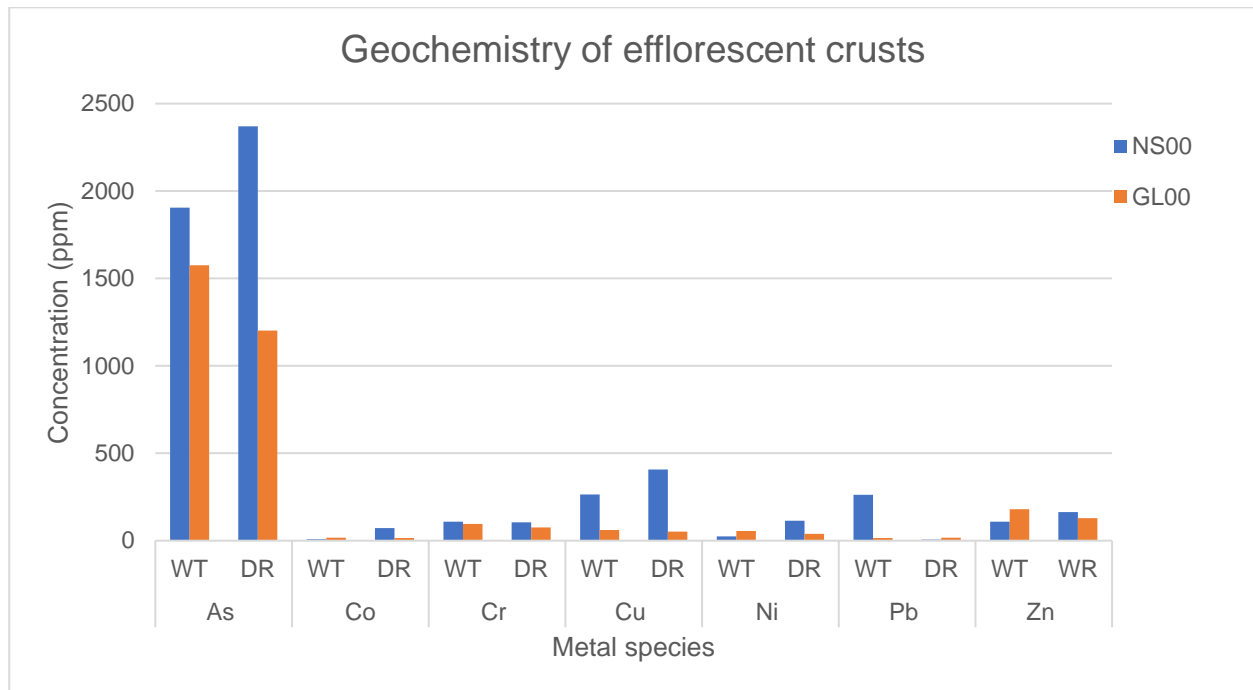


Figure 16 Trace elements geochemistry of efflorescent salts from the Nestor and Glynn Lydenburg MTSF.

The chemical analyses of efflorescent crusts from the Nestor MTSF confirmed the presence of potential toxic elements (PTEs), namely, arsenic (As), copper (Cu), and lead (Pb) in their structure that can easily be released to the nearby water bodies and soils by dissolution. These elements' concentrations are exceeding the South African guidelines on the soil screening for the safety of environment health (Table 12; DEA, 2013). Therefore, the dissolution of the efflorescent crusts in the Nestor MTSF is a potential source of contamination during the wet season. The only potential contaminant from the Glynn Lydenburg MTSF efflorescent crusts is arsenic, which require further investigation in terms of its source. However, this As-enrichment in these precipitated salts can be attributed to the presence of arsenopyrite in the ore of the Glynn Lydenburg Mine.

Table 12 Distribution of metal species in efflorescent crusts (mg/kg) and soil screening values for metals (DEA, 2013).

Metal	Glynn Lydenburg TSF	Nestor TSF	All land uses, protective of water resources	Informal residential	Standard residential	Commercial/Industrial	Protection of Ecosystem Health
As	~1900	~1600	~1900	~1600	~1900	~1600	~1900
Co	~10	~10	~10	~10	~10	~10	~10
Cr	~100	~100	~100	~100	~100	~100	~100
Cu	~250	~100	~250	~100	~250	~100	~250
Ni	~10	~10	~10	~10	~10	~10	~10
Pb	~250	~10	~250	~10	~250	~10	~250
Zn	~100	~150	~100	~150	~100	~150	~100

As	1202-1575	1904-2371	5.8	23	48	150	580
Co	15-17	8.1-72	300	300	630	5000	22000
Cr (VI)	75-96	105-108	6.5	6.5	13	40	260
Cu	52-62	263-408	16	110	230	19000	16
Ni	39-55	24-115	91	620	1200	10000	1400
Pb	15-17	63-262	20	110	230	1900	100
Zn	129-180	108-163	240	9200	19000	150000	240

While As is the only potential contaminant from the Glynn's Lydenburg MTSF, the potential contaminants from the Nestor MTSF efflorescent crusts are As, Cu and Pb; these metal species concentrations occurred in excess of the National Norms and Standards for the Remediation of Contaminated Land and Soils in the Republic of South Africa (DEA, 2013).

4.2.2. Mineralogy of efflorescent crusts

In terms of mineralogy, the efflorescent crusts from each MTSF were characterised by unique mineral assemblages (Figure 17). The minerals identified in the efflorescent crusts are of primary, secondary, and tertiary origin. Because secondary soluble salts stockpile acid as well as metal species in their compacted period they are environmentally hazardous. During periods of rainfall or wetness, their dissolution may produce possibly harmful flushes of acid and metal species into surface and groundwater. (Nordstrom and Alpers, 1999). The salts developed on the MTSFs were of botryoidal efflorescence in inconstant colours (green, yellow, and white), signifying a paragenetic system of sulphates having different solubilities and degrees of dehydration.

In the efflorescent crusts of the Nestor MTSF, quartz predominates the primary minerals, followed by the tertiary mineral ferricopiapite. In addition, these efflorescent crusts contain the secondary clay mineral kaolinite. In terms of acid producing minerals, the Nestor MTSF contains ferricopiapite, which is the hydrated soluble iron sulphates. This implies that the main primary iron mineral accumulated in the MTSF is probably pyrite. The dissolution of these soluble sulphate salts can produce acidic solutions with elevated concentrations of dissolved metals during the wet season. The Glynn's Lydenburg MTSF efflorescent crusts are composed of the primary minerals quartz and dolomite. The secondary mineral gypsum, which is a precipitate of calcium, is also present in these efflorescent crusts. There are no acid producing minerals present in the Glynn's Lydenburg MTSF's efflorescent crusts. Based on their large external area and capacity to sorb dissolved pollutants, these specific minerals (especially dolomite) can be important in self-

mitigation of metal-laden acidic Nestor MTSF drainages. For example, As co-precipitates with the Fe(III) sulphate, Zn and Cu are primarily incorporated into Fe(II) sulphates, and hazardous elements such as As^{5+} , Cr^{6+} , and Pb^{2+} are essentially co-precipitated with minerals of the jarosite group. The co-precipitation of the potentially toxic elements with sulphates and sulpharsenates of Fe had been revealed to be a major tool in governing the concentrations of hazardous elements in pore solutions of high sulphide mine wastes (Gomes and Favas 2006).

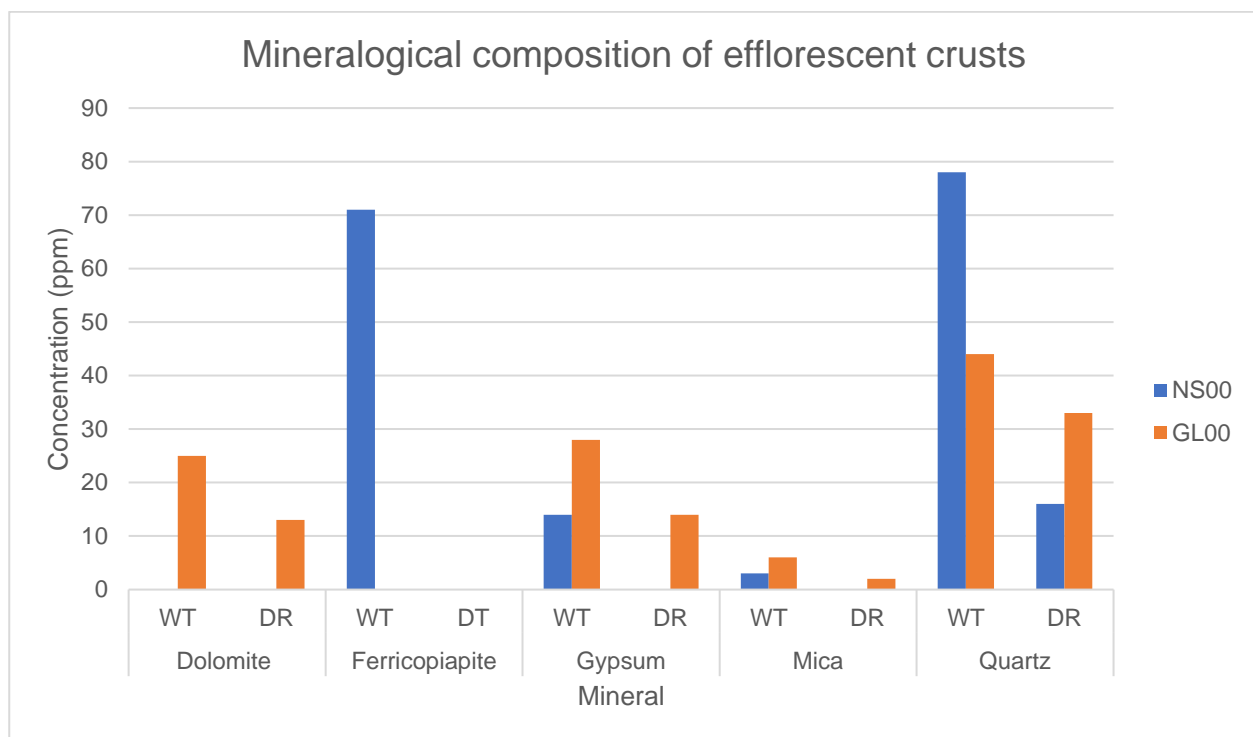


Figure 17 Mineralogical composition of efflorescent crusts from the Nestor (NS00) and Glynn's Lydenburg (GL00) MTSFs.

4.3. Soil geochemistry and mineralogy

Metal species are natural constituents of soils, and their concentrations vary depending on the parent material. There has been an increase in the concentrations of metal species in soils because of human activities such as industrial discharges, fertilizers distribution, pesticides, waste disposal, and air pollution. In order to assess the presence and intensity of anthropogenic contaminant depositions on surface soils and stream sediments, the Chemical Index of Alteration (CIA), Enrichment Factor (EF) in metals as well as Geoaccumulation Index (Igeo) indicators were applied.

Soil samples collected near mine tailings storage facilities SN and SG (MTSFs) and those that were collected away from mining activities showed variation in terms of geochemistry and mineralogy.

4.3.1. Soil surrounding mine tailings storage facilities

In order to assess the potential impacts due to mine tailings storage facilities (MTSFs), soil samples collected near the Nestor (SN) and Glynn's Lydenburg (SG) MTSFs were analysed and the results are discussed below.

4.3.1.1. Geochemistry of soil near Nestor MTSF

Eight soil samples collected near the Nestor MTSF showed variation in terms of major element concentrations (Table 13). The dominant major element is the resistance silica at the range from 52-87 wt. %, followed by aluminium oxide (3-18 wt. %), iron oxide (3.62-11.54 wt. %), with lesser concentrations of potassium oxide and titanium oxide (up to 1.62 and 1.11 wt. % respectively). Also occurring in lower concentrations are oxides of calcium, magnesium, sodium, phosphorus and chromium. Rose et al. (1979) identified the median value for Fe oxide as 2.1 wt. % in soils, which is less than what is found in this study (up to 21.50 wt. %).

Table 13 Major elemental composition of soil near the Nestor MTSF.

Sample ID	Si (wt. %)	Ti (wt. %)	Al (wt. %)	Fe ₂ (t) (wt. %)	Mn (wt. %)	Mg (wt. %)	Ca (wt. %)	Na (wt. %)	K (wt. %)	P (wt. %)	Cr (wt. %)
SN01	87.37	0.44	2.69	6.44	0.012	0.13	0.02	0.06	0.62	0.035	0.02
SN02	51.58	1.05	17.64	11.54	0.414	0.48	0.05	0.05	0.81	0.066	0.051
SN03	83.37	0.48	3.1	3.62	0.017	0.11	0.02	0.05	0.93	0.025	0.018
SN04	62.12	0.9	16.47	10.54	0.391	0.45	0.03	0.04	0.66	0.046	0.054
SN05	77.19	0.74	7.51	6.58	0.049	0.29	0.02	0.06	1.53	0.062	0.027
SN06	69.77	0.56	12.07	6.75	0.05	0.5	0.04	0.06	0.72	0.057	0.035
SN07	57.97	1.11	16.74	8.94	0.078	0.23	0.08	0.1	0.42	0.106	0.038
SN08	64.69	0.75	13.33	8.04	0.257	0.61	0.25	0.08	1.62	0.149	0.048

There is also a large variation in terms of trace element concentrations on soils surrounding the Nestor MTSF (Table 14). The soil samples collected near the main MTSF (SN01, SN03, and SN05) are highly enriched in As and it showed a decreasing trend with a distance from the MTSF and at SN07, of about a kilometre away, which was collected before the confluence with the Klein

Sabie River, the value was only 18mg/kg. It should be noted that all the samples are enriched in chromium.

Table 14 Geochemistry of soil near the Nestor MTSF.

Sample ID	As (mg/kg)	Co (mg/kg)	Cr (mg/kg)	Cu (mg/kg)	Ni (mg/kg)	Pb (mg/kg)	Zn (mg/kg)
SN01	419	5.1	125	55	24	21	15
SN02	13	86	334	84	130	30	27
SN03	187	6	65	28	16	13	6
SN04	8	46	319	86	156	16	30
SN05	234	11	143	50	40	37	12
SN06	6	14	218	36	85	8.9	19
SN07	18	11	261	63	58	17	21
SN08	44	34	337	83	90	31	93
Normal Soil	6	8	-	30	15	14	90

Normal soil (Bowen, 1979), -, not given.

All concentrations of metal species (As, Co, Cr, Ni, Pb, and Zn) in the soil near the Nestor MTSF are within guidelines of South African soil screening, National Norms and Standards for Remediation of Contaminated Land and Soil Quality in the Republic of South Africa except for Cu (Table 12; DEA, 2013). However, these concentrations occur above the normal soil concentrations (Table 13; Bowen, 1979) with few exceptions such as low Co, Cu, Pb, and Zn at SN03.

4.3.1.2. Mineralogy of soil near Nestor MTSF

In terms of mineral assemblage, quartz is the dominant primary mineral in the soils surrounding the Nestor MTSF ranging between 66.2 and 94.4 wt. % followed by mica (up to 22 wt. %; Table 15). In addition, the secondary minerals such as gibbsite, goethite, gibbsite, and magnesioferrite are present in various concentrations. Clay minerals occur in low concentration and are represented by kaolinite and smectite that were found only at SN05 (0.1 wt. %).

Table 15 Mineralogical composition of soils near the Nestor MTSF.

Sample ID	Quartz (wt. %)	Mica (wt. %)	Gibbsite (wt. %)	Goethite (wt. %)	Magnesioferrite (wt. %)	Kaolinite (wt. %)	Smectite (wt. %)	Clinocllore (wt. %)	Almandine (wt. %)
SN01	94.4	4.2	ND	1.4	ND	ND	ND	ND	ND
SN02	66.5	2.5	20.5	ND	0.3	ND	0.2	ND	ND
SN03	88.2	10.6	ND	1.2	ND	ND	ND	ND	ND
SN04	82.1	ND	17.6	ND	ND	ND	0.3	ND	ND
SN05	83.5	15.8	ND	0.6	ND	0.1	0.1	ND	ND
SN06	92.8	4.5	ND	ND	ND	ND	0.6	ND	2.1
SN07	71.8	ND	24.8	ND	ND	ND	ND	3.4	ND
SN08	66.2	22	9.4	ND	ND	ND	ND	2.4	ND

4.3.1.3. Geochemistry of soil near Glynns Lydenburg MTSF

Seven samples, collected around the Glynns Lydenburg MTSF, show variation in terms of major elemental composition (Table 16). The principal major element is quartz (47.15-66.73), followed by aluminium oxide (7.38-16.20 wt. %), iron oxide (7.38-12.20 wt. %), calcium oxide (0.02-4.22-wt. %), magnesium oxide (0.36-3.13 wt. %), potassium oxide (0.40-2.08 wt. %), and titanium oxide (0.13-1.80 wt. %). Occurring in low concentrations of less than one wt. % are oxides of sodium, phosphorus, and chromium.

Table 16 Major elemental composition of soils around the Glynns Lydenburg MTSF.

Sample ID	SiO ₂ (wt. %)	TiO ₂ (wt. %)	Al ₂ O ₃ (wt. %)	Fe ₂ O ₃ (t) (wt. %)	MnO (wt. %)	MgO (wt. %)	CaO (wt. %)	Na ₂ O (wt. %)	K ₂ O (wt. %)	P ₂ O ₅ (wt. %)	Cr ₂ O ₃ (wt. %)
SG01	63.57	0.26	5.08	10.76	0.186	2.89	4	0.08	1.19	0.109	0.029
SG02	47.15	0.13	3.28	7.38	0.122	2.4	3.12	0.05	0.98	0.063	0.015
SG03	64.08	0.25	6.91	10.56	0.176	1.96	2.28	0.08	2.08	0.134	0.029
SG04	64.4	1.41	11.31	12.2	0.494	0.26	0.2	0.07	0.38	0.112	0.037
SG05	57.55	1.71	16.2	11.28	0.607	0.39	0.13	0.06	0.4	0.124	0.039
SG06	66.18	0.18	4.06	10.61	0.158	3.08	4.07	0.07	1.18	0.082	0.02
SG07	66.73	0.14	3.52	9.87	0.174	3.13	4.22	0.07	1.03	0.088	0.021
SG08	53.35	1.8	17.77	12.93	0.37	0.36	0.22	BD	0.47	0.16	0.04

BD, below detection limit

Based on outcomes as of the XRF analyses, displayed in Table 17, the soil samples taken near the Glynns Lydenburg MTSF shows high enrichment in As (SG01, SG02, SG03, SG06, and SG07) exceeding guidelines of South African soil screening, National Norms and Standards for Remediation of Contaminated Land and Soil Quality (Table 12; DEA, 2013). In addition, the concentrations of the base metals Cr, Zn, Ni, Cu, and Pb in decreasing order with values of Cu occurring above those stipulated by DEA (2013). However, all the soil samples collected away from the tailings storage facility show a low concentration of the metalloid As, with elevated concentrations of Cu exceeding the guidelines of South African soil screening, National Norms and Standards for Remediation of Contaminated Land and Soil Quality (DEA, 2013).

Table 17: Geochemistry of trace elements near Glynns Lydenburg MTSF.

Sample ID	As (mg/kg)	Co (mg/kg)	Cr (mg/kg)	Cu (mg/kg)	Ni (mg/kg)	Pb (mg/kg)	Zn (mg/kg)
SG01	1981	25	166	87	66	37	227
SG02	1870	24	113	79	60	26	187
SG03	2027	23	186	34	73	66	226
SG04	19	58	202	83	90	22	68
SG05	30	60.5	249	113	139	21	51
SG06	1896	24.1	115	47	57	31	141
SG07	1864	24.0	117	49	59	41	163
SG08	305	14	272	46	38	19	13
Normal Soil	6	8	-	30	15	14	90

Normal Soil (Bowen, 1979), not given

There is a very high difference in terms of soil geochemistry between the two sites, however, the soil surrounding the Glynns Lydenburg MTSF is more enriched in metal species when compared to the soil surrounding the Nestor MTSF, especially As and Zn. This could pose a potential threat in terms of rehabilitating the Nestor MTSF using the materials from the Glynns Lydenburg MTSF as this could lead to metal contamination in the proximity of the site.

4.3.1.4. Mineralogy of soil near Glynns Lydenburg MTSF

The following minerals were detected in the soil surrounding the Glynns Lydenburg MTSF: quartz, dolomite, mica (primary minerals), gibbsite, goethite, magnesioferrite (secondary minerals) as well as kaolinite and smectite (clay minerals). Quartz shows dominance in terms of mineralogical

composition (up to 87.1 wt. % for sample SG08), followed by the clay mineral kaolinite (22.9 wt. % at SG05), and the primary carbonate mineral dolomite (up to 20 wt. % at SG01; Table 18).

Table 18 Mineralogical composition of soil near Glynn's Lydenburg MTSF.

Sample ID	Quartz (wt. %)	Dolomite (wt. %)	Gibbsite (wt. %)	Goethite (wt. %)	Kaolinite (wt. %)	Mica (wt. %)	Magnesioferrite (wt. %)	Smectite (wt. %)
SG01	72.6	20.0	ND	ND	ND	7.4	ND	ND
SG02	74.0	17.4	ND	ND	ND	8.6	ND	ND
SG03	67.4	13.1	ND	1.1	ND	18.4	ND	ND
SG04	78.2	ND	13.3	1.5	3.9	2.8	ND	0.3
SG05	58.0	ND	12.5	ND	22.9	6.6	ND	ND
SG06	71.1	20.1	ND	ND	ND	8.7	0.1	ND
SG07	71.8	19.0	ND	ND	ND	9.2	ND	ND
SG08	87.1	ND	ND	1.2	ND	11.6	ND	ND

4.3.2. Geochemistry and mineralogy of soils away from mining activities

Four soil samples were collected in areas away from any of the mining activities to assess the difference concerning mine pollution of the soils as well as uncontaminated sites. These sites are underlain by various lithologies, namely, granite, sandstone, dolomite, and quaternary alluvium.

4.3.2.1. Soil geochemistry

Table 19 shows the results of soil samples collected away from mining activities expressed in mg/kg dry weight (DW). There is a low metal species concentration in the soil away from the mining activities with the exception of Cr. This variation can be attributed to the underlying rocks, namely, quaternary alluvium at SB26, dolomite (Malmani Subgroup) at SB27 sandstone (Black Reef Formation) at SB28, and granite (Nelspruit Suite) at SB29. No concentrations of As were detected at site SB27 and SB29 and the concentrations of other metals (Zn, Ni, Cu, Pb Cr, and Co) are lower than at site SB27 and SB28; most probably influenced by the underlying geology.

At sample point SB27, associated with the Malmani Subgroup comprising mostly of dolomite, there are elevated concentrations of metals Cr, Ni, Cu, and Co in ascending order. Similar elemental association can also be observed at SB28, which is associated with the Black Reef

Formation. This elemental association is commonly associated with possible chrome or platinum-group elements mineralisation. There are lower concentrations of these metals (Cr, Ni, Cu, and Co) at SB26, which is mostly quaternary deposits as well as SB29 that is located on the Nelspruit granite.

Table 19 Geochemistry of soils in the Sabie area.

Sample Id	As (mg/kg)	Co (mg/kg)	Cr (mg/kg)	Cu (mg/kg)	Ni (mg/kg)	Pb (mg/kg)	Zn (mg/kg)
SB26	ND	7.2	90	29	28	15	42
SB27	20	58	386	102	147	22	60
SB28	38	47	142	65	65	13	22
SB29	ND	3.2	28	12	13	17	18
Normal Soil	6	8	-	30	15	14	90

Normal Soil (Bowen, 1979), -, not given

The concentrations of all metal species in the soils away from the mining activities occur in concentrations below the South African guidelines on soil screening, National Norms and Standards for Remediation of Contaminated Land in the Republic of South Africa (DEA, 2013; Table 8), except for Cr at SB27 and Cu at SB27 and 28 respectively. However, most of these metal species (As, Co, Cu, and Ni at SB27 and SB28) occur above normal soil values (Bowen, 1979).

4.3.2.2. Mineralogical composition of soils away from mining activities

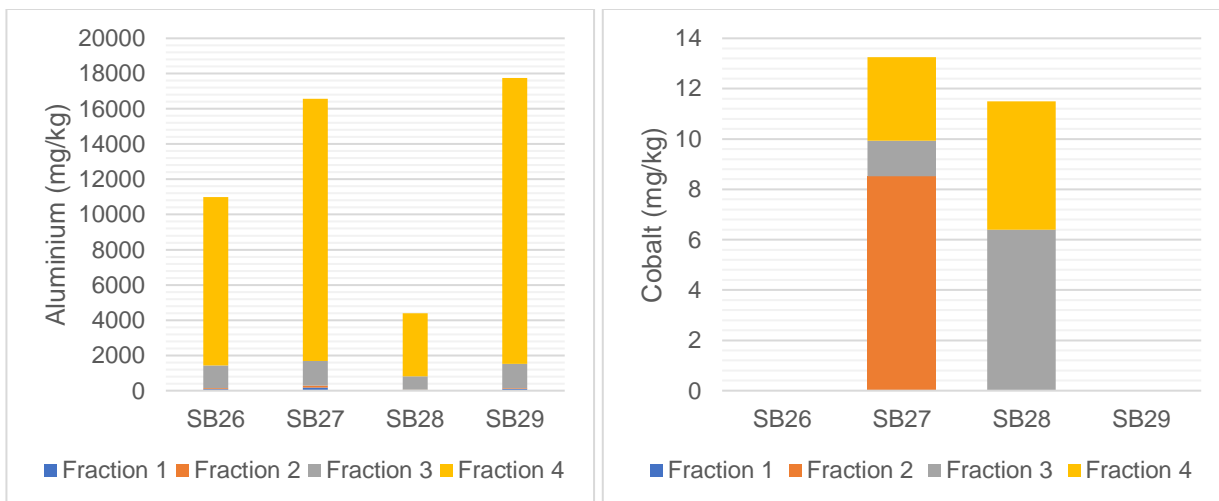
There is a wide variation in terms of mineralogy of soils away from mining activities (Table 20). The mineralogy of soils away from mining activities is composed of quartz as major primary mineral in all samples. Other primary minerals, namely, mica, pyrite, K-feldspar, and plagioclase were not all detected in the samples. In addition, gibbsite and kaolinite were also found in the soil samples.

Table 20 Mineralogy of soils away from mining activities.

Sample Id	Quartz (wt. %)	Mica (wt. %)	Gibbsite (wt. %)	Pyrite (wt. %)	K-Feldspar (wt. %)	Plagioclase (wt. %)	Kaolinite (wt. %)
SB26	25	1	6	ND	38	26	4
SB27	79	7	7	ND	ND	ND	7
SB28	90	4	5	ND	ND	ND	1

4.3.2.3. Speciation of metals in soils away from the mining activities

The sequential extraction of soil from four different locations away from the mining activities showed variation in terms of metal species distribution in various fractions (Annexure C). Figure 18 shows the concentrations of selected trace elements (Al, Mn, Fe, As, Ni, Cr, Zn, Co, Cu as well as Pb) extracted from the soil. These elements were selected because they were prevalent in typical soil samples. Aluminium is highly partitioned in the third and fourth fractions. Cobalt was absent at some sampling sites (SB26 and SB29) and was found in different fractions at SB27 and SB28. In the SB27 sample, Co is highly partitioned in the bioavailable Fe-Mn oxide fraction while at SB28 it is concentrated in the F3 and F4 fractions. There was no concentrations of Co, Cr, and Cu extracted from F1 in all soil samples. In addition, there was no Cr extracted from F2 and it is primarily partitioned in the inert fraction. This indicates that these metals were not anthropogenically introduced into the soil. However, significant concentrations of these elements were found in the fourth fraction indicating that they were incorporated into the mineral phase and therefore are of natural geochemical origin. The majority of trace elements that were extracted are found in the inert fraction (Al, Cr, Cu, Ni, As, Zn, Pb, and Fe); suggesting a geogenic source for these elements.



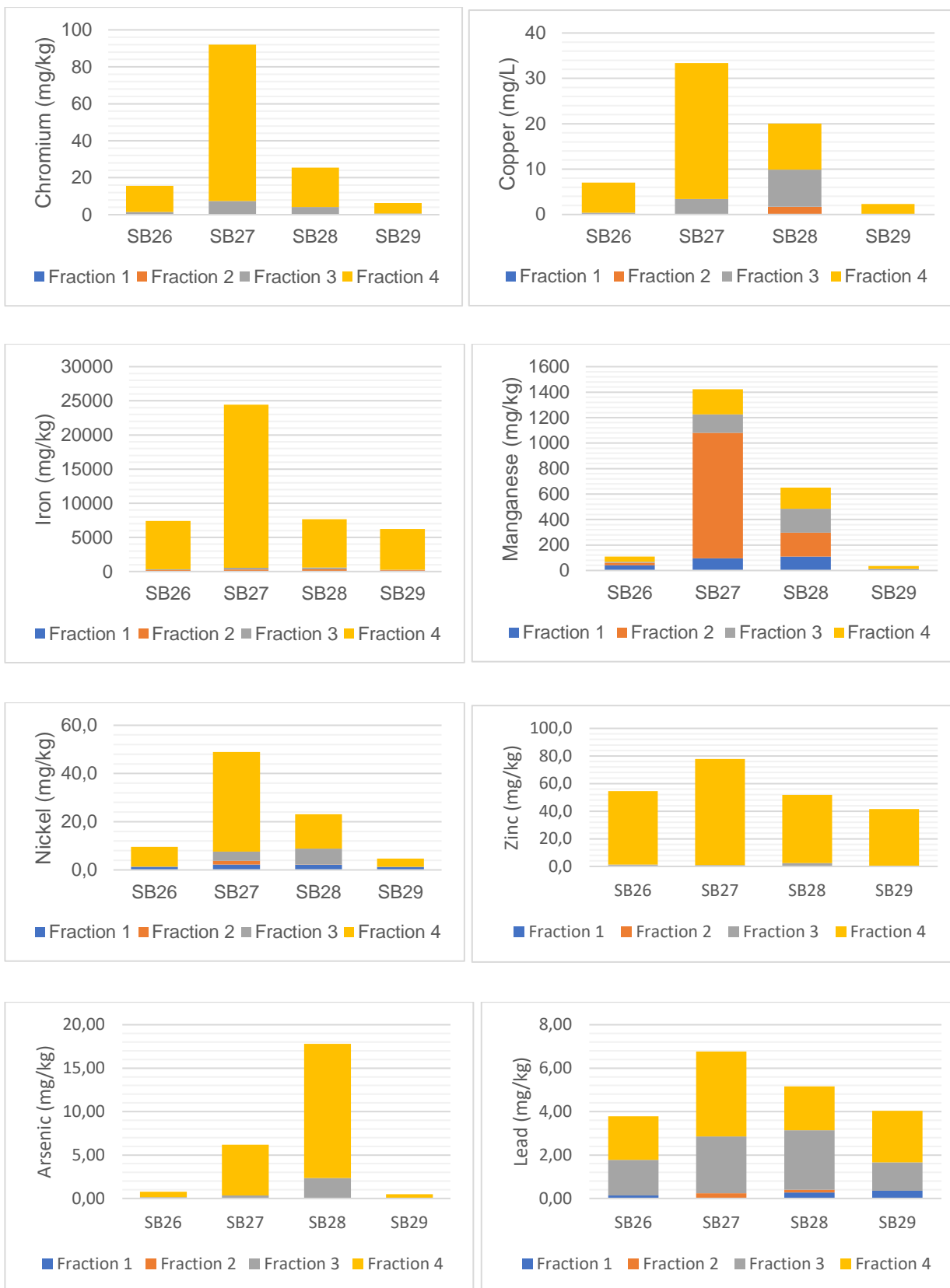


Figure 18 Metal species concentrations (mg/kg) in different fractions of soils away from mining activities.

4.4. Stream sediment geochemistry and mineralogy

4.4.1. Stream sediment and geochemistry

The geochemistry of the Sabie River system is a function of a complex relationship between a range of factors that include the underlying geology and area covered, flow dynamics, land use, weathering processes and redox reactions.

4.4.1.1. Major elements in stream sediments

Table 21 displays the data of XRF examination of the main elements as weight percentages (wt. percent) of the matching oxides. More than 75% of the main elements in all stream sediment samples were identified as Si-Al-Fe components, indicating that the sediments comprise a higher percentage of quartz, feldspar, clay minerals, and micas. The subsequent oxides were found to be the most prevalent in all sites examined: SiO₂ (40.24-86.15%), Al₂O₃ (5.67-19.52%), Fe₂O₃ (1.19-11.75%), K₂O (0.98-3.11%), Na₂O (0.08-2.30%), CaO (0.12-1.92), Ti₂O (0.14-1.38%), MgO (0.20-1.63%), MnO (0.02-0.89%), P₂O₅ (0.01-0.10%) and Cr₂O₅ (0.007-0.102%). The essential element Fe component in the oxide ranged from 1.81-11.75 wt. % with a range of 5.31 wt. % in the wet season and 1.19-11.53 wt. % with range of 5.56 wt. % during the dry season, respectively. This average is higher than estimated in river sediments, measured as 4.8 wt. % (McLennan and Murray, 1999).

Rock types covering most part of the study were most likely the cause for the occurrence of these minerals. The prevailing elements Si, Al, Fe, Ti and Mn are theoretically hazardous to the aquatic environment. Upstream of the Sabie River catchment, Fe and Al are high compared to downstream. However, these concentrations were less at SB11 reflecting the dolomitic type of underlying rock at this particular site.

Table 21 Major elemental composition of stream sediment of the Sabie River system (wt. %).

Sample ID	SiO ₂ (wt. %)		Al ₂ O ₃ (wt. %)		Fe ₂ O ₃ (wt. %)		MnO (wt. %)		MgO (wt. %)		CaO (wt. %)		K ₂ O (wt. %)	
	WT	DR	WT	DR	WT	DR	WT	DR	WT	DR	WT	DR	WT	DR
SB01	48.83	51.19	19.52	18.7	11.75	11.53	0.16	0.12	0.73	0.95	0.52	0.49	1.44	1.7
SB02	68.74	60.48	12.95	15.2	4.77	9.69	0.14	0.19	0.79	2.09	1.63	1.74	2.79	1.72
SB03	68.42	72.08	8.55	7.9	10.28	8.72	0.23	0.13	0.6	0.49	0.35	0.31	1.02	1.14
SB04	77.51	63.1	9.02	12	3.21	8.82	0.06	0.18	0.77	0.47	0.72	0.34	2.29	1.72
SB05	66.03	56.92	12.25	14.2	6.75	8.41	0.12	0.15	0.54	0.52	0.4	0.47	2.22	1.94

SB06	70.31	74.26	10.35	9.19	7.11	6.32	0.1	0.06	0.51	0.4	0.6	0.56	2.29	2.35
SB07	73.52	79.25	10.91	8.84	4.56	3.5	0.1	0.07	0.44	0.27	0.6	0.65	2.61	3.03
SB08	72.88	87.13	11.8	6.15	3.39	1.19	0.09	0.02	0.36	0.12	0.82	0.48	2.73	2.2
SB09	83.85	65.76	7.5	11.7	1.81	10.17	0.04	0.89	0.43	0.63	0.58	0.35	2.13	1.02
SB10	40.24	57.1	17.04	17.6	9.78	10.07	0.12	0.08	0.68	1.14	0.81	0.69	1.32	2.02
SB11	69.86	80.82	6.02	6.14	3.14	2.73	0.27	0.22	1.3	1.5	1.87	1.92	1.25	1.41
SB12	82.65	60.67	5.67	10.3	5.83	10.04	0.17	0.24	0.41	0.5	0.21	0.62	1.02	1.25
SB13	70.85	85.28	11.06	7.46	8.44	1.38	0.83	0.04	0.62	0.28	0.19	0.54	1.05	2.76
SB14	79.01	81.55	7.43	6.79	6.01	5.08	0.48	0.28	0.42	0.33	0.12	0.12	2.12	2
SB15	57.52	70.89	25.2	15.1	3.75	2.77	0.04	0.09	0.54	0.42	0.18	0.33	4.45	5.51
SB16	79.18	84.63	9.26	7.51	3.33	1.66	0.03	0.02	0.49	0.29	0.46	0.44	3.17	3.04
SB17	80.19	66.59	9.57	15.3	1.62	4.09	0.02	0.06	0.3	0.51	0.52	0.87	3.12	2.92
SB18	78.67	85.66	9.44	6.59	3.31	2.4	0.14	0.18	0.4	0.23	0.57	0.25	2.47	1.88
SB19	86.15	91.37	6.28	3.38	2.21	1.32	0.02	0.02	0.3	0.15	0.18	0.21	1.36	0.98
SB20	82.23	65.46	8.58	14.5	1.97	4.15	0.04	0.11	0.27	0.6	0.77	1.39	2.83	3.11
SB21	65.15	76.68	13.61	10.1	6.73	2.65	0.13	0.04	1.63	1.08	1.25	1.33	2.16	2.9
Mean	71.61	72.23	10.97	10.7	5.31	5.56	0.15	0.15	0.59	0.62	0.61	0.67	2.21	2.22
SD	11.28	11.64	4.63	4.26	2.91	3.58	0.18	0.18	0.32	0.49	0.47	0.5	0.86	1.02
Wadopohl (1995)	66.8		15.1		4.09		0.07		2.3		4.24		3.19	

WT, wet season; DR, dry season

Values of chemical index of alteration (CIA) ranging between 45 and 55 indicates moderate weathering of the catchment area's rocks, while a value of 100 indicates extreme weathering, according to Nesbitt and Young (1982). In the Sabie River system, the CIA value of the Nestor MTSF was 74.03 and 75.6 (SB00) in the wet and dry seasons, respectively, but varied from 53.19 to 88.58 in the stream sediment the wet and dry seasons (SB01-09; Table 22). The wet and dry seasons both had high CIA values of 88.46 and 82.33. The underlying rocks, which are dolomite in the upstream of the River system and shales in relation to the Nestor gold mine mineralization, have an impact on this variation. This implies that the Sabie River experiences a wide range of chemical weathering. However, low CIA values were recorded at the granitic rock-underlain locations SB08, SB16, SB17, SB18, SB20, and SB21.

Table 22 Chemical indices of weathering in the Sabie River catchment.

Sample number	Chemical Index of Weathering (CIW)	
	WT	DR
SB00	74.03	75.6
SB01	88.58	86.33
SB02	53.19	82.26
SB03	83.96	93.16
SB04	68.94	82.3
SB05	72.73	77.78
SB06	64.52	62.07
SB07	61.76	57.14
SB08	56.10	48.11
SB09	77.29	89.26
SB10	88.46	82.33
SB11	66.49	60.18
SB12	50.88	84.33
SB13	88.75	49.01
SB14	72.44	70.84
SB15	75.93	56.96
SB16	57.43	53.02
SB17	50.43	62.65
SB18	56.22	62.93
SB19	70.57	63.74
SB20	49.85	50.45
SB21	66.20	49.44

WT, wet season; DR, dry season

Pearson correlation analysis reveals a substantial positive relationship amongst Fe and Ti and Al, Mg and Al, and P and Fe. Strong positive correlations amongst Ti with Al and Ca, Fe with Mg, and Mg with Cr and Ca, therefore, these element groups have similar input sources and/or close mineral associations.

4.4.1.2. Trace elements concentrations of the stream sediments

Table 23 shows the concentrations of trace element in the Sabie River system. Based on the XRF analysis, the mean sediment trace element concentrations show different increasing orders with seasons and the following orders were observed Cr>As>Cu>Zn>Ni>Co>Pb in the wet season and Cr>Cu>Zn>As>Ni>Co>Pb during the dry season. A significant variation was observed for Cu and Zn which were mostly highly concentrated during the dry season, while As was highly concentrated in the wet season.

There are currently no sediment quality guidelines (SQGs) in South Africa, so this study used the most widely used approach, TEC-ERC-ERM-PEC-SEC (Burton, 2002) from consensus-based guidelines (MacDonald et al., 2000; Table 15). Monitoring and analysing the results show that the metals species observed in sediments accumulated in higher concentrations in the study area, potentially causing toxicity to aquatic ecosystems. There are two sets of guidelines for sediment quality that were used to confirm the presence of toxicity and assess the adverse biological effects of contaminations. These applied SQGs are: toxic effect concentrations (TECs) as well as probable effect concentrations (PECs), where TEL denotes concentration below which toxic effects on aquatic organisms are unlikely to occur; whereas PEC denotes concentration which adverse effects may occur (CCME, 2001, McDonald et al., 2000; Long et al., 1998). Table 23 shows the results of comparisons between SQGs and metal concentrations.

From Table 23, the composition of As in stream sediment samples averages at 92.6 mg/kg with a standard deviation of 120.5 in the wet season; during the dry season, the average is 80.4 mg/kg with a standard deviation of 118.7. There are high concentrations of As recorded from the upper parts of the Sabie River system at SB03, and these decreased downstream towards the Kruger National Park as lower concentrations were recorded at SB08 and SB09 respectively. No As concentrations were recorded on the samples from the Goldstream (SB16), Sabana River (SB17), Sunlight River (SB19) and the Bega River (SB21). Furthermore, the As concentrations recorded, exceeded TELs in all samples (McDonald et al., 2000). The samples located near the mine sites had concentrations above PEC (SB12 Klein Sabie, SB14 Spitskop River, SB15 Rietfontein drainage). All these concentrations are larger than were maintained at SB03 (Sabie River) going downstream (SB07). This implies that there is a potential of adverse effects due to As on the Sabie River system.

Chromium averages 159.5 mg/kg with a standard deviation of 155.8 in the wet season; and 146.9 mg/kg average with a standard deviation of 100.3 during the dry season, indicating that Cr is prevalent in the study area. Meanwhile, the range is between 7 and 263 mg/kg in the wet season

as well as 4.5 and 382 mg/kg in the dry season. Toxic concentrations of 263 and 382 will pose a debilitating effect to the Sabie River system, thus monitoring is required at such sites. Cr concentrations in sediment samples were higher than other metals, most likely due to the direct discharge of untreated fertilizer waste (SB01-21). The higher Cr concentration measured in the Bega River (SB21) during the dry season indicates that its input could be derived from either residential or industrial wastes.

There are higher concentrations of Cu at the Rietfontein mine drainage (SB16) especially during the dry season (up to 1180 mg/kg DW), which can be attributed to the mineral chalcopyrite present in the ore from this mine site.

Table 23 shows that the metal species such as Ni, As, Cu, as well as Cr in most samples occur above the PEC guideline for a marine ecosystem, which implies that probable adverse effects might result in the ecosystem.

Table 23 Trace elements geochemistry of sediment from Sabie River catchment (mg/kg, dry weight).

Sample ID	As (mg/kg)		Co(mg/kg)		Cr (mg/kg)		Cu (mg/kg)		Ni (mg/kg)		Pb (mg/kg)		Zn (mg/kg)	
	WT	DR	WT	DR	WT	DR	WT	DR	WT	DR	WT	DR	WT	DR
SB01	22.9	16.8	36.8	37.9	262.8	276.7	85.6	77.8	102	104	22.8	20.9	88.9	89.9
SB02	8.0	14.8	18.9	35.8	215	273	31.9	64.6	36.9	93.6	16.8	30.8	48.9	72.8
SB03	383	293.5	38.9	35.8	193	205	78.9	74.8	76.8	81.9	17.8	17.8	136	110
SB04	55.9	322.1	14.9	34.8	119.2	154.9	30.9	221.9	24.5	72.9	11.9	23.2	30.9	95.5
SB05	269.8	276.9	24.7	30.8	109.6	135.7	102.8	158.7	48.5	64.6	15.5	19.9	75.5	92.6
SB06	185.7	278.6	18.6	16.7	107.7	110.5	51.9	40.8	37.8	37.9	12.8	12.9	54.5	46.7
SB07	147.9	ND	16.8	13.7	92.6	88.8	39.8	19.8	32.5	35.8	10.9	15.9	42.9	57.9
SB08	31.6	12.8	10.9	ND	68.6	77.7	19.8	5.9	17.5	8.0	11.8	6.0	35.8	8.9
SB09	16.9	15.8	6.8	61.9	80.8	240.1	9.9	67.8	16.8	102	6.9	13.8	14.6	64.9
SB10	15.9	18.5	32.8	32.7	235.5	267.5	72.9	62.8	82.8	91.8	17.8	19.8	82.9	82.9
SB11	22.8	17.7	21.7	18.5	252.9	381.8	34.8	26.6	40.7	37.9	26.8	12.8	44.8	24.4
SB12	169.5	233.5	33.9	42.8	182.9	201.9	66.7	177.7	55.9	108	11.9	38.9	84.9	295
SB13	12.5	10.5	60.5	2.9	210.5	51.8	57.8	8.0	84.7	14.8	10.8	7.9	54.6	6.9
SB14	132.7	185.6	73.9	88.7	161.5	206.6	110.6	146.6	83.5	86.8	26.6	28.8	63.8	48.8
SB15	89.9	80.5	12.7	17.8	18.9	23.9	419.0	1182	12.9	15.8	51.9	24.8	35.8	39.9
SB16	ND	ND	5.9	ND	38.5	23.9	6.9	5.0	13.7	9.9	10.0	8.9	23.7	13.7

SB17	ND	ND	3.9	10.9	59.8	119.6	5.9	14.7	17.7	46.8	8.1	11.8	10.8	38.8
SB18	12.8	6.9	22.8	24.5	58.9	80.8	30.9	32.9	1.9	41.7	8.0	7.0	25.7	16.9
SB19	ND	ND	5.7	ND	37.9	23.9	7.9	3.9	8.9	5.8	5.1	2.9	12.8	6.0
SB20	ND	88.7	4.9	8.9	34.9	84.9	7.0	18.5	9.0	21.5	8.9	9.2	13.8	23.6
SB21	ND	ND	37.8	9.9	709.7	239.7	39.9	10.0	173	40.8	15.9	9.0	79.9	24.8
Mean	93.4	81.0	25.1	26.0	158.3	154.5	67.2	114.9	49.0	54.5	16.7	15.9	51.2	81.4
SD	121.4	119.4	17.9	21.9	145.5	100.3	85.2	253.0	38.9	35.2	10.9	10.0	32.0	56.6
TEL	5.9				37.3		35.7		18		35		123	
PEC	33				111		149		48.6		128		459	

WT, wet season; DR, dry season; ND, not detected; TEL: threshold effect level (MacDonald *et al.*, 2000); PEC, probable effect concentration (MacDonald *et al.*, 2000)

There are no sediment quality guidelines for Co; therefore, values for upper continental crust were used for comparison. In the Sabie River the values of Co are above upper continental crust limits (SB 01, 02, 03, 04, 05, 06, 08, and 12). Due to lower water flowing during the winter, which might help toxic metal species accumulate in sediments, metal concentrations were lower in winter compared to summer.

The elemental composition of As, Co, Cr, and Ni suggests that the ores of the Sabie River catchment are associated with deep-seated magmatic and hydrothermal activity.

4.4.1.2.1. Sabie River (samples SB01-09)

There is huge variation in terms of As distribution in the samples from the Sabie River system (Fig. 19). High concentrations of As are reported from the Nestor MTSF (MTSF) compared to the samples from the Sabie River (SB01-SB09; Annexure A, Fig. 24-32) with an exception of sample SB03 during the wet season. Along the Sabie River, the values of Cr show a declining trend downstream (SB09, lowermost; Annexure A, Fig. 31) compared to values upstream (SB1 that is uppermost; Annexure A, Fig. 24). The concentration of Cr in the upper parts of the Sabie River is lower than that of the Nestor MTSF sample and it showed fluctuations with seasons. This can be attributed to the local geology, which is comprised of sediments enriched in these two elements at these particular locations (As and Cr). The As concentrations are above TEL and PEC for all samples except for site 02, 08 and 09, that had concentrations below PEC, implying that arsenic poisoning is likely to occur (Table 23).

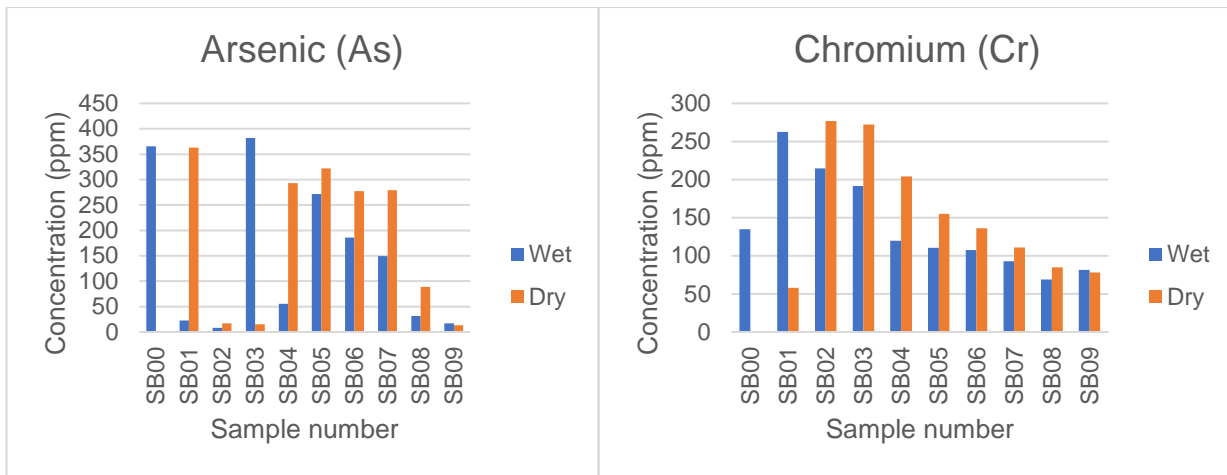


Figure 19 Seasonal variation in arsenic and chromium concentrations in the Sabie River.

4.4.1.2.2. Lone Creek (sample SB10)

The Cr concentrations were high at this sample site (236 mg/kg DW), taken just before the confluence with the Sabie River (Fig. 20). Also occurring in concentrations above PEC is Ni (83 mg/kg DW). There is no significant difference in metal concentrations between this site and SB01, which is located after the confluence of the two rivers (about 2 km downstream).

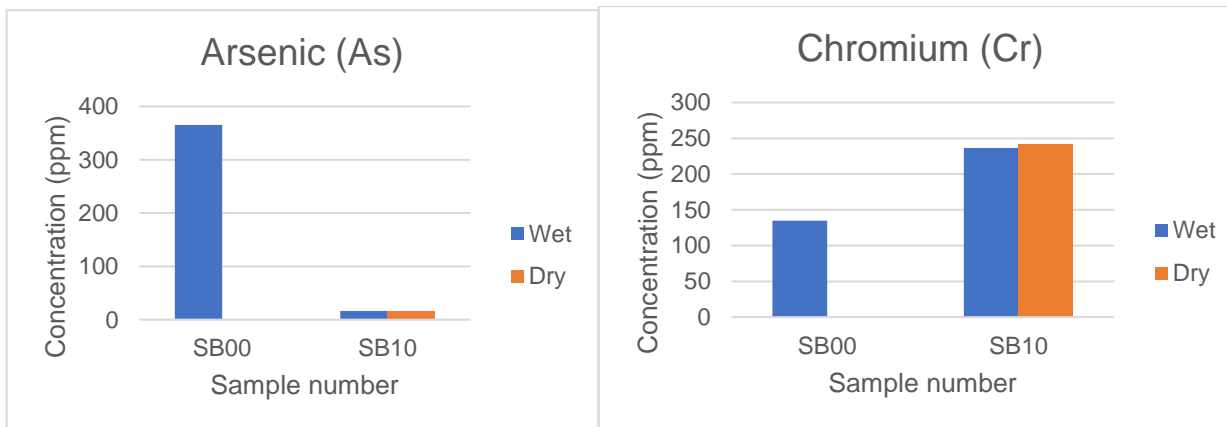


Figure 20 Seasonal variation in arsenic and chromium concentrations in the Lone Creek River.

4.4.1.2.3. Glynn's (sample SB11)

This is small stream flowing on the eastern side of the Glynn's Lydenburg MTSF. The concentrations of Cr and Ni were above both TEL (37.3 and 18 mg DW respectively) guidelines. In addition, the concentrations of the Cr are also above PEC guideline.

4.4.1.2.4. Klein Sabie River (samples SB12 and 13)

The concentrations of Cr and Ni are above TEL (37.3 and 18 respectively) and PEC (111 and 48.6 mg/kg DW respectively) at SB12, which is located near the Sabie Waterfalls, after the confluence with the AMD stream from Nestor TSF. In addition, sediments from this site consist of high As concentrations (170 ppm and 234 mg/kg DW in the wet and the dry seasons respectively), above PEC guidelines.

4.4.1.2.5. Spitskop River (sample SB14)

The stream sediment in Spitskop River contained elevated concentrations of As, Cr, Cu, as well as Ni that exceeded PEC guidelines. There were illegal mining activities observed at the upper reaches of the river, which implies that there is a possibility of adverse effects on aquatic organisms because of those metal species.

4.4.1.2.6. Riet-mine (sample SB15)

This is the drainage located west of Rietfontein mine adit, flowing in a north-easterly direction towards the Sabie River. Drainage sediments were found to be enriched in Cu and As and they were above PEC guidelines. The concentrations of Pb also poses a threat to aquatic life as they were above probable effect concentrations (MacDonald *et al.*, 2000). The elevated As and Cu concentrations at this site can be accredited to the existence of arsenic, bismuth as well as copper sulphides existing in the ore from the Rietfontein mine.

4.4.1.2.7. Goldstream (sample SB16)

The concentrations of all metal species are within SQGs (MacDonald *et al.*, 2000) except for the Cr, which was just above the TEL at 39 mg/kg DW.

4.4.1.2.8. Sabana River (sample SB17)

All metal concentrations are below the TEL values with the exception of Cr (60 mg/kg DW). At this sample site, no concentrations of As were recorded. There are minimum external environmental stressors in this point.

4.4.1.2.9. Mac-Mac River (sample SB18)

Forestry is the main activity around this sample point and there were no mining activities observed. The sediments were enriched in As, Cr and Ni and with concentrations above the TEL guideline and pose potential metal species enrichment.

4.4.1.2.10. Sunlight River (sample SB19)

Located near the Mac-Mac River (SB18), forestry is also the main activity taking place in the area. Only Cr concentrations were above TEL (38 mg/kg DW) and all metal concentrations were within the SQGs while As was below detection limits.

4.4.1.2.11. Nkambeni River/Noord Sand (sample SB20)

In this site, metals of concern are Cr and Ni as they were above TEL (37.3 and 18 ppm respectively) values. In addition, As poisoning is likely on sediments as the concentrations are above TEL (5.9 mg/kg DW) guideline.

4.4.1.2.12. Bega River (sample SB21)

This is a branch of the Sand River, which is a branch of the Sabie River. No concentrations of As were recorded (below detection limits) at this sample site, however very high concentrations of Cr were recorded at this site (710 mg/kg DW). Also occurring above PEC guideline during the wet season, was the concentration of Ni.

4.4.1.2.13. Enrichment factor (EF)

According to Zhang and Liu (2002), sediment EF values around 1.0 specify that the element in question be primarily derived from crustal material and/or weathering processes, whereas EF values much greater than 1.0 specify that the element is anthropogenic. Snzefer et al. (1996) and Chen et al. (2007) developed six contamination categories based on enrichment factor values (Table 24).

Table 24 Values for enrichment factor.

EF<3	Minor enrichment (anthropogenic impact)
EF= 3-5	Moderate enrichment
EF= 5-10	Moderately severe enrichment
EF= 10-25	Severe enrichment
EF= 25-50	Very severe enrichment
EF>50	Extremely severe enrichment

The EF values for trace elements in the Sabie River system shows insignificant to acute enrichment (Table 25). While elements like Zn, Ni, Cu, Pb, As, as well as Cr revealed a high level

of contamination with EF of greater than six (6); 1EF3 were revealed by cobalt. However, Pb, Ni, Cr, as well as Cu fluctuated dependent on season, wherein they had CV values of less than six.

Table 25 Trace metals enrichment factor.

Sample ID	As		Co		Cr		Cu		Ni		Pb		Zn	
	WT	DR	WT	DR	WT	DR	WT	DR	WT	DR	WT	DR	WT	DR
SB01	1.45	1.34	1.44	0.89	3.63	1.99	2.28	1.37	2.95	1.43	2.52	1.77	2.77	3.08
SB02	0.4	1.23	0.6	0.88	2.34	2.03	0.68	1.19	0.86	1.36	1.47	2.72	1.22	2.6
SB03	49.62	48.19	3.05	1.75	5.37	3.05	4.26	2.74	4.57	2.37	3.87	3.16	8.6	7.75
SB04	3.25	31.94	0.53	1.03	1.51	1.4	0.74	4.89	0.66	1.27	1.17	2.54	0.87	4.12
SB05	17.63	26.23	0.97	0.87	1.55	1.17	2.79	3.35	1.46	1.08	1.75	2.02	2.41	3.81
SB06	12.81	26.83	0.79	0.48	1.6	0.97	1.49	0.88	1.2	0.64	1.47	1.33	1.85	1.95
SB07	14.12	0	1.01	0.32	1.9	0.62	1.59	0.34	1.45	0.49	1.79	1.32	1.97	1.94
SB08	2.32	1.81	0.47	0	1.09	0.98	0.6	0.19	0.61	0.19	1.45	0.81	1.28	0.56
SB09	1.64	2.63	0.42	3.02	1.66	3.6	0.4	2.49	0.75	2.92	1.14	2.46	0.7	4.55
SB10	1.21	1.29	1.48	0.66	3.8	1.66	2.24	0.95	2.84	1.1	2.32	1.45	3.01	2.44
SB11	2.72	2.56	1.6	0.8	6.52	4.93	1.76	0.85	2.27	0.95	5.56	1.97	2.64	1.54
SB12	26.68	40.63	3.28	2.21	6.19	3.19	4.39	6.79	4	3.27	3.19	7.22	6.5	22.07
SB13	1.64	1.21	4.61	0.1	5.58	0.52	2.97	0.19	4.79	0.29	2.25	0.94	3.32	0.34
SB14	9.61	17.35	3.26	2.46	2.52	1.76	3.33	3.05	2.76	1.43	3.33	2.89	2.25	1.98
SB15	1.97	2.3	0.17	0.15	0.09	0.06	3.81	7.45	0.13	0.08	1.92	0.76	0.39	0.5
SB16	0	0	0.29	0	0.66	0.17	0.23	0.08	0.51	0.14	1.25	0.77	0.92	0.49
SB17	0	0	0.18	0.27	0.9	0.9	0.18	0.27	0.56	0.68	0.9	1.05	0.37	1.39
SB18	0.99	1.01	0.98	1.01	0.99	1	0.99	1	1	1	0.99	0.97	1	1
SB19	0	0	0.54	0	1.13	0.57	0.48	0.26	0.59	0.29	1.07	0.93	0.85	0.63
SB20	0	8.43	0.22	0.27	0.54	0.73	0.2	0.4	0.29	0.37	1.11	0.9	0.48	0.94
SB21	0	0	1.84	0.29	12	2.13	1.31	0.21	6.19	0.7	2.12	0.91	3.08	1.06
Min	0	0	0.17	0	0.09	0.52	0.18	0.08	0.13	0.08	0.9	0.76	0.48	0.34
Max	49.62	48.19	3.05	3.02	12	4.93	4.26	7.45	4.57	3.27	5.56	7.22	8.6	22.1

WT, wet season; DR, dry season

The geological background of the catchment area is controlled by metamorphic and granitic rocks, which are composed of minerals that can encompass trace elements in their structure. Urban contributions from the catchment shoreline that release a huge bulk of wastewater (Sabie and Hoxane), landfill leachates, and agrochemicals from nearby residential areas (Simile to Skukuza), traffic (release of toxic elements such as Pb and Sb), and abandoned tailings storage facilities are all anthropogenic sources of trace elements (As). Elements such as Zn, Cr, Pb, Co, and Cu are common components of agrochemicals (Forstner and Wittmann, 1981), and urban solid and liquid wastes are high in Cu, Pb, Ni, and Zn (DVWK, 1998).

4.4.1.2.14. Geo-accumulation Index

The geo-accumulation index (I_{geo}) of sediments revealed that As contamination is extremely high at some sites, particularly in winter (Table 26). According to the geo-accumulation index, the Bega River (SB21) has a great probability for Cr and Ni contamination, while the drainage near Rietfontein Mine has a high potential for Cu-Pb contamination (SB15). The geo-accumulation indices revealed unpolluted to moderately polluted sediments for elements such as Cu, Zn, Pb, Co, Pb, and Cr at most sites. Therefore, the toxic elements pollution that is resulting from mine wastes may be likely limited to As.

Table 26 Trace elements geo-accumulation in sediment from the Sabie River system.

Sample ID	As		Co		Cr		Cu		Ni		Pb		Zn	
	WT	DR	WT	DR	WT	DR	WT	DR	WT	DR	WT	DR	WT	DR
SB00	5.64		0.11		0.45		0.5		0.23		1.01	0.63	0.21	
SB01	0.35	0.46	0.35	0.3	0.89	0.65	0.55	0.3	0.72	0.19	0.62	0.93	0.68	1.06
SB02	0.12	0.41	0.19	0.29	0.73	0.64	0.21	0.29	0.27	0.45	0.46	0.54	0.38	0.86
SB03	5.9	7.95	0.37	0.29	0.65	0.48	0.21	0.29	0.55	0.39	0.47	0.72	1.04	1.28
SB04	0.86	8.73	0.14	0.28	0.41	0.37	0.2	0.28	0.18	0.35	0.32	0.6	0.24	1.13
SB05	4.19	7.51	0.23	0.25	0.38	0.32	0.67	0.25	0.35	0.31	0.42	0.39	0.58	1.09
SB06	2.87	7.57	0.18	0.14	0.37	0.26	0.34	0.14	0.27	0.18	0.34	0.48	0.42	0.55
SB07	2.3	0	0.17	0.11	0.32	0.21	0.26	0.11	0.23	0.17	0.3	0.16	0.33	0.68
SB08	0.49	0.35	0.1	0	0.23	0.18	0.13	0	0.13	0.04	0.31	0.42	0.28	0.11
SB09	0.27	0.43	0.07	0.5	0.28	0.57	0.07	0.49	0.12	0.31	0.19	0.6	0.12	0.75
SB10	0.25	0.51	0.31	0.26	0.8	0.63	0.47	0.26	0.6	0.44	0.49	0.39	0.64	0.98
SB11	0.35	0.49	0.21	0.15	0.86	0.9	0.23	0.15	0.6	0.18	0.73	0.48	0.35	0.29

SB12	2.63	6.35	0.33	0.35	0.62	0.48	0.44	0.35	0.4	0.51	0.32	0.24	0.65	3.46
SB13	0.2	0.3	0.59	0.03	0.72	0.12	0.38	0.03	0.61	0.07	0.29	0.87	0.43	0.08
SB14	2.06	5.05	0.71	0.71	0.55	0.49	0.72	0.71	0.6	0.42	0.73	0.75	0.49	0.58
SB15	1.39	2.2	0.42	0.14	0.06	0.06	2.72	0.14	0.09	0.08	1.38	0.27	0.28	0.48
SB16	0	0	0.59	0	0.13	0.06	0.05	0	0.1	0.05	0.25	0.36	0.18	0.16
SB17	0	0	0.04	0.09	0.2	0.28	0.04	0.09	0.13	0.23	0.21	0.2	0.09	0.46
SB18	0.2	0.2	0.2	0.2	0.2	0.19	0.2	0.2	0.2	0.2	0.2	0.1	0.2	0.2
SB19	0	0	0.06	0	0.13	0.05	0.05	0	0.07	0.03	0.12	0.27	0.1	0.06
SB20	0	2.41	0.05	0.08	0.12	0.2	0.05	0.08	0.06	0.11	0.25	0.26	0.11	0.27
SB21	0	0	0.37	0.08	2.4	0.57	0.26	0.08	1.23	0.2	0.43	0.26	0.94	0.29

WT, wet season; DR, dry season

4.4.1.3. Rare earth elements in stream sediments

The concentrations of rare earth elements (REEs) in the Sabie River catchment are shown in Table 27. As the concentration intensities of these elements were below the detection limits, data for Pr, Er, Tb, Ho, Eu, Gd, Tb, Dy, Tm, Gd, and Lu were not included. The mean rare earth elemental levels for Ce and Yb in the samples were marginally greater than the upper continental crust, as per Rudnick and Gao (2003).

Individual REE concentrations in sediments, according to Zhu and Liu (1988), are usually dependent on their respective parent materials. The significant concentrations of REEs observed along the Sabie River catchment can be attributed to the metamorphic and igneous rocks exposed in the Sabie region, such as gneisses, quartzite, and granites (Tayler, 1985). REE concentrations are higher in sediments resulting from metamorphic and granitic rocks, particularly those of the granitic rock type (Herman, 1970; Ure and Bacon, 1970; Reiman and Caritat, 1988; Hu et al., 2006). Anthropogenic contributions like fertilizers, phosphate, manure, and waste effluent can also affect and enrich REE concentrations in sediments (Wang et al., 2004; Protano and Riccobono, 2009).

Table 27 Total REE concentrations in the stream sediment from Sabie River Catchment with descriptive statistics.

Sample ID	Ce (mg/kg)		La (mg/kg)		Nd (mg/kg)		Sm (mg/kg)		Y (mg/kg)		Yb (mg/kg)	
	WT	DR	WT	DR	WT	DR	WT	DR	WT	DR	WT	DR

SB01	95	99	52	27	35	35	ND	ND	28	26	9	4.7
SB02	73	63	39	32	29	29	ND	ND	19	22	ND	4.1
SB03	65	54	25	ND	16	22	ND	ND	20	18	7	3.2
SB04	48	99	22	37	16	35	ND	ND	11	28	ND	ND
SB05	102	119	44	48	33	42	ND	5.7	23	29	4	3.8
SB06	79	59	33	18	29	24	ND	ND	16	14	4	ND
SB07	35	139	8	50	11	42	ND	ND	5	18	ND	ND
SB08	72	12	9	12	24	7.8	ND	ND	10	3.7	ND	ND
SB09	34	68	5	ND	12	18	ND	ND	6	44	ND	5.2
SB10	48	74	18	22	9	27	ND	ND	15	19	ND	3.4
SB11	38	25	24	ND	13	10	ND	ND	11	8.4	ND	ND
SB12	27	69	20	26	9	32	ND	ND	6	44	ND	5.2
SB13	63	13	23	ND	15	6.8	ND	ND	13	3.8	6	ND
SB14	92	92	25	29	17	7.8	ND	ND	13	12	ND	ND
SB15	134	97	72	41	56	38	ND	5.6	35	30	ND	ND
SB16	53	29	32	ND	24	18	ND	ND	16	12	6	ND
SB17	27	131	20	56	9.1	49	ND	7.1	11	24	ND	ND
SB18	44	12	24	11	20	12	ND	ND	7	5.6	7	ND
SB19	29	8.8	18	11	14	9	ND	ND	6.8	4.2	ND	ND
SB20	66	36	33	12	21	16	ND	ND	13	7.4	ND	ND
SB21	81	30	44	ND	28	15	ND	ND	14	8.6	6	ND
Mean	62.14	63.28	28.1	20.57	20.96	23.59	0	0.88	14.23	18.18	2.33	5.2
Min	27	8.8	8	0	9.1	6.8	0	0	5	3.7	0	0
Max	134	139	52	56	56	49	0	7.1	35	44	9	5.2
SD							0					
UCC	63		31		27		4.7		21		2	

WT, wet season; DR, dry season; Min, minimum; Max, maximum, SD, standard deviation; Nd, not detected

Pearson correlation analysis (Table 28) has shown (1) a highly significant correlation between the LREE group (La, Ce, and Nd) and (2) a highly significant correlation between the HREE Y and the LREE La. HREEs Yb and Sm, on the other hand, showed a negative correlation. These

findings point to comparable input sources, endorsing the mutual geochemical properties of the REEs as well as the above-mentioned findings.

Table 28 The Pearson correlation coefficient of REEs in the Sabie River catchment.

	La	Ce	Nd	Y	Yb	Sm
La	1.00					
Ce	0.81	1.00				
Nd	0.89	0.89	1.00			
Y	0.89	0.86	0.85	1.00		
Yb	0.27	0.17	0.20	0.25	1.00	
Sm	0.40	0.30	0.36	0.43	-0.27	1.00

4.4.2. Stream sediment mineralogy

Granite, gneiss, quartzite, and dolomite dominate the uncovered underlying lithologies of Sabie River system. Consequently, surficial sediment samples of stream sediment mineralogy are closely related to the prevailing rock outcrops. All mineral phases observed from the X-ray diffraction (XRD) data analyses are recorded in Table 29. The XRD data was used for qualitative mineralogical determination of seepage and surface water.

The mineralogy of the sediments is dominated by quartz and no variations were found in the sampling during the different seasons (22-93 wt. % and 55-94 wt. % wet and dry seasons respectively) followed by K-feldspar (up to 34 wt. %), and the phyllosilicates (mica & clay) have concentrations varying from 0 to 17 wt. %. In addition, the carbonate mineral dolomite, is only found in the upper parts of the Sabie River system, in the proximity of Glynn's Lydenburg with concentrations of between 1 and 8 wt. % (SB02 and SB11). The principal secondary minerals in the Sabie River system are hematite and gibbsite. The secondary iron oxide mineral hematite, which was mostly found during the dry season in low concentrations of up to 2 wt. % throughout the Sabie River (upstream to downstream). Gibbsite is sporadically present in some samples at the upper reaches of the catchment reaching concentrations of up to 12 wt. %. In terms of clay minerals, kaolinite and smectite represents the class as they occur sporadically within some samples, especially in the upper parts of the Sabie River system.

Table 29 Mineralogical composition of sediments from the Sabie River system.

Sample ID	Quartz (wt. %)		K-feldspar (wt. %)		Dolomite (wt. %)		Hematite (wt. %)		Gibbsite (wt. %)		Kaolinite (wt. %)		Smectite (wt. %)	
	WT	DR	WT	DR	WT	DR	WT	DR	WT	DR	WT	DR	WT	DR
SB01	71	57	1	1	ND	ND	ND	2	5	4	5	15	6	ND
SB02	53	60	14	1	ND	6	ND	1	ND	2	1	11	ND	ND
SB03	88	69	2	9	ND	ND	ND	2	2	3	2	8	ND	ND
SB04	64	62	16	17	ND	ND	ND	1	3	4	2	7	ND	ND
SB05	72	69	10	5	ND	ND	ND	1	3	5	3	11	ND	ND
SB06	51	76	21	7	ND	ND	ND	1	2	1	2	3	ND	ND
SB07	55	71	14	17	ND	ND	ND	1	ND	1	2	2	ND	ND
SB08	67	87	14	7	ND	ND	ND	ND	ND	ND	ND	ND	ND	ND
SB09	73	85	10	1	ND	ND	ND	1	ND	5	ND	2	ND	ND
SB10	58	52	2	ND	ND	ND	ND	1	10	6	4	17	4	ND
SB11	86	74	4	4	3	8	ND	ND	ND	1	ND	3	ND	ND
SB12	84	84	8	1	ND	ND	ND	1	2	3	ND	4	ND	ND
SB13	88	67	ND	21	ND	ND	ND	ND	12	ND	ND	1	ND	ND
SB14	93	85	7	4	ND	ND	ND	ND	ND	ND	ND	3	ND	ND
SB15	22	55	34	21	ND	ND	ND	1	ND	ND	17	4	ND	ND
SB16	61	80	14	11	ND	ND	ND	ND	ND	trace	ND	1	4	ND
SB17	71	62	17	7	ND	ND	ND	ND	ND	trace	ND	5	ND	ND
SB18	72	84	10	6	ND	ND	ND	ND	2	ND	ND	1	ND	ND
SB19	85	94	4	3	ND	ND	ND	ND	3	ND	ND	1	ND	ND
SB20	61	72	14	9	ND	ND	ND	ND	ND	ND	ND	3	ND	ND
SB21	52	73	17	7	ND	ND	ND	ND	ND	ND	ND	ND	ND	2

WT, wet season; DR, dry season

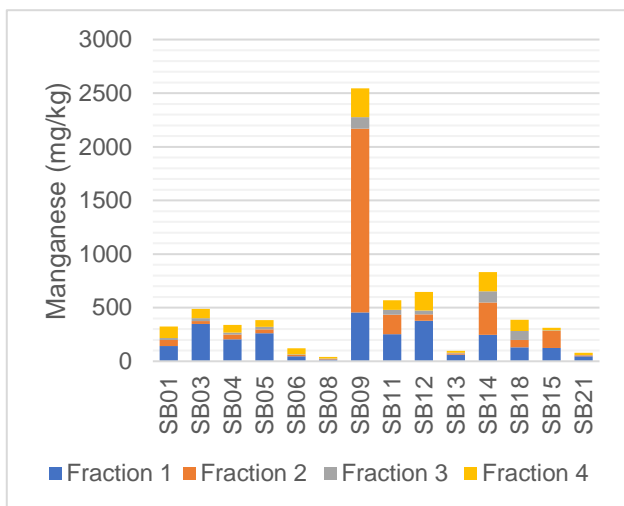
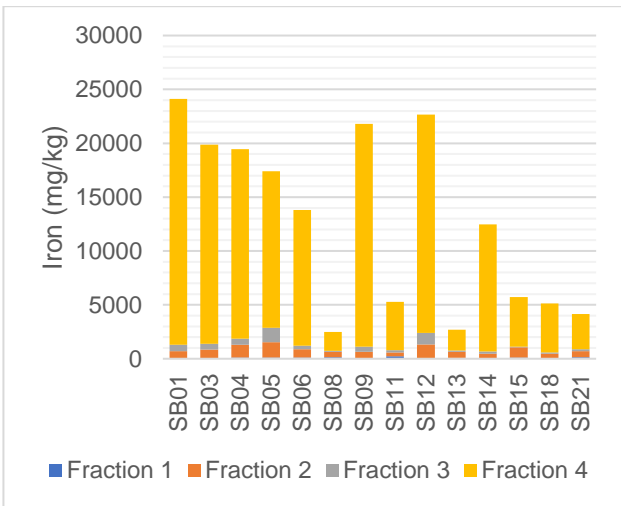
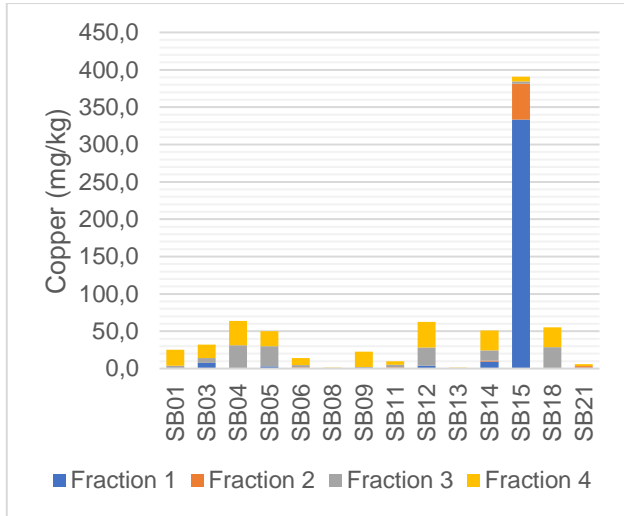
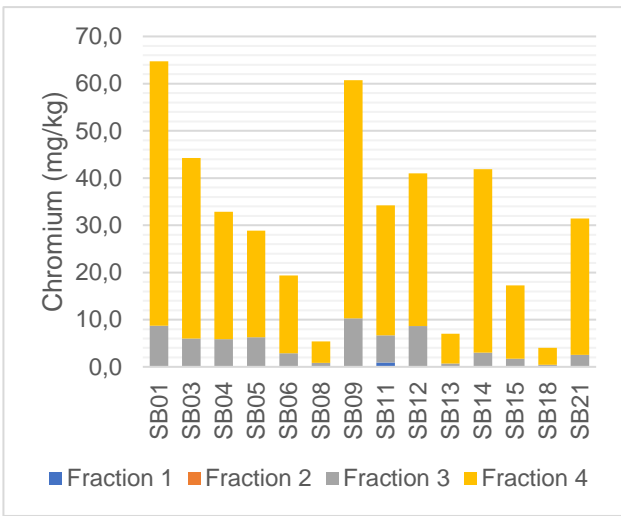
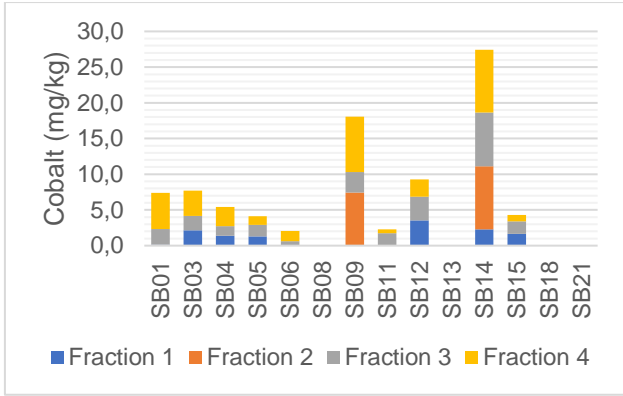
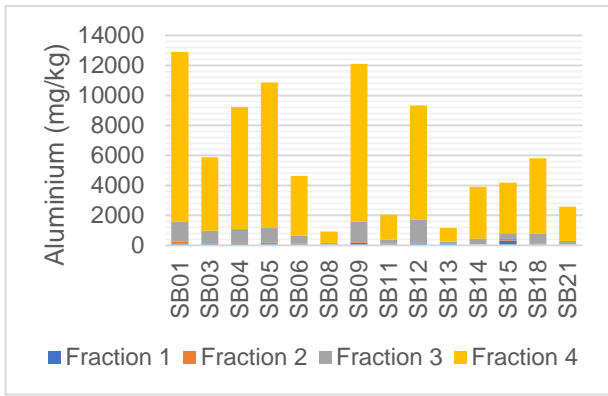
There is a large variation in terms of mineralogy that is influenced by the source rocks and the degree of weathering. The highest concentration of the clay mineral kaolinite is found at the Rietfontein drainage (SB15), which is consistent with geochemical data found Al_2O_3 as the second most dominant major element in this site. This is further supported by the elevated concentrations of K-feldspar that are found at this site that might be microcline as it is located on the granitic rock.

4.4.3. Speciation of metals in stream sediments

To better distinguish the biological and chemical accessibility of the measured metals, a 4-stage sequential extraction was undertaken on the stream sediments (Annexure D). Each phase was extracted into four operationally defined phases: exchangeable, Fe-Mn and carbonate, organics and sulphides, and silicate. Metal concentrations associated with carbonate and Fe-Mn oxide extractions were thought to be chemically moveable because these phases can discharge trace metals into the ecosystem when geochemical conditions change.

The results shows that Al is predominantly partitioned in the inert fraction, which implies that the majority of Al extracted from the sediments of the Sabie River system, is from the geogenic source. A similar trend can be seen for iron, which is also predominant in the inert fraction (Fig. 21). Therefore, Al and Fe toxicity is not a threat to the organisms in the Sabie River system. This can be attributed to the dissolution of clay mineral and incomplete dissolution of the metals (Fe and Al) in the third step (F3) because of the exceedingly high concentrations of these metals. Cobalt was not partitioned in all samples (SB08, SB13, and SB21) and it is highly concentrated in the third and fourth fractions. Anomalous concentration found at SB14 can be ascribed to the illegal mining activities observed in the upper parts of the Spitskop River. The distribution of copper is highly variable, and it is portioned in the exchangeable fraction, predominantly in samples SB15, SB14, SB03, SB05, SB122, and SB21, in decreasing order of abundance. The anomalous concentration observed at SB15 (333 mg/kg) can be attributed to the illegal mining observed on the drainage near abandoned Rietfontein gold mine. Other metal species like As, Cr, Pb, and Zn are highly portioned in the fraction 4 and fraction 3 respectively, implying that they are not bioavailable unless the pH of the water in the river catchment area can be reduced (at F3: bound to carbonate). Therefore, these metal species were not anthropogenically introduced into the sediments.

There is huge variation in terms of manganese distribution as it is found highly partitioned in fraction 1 and fraction 2, which are readily bioavailable. This can be used as an indicator of the degree of pollution from the anthropogenic sources around the Sabie River system. The greater the relative quantity of metal in the exchangeable fraction, the higher the degree of pollution. Higher concentrations of Mn were expected at the upper parts of the Sabie River, since the area is underlain by the dolomite of the Malmani Subgroup.



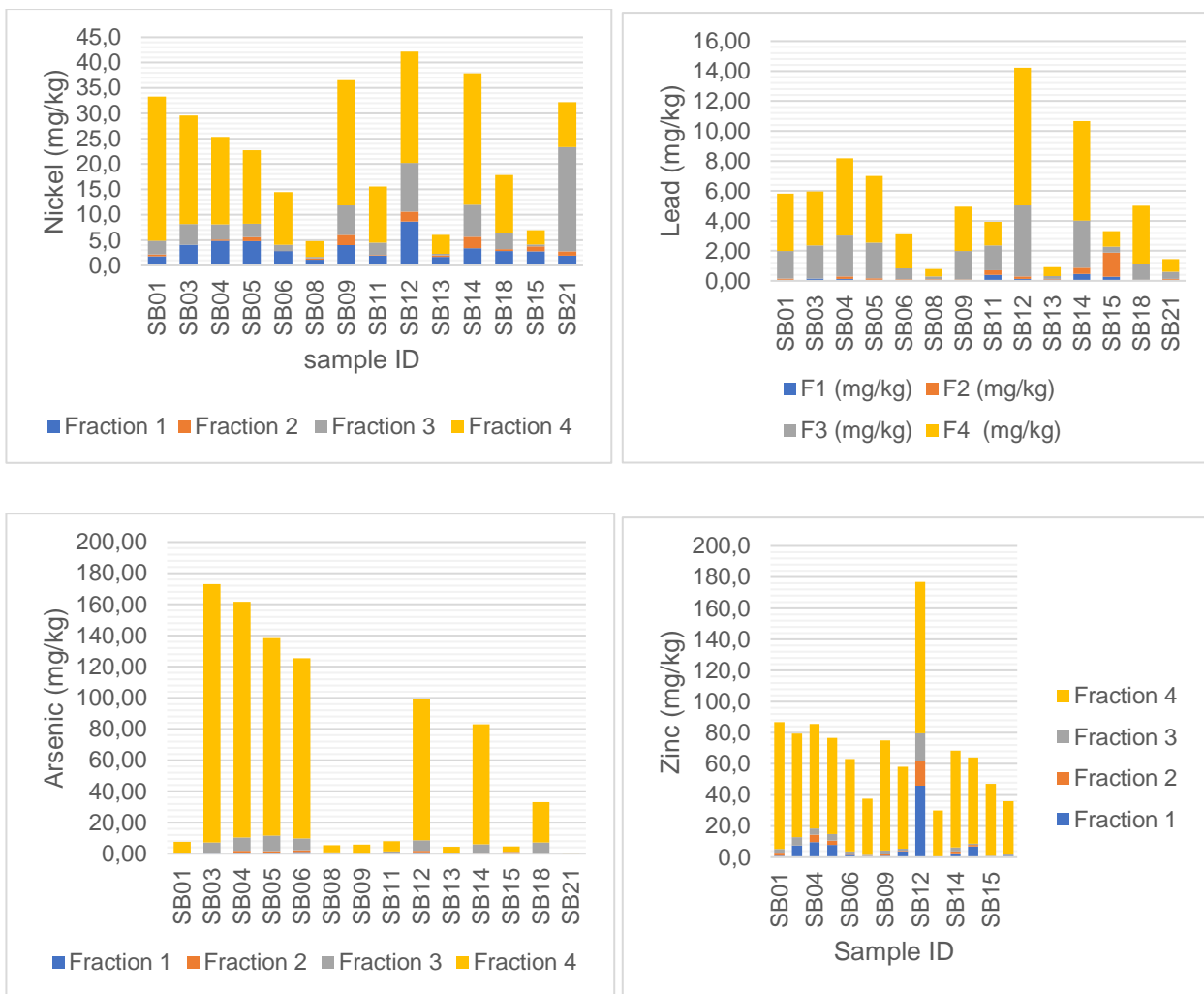


Figure 21 Metal species concentrations (mg/kg) in the different fractions in the stream sediments.

Chromium is distributed only in the third and fourth fractions, the oxidisable organics and sulphides fraction as well as the inert fraction respectively. This implies that Cr may only become bioavailable upon exposure to oxidising conditions. Manganese is highly portioned in the exchangeable and the reducible Fe-Mn oxide/carbonate fractions. Consequently, any change in the ionic structure of water would have a significant influence on the adsorption-desorption and ion exchange processes of Mn ions with main components of sediments. Furthermore, lowering the pH of the water will remobilize Mn due to the reduction of ferric oxide and Mn(IV) under anoxic environments and their subsequent dissolution. Despite its low concentration in the exchangeable fraction, Ni is primarily partitioned in the inert fraction and is unlikely to be mobilized under normal environmental conditions in the Sabie River system. The inert fractions contain the highest concentrations of lead (Pb) and zinc (Zn).

From the sequential extraction of stream sediments, the highest average concentration of the investigated metal species Al, Fe, Co, Mn, Cr, Ni, Cu, Ni, Zn, Pb, and As, is in the silicate (F4) fraction, which implies the geogenic origin of these elements. The concentration of metal species found in the geochemically mobile Fe-Mn oxide and carbonate extractions in the Sabie River system as percent of total metal concentration was found to be in order of Fe>Al>Mn>Zn (Fig. 12). In addition, the metal concentrations of As, Co, Cr, Cu, Ni and Pb are not bioavailable as their concentrations were very low to none. Therefore, the metal species from the sediment of this river system pose little to no threat to the organisms in the system as they originate from the natural source.

4.5. Water Quality

Assessing the water quality should include chemical measures such as pH, dissolved oxygen (DO), nutrients (nitrates and phosphorus), total dissolved solids (TDS), and metal species (Lollar, 2005). All of the above-mentioned parameters were considered for this study and their seasonal variation in the Nestor MTSF seepage and Sabie River system are discussed below.

4.5.1. Spatial distribution of pollutants from mine effluent

Samples of water were taken from AMD around Nestor MTSF to define the distribution of pollutants as well as nature of their species. These include a pond of seepage near the Nestor MTSF and traced downstream to a distance of about 100 m under the Klein Sabie Bridge. In addition, the water decanting from the Rietfontein mine adit was also collected and analysed. The physicochemical data of the mine effluents, namely, pH, electrical conductivity (EC), redox potential (Eh), dissolved oxygen (DO) and alkalinity are shown in Table 30. These parameters suggest a highly variable nature as regards to seasonal continuity, water volume and acidity/alkalinity between the Nestor and the Rietfontein Mines effluents. The pH levels measured at the proximity of the Nestor MTSF is acidic, in the range of 2.5 near MTSF and 3.0 under the bridge respectively that is typical of AMD (Gray, 1998). The concentration of total dissolved solids (TDS) in all samples was also high as indicated by the EC value (up to 3890 $\mu\text{S}/\text{cm}$). However, water decanting from the Rietfontein Mine adit had an alkaline pH of 8.3 coupled with a low redox potential (-35.2 mV) and total alkalinity of 38.9 CaCO_3 equivalent, which is a good quality compared to the seepage from the Nestor MTSF.

Table 30 Physicochemical parameters of Nestor TFS seepage measured onsite.

Sample ID	pH	EC ($\mu\text{S}/\text{cm}$)	Eh (mV)	DO (mg/L)	Alkalinity (mg/L CaCO_3)
NS01	2.5	9740	270.2	5.9	0

NS02	3	1023	221.5	6.8	0
RF01	8.3	890	-35.2	7.5	38.9
SANS (2015)	5-9.7	≤170			
WHO (2011)	7.0-8.5	2500			

The trend of pollution decreased downstream as the lower values were recorded at NS02, where a substantial drop in the Fe concentration was observed, with a subsequent increase in pH of 3.5 along the AMD watercourse (Table 31). This drop can be attributed to precipitation because Fe is less soluble at pH values near four (4). As a result, secondary minerals in the Nestor MTSF efflorescent crusts add to the discharge of Fe and SO₄ in the solution. In terms of water quality, the most challenging pollutants were found in trace amounts, as shown in Table 30. Metal species like as Al, Fe, As, Zn, as well as Cu occur in mine water at higher concentrations than SANS241 (2015) and WHO (2011) guidelines and pose a contamination threat to the receiving water bodies. There was a decrease in metal species concentration from the seepage next to the Nestor MTSF (NS01) to downstream under the Klein Sabie Bridge (NS02) and that can be attributed to precipitation and adsorption species by sediments. In addition, elevated concentrations of metal species and sulphate together with high EC and low pH could suggest that the water is highly polluted. All the concentrations of metal species were within the SANS241 (2015) and WHO (2011) guidelines for the Rietfontein Mine water sample except for As which was slightly high.

Table 31 Major cations, anions, and trace elements of seepage from Nestor TSF.

Sample ID	Ca	Mg	Cl	SO ₄	As	Fe	Al	Mn	Cu	Cr	Zn
	mg/L	mg/L	mg/L	mg/L	mg/L	mg/L	mg/L	mg/L	mg/L	mg/L	mg/L
NS01	68.4	9	47.3	3650	16.1	4964	339.6	11.4	111.3	4.6	25.2
NS02	14.11	3.27	35.2	2970	0.22	15.11	44.8	3.1	0.45	0.1	0.32
RF01	53.3	28.7	113	252	1.26	0.14	0.24	<0.01	<0.01	<0.01	<0.01
SANS241 (2015)	150	70	300	500	0.01	2	0.3	0.4	≤2	≤0.05	0.05
WHO (2011)	<200	50	≤250	≤250	0.01	-	0.1	0.4	2	0.05	2

Based on the chemical composition data, Fe, Al, and Mg are the most common dissolved metal species in the AMD (with Fe>Al>Ca>Mn>Cu>Zn). Therefore, the minerals that are commonly

formed in these AMD environments are mainly Al, Ca, Fe(II), Fe(III), as well as Mg sulphates and (oxy)hydroxysulphates. In the seepage from the Nestor MTSF, Ca and Mg are the major cations while SO_4 and Cl are the major anions and the water type is Fe- SO_4 (Fig. 22).

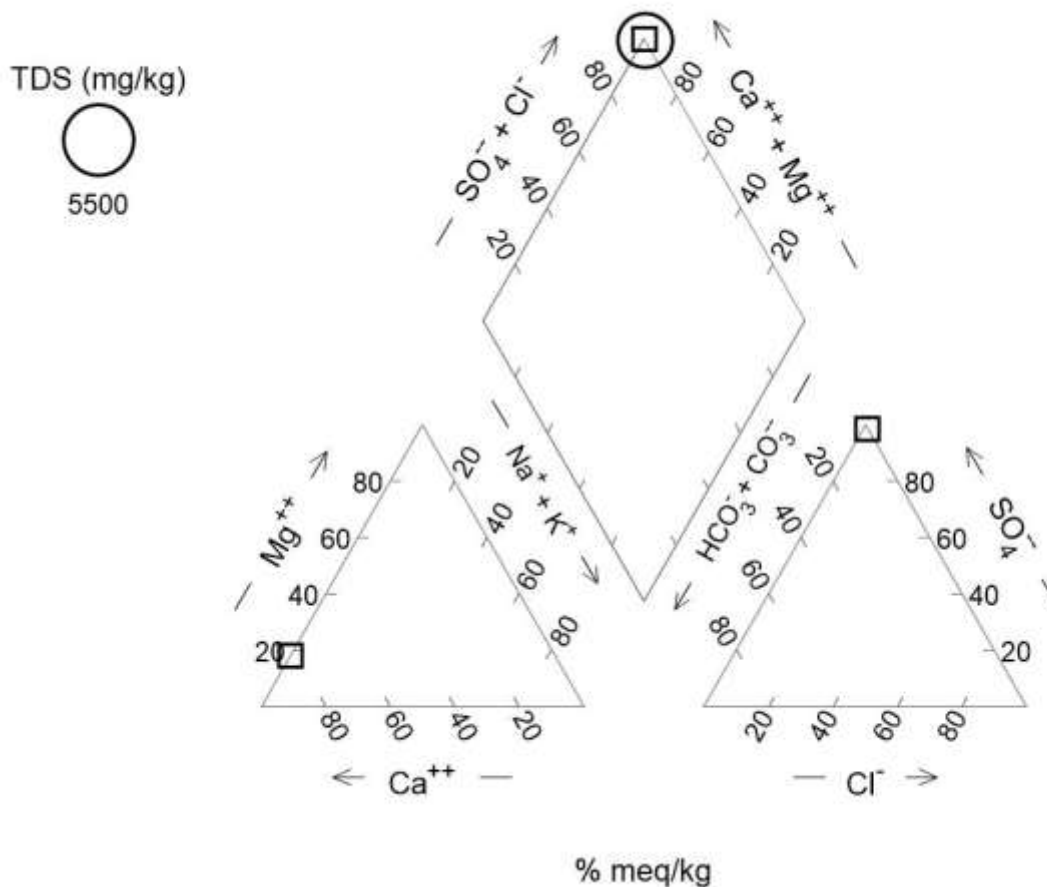


Figure 22 Chemical constituents distribution in Nestor TSF seepage.

4.5.2. Spatial distribution of pollutants in surface water

The hydro chemical characteristic changes of the Sabie River catchment has been investigated. Seasonal variation of parameters, analysed onsite and the alkalinity are presented in Table 32. For both seasons, in the uncontaminated Sabie River system (SB01 to SB21) the pH values were alkaline in all surface water samples with average values of 7.5 in the wet season and 7.9 in the dry season respectively. All pH values noted in both seasons occur in acceptable guideline for (SANS241, 2015). The maximum levels (pH 8.3) are located in the upper part of the catchment (SB03) and this can be ascribed to the presence of dolomite in the bedrock. The values of pH

measured from the Sabie catchment area are a direct meaning of its total dissolved solids (TDS) and specifies concentrations of soluble salts in water. All values recorded in the Sabie River were within SANS241 (2015) and WHO (2011) limits. However, EC values recorded at SB11 located next to Glynn's Lydenburg TSF and SB12 (Klein Sabie River) were slightly above recommended limits with higher values recorded at Nkambeni and Bega Rivers, 295 $\mu\text{S}/\text{cm}$ and 547 $\mu\text{S}/\text{cm}$, respectively. High EC values in these sites can be attributed to human activities, as there was evidence of dumping of wastes at those sites. The values of dissolved oxygen (DO) were above recommended limits by SANS (2005) for both seasons and this can be attributed to aerobic conditions prevailing in the Sabie catchment area. The DO concentrations in water samples indicate changes in the redox state and microbial activity (Gebrekristos et al., 2008). In both seasons, Eh values ranged from -75.9 to -2.6, with a mean of -35.9 in the wet season and -47.41 in the dry season. The alkaline pH within the Sabie catchment is responsible for the low Eh values. This is supported by high values (270.2 mV) recorded at Nestor TSF seepage sample which had acidic pH 2.5.

Table 32 Seasonal distinction of parameters measured in situ and alkalinity (mg/L CaCO_3) measured in surface water of the Sabie catchment.

Sample ID	pH		EC ($\mu\text{S}/\text{cm}$)		Eh (mV)		DO (mg/L)		Alkalinity CaCO_3 (mg/L)	
	WT	DR	WT	DR	WT	DR	WT	DR	WT	DR
SB01	7.8	8.3	78.3	64.7	-37.0	-64.5	7.5	9.5	33.6	29.1
SB02	7.9	7.8	130.0	105.0	-46.2	-40	7.4	8.5	55.2	49.8
SB03	8.1	8.3	153.1	149.1	-50.5	-64.2	7.3	8.7	61.1	60.4
SB04	8.3	8.2	168.0	141.1	-66.9	-64.5	7.8	8.3	59.5	54.6
SB05	8.0	8.2	142.4	101.0	-55.0	-63.2	7.2	9.6	56.2	52.1
SB06	7.3	8.0	120.0	120.5	-41.4	-49.8	6.8	9.1	47.1	50.7
SB07	8.0	8.1	135.4	125.1	-45.9	-50.2	7.1	9.2	37.1	126.0
SB08	7.7	8.1	108.0	119.1	-16.2	-58.4	7.3	9.5	49.9	46.8
SB09	8.0	8.1	128.0	238.0	-55.4	-60.5	6.7	8.3	47.1	87.2
SB10	7.3	8.5	83.7	67.4	-3.6	-75.9	7.1	8.6	39.1	20.1
SB11	6.7	7.5	174.1	174.3	26.9	-30.5	6.2	8.9	72.3	82.9
SB12	7.5	7.6	176.9	183.1	-23.0	-30.7	6.3	9.5	58.1	80.2
SB13	8.3	7.9	140.2	134.5	-51.6	-46.2	8.0	9.0	64.0	64.3
SB14	8.2	8.0	74.0	68.3	-65.9	-50.5	7.1	9.3	32.9	28.2

SB15	7.2	7.7	188.4	194.9	-2.6	-36.8	7.2	7.9	44.3	440.1
SB16	7.8	7.8	93.1	83.7	-44.0	-42.0	6.0	8.3	59.9	24.0
SB17	7.5	7.8	150.6	162.6	-20.7	-40.9	7.6	8.7	33.5	64.6
SB18	8.0	7.5	100.8	109.9	-55.6	-20.9	7.4	9.6	48.7	50.4
SB19	7.7	7.4	44.0	38.8	-37.3	-17.6	6.8	9.2	17.9	16.7
SB20	7.5	7.8	295.0	455.2	-20.2	-32.8	6.5	7.3	72.8	51.5
SB21	7.8	8.1	547.0	610.1	-41.3	-55.6	6.5	8.1	185.3	220.0
Mean	7.7	7.9	154.2	164.1	-35.9	-47.4	7.2	8.8	56	80.9
SD	0.4	0.1	104.1	133.9	23.4	15.7	0.5	0.1	32.7	93.3
SANS241 (2015)	5-9.7		≤1700		-		-		-	
WHO (2011)	7.0-8.5		-		-		-		-	

WT, wet season; DR, dry season; SD, standard deviation; -, no guideline.

There are higher concentrations of combined cations than anions recorded in surface water of Sabie River system. In the surface water of the Sabie catchment, Mg and Ca are the dominant cations while chlorine and sulphate are the dominant anions, respectively (Table 33). The highest values of Ca²⁺ and Mg²⁺ recorded in the upper parts of the Sabie River system can be attributed to the dolomite rocks covering the area. At site SB11, the highest Ca²⁺ and Mg²⁺ were recorded at 20.0 and 10.8 mg/L respectively. However, there were higher concentrations of both cations at Bega River (SB21) covered by granitic rock and this can be attributed to pollution from the local community as observed during site visits.

Table 33 Seasonal variation of cation and anions in the of Sabie catchment.

Sample ID	Ca (mg/L)		Mg (mg/L)		Na (mg/L)		Cl (mg/L)		NO ₃ (mg/L)		SO ₄ (mg/L)	
	WT	DR	WT	DR	WT	DR	WT	DR	WT	DR	WT	DR
SB01	7.3	5.3	4.7	3.2	2.1	1.5	1.5	1.5	1.3	2.1	1.6	1.7
SB02	12.4	10.1	7.7	5.8	1.9	1.6	1.9	1.7	1.9	1.4	1.1	1.3
SB03	14.7	12.7	9.2	7.5	2.6	2.1	2.4	2.4	ND	2.4	5.4	4.5
SB04	14.2	11.7	8.6	6.6	3.0	2.4	5.8	2.6	ND	2.7	5.4	4.8
SB05	12.9	11.2	7.9	6.4	3.6	3.1	3.9	3.5	2.3	2.5	5.1	4.6
SB06	10.8	9.9	6.7	5.8	4.2	3.1	3.7	3.1	3.3	1.6	3.5	3.5

SB07	10.8	27.6	6.8	15.5	4.4	21	4.1	7.3	1.2	1.1	3.9	4.1
SB08	7.6	9.7	4.6	5.3	5.7	6.1	5.8	4.5	1.7	1.3	3.4	19.1
SB09	8.8	24.2	6	9.2	7.1	7.4	7.1	7.3	0.9	1.1	3.3	4.1
SB10	7.9	4.2	5.2	2	1.7	10.1	1.1	3	0.7	0.3	1.4	ND
SB11	17.3	20	10.8	7.6	3.2	10.1	2.9	3.2	0.9	2.2	10.1	1.5
SB12	15.2	15.4	9.1	8.9	4.8	6.2	3.8	7	8.5	1.8	9.4	8.2
SB13	14.1	14.2	8.7	8.5	1.2	2.3	1.4	3	1.2	0.4	ND	ND
SB14	6.3	5.4	4.2	3.5	2.3	2.7	1.6	4	0.6	0.2	ND	ND
SB15	19.2	5.5	7.6	3.7	4.4	2.3	3.8	5	2.9	1.2	32.1	37
SB16	5.4	11	2.5	5.9	9.4	2.6	6.8	2.8	2.6	1.3	1.1	1.1
SB17	10.5	11.5	9.8	8	5.2	6.7	4.8	8.1	1.4	1.1	5.4	4.2
SB18	9.9	11	5.9	5.9	2.7	2.6	2.6	2.8	0.6	1.3	0.8	1.1
SB19	2.8	3.4	1.4	2.6	4.6	5.1	3.6	2.9	2.6	0.5	0.1	0.9
SB20	16.4	11.7	10.7	6	23.4	3.5	24.7	4.9	ND	1.7	19.8	4.5
SB21	25.2	32.5	37.2	37.9	29.6	15.3	45.7	48.7	2.3	6.8	11.8	19.8
Mean	14.4	12.8	8.4	7.9	5.8	5.6	8.5	6.1	1.7	1.7	5.9	6
SD	13.1	7.6	1.5	7.5	1.5	5	2.8	9.9	0.4	1.4	7.7	8.9
SANS241 (2015)	-	-	-	-	≤200	-	≤300	-	≤11	-	≤500	-
WHO (2011)	-	-	-	-	40	-	-	-	50	-	-	-

Note: WT, wet season, DR, dry season; ND, not detected; SD, standard deviation, -, no guideline.

The highest concentration of Cl⁻ at sampling sites are recorded in the lower reaches of the catchment at the Bega River and the Nkambeni River, reaching 48.7 mg/L and 24.7 mg/L. Similarly, SO₄²⁻ concentration at these two particular sites is high (19.8 mg/L) and suggest input from the nearby rural settlement areas. In the upper reaches, the concentration of Cl⁻ and SO₄²⁻ is low at all sampling sites. However, there is high SO₄²⁻ concentration recorded at the drainage near Rietfontein mine (SB15) that might be ascribed to illegal mining activities happening at the site. The concentrations of nutrients (NO₃²⁻ and NO₂⁻) are low in the Sabie River system and they are within SANS241 (2015) and WHO (2011) guidelines.

The seasonal variation in trace metals of the Sabie River system is shown in Table 34. There is no significant difference in measured species concentrations between the wet and dry seasons.

Though the majority of the metal species are below the detection limits, all of these concentrations are within the SANS (2015) and WHO (2015) recommended limits (2011). Although there is no water hardness guideline, high Ca and Mg concentrations are associated with increased water hardness (WHO, 2011). The metal species concentrations dissolved in the water is extremely low, as would be expected in water with a pH greater than 7. These results indicate that metal transport to the sediments could largely be through particulate matter.

Table 34 Seasonal variation of trace metals in the Sabie catchment.

Sample ID	Al (mg/L)		As (mg/L)		Cu (mg/L)		Cr (mg/L)		Fe (mg/L)		Mn (mg/L)		Zn (mg/L)	
	WT	DR	WT	DR	WT	DR	WT	DR	WT	DR	WT	DR	WT	DR
SB01	0.02	<0.01	<0.01	<0.01	<0.01	<0.01	<0.01	<0.01	<0.01	0.02	<0.01	<0.01	<0.01	<0.01
SB02	0.01	<0.01	<0.01	<0.01	<0.01	<0.01	<0.01	<0.01	<0.01	<0.01	<0.01	<0.01	<0.01	<0.01
SB03	<0.01	<0.01	<0.01	<0.01	<0.01	<0.01	<0.01	<0.01	<0.01	0.01	<0.01	0.04	<0.01	<0.01
SB04	<0.01	<0.01	<0.01	<0.01	<0.01	<0.01	<0.01	<0.01	<0.01	0.03	<0.01	0.02	<0.01	<0.01
SB05	<0.01	<0.01	<0.01	<0.01	<0.01	<0.01	<0.01	<0.01	<0.01	0.04	<0.01	0.01	<0.01	<0.01
SB06	<0.01	<0.01	<0.01	<0.01	<0.01	<0.01	<0.01	<0.01	<0.01	0.04	<0.01	<0.01	<0.01	<0.01
SB07	<0.01	<0.01	<0.01	<0.01	<0.01	<0.01	<0.01	<0.01	<0.01	0.17	<0.01	0.16	<0.01	<0.01
SB08	<0.01	<0.01	<0.01	<0.01	<0.01	<0.01	<0.01	<0.01	<0.01	0.12	<0.01	0.02	<0.01	<0.01
SB09	<0.01	<0.01	<0.01	<0.01	<0.01	<0.01	<0.01	<0.01	<0.01	0.11	<0.01	<0.01	<0.01	0.02
SB10	<0.01	0.02	<0.01	0.04	<0.01	<0.01	<0.01	0.01	0.04	<0.01	<0.01	<0.01	<0.01	<0.01
SB11	<0.01	0.01	<0.01	0.02	<0.01	0.08	<0.01	0.01	ND	<0.01	<0.01	0.42	<0.01	<0.01
SB12	<0.01	<0.01	<0.01	0.03	<0.01	0.03	<0.01	<0.01	<0.01	<0.01	0.02	<0.01	<0.01	0.03
SB13	0.04	<0.01	<0.01	0.02	<0.01	0.01	<0.01	0.01	<0.01	<0.01	0	<0.01	<0.01	<0.01
SB14	0.18	<0.01	0.04	0.03	0.01	0.01	<0.01	<0.01	<0.01	0.02	0.02	<0.01	<0.01	<0.01
SB15	<0.01	<0.01	<0.01	<0.01	0.14	0.01	<0.01	0.01	<0.01	<0.01	0.3	<0.01	<0.01	<0.01
SB16	<0.01	<0.01	<0.01	<0.01	<0.01	<0.01	<0.01	<0.01	0.16	<0.01	<0.01	<0.01	<0.01	<0.01
SB17	<0.01	<0.01	<0.01	<0.01	<0.01	<0.01	<0.01	<0.01	0.03	0.18	<0.01	0.05	<0.01	<0.01
SB18	<0.01	<0.01	<0.01	<0.01	<0.01	<0.01	<0.01	<0.01	<0.01	<0.01	<0.01	<0.01	<0.01	<0.01
SB19	<0.01	<0.01	<0.01	<0.01	<0.01	<0.01	<0.01	<0.01	0.11	0.08	<0.01	<0.01	<0.01	<0.01
SB20	<0.01	<0.01	<0.01	<0.01	<0.01	<0.01	<0.01	<0.01	<0.01	0.07	0.09	0.06	<0.01	<0.01
SB21	<0.01	<0.01	<0.01	<0.01	<0.01	<0.01	<0.01	<0.01	<0.01	0.02	<0.01	0.06	<0.01	<0.01
Mean	0.01	0	0	0.01	0.01	0.03	0	0	0.02	0.04	0.02	0.04	0	0

SD	0.04	0.01	0.01	0.01	0.03	0.03	0	0	0.04	0.06	0.07	0.1	0	0
SANS241 (2015)	0.3		0.01		≤2		≤0.05		2		0.4		0.05	
WHO (2011)	-		0.01		2		0.05		-		-		-	

WT, wet season; DR, dry season; SD, standard deviation; -, no guideline.

The AMD from the Nestor MTSF flows downstream towards the Klein Sabie River (about a distance of one kilometer), which is a tributary of the Sabie River. As a result, simple mixing or geochemical reactions like dissolution and precipitation would affect the concentrations of dissolved metals in Sabie River samples.

4.5.3. Metal speciation in water

According to Newman (2015), the chemical form in which an element occurs, or speciation, determines its transport and interaction in the environment. Thus, an element can occur as oxidized, free ion or complexed with organic and inorganic molecules. The input data for metal speciation in the surface water in the Sabie River catchment area is presented in Table 35 and Table 36 presents data for predicted species in mine water. This data was calculated using the PHREEQC modelling program for understanding the behaviour of metals in the surface water.

Calcium chemical species concentrations calculated for all water samples analysed in both wet and dry seasons revealed a predominance in the II oxidation state (>93%), with the remainder being complexes with carbonates (CaHCO_3 & CaCO_3), nitrate (CaNO_3), sulphate (CaSO_4), and chloride (CaCl). In the case of Mg, the most principal chemical species was Mg^{+2} (>94%) analysed in both dry and wet seasons. Other chemical species of Mg were MgOH^+ , MgF^+ , MgCl^+ , MgSO_4 and carbonates (MgCO_3 & MgHCO_3). Based on these results, the bioavailability of both Ca and Mg is likely to occur, however, this will be decreased as they also form complexes with carbonates.

According to Sirkiä et al. (1999) the Cu^{2+} ions complexes CuCO_3 (aq), $[\text{Cu}(\text{HCO}_3)_2]$, $\text{Cu}(\text{OH})_3^-$ and $[\text{Cu}(\text{OH})_4]^{2-}$ are present in water with high concentrations of hydrogen carbonates. From speciation modelling, Cu was predicted as being likely to precipitate as CuCO_3 and $\text{Cu}(\text{CO}_3)_2^{-2}$. The concentrations of CuCO_3 ranged between 52.15-89.22% in the wet season and 50.45-90.52% in the dry season. On the other hand, the concentrations of $\text{Cu}(\text{CO}_3)_2^{-2}$ ranged between 0.13 to 3.68% and 0.04 to 6.51 in both dry and wet seasons respectively. The other species predicted for Cu were free hydrated ion (CuOH), CuHCO_3 and precipitates (CuSO_4 and $\text{Cu}(\text{OH})_2$).

The predominance species of Fe was Fe^{+2} with concentrations ranging between 91.16 to 98.19 and 93.79% to 99.30% in both seasons. The residual Fe was predicted to exist in the form FeOH , FeSO_4 and FeHCO_3 . Also showing a similar dominance in terms of speciation was Mn, which showed dominance in Mn^{+2} chemical species. The range for Mn^{+2} was 69.45 to 95.80% (wet season) and 59.01 to 91.03% (dry season). There is also a likelihood of Mn species to precipitate as carbonate-based concentrations of MnCO_3 (up to 27.77% in the wet season and 36.90% in the dry season) and MnHCO_3 (up to 3.53% in the wet season and 3.15% in the dry season). Some of the predicted chemical species of Mn are MnOH , MnSO_4 and MnNO_3 .

Most of the Al species were likely to dissolve as hydroxides. The main species predicted for Al was $\text{Al}(\text{OH})_4^-$ which ranged between 57.698 to 99.02% in the wet season and 89.31 to 98.88% during the dry season. According to Barabás, (1998) $\text{Al}(\text{OH})_4^-$ is more predominant in alkaline waters. Other predicted species of Al were $\text{Al}(\text{OH})$, $\text{Al}(\text{OH})_2$ and $\text{Al}(\text{OH})_3$. Also, Cr was likely to precipitate as hydroxide (CrOH) with concentrations ranging between 97.16 to 99.93% (wet season) and 99.55 to 99.93% (dry season); consistent with (Świetlik, 1998) at pH of about 8. Cr^{+2} was the other predicted chemical species of Cr with concentrations ranging between 0.07 and 2.84% (wet season) and 0.02 to 0.45% (dry season).

Table 35 Maximum percentages of speciated metals measured in surface water in the Sabie River catchment.

Speciated forms	Wet season %Range	Dry season %Range
Ca^{+2}	94.21-99.41	93.55-98.88
CaCl^+	0.01-0.76	0.01-0.21
CaSO_4 (aq)	0.01-4.01	0.15-2.53
CaNO_3^+	0.01-3.62	0.01-0.12
CaOHCO_3^+	0.67-3.17	0.28-2.89
CaCO_3 (aq)	0.03-1.26	0.03-1.68
Mg^{+2}	95.56-99.55	94.80-99.55
MgOH^+	0.01-0.07	0.01-0.03
MgF^+	0.01-0.06	0.01-0.05

MgCl ⁺	0.01-0.10	0.01-0.06
MgSO ₄ (aq)	0.12-2.30	0.14-1.28
MgCO ₃ (aq)	0.02-0.63	0.05-0.85
MgHCO ₃	0.47-2.49	0.47-2.65
Fe ⁺²	91.16-98.19	93.79-99.30
FeOH ⁺	0.10-6.15	0.29-2.98
FeCl ⁺	0.03-0.05	0.06
FeSO ₄ (aq)	0.13-4.24	0.15-2.64
FeHCO ₃ ⁺	0.39-3.18	0.26-1.71
Al ⁺³	0.052	
Al(OH) ₂ ⁺	0.01-1.40	0.03-2.48
Al(OH) ⁺	0.13-17.70	0.03-1.40
Al(OH) ₃ (aq)	0.97-23.10	1.08-6.22
Al(OH) ₄ ⁻	57.70-99.02	89.31-98.88
Cr ⁺²	0.07-2.84	0.02-0.45
CrOH ⁺	97.16-99.93	99.55-99.93
Cu ⁺²	1.74-39.63	1.22-15.01
CuOH ⁺	4.01-21.31	2.31-12.96
CuOH ₃ ⁻	0.02-0.36	0.02-0.06
Cu(OH) ₂ (aq)	0.02-3.47	0.12-1.92
CuSO ₄ (aq)	0.01-1.49	0.01-0.14

CuCO ₃ (aq)	52.15-89.22	50.45-90.52
Cu(CO ₃) ₂ ⁻²	0.13-3.68	0.04-6.51
CuHCO ₃ ⁺	0.10-2.53	0.10-0.58
Mn ⁺²	69.45-95.80	59.01-91.03
MnCO ₃ (aq)	3.35-27.77	0.01-36.90
MnOH ⁺	0.04-0.23	0.01-1.17
MnF ⁺	0.01-0.03	0.07-0.09
MnCl ⁺	0.01-0.36	0.01-0.07
MnSO ₄ (aq)	0.01-2.95	0.02-1.66
MnNO ₃ ⁺	0.01-0.85	0.01-0.03
MnHCO ₃	0.60-3.53	0.76-3.15

Table 35 shows the results of speciation modeling on water samples, with saturation indices (SI) taken into account. According to Zhu and Anderson (2002), saturation indices are an indication of a solution's saturation with respect to a mineral, with a positive SI indicating supersaturation and a negative SI indicating undersaturation. All minerals dissolved in the water samples from the Sabie River system were found to be undersaturated.

However, the predicted chemical species from the Nestor MTSF seepage were different from the ones predicted for surface water (Table 36). Most cations were predicted to likely precipitate as sulphates, namely, Ca, Mg, Fe and Cu.

Table 36 Range of highest speciated forms of metals from Nestor TSF seepage.

Element	Speciated forms	Wet season
		%Range
Ca	CaSO ₄ (aq)	65.31

	Ca ⁺²	34.47
	CaHCO ₃ ⁺	0.18
	CaCl ⁺	0.04
Mg	MgSO ₄ (aq)	60.01
	Mg ⁺²	39.74
	MgHCO ₃ ⁺	0.17
	MgCl ⁺	0.07
	MgF ⁺	0.02
Fe	FeSO ₄ (aq)	66.82
	Fe ⁺²	33.00
	FeHCO ₃ ⁺	0.17
Al	AlF ₂ ⁺	55.71
	AlF ⁺²	17.17
	Al(SO ₄) ₂ ⁻	10.62
	AlF ₃ (aq)	8.81
	AlSO ₄ ⁺	7.19
	Al ⁺³	0.39
	AlF ₄ ⁻	0.12
Cr	Cr ⁺²	99.89
	CrOH ⁺	0.11
Cu	CuSO ₄ (aq)	64.58
	Cu ⁺²	34.24
	CuHCO ₃ ⁺	0.87
	CuHSO ₄ ⁺	0.28
	CuCl ⁺	0.03
	CuF ⁺	0.01

Soluble Al⁺³ predominates in an acidic condition while insoluble Al(OH)₃ predominates in a neutral condition (Barabás, 1998). Based on speciation, Al is likely to form complexes with both fluorine sulphate. The dominant species was AlF₂⁺ (55.71%) followed by AlF⁺² (17.17%), Al(SO₄)₂, AlSO₄⁺ (7.19%), AlF₄⁻ and few concentrations of soluble Al⁺³ (0.39%). For Cr chemical speciation, the

most dominant species predicted was Cr^{+2} at 99.89% and the remainder was CrOH (0.11%). Based on the saturation index, all minerals in the seepage from Nestor MTSF are undersaturated with the exception of gypsum, which was close to saturation (SI of -0.92). Figure 23 shows the trilinear piper diagrams for both seepages from the Nestor TSF and surface water collected from the Sabie catchment.

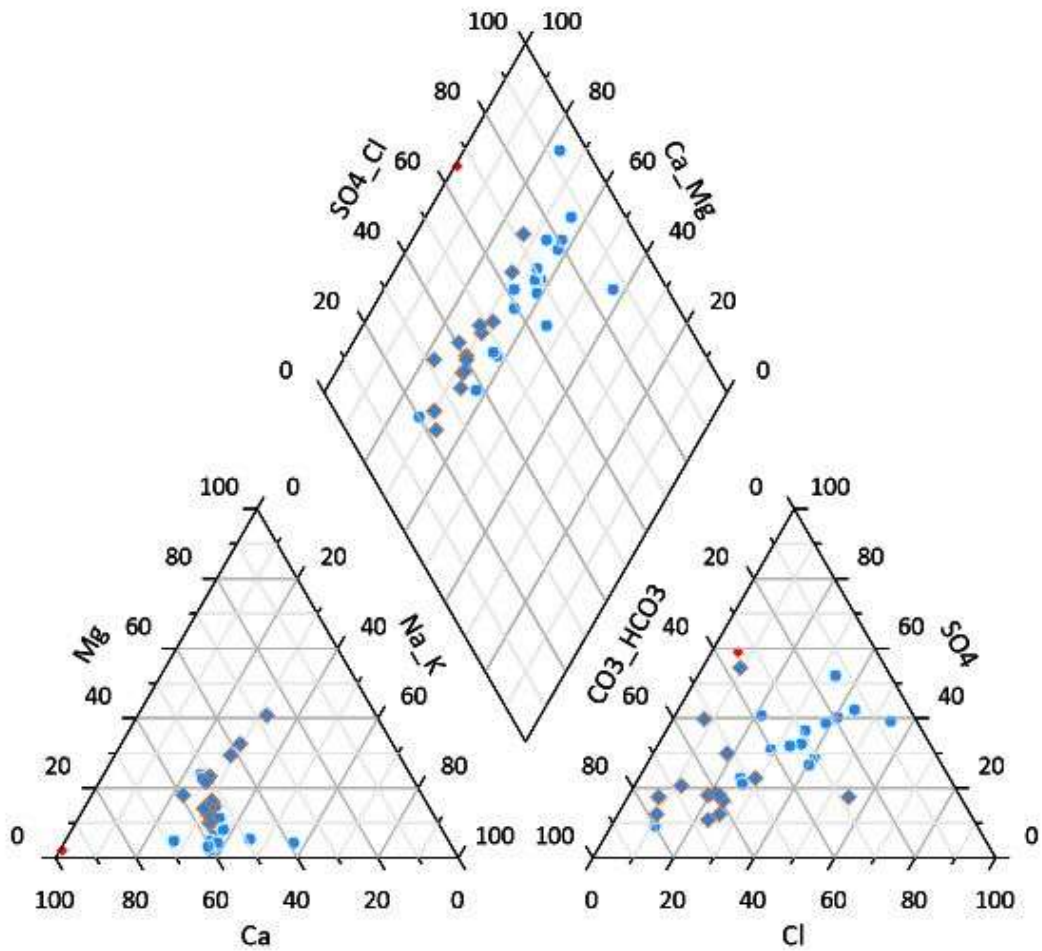


Figure 23 Piper plot for Nestor MTSF seepage (red) and surface water for wet (blue) and dry (orange) seasons

CHAPTER FIVE

5. Mitigation measures of the mine tailings storage facilities in the Sabie River catchment

The scale of the environmental problems caused by acid mine drainage (AMD) has motivated substantial research and development of remediation actions. AMD prevention technologies are aimed at changing the chemical, biological and physical nature of the mine wastes. The rehabilitation of the sensitive mine discarded dumping site can simply be accomplished when scheduled in before and incorporated in the mining construction cycle, as per principles of "Designing for Closure" (Aubertin et al., 2002; 2016). There is no general solution to the impacts caused by AMD from mining activities.

According to the Mineral and Petroleum Resources Development Act 28; 2002 (MPRDA, 2002), mining companies are required to have both an environmental management program and plan respectively (MPRDA, 2002). Mining companies should budget for the financial costs of rehabilitating the environment following the closure of mining operations, as well as the costs of mitigating environmental impacts if they occur. Mining commenced in 1872 in the Sabie Goldfield and that was before the development of MPRDA (2002). Therefore, there is no quantitative information on pre-mining water, rock, soil, and biota conditions in the Sabie Goldfield. The Nestor and Glynns Lydenburg mine tailings storage facilities (MTSFs) are the most visible signs of past mining activities in this mining district. The primary goal of this research was to strategize a management plan for the Nestor MTSF. The surfaces of the mine tailings storage facility need to be restored to a stable natural condition while minimizing the degradation of the surrounding environment from metal pollution.

Lusunzi (2018) assessed the geochemical properties of the two MTSFs for the potential AMD formation in the Sabie Goldfield. The study concluded that the Nestor MTSF is acid generating while the Glynns Lydenburg MTSF is alkaline-generating. Compared to the Glynns Lydenburg MTSF, there is sufficient data that the mine tailings from the Nestor MTSF may result in pollution of the air (through volatilization and fugitive dust productions); surface water of the Sabie River system (from surface runoff and groundwater seepage); groundwater (through leaching/infiltration); surrounding soils because of erosion (including fugitive dust emission/deposition and tracking); sediments (from surface runoff, flowing seepage and leaching); and biota (as a result of biological uptake and bioaccumulation). Furthermore, the rehabilitation of the Nestor MTSF was recommended.

The Glynns Lydenburg MTSF has vegetation growing on it and no evidence of weathering and erosion were observed at this site. In this study, the tailings from the acid generating tailings from the Nestor MTSF (AG) were collected and mixed with the acid neutralizing tailings materials from the Glynns Lydenburg MTSF (AN) at 25:75 wt. % AN/AG and 50:50 wt. % AG/AN (4.1.1). Two mixtures generated MIX25 and MIX50 had been classified as net alkaline producing based on the acid base accounting (ABA) static tests performed. This was aimed at assessing the suitability of the alkaline-generating materials from the Glynns Lydenburg MTSF to rehabilitate the Nestor MTSF through capping. According to the ABA data, the acid-generating capabilities of the gold mine tailings from the Nestor MTSF (AG), are considered to be potentially acid forming (PAF) using traditional classification criteria. The low paste pH of AG confirms that the tailings are acidic and they are generating an acidic effluent (AMD) evident during onsite analyses and from laboratory results. Due to the highly acidic conditions of the AG tailings (paste pH of 2.5), ferric iron will be the primary oxidizer of the sulphide minerals and will result in a higher acid generating potential and a high quantity of stored acidity. In order to protect downstream water resources, the Nestor MTSF should be rehabilitated. The gold mine tailings from the Glynns Lydenburg MTSF (AN) can be considered to be net alkaline forming (NAF). However, these may still generate alkaline mine drainage. Thus, using the alkaline tailings as a cover for the acid-generating tailings may prevent acid drainage and prevent and/or treat AMD generated by the acid-generating gold mine tailings. Using the alkaline mine tailings would be a more economically feasible option compared to other treatment options such as using lime or limestone which is a resource and allows for the co-disposal of mine waste. These tailings material will provide a medium for establishing sustainable vegetation on the Nestor MTSF as they proved to support the vegetation growth at the Glynns Lydenburg MTSF.

In terms of stability, the Nestor MTSF is both physically and chemically unstable. There was no vegetation growing on the Nestor MTSF as observed during site visits and it was highly weathered. In addition, a low pH and metal-rich seepages from the MTSF and tailings that are highly weathered, were eroded downstream towards the Klein-Sabie River. The absence of plant growth allows for erosion and the penetration of water and oxygen into the acid-generating mine tailings, which increases the rate and extent of acid generation.

The remediation of contaminated soil and sediment necessitates a detailed onsite classification of the speciation of the potential hazardous elements as well as their transformations with over time and space. There are high concentrations of the metalloid As in both Nestor and Glynns Lydenburg MTSF, which is of geogenic source based on the speciation results (Chapter 4: 4.1.2.1). Recently, the phytoextraction technology has been suggested as an effective tool in As clean-up. A substantial amount of grass-like plant growth was observed on the surface of the

Glynns Lydenburg MTSF. This plant growth will thus limit the extent of erosion and penetration of water and oxygen into the mine tailings pile. MIX25 and MIX50 both seem to be suitable options to treat and prevent further acid generation caused by the acid-generating gold mine tailings (AG). However, a MIX25 (25 wt. % AN to 75 wt. % AG ratio) would be the more economically feasible option. This implies that tailings from the Glynns Lydenburg Mine can be used to rehabilitate the Nestor MTSF by forming a base through which vegetation will grow. Therefore, a dry cover system, that is store-and-release cover system, will be suitable rehabilitation technology in the Nestor MTSF using materials from Glynns Lydenburg MTSF. This cover system will help in dust and erosion control, improves chemical stability of AMD thereby controlling contaminants release and provision of a growth medium for establishment of vegetation in the Nestor MTSF.

Lime-based technologies cannot be used as a solution because seepages occur only during the rainy season and may produce incorrect results when no seepage occurs. Passive treatment has gained popularity lately and has been widely investigated. There are various parameters that should be considered before implementing these systems, which include drainage chemistry, flow rate, and the topography of the area (Hedin and Nairn, 1992; Hedin *et al.*, 1994). However, the drainage chemistry of the Nestor MTSF effluents is characterized by a low pH (2.5), elevated metal concentration especially Fe and Al at 4964.0 mg/L and 72 mg/L correspondingly, high acidity (>90 mg/L) and there is a periodic flow rate that is influenced by rainfall. This will hinder the application of passive treatment systems at the site as these systems incorporate the flow rate in their design parameters and the metal concentrations are too high at this particular site. An evolving phytoremediation technology can also be considered to remediate the Nestor MTSF. This technique should either be phytostabilisation or phytoextraction using material from Glynns Lydenburg MTSF as the base layer. Additionally, the Glynns Lydenburg MTSF is located less than 5 km from the Nestor MTSF, making it a more economical feasible option.

The capping or covering of solid mining waste is an effective technology for isolating contaminants. Therefore, capping of the acidic Nestor MTSF with materials from the Glynns Lydenburg MTSF is recommended for the rehabilitation of the acidic Nestor MTSF. Grading of the slopes should be done prior to capping of the MTSF in order to stabilize the pile and reduce erosion. In addition, stormwater control structures such as drainage channels and retention ponds should be incorporated in the design. Because the alkaline tailings material from the Glynns Lydenburg MTSF are already ground and are located less than 2 km from the acidic tailings of the Nestor MTSF, the proposed solution will be cost-effective in terms of handling and transportation. MIX25 and MIX50 were classified as alkaline producing based on ABA tests performed, therefore this solution will work indefinitely to remediate the Nestor MTSF. As a result,

if the materials are properly mixed, no secondary contamination can be expected (ratios of MIX25 and MIX50).

CHAPTER SIX

6. Conclusion

The Nestor mine tailings storage facility (MTSF) is situated in the Sabie Goldfield, which is a semi-arid area with high rate of evaporation in winter season. Geochemical as well as hydrological studies were carried out to categorize the probable pollution and ecological concerns associated with the potentially harmful trace elements in the Sabie River system. Chemistry of acid mine drainage (AMD) is highly dependent on mineralogy of the mine wastes, revealing a high dissolution rate of pyrite and the associated sulphides in the Nestor mine tailings storage facility (MTSF). Total metal species concentrations in stream sediment samples varied significantly, with elevated concentrations in winter (dry season) compared to summer (wet season). In comparison to metal concentrations found in mine wastes, stream sediments had low metal (loid) concentrations of chromium (Cr), lead (Pb), copper (Cu), zinc (Zn), nickel (Ni), and arsenic (As). The mainstream of metal contamination, on the other hand, is removed over a short spatial distance, implying that mining activities cause little or no pollution in the Sabie River system. According to the pollution load index, geo-accumulation index, and contamination factor the sediments ranged from unpolluted to extremely polluted in arsenic.

Acid producing minerals ferricopiapite and pyrrhotite found in the Nestor MTSF efflorescent crusts are potential sources of acidity and metal transportation while acid neutralizing mineral of dolomite dominated efflorescent crusts of Glynn's Lydenburg MTSF. This is consistent with mineralogical composition from previous studies, which noted the existence of acid producing minerals in the vicinity of Nestor TSF (ferricopiapite and fibroferrite) and acid neutralizing minerals in the vicinity of Glynn's Lydenburg (calcite and dolomite). This variation can be attributed to geogenic source of Malmani dolomite rock for the Glynn's Lydenburg and shale as the source rock for Nestor Mine. While the oxidation of sulphide minerals, particularly pyrite (FeS_2), is the primary source of AMD related to Nestor MTSF, existing characteristics of the AMD in the efflorescent crusts and weathered tailings is directly related to secondary minerals. Therefore, efflorescent crusts from Nestor MTSF are the potential source of water pollution to the adjacent Klein-Sabie River and in turn the main Sabie River catchment.

The result of sequential extraction analyses confirmed trace metals attenuation via dilution and precipitation from water to sediments in descending order $\text{Co} < \text{Pb} < \text{Ni} < \text{Cu} < \text{Cr} < \text{Zn} < \text{As} < \text{Mn} < \text{Al} < \text{Fe}$.

The silicate (residual) fraction has the highest average concentration of investigated metal species. As a result, the AMD-mediated release from the Nestor MTSF is not expected to have a

significant impact on the Sabie River system. The sediment from the Sabie River system has enough capacity to act as a sink for metal species as long as the pH remains above 7 and the dissolved salts levels do not rise significantly.

Throughout the Sabie River catchment (from upstream to downstream), the surface water is alkaline and the concentrations of metal species are within limits permitted by SANS241 (2015) and WHO (2011). However, the seepage from the Nestor MTSF had low pH and elevated metal species concentrations, namely, Fe, Al, As, Mn, Cu and Co exceeding limits for drinking water. It was observed from the research that there was no statistically substantial variation between physicochemical parameters measured in surface water samples collected in different seasons - summer and winter). The results from PHRREQC modelling had shown that cation exchange played a substantial part in regulating the chemistry of surface water in the Sabie River system. There is no AMD in the Sabie River system based on findings from this study. As a result, contamination sources in the Sabie River system should be closely monitored. Passive geochemical treatment systems such as open limestone channels (OLCs) and limestone leach beds (LLBs) cannot be considered for the treatment of seepage from the Nestor MTSF. The dry cover system is required at the Nestor MTSF in order to mitigate the acid mine drainage impacts downstream into the Sabie River system. Using the materials from the Glynn's Lydenburg MTSF as a base cover, the vegetation will grow on the Nestor MTSF as supported by the geochemical modelling.

From the comprehensive data obtained during the investigation into MTSFs, it became apparent that the metal pollutants were Mn, Al, Cu, Zn, Ni, and Cr. In addition to these metal species, the metalloid As was also observed. The dispersion into the Sabie River system was observed with AMD being released from the Nestor MTSF, whilst no AMD pollution was observed for the Glynn's Lydenburg MTSF due to the fact that it is situated on the dolomite, causing a more neutral environment.

The research objectives were reached, and it was found that pyrite (the main Fe-bearing mineral) was the main mineral responsible for the pollution from the Nestor MTSF, but the metal Mn was detected, causing further concern. The trace elements (Co, Cu, Zn, Ni, Cr, and Pb) were found to be immobile and did not contribute to the pollution problem. The hypothesis was proved and a decision about the remediation of the Nestor MTSF can be made.

6.1. Recommendations

The rehabilitation of the Nestor MTSF should be a top priority, according to the findings from this study. The tailings material from Glynn's Lydenburg can be used as a cover for possible

vegetation growth in the Nestor MTSF considering their location and geochemistry. However, assaying of possible gold recovery should be done in advance. In addition, kinetic tests should be conducted on the Nestor MTSF (AG) and the Glynns Lydenburg MTSF (AN) samples to evaluate the acid and alkaline characteristics of the respective samples in detail. A set of columns should be conducted where the alkaline tailings (AN) are used as a cover, covering the acidic tailings (AG) to determine whether it would be a feasible option to treat and prevent further acid generation. Kinetic tests with a 25 wt. % AN:75 wt. % AG ratio should be conducted which corresponds to the MIX25 sample that was evaluated in this study.

A management strategy for the acid-producing Nestor MTSF can be put in place to ensure no further pollution (or at least a limited release of pollutants) can occur in future. A mitigation process is being discussed that involves all relevant partners as the mines have been abandoned and Government is now the custodian of the pollution mitigation, involving various role players (of Government and State Owned Entities such as Council for Geoscience and Mintek). This process falls outside the scope of this thesis and will be an ongoing process in future.

REFERENCES

ACMER (2005) Australian Centre for Mineral Extension and Research, 'A Summary of Passive and Active Treatment Technologies for Acid and Metalliferous Drainage (AMD)'. Proceedings of the 5th Australian Workshop on Acid Drainage.

Adams, N., Carroll, D., Madalinski, K., Rock, S., Wilson, T., Pivetz, B. (2000) 'Introduction to phytoremediation'. National Risk Management Research Laboratory Office of Research and Development U.S. Environmental Protection Agency Cincinnati, Ohio 45268.

Ahluwalia, S.S. and Goyal, D. (2007) 'Microbial and plant derived biomass for removal of heavy metal wastewater'. *Biosource Technology*, **Vol.** 98; pp. 2243-2257

Ahmed, A.H.M., Noufal, K.N., Masroor, A.M., and Tavheed, K.T. (2016) 'Petrography and geochemistry of Jumara Dome sediments, Kachchh Basin: Implications for provenance, tectonic setting and weathering intensity'. *Chinese J. of Geochem*, **Vol.** 33; pp. 9-23.

Al-Thani H, Koç M, Isaifan RJ. (2018b) 'A review on the direct effect of particulate atmospheric pollution on materials and its mitigation for sustainable cities and societies'. *J. Environ Sci Poll Res*, **Vol.** 25(28); pp. 27839–27857.

Ali, M.M., Ali, M.L., Islam, S., Rahman, Z. (2016) 'Preliminary assessment of heavy metals in water and sediment of Karnaphuli River, Bangladesh'. *J. Environ Nanotechnology, Monitoring and Management*, **Vol.** 5; pp. 27-35.

Alkorta, I., Herná'ndez-Allica, J., Becerril, J. M., Amezaga, I., Albizu, I., and Garbisu, C. (2004) 'Recent findings on the phytoremediation of soils contaminated with environmentally toxic heavy metals and metalloids such as zinc, cadmium, lead, and arsenic'. *Reviews in Environmental Science and Bio/Technology*, **Vol.** 3; pp. 71–90.

Allen, H.E. (1993) 'The significance of trace metal speciation for water, sediment, and soil quality criteria and standards'. *J. Sci Tot Environ*, **Vol.** 134; pp. 23-45.

Alpers, C.N., Nordstrom, D.K., Thompson, J.M. (1994b) 'Seasonal variations of Zn/Cu ratios in acid mine water from Iron Mountain, California'. In: Alpers, C.N., Blowes, D.W. (Eds.), *Environmental Geochemistry of Sulfide Oxidation*, *Am. J. Chem. Soc. Symp. Ser*, **Vol.** 550; 324–344.

Ammann, A. A. (2017) 'SPECIAL FEATURE : Inductively coupled plasma mass spectrometry (ICP MS): a versatile tool', (April 2007). doi: 10.1002/jms.1206.

APHA (1998) American Public Health Association '*Standard Methods for the Examination of Water and Waste Water*', 20th Edition, Washington DC.

Apallaro, C. et al. (2011) ' Investigation of rock-to-water release and fate of major, minor, and trace elements in the metabasalt–serpentinite shallow aquifer of Mt. Reventino(CZ, Italy) by reaction path modelling'. *J. App Geochem*, **Vol.** 26; pp. 1722-1740.

Arenus-Lago, D., Andrade, M.L., Lago-Vila, M., Rodríguez-Seijo, A., Vega, F. A. (2014) 'Sequential extraction of heavy metals in soils from a copper mine : Distribution in geochemical fractions', Elsevier B.V. *J. Geoderma*, **Vol.** 230–231; pp. 108–118.

Armienta, M.A. and Segovia, N. (2008) 'Arsenic and fluoride in the groundwater of Mexico'. *J. Environ Geochem and Health*, **Vol.** 30; pp. 345-353.

Armstrong-Altrin, J.S. et al. (2012) 'Geochemistry of beach sands along the western Gulf of Mexico, Mexico: Implication for provenance'. *J. Chemie der Erde*, **Vol.** 72; pp. 345-362.

Aseniero, J.P.J., Opiso, E.M., Banda, M.H.T. and Tabelin, C.B. (2019) 'Potential utilization of artisanal gold-mine tailings as geopolymeric source material: preliminary investigation'. *J. SN Appl. Sci*, **Vol.** 1; pp. 35.

Aubertin, M., Bussière, B., Bernier, L. (2002) 'Environnement et Gestion des Rejets Miniers'. Published by Presses Polytechnique Internationales'.

Aubertin, M., ASCE, M., Bussière, B., Pabst, T., James, M., Mbonimpa, M. (2016) 'Review of reclamation techniques for acid generating mine wastes upon closure of disposal sites'. *J. Min Eng*, **Vol.** 126; pp. 207-220.

Ahalya, A., Ramchandra, T.V., Kanmadi, R.D. (2003) *Research J. of Chem. & Environment*, **Vol.** 7(4).

Badawy, S.H., Helal, M.I.D., Chaudri, A.M., Lawlor, K. and McGrath, S.P. (2002) 'Heavy metals in the environment, soil solid-phase controls lead activity in soil solution'. *J. Environ. Qual*, **Vol.** 31; pp. 162–167.

- Badhurahman, A., Gautama, R.S., Kusuma, G.J. (2020) 'REE Enrichment Pattern in Acid Mine Drainage and Overburden from Coal Mine in Indonesia'. IMWA 2020 "Mine Water Solutions" (Pope, J.; Wolkersdorfer, Ch.; Weber, A.; Sartz, A.; Wolkersdorfer, K. (Editors).
- Bain, J.G., Meyer, K.U., Blowes, D.W., Frind, E.O., Molson, J.W.H., Kahnt, R., Jenk, U. (2001) 'Modelling the closure-related geochemical evolution of groundwater at a former uranium mine'. *J. Cont Hydrol*, **Vol.** 52; pp. 109-135.
- Baiq, D.K. and Christopher, A. (2014) 'Gold Phytomining: A New Idea for Environmental Sustainability in Indonesia'. *Indonesian J. on Geoscience*, **Vol.** 1; pp. 1-7.
- Barabás, K. (1998) 'Environmental health criteria 198', *Environmental Health Criteria*, (**198**), pp. 1–140.
- Barakat, S. and Giusti, L. (2003) 'Chromium speciation in a river system in Veneto (Italy) affected by tannery effluent'. *J. Phys. IV (Proc.)*, **Vol.** 107(1); pp. 115–118.
- Barabasz W, Albinska D, Jaskowska M, Lipiec J. (2002) 'Ecotoxicology of Aluminium'. *J. Pol Environ Stud*, **Vol.** 11(3); pp. 199–203.
- Barceló, J. and Poschenrieder, C. (2003) 'Importance of phenolics in rhizosphere and roots for plant-metal relationships'. *Pcoc. 7th Int. Conf. on the Biogeochem of Trace Elements*. Uppsala '03. SYMP02-Biotic and Abiotic Processes in Soil Rhizosphere. **Vol.** 2; pp. 162-163.
- Baker, B.J. and Banfield, J.F. (2003) 'Microbial communities in acid mine drainage'. *FEMS Microbiology Ecology*, **Vol.** 44(2); pp. 139-152.
- Barros, L.M., Macedo, G.R., Duarte, M.M., Silva, E.P. and Lobato, K.C.L. (2003). Biosorption of cadmium using fungus *Aspergillus niger*. *J. Braz Chem Eng*, **Vol.** 20; pp. 229-239.
- Batsala, M., Chandu, B., Sakala, B., Nama, S. and Domatoti, S. (2012) 'INDUCTIVELY COUPLED PLASMA MASS SPECTROMETRY (ICP-MS)'. *IJRPC*, **Vol.** 2(3); pp. 671-680.
- Barbieri, M. (2016) 'The Importance of Enrichment Factor (EF) and Geoaccumulation Index (Igeo) to Evaluate the Soil Contamination'. *J Geol Geop*, **Vol.** 5; pp. 237. doi:10.4172/2381-8719.1000237
- Barnhisel, R., Darmody, R. and Daniels, L. (2000) 'Reclamation of drastically disturbed lands'. *ASA Special Publ*, **Vol.** 41. ASA, Madison, WI.

Barton, J.M. Jr. (1983) 'Isotopic constraints on possible tectonic models for crustal evolution in the Barberton granite-greenstone terrane, southern Africa'. *In: Anhaeusser, C.R. (Ed.), Contributions to the Geology of the Barberton Mountain Land. Spec. Publ. Geol. Soc. S. Afr, Vol. 9; pp. 73–79.*

Bell, A.V. (1988) 'Acid waste rock management at Canadian base metal mines'. Paper presented at the 1988 Mine Drainage and Surface Reclamation Conference sponsored by the American Society for Surface Mining and Reclamation and the U.S. Department of Interior (Bureau of Mines and Office of Surface Mining Reclamation and Enforcement), April 17-22, Pittsburg, Pennsylvania.

Ben Ali, H., Neculita, C., Molson, J., Maqsoud, A. (2019) 'Efficiency of batch biochemical reactors for mine drainage treatment at low temperature and high salinity'. *J. Appl Geochem, Vol. 103; pp. 40-49.*

Benamer, M. (2014) 'Chemical speciation and spatial distribution of heavy metals and their adsorption onto sediments of the Berg River, South Africa'. PhD thesis, University of Cape Town.

Benson, C.H., Óren, A.H., Gates, W.P. (2010) 'Hydraulic conductivity of two geosynthetic clay liners permeated with a peralkaline solution'. *Geotext Geomembr, Vol. 28; pp. 206-218.*

Bentley, P.N. (1995) 'The Sabie-Pilgrim's Rest gold fields- is there a future for small scale underground gold mining?'. *In Extended Abstracts, Centennial Geocongress '95, Johannesburg. (J.M. Burton and Y.E. Copperthwaite, eds): Geol Soc S.A, pp. 52-55.*

Benzaazoua, B., Bussière, B., Kongolo, M., McLaughlin, J. and Marion, P. (2000) 'Environmental Desulphurisation of four Canadian mine tailings using froth flotation'. *J. Int Min Proc, Vol. 60(1); pp. 57-74.*

Benzaazoua, M., Belem, T., Bussière, B. (2002) 'Chemical factors that influence the performance of mine sulphidic paste backfill'. *J. Cement and Concrete Res, Vol. 32; pp. 1133-1144.*

Bertling, S., Wallinder, I.O., Leygraf, Ch. and Kleja, D.B. (2006) 'Occurrence and fate of corrosion-induced zinc in runoff water from external structures'. *Sci. Total Environ., Vol. 367; pp. 908–923.*

Blaylock, M. J. and Huang, J. W. 2000. Phytoextraction of metals. *In: Raskin, I. and B.D. Ensley (Eds). Phytoremediation of toxic metals: using plants to clean-up the environment'. New York, John Wiley & Sons, Inc.*

Blowes, D.W., Ptacek, C. J., Benner, S.G., McRae, Che, Bennett, T.A. and Puls, R.W. (2000) 'Treatment of inorganic contaminants using permeable reactive barriers'. *J. Con Hydrol*, **Vol.** 45 (1-2); pp. 123-137.

Blowes, D.W., Ptacek, C.J., Jambor, J.L., Weisener, C.G. (2003) 'The geochemistry of acid mine drainage'. In: Holland, H.D., Turekian, K.K. (Eds.), *Treatise on Geochemistry*, Ch 9.05. Pergamon, Oxford.

Boer R.H., Bsukes G.J., Meyer F.M., and Smith C.B. (1993a) 'Fluoride precipitates in silicate wet-chemistry: implications on REE fractionation'. *J. Chem. Geol*, **Vol.** 104; pp. 93-98.

Boer, R. H. (1995) 'A dissertation submitted to the Faculty, of Science, University of the Witwatersrand, Johannesburg, for the Degree of Doctor of Philosophy Johannesburg, 1995'.

Boer, R. H., Meyer, F.M., Robb, L.J., Graney, J.R., Vennemann, T.W., Kosoler, S.E. (1995) 'Mesothermal-type mineralization in the Sabie-Pilgrim's Rest gold field, South Africa', *J. Econ Geol*, **Vol.** 90(4); pp. 860–876.

Bouazza, A. (2002) 'Geosynthetic clay liner'. *Geotext Geomembr*, **Vol.** 20; pp. 3-17.

Bourg, A.C.M. (1995) 'Speciation of heavy metals in soils and groundwater and implications for their natural and provoked mobility'. In: Salomons, W., Förstner, U., Mader, P. (Eds.). *Heavy Metals*. Springer, Berlin.

Bourg, A. C. M., and Darmendrail, D. (1992) 'Effect of dissolved organic matter and pH on the migration of zinc through river bank sediments'. *J. Environ Tech*, **Vol.** 13; pp. 695-700.

Bowen, H.J.M. (1980) 'Environmental Chemistry', Academic Press, London.

Bradshaw, S.L., Benson, C.H., Rauen, T.L. (2016) 'Hydraulic conductivity of geosynthetic clay liners to recirculated municipal solid waste leachates'. *J. Geotech, Geoenviron*, **Vol.** 142; pp. 401507.

Brodie, G.A. Hammer, D. A. and Tomljanovich, D. A. (1988) 'An Evaluation of substrate Types in Constructed Wetlands Acid Drainage Treatment systems, *In: Proc. 1988 Mine Drainage and Reclam. Conf April 17-22.*

Brime, C. (1985) 'The accuracy of X-ray diffraction methods for determining mineral mixtures. *Mineralogical Magazine*, **Vol.** 49(353); pp. 531-538.

Brodie, G.A., Hammer, D.A. and Tomljanovich, D.A. (1988) 'Constructed Wetlands for Acid Drainage Control in the Tennessee Valley'. *In: Proceedings American Society of Mining and Reclamation*; pp. 325-331.

Brooks, R.R., Chambers, M.F. and Nicks, L.J. (1998) 'Phytomining'. *Trends in Plant Science*, **Vol.** 3; pp. 359-362.

Brown, G.E. (1990) 'Spectroscopic studies of chemisorption reaction mechanisms at oxide-water interfaces'. *In: Mineral-Water Interfaces Geochem*, M.F. Hocheller, Jr. and A.F. White (Eds.). Mineralogical Society of America, Washington, DC. **Vol.** 23; pp. 309-363.

Brown, P.L. and Markich, S.J. (2000) 'Evaluation of the free ion activity model of metal-organism interaction: extension of the conceptual model'. *J. Aquat. Toxicol*, **Vol.** 51; pp. 177-194.

Button, A., 1973 'A regional study of the stratigraphy and development of the Transvaal basin in the eastern and northeastern Transvaal': Ph.D. thesis (unpubl.), University of Witwatersrand.

Burns, A.S., Pugh, C.W., Segid, Y.T., Behum, P.T., Lefticariu, E., Benders, K.S. (2012) 'Performance and microbial community dynamics of a sulphate-reducing bioreactor treating coal generated acid mine drainage'. *J. Biodegrad*, **Vol.** 23(3); pp. 415-429.

Camden-Smith, B., Mthombeni, P., Johnson, R.H., Weiersbye, I.M. and Tutu, H. (2014) 'The Release and Transport of Metals Arising from Gold Mining Tailings Storage Facilities in the Witwatersrand, South Africa'. *An Interdisciplinary Response to Mine Water Challenges - Sui, Sun & Wang (eds)*, China University of Mining and Technology Press, Xuzhou, ISBN 978-7-5646-2437-8.

Camden-Smith, B.P.C. and Tutu, H. (2014) 'Geochemical modelling of the evolution and fate of metal pollutants arising from an abandoned gold mine tailings facility in Johannesburg'. *J. Water Science & Technology*. DOI: 10.2166/wst.2014.028 .

Caruso, J.A., Klaue, B., Michalke, B. and Rocked, D.M. (2000) 'Group assessment: elemental speciation'. *J. Ecotox & Environ Saf*, **Vol.** 56; pp. 32-44.

Castello, C. (2003) 'Acid Mine Drainage: Innovative Treatment Technologies', U.S. Environmental Protection Agency, Office of Solid Waste and Emergency Response Technology Innovation Office, Washington, D.C.

Chaney, R. L, Malik, M. Li, Y.M., Brown, S.L., Angle, J. S. and Baker, A.J.M. (1997) 'Phytoremediation of soil metals'. *J. Biotechn*, **Vol.** 8; pp. 279-284.

Charlton, S. R., and Parkhurst, D. L. (2002) 'PHREEQCI—A Graphical User Interface to the Geochemical Model PHREEQC'.

Chauhan, G., Pant, K.K., Nigam, K.D.P. (2015) 'Chelation technology: a promising green approach for resource management and waste minimization'. *J. Environ. Sci: Processes Impacts*, **Vol.** 17; pp. 12–40.

Chaudhry, T. M., Hayes, W. J., Khan, A. G., & Khoo, C. S. (1998) 'Phytoremediation – Focusing on accumulator plants that remediate metal-contaminated soils'. *Austral-asian J. . Ecotoxicology*, **Vol.** 4; pp. 37–51.

Chen, Q.Y., Brocato, J., Laulicht, F., Costa, M. (2017) 'Mechanisms of Nickel Carcinogenesis'. *J. Mol & Int Toxicol*; pp. 181-197.

Chetty, S., Pillay, L., Humphries, M.S. (2021) 'Gold mining's toxic legacy: Pollutant transport and accumulation in the Klip River catchment, Johannesburg'. *S. Afr J. Sci*, **Vol.** 117(7/8).

Christensen, B., Laake, M. and Lien, T. (1995) Personal communications (abstract of Norwegian Institute for Water Research) to Mr. Grant Feasby, MEND Secretariat.

Christenson, H., Weber, P., Pope, J., Newman, N., Olds, W., Trumm, D. (2017) ' Enhancing mine drainage treatment by sulfate reducing'. In: Wolkersdorfer C, Sartz L, Sillanpää M, Häkkinen A (Editors), IMWA2017 Mine Water and Circular Economy, Lappeenranta, Finland (Lappeenranta University of Technology). **Vol.** 3; pp. 1196-1203.

Clayton, G.D. and Clayton, F.E. (1994) 'Patty's Industrial Hygiene Toxicology. 4th Edn., A Wiley-Interscience Publication, New York.

Clendenin, C.W.. Jr. (1989) 'Tectonic influence on the evolution of the Early Proterozoic Transvaal Sea, southern Africa': Ph.D. Thesis (unpubl.), Johannesburg, University of Witwatersrand.

Cornell, R.M., Schwertmann, U. (2003) 'Adsorption of Ions and Molecules, The Iron Oxides: Structure, Properties, Reactions, Occurrences and Uses', Second Edition. Wiley-VCH Verlag GmbH and Co. KGaA, Weinheim, 253-287.

Coupland, K., Rowe, O., Hallberg, K.B. and Johnson, D.B. (2004) 'Biogeochemistry of a subterranean acidic mine water body at an abandoned copper mine'. Mine water– process, policy and progress In: Jarvis A.P., Dudgeon, B.A. and Younger, P.L. (eds.) University of Newcastle upon Tyne, UK. **Vol.** 1; pp. 113–119.

Cravotta, C.A. and Trahan, M.K. (1999) 'Limestone drains to increase pH and remove dissolved metals from acidic mine drainage'. *J. Appl Geochem*, **Vol.** 14; pp. 581-606.

Cravotta, C.A., Ward, S.J., Koury, D.J. and Koch, R.D. (2004) 'Optimization of limestone drains for long-term treatment of mine drainage, Swatara Creek Basin, Schuylkill County, PA'. 366-411. *In: Proceedings of the 2004 National Meeting of the American Society of Mining and Reclamation and the 25th West Virginia Surface Mine Drainage Task Force. Morgantown, West Virginia. 18-22 April.*

Crawford, J. (1999) 'Geochemical Modelling – A Review of Current Capabilities and Future Directions'. *Natur Vards Verket (Swedish Environmental Protection Agency)*.

Dallas, H. and Day, .J (2004) 'The Effect of Water Quality Variables on Aquatic Ecosystems: A Review'. WRC Technical Report No. 224/04, Water Research Commission, Pretoria, South Africa.

Das, R. and Maiti, S.K. (2016) Estimation of carbon sequestration in reclaimed coalmine degraded land dominated by *Albizia lebbeck*, *Dalbergia sissoo* and *Bambusa arundinacea* plantation: A case study from Jharia Coalfields, India *Int J. Coal Sci Technol.* **3** (2), 246–66.

Davis, B. & Day, J. (1998). 'Vanishing Waters'. U.C.T. Press, University of Cape Town, South Africa, 487.

Davis, A., Drexler, J.W., Ruby, M.V., and Nicholson, A. (1993) 'Micromineralogy of mine wastes in relation to lead bioavailability', Butte, Montana: *J. Environ Sci and Techno*, **Vol.** 27; pp. 1415–1425.

DEA (Department of Environmental Affairs) (2013) 'National Environmental Management: Waste Act: National Norms and Standards for the remediation of contaminated land and soil quality'.

Deacon, A.R. (1996) 'Sabie Sand IFR Workshop Starter Document'. Department of Water Affairs and Forestry, Pretoria, South Africa.

Delgado, J., Barba-Brioso, C., Nieto, J.M., Boski, T. (2011) 'Science of the Total Environment Speciation and ecological risk of toxic elements in estuarine sediments affected by multiple anthropogenic contributions (Guadiana saltmarshes , SW Iberian Peninsula): I . Surficial sediments'. *J. Sci Tot Environ*, **Vol.** 409; pp. 3666-3679.

Dermont, G., Bergeron, M., Mercier, G., Richer-Lafleche, M., 2008. 'Soil washing for metal removal: a review of physical/chemical technologies and field applications'. *J. Hazard. Mater*, **Vol.** 152; pp. 1–31.

Derviř, B. (2013) ' Using the Sediment Quality Triad to Characterize Toxic Conditions in the Chesapeake Bay (2002): An Assessmet of Tidal River Segments in the Bohemia, Elk, Northeast, and Severn Rivers'. *J. of Chem Info and Model.* **Vol.** 53; pp. 1689-1699.

Dierberg ,F.E., DeBusk, T.A., Goulet, N.A. (1987) 'Aquatic plants for water treatment and resource recovery'. In: Reddy KR, Smith WH (eds) Magnolia, Orlando.

Dinu, L.R., Stefanescu, M., Patroescu, V., Cosma, C., Cristea, I., Badescu, V., Alexie, M. (2016) 'Trials For The Improvement Of The Ettringite Process For The Mine Water Treatment'. *J. Environ Prot & Ecol*, **Vol.** 17(1); pp. 83–93.

Dinu, L.R. et al. (2016) 'Towards Mining the Mine Water-Recovery of Aluminium and Manganese'. *J. Environ and Indus*, pp. 365-370.

Dos Reis, C.A., Da Silva, A.B., Landgraf, P.R.C., Batista, J.A., Jacome, G.A.R. (2018) 'Bioreactor in the micropropagation of ornamental pineapple'. *J. Ornamental Horticulture*, **Vol.** 24; pp. 182-187.

Drapeau et al., (2021) 'Lead Mobilization and Speciation in Mining Waste: Experiments and Modeling'. *J. Minerals*, **Vol.** 11; pp. 606. <https://doi.org/10.3390/min11060606>.

Drogowska, M., Brossard, L. and Me´nard, H. (1994) 'Comparative study of copper behaviour in bicarbonate and phosphate aqueous solutions and effect of chloride ions'. *J. Appl. Electrochem*, **Vol.** 24(4); pp. 344–349.

Dudeney, A.W.L., (1997) 'Removal and utilization of iron from contaminated waters', *Clay Techn*, **Vol.** 54; pp. 8-10.

Duggan, L.A., Wildeman, and D.M. Updegraff, D.M. (1992) The aerobic removal of manganese from mine drainage by an algal mixture containing Cladophora. In: Proceedings, Ninth American Society for Surface Mining and Reclamation Conference, Duluth, MN. June 14-18.

Dushenkov, V., P. Kumar, H. M. and Raskin, I. (1995) 'Rhizofiltration: the use of plants to remove heavy metals from arduous streams'. *J. Environ Sci and Technol*, **Vol.** 29; pp. 1239-1245.

Dussel, E. (1994) 'Bioavailability of Metals'. J. De la "conquista" a la "colonización" del mundo de la vida (Lebenswelt). 10-18.

DWAF (1996) Department of Water Affairs and Forestry. 'South African Water Quality Guidelines', **8**, Field Guide, Pretoria, South Africa.

Edinger, E. (2012) 'Gold mining and submarine tailings disposal: Review and case study'. *J. Oceanography*, **Vol.** 25(2); pp. 184–199.

Edwards, K.J., Bond, P.L., Druschell, G.K., McGuire, M.M., Hamers, R.J. and Banfield, J.F. (2000) 'Geochemical and biological aspects of sulphide mineral dissolution: lessons from Iron Mountain, California'. *J. Chem Geol*, **Vol.** 169(3-4); pp. 383-397.

Eger, P. (1994) 'Wetland treatment for trace metal removal from mine drainage: the importance of aerobic and anaerobic processes'. *J. Water Sci. Technol.* **29**, 249-256.

Elder, J.F. (1989) 'Metal biogeochemistry in surface-water systems—A review of principles and concepts'. *U.S. Geol Sur Circular*. **Vol.** 1013; pp. 43.

Edokpayi, J.N., Odiyo, J.O., O.E. and Titus Msagati, A.M. (2016) 'Assessment of Trace Metals Contamination of Surface Water and Sediment: A Case Study of Mvudi River, South Africa'. *J. Sustainability (Switzerland)*, **Vol.** 8; pp. 1-13.

Egloffstein, T.A. (2001) 'Natural bentonites-influence of the ion exchange and partial discation on permeability and self-healing capacity of bentonites used in GCLs'. *Geotex Geomembr*, **Vol.** 19; pp. 427-444.

Figuroa, L., Landkamer, L., Drennan, D., Sharp, J., Lee, I. (2016) 'Sulfate Reducing Bioreactor Longevity Estimates Based on Substrate Characterization and Initial Carbon Release'. IMWA Proceedings; 952-956.

Florinsky, I.V. (2000) 'Relationship between topographically expressed zones of flow accumulation and sites of fault intersection: analysis by means of digital terrain modeling'. *J. Environ. Model. Sof*, **Vol.** 15; pp. 87–100.

Ford, C.T. (1974) 'Use of limestone in AMD treatment'. Coal mine drain res., 5th Coal and the env. tech. Conf., Louisville, Ky. Proceedings; pp. 205-228.

Ford, K.L. (2003) 'Passive treatment systems for acid mine drainage'. Technical Note 409. BLM/ST/ST-02/001+3596. *US Bureau of Land Management Papers* 19.

Fosso-Kankeu, E., Mulaba-Bafubiandi, A. F., Mamba, B. B., Barnard, T. G. (2011) 'Prediction of Metal Adsorption Behaviour in the Remediation of Water Contamination Using Indigenous Microorganisms'. *J. Environ. Mgt*, **Vol.** 92(10); pp. 2786–2793.

Fosso-Kankeu, E., Manyatshe, A. and Waanders, F. (2017) ' Mobility potential of metals in acid mine drainage occurring in the Highveld area of Mpumalanga Province in South Africa: Implication of sediments and efflorescent crusts'. *J. Int Biodeterioration & Biodegradation*, **Vol.** 119; pp. 661-670.

Galán, E. *et al.* (2003) 'Heavy metal partitioning in river sediments severely polluted by acid mine drainage in the Iberian Pyrite Belt'. *J. Appl Geochemi*, **Vol.** 18; pp. 409-421.

Garbisu, C. & Alkorta, I. (2001) 'Phytoextraction: a cost-effective plant-based technology for removal of metals from the environment'. *J. Biores Technol*, **Vol.** 77; pp. 229-236.

Gardea-Torresdey, J.L., de la Rosa, G. Peralta-Videa, J.R., Montes, M. Cruz-Jimenez, G. and Cano- Aguilera, I. (2005) 'Differential uptake and transport of trivalent and hexavalent chromium by tumbleweed (*Salsola kali*)'. *Arch Environ Contam Toxicol*. PMID:15696348.

Gazea, B., Adam, K., Kontopoulos, A. (1996) 'A review of passive systems for the treatment of acid mine drainage'. *J. Miner. Eng*, **Vol.** 9; pp. 23–42.

Gebrekrstos, R. A., Pretorius, J. A. and Usher, B. H. (2008) Manual for Site Assessment at DNAPL Contaminated Sites in South Africa Report to the Water Research Commission.

Geidel, G. and Caruccio, F.T. (1984) 'Evaluation of a surface limestone for controlling acid mine drainage from abandoned strip mines'. Sewellsville, Ohio. Final report. BP-84-148532: 185.

Glass, D.J. (2000) 'Economic potential of phytoremediation'. In: Raskin I and Ensley DB (Eds) *Phytoremediation of Toxic Metals* (pp.15-31). John Wiley & Sons, New York, USA.

Gleisner, M. (2005) 'Quantification of mineral weathering rates in sulfidic mine tailings under water-saturated conditions'. Thesis submitted to the Department of Geology and Geochemistry, Stockholm University, Stockholm, Sweden.

Goldberg, D.E. (1954) 'Marine geochemistry 1. Chemical Scavengers of the Sea'. *Scripps Institution of Oceanography, J. Geol*, **Vol.** 62(3); pp. 249-265.

Gomes, M.E.P., Favas, P.J.C., (2006) 'Mineralogical controls on mine drainage of the abandoned Ervedosa tin mine in north-eastern Portugal'. *J. Appl Geochem*, **Vol.** 21; pp. 1322–1334.

- Goulbourne, E., Matin, M., Zychlinsky, E. and Matin, A. (1998) 'Mechanism of Δ pH maintenance in active and inactive cells of an obligately acidophilic bacterium'. *J. Bacteriology*, **Vol.** 166; pp. 59-65.
- Gouws, P. and Coetzee, P.P. (1996) 'Determination and partitioning of heavy metals in the sediments of the Vaal Dam System by sequential extraction'. *Department of Chemistry and Biochemistry, Rand Afrikaans University, South Africa*, **Vol.** 23(3); pp. 217-226.
- Gramowska, H., Krzyzaniak, I., Baralkiewicz, D. Goldyn, R., (2010) 'Environmental applications of ICP-MS for simultaneous determination of trace elements and statistical data analysis'. *Environ Monit Assess*, **Vol.** 160; pp. 479–490.
- Gray, N.F. (1998) 'Acid Mine Drainage Composition and Implications on lotic systems'. *J. Water Res*, **Vol.** 32(7); pp. 2122-2134.
- Greenfield, R., van Vuren, J.H.J., Epener, V. (2007) 'Determination of sediment quality in the Nyl River system, Limpopo Province, South Africa'. *J. Water S.A*, **Vol.** 33(5); pp. 693-700.
- Greenwood, N.N. and Earnshaw, A. (1998) '*Chemistry of the elements*'. Second Edition. Butterworth-Heinemann, Oxford.
- Grijalva, V.M.G. (2009) 'Biological and physical-chemical methods for treatment of semiconductor manufacturing effluents. Doctor of Philosophy, University of Arizona, USA.
- Grover, B.P.C., Johnson, R.H., Tutu, H. (2016) 'Leachability of metals from gold tailings by rainwater: An experimental and geochemical modelling approach'. *Water SA*, **Vol.** 42(1); pp. 38-42.
- Gupta, R., Ahuja, P., Khan, S., Saxena, R.K. and Mohapatra, H. (2000) 'Microbial biosorbents: Meeting challenges of heavy metal pollution in aqueous solutions'. *Current Sci*, **Vol.** 78; pp. 967-973.
- Gupta, B., Kumar, R. and Rani, M. (2013) 'Speciation of heavy metals in water and sediments of an urban lake system'. *Journal of Environ Sci and Health, Part A*. **Vol.** 48; pp. 1231–1242.
- Gusek, J.J. (1995) 'Passive-treatment of acid rock drainage: What is the potential bottom line?'. *International J. Rock Mec, Min Sci & Geomechanics*.

Gusek, J.J. (2004) 'Scaling up design challenges for large scale sulfate reducing bioreactors'. Proceedings America Society of Mining and Reclamation'. <http://dx.doi.org/10.21000/JASMR04010752>.

Gusek, J. (2005) 'Design challenges for large scale sulfate reducing bioreactors'. *J. Cont Soils, Sed & Wat*, **Vol.** 9; pp. 33-44.

Gusek, J.J. and Plocus, V. (2016) 'Case Study: 20 Years of Acid Rock Drainage Chemistry Improvements after a Bactericide Application. *J. Amer Soc of Min & Reclam*, **Vol.** 5(1); pp. 67-85

Gusek, J.J., Corcutt, T., and Josselyn, L. (2021) 'Using Spent Brewery Grain to Suppress Acid Rock Drainage from Historic Tailings'. *Reclamation Matters*; pp. 21-28.

Gusek, J.J. (2022) 'Revisiting Bactericides: a 40-Year-Old (and Counting) Technology to Suppress Acid Rock Drainage'. 12th International Conference on Acid Rock Drainage', Australia.

Habs, H., Simon, B., Thiedemann, K.U. and Howe, P. (1997) '*Aluminium, environmental health criteria 194*'. World Health Organization, WHO Library Cataloguing in Publication Data, Geneva.

Hammarstrom, J.M., Sibrell, P.L., Belkin, H.E. (2003) 'Characterization of limestone reacted with acid-mine drainage in a pulsed limestone bed treatment system at the Friendship Hill National Historical Site, Pennsylvania, USA'. *J. Appl Geochem*, **Vol.** 18(11); pp. 1705-1721.

Han, Y.S., Youm, S.J., Oh, C., Cho, Y.C., Ahn, J.S. (2017) 'Geochemical and eco-toxicological characteristics of streamwater and its sediments affected by acid mine drainage'. *J. Catena*, **Vol.** 148; pp. 52-59.

Harley, M. and Charlesworth, E.G. (1990) 'The mineralization at Elandshoogte Gold Mine, eastern Transvaal, South Africa. Economic Geology Research Unit, Univ. Witwatersrand, Johannesburg, Information Circular 226.

Harley, M. and Charlesworth, E.G. (1991a) 'Comprehensive deformation of a pre-Bushveld diabasic sill, Sudwala, eastern Transvaal, S. Afr.', *J. Geol*, **Vol.** 94(5/6); pp. 348-354.

Harley, M. and Charlesworth, E.G. (1992) 'Thrust-controlled gold mineralization at the Elandshoogte mine, Sabie-Pilgrim's Rest goldfield, South Africa': *Mineralium Deposita*, **Vol.** 27; pp. 122-128.

Harries, J.A., Birch, P., Short, C.K. (1989) 'Changes in the microbial community and physico-chemical characteristics of topsoil stockpiled during opencast mining. *Soil Use and Mgt*, **Vol.** 5; pp. 161-168.

Hartman, W.J. Jr (1975) 'An evaluation of land treatment of municipal wastewater and physical siting of facility installations'. Washington, DC; US Department of Army.

Hartman, M.D., Baron, J.S., Ojima, D.S. (2007) 'Application of a coupled ecosystem-chemical equilibrium model, DayCent-Chem, to stream and soil chemistry in a Rocky Mountain watershed'. *Ecological Modeling*, **Vol.** 200(3-4); pp. 493-510.

Hazermoshar, A., Lak, R., Espahbood, M.R., Ghadimvand, N.K., Farajzadeh, R. (2016) 'Geochemical, Sedimentological and Mineralogical Characterization of Surficial Sediments in Eynak Marsh (North of Iran)'. *Open J. Geol*, **Vol.** 6; pp. 640-659.

Health, C. *et al.* (2015) 'SANS 241-1 : 2015 - Edition 2'.

Hedin, R.S. and Nairn, R.W. (1992) 'Passive treatment of coal mine drainage'. Course notes for workshop. Pittsburgh, PA, US Bureau of Mines.

Hedin, R.S., Nairn, R.W., Kleinmann, R.L.P. (1994) 'Passive treatment of coal mine drainage'. US Bureau of Mines Information Circular Number 9389.

Hedin, R.S. (2002) 'Recovery of Marketable Iron Oxide from Mine Drainage'. National Meeting of the American Society of Mining and Reclamation, Lexington KY, June 9-13; 517-526.

Holner, S. (2015) 'Removal of Heavy Metals from wastewater: A review'. *IJAIEEM*, **Vol.** 10(4); pp. 19-22.

Halnor, S. & Ubale, M. (2013) 'Int. J. of Recent Trends in Sc.& Tech. Sp. Issue ACTRA-India; pp. 38-42.

Horng, Ch., Wang, Sh. and Cheng, I. (2009) 'Effects of sediment-bound Cd, Pb, and Ni on the growth, feeding, and survival of *Capitella* sp. I'. *J. Exp. Mar. Biol. Ecol*, **Vol.** 371; pp. 68–76

Hurst, A. and Morton, A.C. (2014) 'Provenance models: The role of sandstone mineral-chemical stratigraphy'. *Geol Soc Special Publication*, **Vol.** 386(1); pp. 7-26.

Hutchison, I.P.G. and Ellison, R.D. (1992) *Mine Waste Management, a Resource for Mining Industry Professionals, Regulators and Consulting Engineers*. Lewis Publishers.

Ibrhaim, A. and Aly, A.A. (2014) 'Geochemical and Mineralogical Characters of the Coastal Plain Sediments of the Arabian Gulf, Kuwait'. *J. Geol & Geosci*, **Vol.** 3; pp. 1-9.

Ibrahim, K.M. and El-Naqa, A.R. (2018) 'Inverse geochemical modeling of groundwater salinization in Azraq Basin, Jordan'. *Arabian J. Geosci*, **Vol.** 11; pp. 237.

Islam, M.S., Ahmed, M.K., Raknuzzaman, M., Habibullah-ALMamun, M., Islam M.K, (2015c) 'Heavy metal pollution in surface water and sediment: a preliminary assessment of an urban river in a developing country'. *Ecol.Indic*, **Vol.** 48; pp. 282-291.

ITRC, Interstate Technology & Regulatory Council (2011) 'Permeable Reactive Barrier: Technology Update'. PRB: Technology Update Team, Washington, D.C.

Jan, S. and Parray, J. (2016) 'Phytoremediation- A Green Technology'. *Approaches to Heavy Metal Tolerance in Plants*. DOI 10.1007/978-981-10-1693-6_5.

Jacques, D., Šimůnek, J. (2004) 'User manual of the Multicomponent variablysaturated transport model HP1 (Version 1.0): Description, Verification and Examples'. SCK.CEN, *Mol, Belgium*, BLG-**Vol.** 998.

Jimenez, Y.P., Justel, F, Casas, J.M. (2022) 'Model speciation and solubility of sodium molybdate in water, 0-110 °C'. *J. Molecular Liquids*, ISSN 0167-7322.

Jin, S., Fallgren, P.H., Morris, J.M. and Cooper, J.S. (2008) 'Source Treatment of Acid Mine Drainage at a Backfilled Coal Mine Using Remote Sensing and Biogeochemistry'. *Water, Air Soil Pol*, **Vol.** 188; pp. 205-212.

Jiwik, R., Payant, S. and Wheel, K. (1989) 'Control of acid generation from reactive waste rock with the use of chemicals'. Paper presented at the Tailings and Effluent Management Symposium at the 28th Annual C.I.M. Conference of Metallurgists, Halifax, N.S., 20-24 August.

Johnson, D.B. and Hallberg., K.B. (2005) 'Acid mine drainage remediation options': a review: *Sci Tot Environ*, **Vol.** 338; pp. 3-14.

Jones, C. (1990) 'Hydrogeological assessment and development of amd control technology for myra falls waste rock'. *Northwest Geochem #204* - 26 Bastion Square, Victoria, B.C.

Jones, A., Rigopoulos, S., Zauner, R. (2004) 'Crystallization and precipitation engineering'. In: Barbosa-Póvoa A., Matos H. (eds), Elsevier. *Computer aided chem eng*, **Vol.**18; pp. 75-86.

Jung, M.C. (2001) 'Heavy metal contamination of soils and waters in and around the Imcheon Au-Ag mine, Korea'. *J. Appl Geochem*, **Vol.** 16; pp. 1369-1375.

Kabata-Pendias, A. (2000) 'Biogeochemistry of cadmium'. *Committee "Man and the environment"* under the Presidium of the Polish Academy of Science, **Vol.** 26; pp. 17–24.

Kabata-Pendias, A. and Pendias, H. (2000) 'Trace elements in soils and plants'. *CRC Press Boca Raton*, London New York Washington D.C.

Källvenius, G., Ekberg, C. (2003) 'TACK—a program coupling chemical kinetics with a two-dimensional transport model in geochemical systems'. *Computers & Geosciences*, **Vol.** 29(4); pp. 511-521.

Kama, S. and Davis, D. (1991) 'A review of geochronology from the Barberton Mountain Land, In Two Cratons and an Orogen'- Excursion Guidebook and Review Articles for a Field Workshop through Selected Archaean Terranes of Swaziland, South Africa and Zimbabwe (ed, D. Ashwal), IGCP Project 280; pp. 59-68.

Kannan, N. Sarojini, P. (2010) *Ind. J. Env. Prot.*, 30(5), 404-408.

Kapoor, A., Viraraghavan, T. and Cullimore, D.R. (1999) 'Removal of heavy metals using the fungus *Aspergillus niger*'. *Biores Techn*, **Vol.** 70; pp. 95-104.

Karabelnik, K., Noorvee, A., Pöldvere, E., Mander, Ü. (2008) 'Batch-operation as a method to enhance oxygen supply in a constructed wetland'. *WIT Transactions on the Built Environment*. **Vol.** 100; pp. 131-142. WIT Press.

Karukstis, K.K. and Van Hecke, G.R. (2003) '*Chemistry Connections: The Chemical Basis of Everyday Phenomena*'. Academic Press/Elsevier Science, San Diego.

Kay, S.H., Haller, W.T., Garrard, L.A. (1984) 'Effect of heavy metals on water hyacinths [*Eichhornia crassipes* (Mart.) Solms]'. *Aquatic Toxicology*, **Vol.** 5; pp. 117-128.

Khalid, A., Khan, A.T., Alam, J., Anwar, M.S. (2015) 'X-Ray Fluorescence (XRF) spectrometry for materials analysis and "discovering" the atomic number'. Version 2015-1.

Kilborn (1999) '*Review of Passive Systems for Treatment of Acid Mine Drainage*'. Mine Environment Neutral Drainage (MEND) Report 3.14.1.

Kinniburgh, D.G., Cooper, D.M., 2010. 'PhreePlot—Creating graphical output with PHREEQC'. Accessed March 23, 2010. <http://www.phreeplot.org>.

Kitaura, H., Nakao, N., Yoshida, N., Yamada, T. (2003) 'Induced sensitization to nickel in guinea pigs immunized with mycobacteria by injection of purified protein derivative with nickel'. *New Microbiol*, **Vol.** 26(1); pp. 101.

Kleinmann, R.L.P. and Erickson, P.M. (1983) 'Control of Acid Mine Drainage from Coal Refuse using Anionic Surfactants', U.S. Bureau of Mines Report of Investigations 8847.

Kleinmann, R.L.P. (1998) (in) Brady, Smith, and Schueck (Eds) 'Bactericidal Control of Acidic Drainage'. In 'Coal Mine Drainage Prediction and Pollution Prevention in Pennsylvania'. (Pennsylvania Department of Environmental Protection: Harrisburg, PA).

Kolkstad, D., Benson, C.H., Edil, T. (2004) 'Hydraulic conductivity and swell of non prehydrated geosynthetic clay liners permeated with multi-species organic solutions'. *J Geotech Geoenviron*, **Vol.** 130; pp. 1236-1249.

Kousi, P., Remoundaki, E., Hatzikioseyan, A., Tsezos, M. (2015) 'Sulphate-reducing bioreactors: current practices and perspectives'. *IWA Balkan Young Water Professional*, May 10-12; pp. 409-417.

Khorasanipour, M., Tagestani, M.H., Naseh, R., Hajmohammadi, H. (2012) 'Chemical Fractionation and Contamination Intensity of Trace Elements in Stream Sediments at the Sarcheshmeh Porphyry Copper Mine, SE Iran'. *J. Mine Water and the Environ*, **Vol.** 31(3); pp. 199-213.

Khorasanipour, M., Tagestani, M.H., Naseh, R., Hajmohammadi, H. (2012) 'Chemical Fractionation and Contamination Intensity of Trace Elements in Stream Sediments at the Sarcheshmeh', *Mine Water and the Environ*, **Vol.** 31(3); pp. 199–213. doi: 10.1007/s10230-012-0198-0.

Kroschwitz, J.I., Seidel, A. (2006) 'Kirk-Othmer encyclopedia of chemical technology, Wiley.

Kuipers, J.R., Maest, A.S., McHardy, K.A. and Lawson, G. (2006) 'Comparison of Predicted and Actual Water Quality at Hardrock Mine: The reliability of predictions in Environmental Impact Statements'. Kuipers & Associates, PO Box 641, Butte, MT USA, 59703.

Langergraber, G. (2008) 'Modeling of Processes in Subsurface Flow Constructed Wetlands: A Review'. *J. Vadose Zone*, **Vol.** 7(2); pp. 830-842.

Langmuir, D. (1978) 'Uranium solution-mineral equilibria at low temperature with applications to sedimentary deposits. *Geochim. Cosmochim. Acta*, **Vol.** 42; pp. 547-569.

Lapakko, K. (1993b) 'Mine Waste Drainage Quality Prediction: A Literature Review'. Draft Paper. Minnesota Department of Natural Resources, Division of Minerals, St. Paul, MN.

Larney, F.J. and Clark, D. (2012) 'The role of organic amendments in soil reclamation: A review'. *Canadian J. Soil Sci*, **Vol.** 92; pp. 19-38.

Lasat, M.M. (2002) 'Phytoextraction of metals from contaminated soil: A view of plant/soil/metal interaction and assessment of pertinent agronomic issues'. *J. Haz sube Res*, **Vol.** 2; pp. 1-25.

Lawrence, R. (1990) 'Prediction of the Behavior of Mining and Processing Wastes in the Environment'. In: *Proc. Western Regional Symposium on Mining and Mineral Processing Wastes*. Edited by Fiona Doyle, Published by the Society for Mining, Metallurgy, and Exploration, Inc., Littleton, CO.

Leathen, W.W., Bradley, S. Jr, and McIntyre, L.D. (1953) 'The role of bacteria in the formation of acid from certain sulfuritic constituents associated with bituminous coal, Part 2. Ferrous iron oxidizing bacteria'. *J. Appl Microbio*, **Vol.** 1; pp. 65-68.

Lee, P.K., Kang, M.J., Choi, S.-H., and Touray, J.-C. (2005) 'Sulfide oxidation and the natural attenuation of arsenic and trace metals in the waste rocks of the abandoned Seobo tungsten mine, Korea'. *J. Appl Geochem*, **Vol.** 20; pp. 1687-1703.

Lefticariu, E., Walters, C., Pugh, C.W., Bander, K.S. (2015) ' Sulfate reducing bioreactor dependence on organic substrates for remediation of coal-generated acid mine drainage: Field experiments. *J. Appl Geochem*, **Vol.** 63; pp. 70-82.

Leštan, D., Luo, C.L., Li, X.D. (2008) 'The use of chelating agents in the remediation of metal-contaminated soils: a review'. *Environ. Pollut*, **Vol.** 153; pp. 3–13.

Levinson, A.A. (1974) 'Introduction to exploration geochemistry'. *Applied Publishing Ltd.*, Wilmette, Illinois, USA.

Levy, D.B., Custis, K.H., Casey, W.H., Rock, P.A., 1997a 'The aqueous geochemistry of the abandoned Spenceville copper pit, Nevada County, California'. *J. Environ. Qual*, **Vol.** 26; pp. 233–243.

Levy, D.B., Custis, K.H., Casey, W.H., Rock, P.A. (1997b) 'A comparison of metal attenuation in mine residue and over- burden material from an abandoned copper mine'. *J. Appl. Geochem*, **Vol.** 12; pp. 203–211.

Lewis, A.E., Seckler, M.M., Kramer, H., van Rosmalen, G.M. (2015) 'Industrial crystallization: fundamentals and applications'. Cambridge University Press.

Liao, J., Chen, J., Ru, X., Chen, J., Wu, H., Wei, C. (2017) 'Heavy metals in river surface sediments affected with multiple pollution sources, South China: Distribution, enrichment and source apportionment'. *Journal of Geochemical Exploration*, **Vol.** 176; pp. 9-19.

Lindsay, M.B.J., Blowes, D.W., Condon, P.D. and Ptacek, C.J. (2010) 'Treatment of Pore Water in Mine Tailings Using Organic Carbon Amendment's. Paper presented at the 2010 GSA Denver Annual Meeting (31 October –3 November) Paper No. 157-7.

List, R. (1989) 'Subaqueous Disposal of Reactive Mine Wastes: An Overview June 1989 Sommaire'. MEND Project 2.11.1a.

Liu, J. and Neretnieks, I. (2009) 'Coupled transport/reaction modelling of copper canister corrosion aided by microbial processes'. *Radiochimica Acta*.

Luoma, S.N. (1985) 'Biological availability of sediment-bound trace metals'. *J. La Baie de Seine. Colloque National du CNRS, 24-26 avril*, 347-362.

Lusunzi, R., Gumbo, J.R., Yibas, B., Novhe, O. (2017) 'Geochemical and Mineralogical Characterization of Gold Mine Tailings for the potential of acid mine drainage in the Sabie-Pilgrim's Rest goldfields, South Africa'.-In: Wolkersdorfer C, Sartz L, Sillanpää M, Häkkinen A (Editors): Mine Water and Circular Economy, Lappeenranta, Finland (Lappeenranta University of Technology).

Lusunzi, R., Gumbo, J.R., Yibas, B., Novhe, O. (2018) 'Acid Base Accounting (ABA) of mine tailings for the Potential of Acid Mine Drainage in the Sabie- Pilgrim ' s Rest Goldfields , South Africa'. – In: Wolkersdorfer, Ch.; Sartz, L.; Weber, A.; Burgess, J. & Tremblay, G. (Editors): Mine Water – Risk to Opportunity; Pretoria, South Africa (Tshwane University of Technology).

Lusunzi, R. (2018) 'Geochemical and mineralogical characterization of gold mine tailings for the potential of acid mine drainage in the Sabie-Pilgrim's Rest goldfields'. MSc Thesis, University of Venda.

Ma, J., Su, G., Zhang, X. and Huang, W. (2016) 'Adsorption of Heavy Metal Ions from Aqueous Solutions by Bentonite Nanocomposites'. *J. Water Environ. Res*, **Vol.** 88(8); pp. 741–746.

MacDonald, D. D., Ingersoll, C. G. and Berger, T. A. (2000) 'Development and evaluation of consensus-based sediment quality guidelines for freshwater ecosystems', *Archives of Environmental Contamination and Toxicology*, **Vol.** 39(1); pp. 20–31.

Malmström, M.E., Destouni, G., Martinet, P. (2004) 'Modeling expected solute concentration in randomly heterogeneous flow systems with multicomponent reactions'. *J. Environ Sci & Techn.* **Vol.** 38(9); pp. 2673-2679.

Manahan, S.E. (2003) '*Toxicological chemistry and biochemistry*'. Lewis Publishers, CRC Press Company, Boca Raton- London-New York-Washington.

Manyatshe, A., Fosso-Kankeu, E., Waanders, F. and Tutu, H. (2017) 'Metal retention potential of sediment and water quality in the Mooi River , South Africa Metal retention potential of sediment and water quality in the Mooi River , South Africa'. *J. Desalination and Water Treatment*, **Vol.** 66; pp. 346–357.

Mao, X., Prommer, H., Barry, D.A., Langevin, C.D., Panteleit, B., Li, L. (2006) 'Three-dimensional model for multi-component reactive transport with variable density groundwater flow'. *Environl Model & Soft*, **Vol.** 21(5); pp. 615-628.

Marani, D., Macchi, G. and Pagano, M. (1995) 'Lead Precipitation in the Presence of Sulphate and Carbonate: Testing of Thermodynamic Predictions'. *Water Res*, **Vol.** 29; pp. 1085–1092.

Marini, L. (2013) ' Reaction Path Modeling: Theoretical Aspects and Applications'. *J. Medical Geochemistry*, DOI: 10.1007/978-94-007-4372-4_4.

Maree, J.P., du Plesis, P., Vander, W.C. (1992) 'Treatment of acidic effluents with limestone instead of lime'. *J. Water Sci. Tech*, **Vol.** 26(1-2); pp. 345-355.

Maree, J.P. *et al.* (2004) 'Design criteria for limestone neutralization at a nickel mine, Mine water and the environment'. *J. Mine Water and Environ*, **Vol.** 23; pp.152-156.

Maree, J.P., de Beer, M., Strydom, W.F., Christie, A.D.M. and Waanders, F.B. (2004) 'Neutralizing Coal Mine Effluent with Limestone to Decrease Metals and Sulphate Concentrations'. *J. Mine water and environ*, **Vol.** 23; pp. 81-86.

Maree, J.P., Theron, D., Nengovhela, N.R. and Hlabela, P.S. (2005) 'Sulphur from smelter gases and sulphate-rich effluents'. *J. S. Afr. Inst. Min. Metall*, **Vol.** 105; pp. 1-4.

Martin, D. McB., Clendenin, C. W., Krapez, B., McNaughton, N. J. (1998) 'Tectonic and geochronological constraints on late Archean and Palaeoproterozoic stratigraphic correlation within and between the Kaapvaal and Pilbara Cratons'. *J. Geol. Soc. London*, **Vol.** 155; pp. 311-145.

Mashifana, T., Sithole, N. and Mkhonto, E. (2019) 'Stabilization of gold mine tailings: The effect of hydrated lime on the unconfined compressive strength'. *IOP Conf. Ser.: Mater. Sci. Eng*, **Vol.** 652; pp. 012-045.

Masliy, A.N., Shapnik, M.S. and Kuznetsov, A.M. (2000) Quantum-chemical investigation of electrochemical processes. Part I. Investigation of the mechanism of Zn(II) complex electroreduction from alkaline water solutions. *Quantum-chemical simulation, chemistry and computational simulation. Butlerov Commun*, **Vol.** 3; pp. 1–6.

Matabane, D.L., Godeto, T.W, Mampa, R.M. and Abayneh A. Ambushe, A.A. (2021) 'Sequential Extraction and Risk Assessment of Potentially Toxic Elements in River Sediments'. *J. Minerals*, **Vol.** 874(2); 1-18.

Mateo-Sagasta, J., Zadeh, S.,M. Turrall, H. (2017) 'Water pollution from agriculture: a global review'. Food and Agriculture Organization of the United Nations Rome, 2017 and the International Water Management Institute on behalf of the Water Land and Ecosystems research program Colombo.

Mattielli, N., Petit, J.C.J., Deboudt, K., Flament, P., Perdrix, E., Taillez, A., Rimetz-Planchon, J. and Weis, D. (2009) 'Zn isotope study of atmospheric emissions and dry depositions within a 5 km radius of a Pb-Zn refinery'. *J.Atmos. Environ*, **Vol.** 43; pp. 1265–1272.

Maurya, A.K. Sharma, R.K. Kumar, A. Joseph, P.E. (2007) *Ind.J. Env. Prot.*, 27(3), 272-275.

McCarthy, T.S. (2011) 'The impact of acid mine drainage in South Africa'. *S. Afr. J. Sci.* **Vol.** 107; pp. 1-7.

McCloskey, A.L., Bless, D., US. Department of Energy (2005) 'Prevention of Acid Mine Drainage Generation from Open-pit Highwalls — Final Report Mine Waste Technology Program Activity III , Project 26'. *J. Environmental Protection*, EPA/600/R-05/060 July.

- McGrath, S.P., Zhao, F.J. and Lombi, E. (2001) 'Plant rhizosphere processes involved in phytoremediation of metal-contaminated soils'. *Plant Soil*, **Vol.** 232; pp. 207-214.
- McKinney, J.D. and Rodgers, R. (1992) 'Metal bioavailability- EPA workshop identified research needs: *Environ Sci & Techn*, **Vol.** 26; pp, 1298-1299.
- Meagher, R. B. (2000) 'Phytoremediation of toxic elemental and organic pollutants'. *Current Opinion in Plant Biology*, **Vol.** 3; pp. 153–162.
- Menezes, J.C.S.S., Silva, R.A., Arce, I.S., Schneider, I.A.H. (2009) 'Production of a polyferric sulphate chemical coagulant by selective precipitation of iron from acidic coal mine drainage'. *J. Mine Water and the Environ*, **Vol.** 28(4); pp. 311-314.
- Menezes, J.C.S.S., Silva, R.A., Arce, I.S., Schneider, I.A.H. (2010) 'Production of a polyaluminum sulphate coagulant by chemical precipitation of a coal mining acid drainage'. *Minerals Engineering*, **Vol.** 23(3); pp. 249-251.
- Meyer, F.M. (1988) 'Environment of ore formation in the Sabie-Pilgrim's Rest Goldfield, South Africa'. *Abstr. Congr. Geol. Soc. S. Afr.*, pp. 427-430.
- Midgley, D.C., Pitman, W.V. and Middleton, B.J. (1994) 'Surface Water Resources of South Africa'. Volumes I, II, III, IV, V and VI, Reports No's. 298/1.1/94, 298/2.1/94, 298/3.1/94, 298/4.1/94, 298/5.1/94 and 298/6.1/94, Water Research Commission, Pretoria, South Africa.
- Mo, S.C., Choi, D.S. and Robinson, J.W. (1989) 'Uptake of mercury from aqueous solutions by duckweed: The effect of pH, copper and humic acid'. *J. Env. Sci. Health*, **Vol.** A24; pp. 135–146.
- Mohammad FS, Al Zubaidy IAH, Bassioni G. (2014) 'A comparison of aluminum leaching processes in tap and drinking water'. *Int J Electrochem Sci*, **Vol.** 9; pp. 3118–3129.
- Mold M, Cottle J, King A, Exley C. (2019b) 'Intracellular Aluminium in inflammatory and glial cells in cerebral amyloid Angiopathy: a case report'. *Int J Environ Res & Public Health*, **Vol.** 16(8); pp. 1–10. doi: 10.3390/ijerph16081459.
- Moncur, M.C., Ptacek, C.J., Blowes D.W., Jambor, J.L. (2005) 'Release, transport and attenuation of metals from an old tailings impoundment'. *J. Appl Geochem*, **Vol.** 20; pp. 639–659.
- Moore, M.R., Imray, P., Dameron, Ch., Callan, P., Langley, A. and Mangas, S. (1996) 'Copper, Report of an International Meeting 20–21 June 1996 Brisbane, Metal Series, No. 3., National Environmental Health Forum.

Moreira, K. (2018) 'Design improvements to sulfate-reducing bioreactors for mine-influenced stream remediation in cold climates'. Graduate Theses & Non-Theses. 163. https://digitalcommons.mtech.edu/grad_rsch/163.

Mugwabana, T. (2018) 'Sediment patterns and source areas within the Letaba River, Kruger National Park, South Africa'. MSc Thesis, University of Witwatersrand.

Munganyinka et al. (2022) 'Potential Uses of Artisanal Gold Mine Tailings, with an Emphasis on the Role of Centrifugal Separation Technique'. *J. Sustainability*, **Vol.** 14; pp. 8130.

Muzerengi, C. (2017) 'Enrichment and Geoaccumulation of Pb, Zn, As, Cd and Cr in soils near New Union Gold Mine, Limpopo Province of South Africa'. IMWA Conference "Mine Water and Circular Economy", Lappeenranta, Finland (Wolkersdorfer C, Sartz L, Sillanpää M, Häkkinen A :Editors)

Naicker, K., Cukrowskaa, E., McCarthy, T.S. (2003) 'Acid mine drainage arising from gold mining activity in Johannesburg, South Africa and environs'. *J. Environ Pollution*, **Vol.** 122; pp. 29-40.

Nde, S.C. and Mathuthu, M. (2018) 'Assessment of Potentially Toxic Elements as Non-Point Sources of Contamination in the Upper Crocodile Catchment area, North-West Province, South Africa'. *J. Int Environ Res & Public Health*, **Vol.** 14; pp. 1-12.

Neculita, C., Zagury, G.J., Bussiere, B. (2007) 'Passive treatment of acid mine drainage in bioreactors using sulfate-reducing bacteria'. *J. Environ. Qual*, **Vol.** 36; pp. 1–16.

Nemati, K.; Abu Bakar, N.K.; Sobhanzadeh, E.; Abas, M.R. (2009) 'A modification of the BCR sequential extraction procedure to investigate the potential mobility of copper and zinc in shrimp aquaculture sludge'. *Microchem. J*, **Vol.** 92; pp. 165–169.

Nemati, K.; Abu Bakar, N.K.; Abas, M.R.; Sobhanzadeh, E. (2011) 'Speciation of heavy metals by modified BCR sequential extraction procedure in different depths of sediments from Sungai Buloh, Selangor, Malaysia'. *J. Hazard. Mater*, **Vol.** 192; pp. 402–410.

Nengovhela, A.C. Yibas, B., Ogola, J.S. (2007) 'Characterisation of gold tailings dams of the Witwatersrand Basin with reference to their acid mine drainage potential, Johannesburg, South Africa'. *Water SA*, **Vol.** 32(4); pp. 499-506.

Nesbitt, W. and Young, G. M. (1982) 'Nesbitt_82 (1). Early Proterozoic climates and plate motions inferred from major elements chemistry of lutites'.

Netshiongolwe, K.E. (2018) 'GEOCHEMICAL CHARACTERISATION OF GOLD TAILINGS FOOTPRINTS ON THE CENTRAL RAND GOLDFIELD'. Msc Thesis, University of South Africa.

Netshitungulwana, R. and Yibas, B. (2012) 'Stream sediment geochemistry of the Olifants catchment, South Africa: Implication for acid mine drainage'. *International Mine Water Association Symposium (2012: Bunbury, Western Australia) Proceedings*. pp, 257-264.

Newman, M.C. and Jagoe, C.H. (1994) 'Inorganic toxicants-ligands and the bioavailability of metals in aquatic environments; in Hamelink, J.L., Landrum, P.F., Bergman, H.L. and Benson, W.H. (eds.), Bioavailability- Physical, Chemical, and Biological Interactions, SETAC Spec. Pub. Series: CRC Press, Inc., Boca Raton, Fla.

Newman, M.C. (2015). 'Fundamentals of Ecotoxicology'. *J. Sci of Poll*. Fourth Edition. CRC Press, Taylor & Francis Group. Boca Raton.

Ngriagu, J.O. and Pacyna, J.M. (1998) 'Quantitative assessment of worldwide contamination of air, water and soils by trace metals'. *Nature*, **Vol.** 333; pp. 134, 1988.

Nishimoto, N.; Yamamoto, Y.; Yamagata, S.; Igarashi, T.; Tomiyama, S. (2021) 'Acid Mine Drainage Sources and Impact on Groundwater at the Osarizawa Mine, Japan'. *J. Minerals*. **Vol.** 11; pp. 998.

Nieboer, E. and Fletcher, G.G. (1996) 'Determinants of reactivity in metal toxicology, in Chang, L.W. (ed.) Toxicology of Metals: CRC Press, Boca Raton, Fla., pp. 113-132.

Nordstrom, D.K. and Alpers, C.N. (1999) 'Geochemistry of acid mine waters'. In: G.S. Plumlee and M.J. Logsdon (Eds.). The Environmental Geochemistry of Mineral Deposits, Society of Economic Geologists, Littleton. **Vol.** 6A; pp. 133-160.

Nordstrom, D. K. (2007) 'Modeling Low-Temperature Geochemical Processes'. *Treatise on Geochem.* (1-38) Pergamon: Oxford.

Novhe, N.O., Yibas, B., Netshitungulwana, R., Lusunzi, R. (2014) 'Geochemical and Mineralogical Characterization of Mine Residue Deposits in the Komati/Crocodile Catchment, South Africa: an Assessment for Acid/Alkaline Drainage'. In: Sui, Sun & Wang (eds) IMWA, An Interdisciplinary Response to Mine Water Challenges.

Nowack, B. and Vanbriesen, J. (2005) 'Chelating agents in the environment'. In: Nowack, B., Vanbriesen, J. (Eds.), Biogeochemistry of Chelating Agents. ACS Symposium Series, Washington DC.

Nsiah, P.K. and Schaaf, W. (2019) 'Effect of topsoil stockpiling on soil properties and organic amendments on tree growth during gold mine reclamation in Ghana'. *J. Amer Soc Mining and Reclamation*, **Vol.** 8(1); pp. 45-68.

Obiri-Nyarko, F., Grajales-Mesa, S.J. and Malina, G. (2014) 'An Overview of Permeable Reactive Barriers for In Situ Sustainable Groundwater Remediation'. *J. Chemosphere*. **Vol.** 111; pp. 243-259.

Obreque-Contreras, J Pérez-Flores, D. Gutiérrez, P. and Chávez-Crooker, P. (2015) 'Acid Mine Drainage in Chile: An Opportunity to Apply Bioremediation Technology'. *Hydl. Current Research*, **Vol.** 6(3), doi:10.4172/2157-7587.1000215.

Oelofse, S. (2008) 'Mine water pollution—acid mine decant, effluent and treatment: A consideration of key emerging issues that may impact the state of the environment'. Emerging Issues Paper: *Mine Water Pollut*, pp. 83–91.

Pabst, T., Bussière, B., Aubertin, M. Molson, J. (2018) 'Comparative performance of cover systems to prevent acid mine drainage from pre-oxidized tailings: A numerical hydro-geochemical assessment'. *J. Contaminant Hydrology*, **Vol.** 214: pp. 39-53.

Pagnanelli, F., Moscardini, E., Giuliano, V., Toro, L. (2004) 'Sequential extraction of heavy metals in river sediments of an abandoned pyrite mining area: Pollution detection and affinity series'. *J. Environmental Pollution*, **Vol.** 132(2); pp. 189-201.

Patil, Y.B. and Paknikar, K.M. (2000) 'Development of a process for biotransformation of metal cyanides from waste waters'. *J. Process Biochem*, **Vol.** 35(10); pp. 1139-1151.

Patil, S.J. Bhole, A.G., Natarajan, G.S. (2008) *J. of Environmental Sc.& Engg.*, Vol.48, No.3, 203-208.

Parish, R.V. (1977) 'The metallic elements': Longman Inc., New York.

Parisi, D., Horneman, J. and Rastogi, V. (1994) 'Use of Bactericides to Control Acid Mine Drainage from Surface Operations'. Paper presented at the International Land Reclamation and Mine Drainage Conference on the Third International Conference on the Abatement of Acidic Drainage, Pittsburgh, PA, April 24-29. **Vol.** 2; pp. 319 – 325.

Parkhurst, D.L. and Appelo, C.A.J. (1999) 'User's guide to PHREEQC (Version 2)—A computer program for speciation, batch-reaction, one-dimensional transport, and inverse geochemical calculations': U.S. Geological Survey Water-Resources Investigations Report 99–4259. 312.

Parkhurst, D.L., Kipp, K.L., and Charlton, S.R. (2010) 'PHAST version 2 —A program for simulating groundwater flow, solute transport, and multicomponent geochemical reactions. U. S. Geological Survey Techniques and Methods.

Parkhurst, D.L., Kipp, K.L., and Engesgaard, P., and Charlton, S.R. (2004) 'PHAST—A program for simulating ground-water flow, solute transport, and multicomponent geochemical reactions. U. S. Geological Survey Techniques and Methods.

Paul, M. J. and Meyer, J.L. (2001) 'Streams in the urban landscape'. *Annu. Rev. Ecol.Syst*, **Vol.** 32; pp. 333–65.

Peikam, E.N. and Jalali, M. (2016) 'Application of inverse geochemical modelling for predicting surface waterchemistry in Ekbatan watershed, Hamedan, western Iran'. *J. Hydrol Sci*, **Vol.** 61(6); pp. 1124-1134.

Peters, R.W. (1999) 'Chelant extraction of heavy metals from contaminated soils'. *J. Hazard. Mater*, **Vol.** 66; pp. 151–210.

Pichtel, J.R. and Dick, W.A. (1991) 'Influence of Biological Inhibitors on the Oxidation of Pyritic Mine Spoil'. *Soil Biol and Biochem*, **Vol.** 23(2); pp. 109-116.

Plumlee, G.S., Logsdon, M.J. (1999) 'The Environmental Geochemistry of Ore Deposits. Part A: Processes, Techniques, and Health Issues'. *Reviews in Economic Geology Society of Economic Geologist*.

Plumlee, G.S. and Logsdon, M.J. (2010) ' An Earth-system science toolkit for environmentally friendly mineral resource development'. *J. Reviews in Econ Geol*, **Vol.** 6A; pp. 1-27.

Potgieter, J.H., Potgieter-Vermaak, S.S. and Kalibantonga, P.D. (2006) 'Heavy metal removal from solution by palygorskite clay'. *J. Min Eng*, **Vol.** 19; pp. 463-470.

Prach, K., Pyšek, P. and Bastl, M. (2001) 'Spontaneous vegetation succession in human-disturbed habitats: a pattern across seres'. *Appl. Veg. Sci*, **Vol.** 4; pp. 83-88.

Prasad M. N. V. and Freitas, H. M. O. (2003) 'Metal hyper-accumulation in plants-Biodiversity prospecting for phytoremediation technology'. *J. Elec J Biotechn*, **Vol.** 6(3); pp. 285.

Pretorius, D.A. (1994) 'From Paardekraal to Langlagte: The search for gold in South Africa, 1852-1866: Information Circular, Economic Geology Research Unit, University of Witwatersrand, Johannesburg.

Prichard, A. (2012) 'Monitoring the Effects of Surface-Coal-Mine-Reclamation on Soil Biological Properties'.

Prommer, H., Davis, G.B., Barry, D.A. (1999) 'PHT3D—A three-dimensional biogeochemical transport model for modelling natural and enhanced remediation, in: Johnston, C.D. (Ed.), Contaminated Site Remediation: Challenges Posed by Urban and Industrial Contaminants. Centre for Groundwater Studies, Fremantle, Western Australia.

Pulford, I. D. and Waston, C. (2003) 'Phytoremediation of heavy metal – contaminated land by tree a review'. *Environ Int*, **Vol.** 29; pp. 592-540.

Puzon, G.J., Roberts, A.R., Kramer, D.M., Xun, L., 2005. 'Formation of soluble organo-chromium(III) complexes after chromate reduction in the presence of cellular organics'. *Environ. Sci. Technol*, **Vol.** 39; pp. 2811–2817.

Puzon, G.J., Tokala, R. K., Zhang, H., Yonge, D., Peyton, Brent M., Xun, L. (2008) 'Mobility and recalcitrance of organo-chromium(III) complexes'. *Chemosphere*, **Vol.** 70(11) pp. 2054-2059.

Rai, V.K., Ranman, N.S., Choudhary, S.K., Rai, S. (2014) 'Top Soil Management in Coal Mines: A Paradigm Shift Required in Approach'. *J. Int Innov Res Adv Eng*, **Vol.** 1; pp. 448-454.

Ranville, M., Rough, D. and Flegal, A. R. (2004) 'Metal attenuation at the abandoned Spenceville copper mine', *J. Appl Geochem*, **Vol.** 19.

Rao, S.R., Gehr, R., Riendeau, M., Lu, D., Finch, J.A. (1992) 'Acid mine drainage as a coagulant'. *J. Min Eng*, **Vol.** 5(9); pp. 1011-1020.

Rastogi, V. (1990) 'AML Award'. Reclamation Newsletter 13(2), July 1990. Canadian Land Reclamation Association and American Society for Surface Mining and Reclamation. (ed CB Powter).

Rees, B., Bowel, R., Dey, M., Williams, K. (2001) 'Passive treatment: A walk away solution?' *Mining Environmental Management*'.

Ringbom, A. (1967) 'Les complexes en chimie analytique: comment choisir rationnellement les meilleures méthodes d'analyse complexométrique. Dunod, Paris.

Robb, L.J. (1978) 'A general geological description of the Archaean granitic terrane between Nelspruit and Bushbuckridge, eastern Transvaal'. *Trans. Geol. Soc. S.A.* **Vol.** 81; pp. 331–338.

Robb, L.J. Anhaeusser, C.R. and van Nierop, D.A. (1983) 'The recognition of Nelspruit batholith north of the Barberton greenstone belt and its significance in terms of Archean crustal evolution': *Geol Soc of S.A*, **Vol.** 9; pp. 117-130.

Robb, L.J. (1994c). 'Cunning Moor Tonalite'. *In*: Johnson, M.R. (Ed.), *Catalogue of South African Lithostratigraphic Units*. S. Afr. Comm. Strat., **5-11–5-12**.

Robinson, B.H., Leblanc, M. and Petit, D. (1998) 'The potential of *Thlaspi caerulescens* for phytoremediation of contaminated soils. *Plant Soil*, **Vol.** 203; pp. 47-56.

Roubířková, A. (2013) ' Interactions of soil fauna and plants during succession on spoil heaps after brown coal mining'. PhD thesis. Charles University in Prague.

Rose AW (2010) 'Advances in passive treatment of coal mine drainage 1998–2009'. *In*: Proceedings of the 27th ASMR, Pittsburgh, PA. 847–887.

Rose, A.W. and Lourenso, F.J. (2000) 'Evaluation of two open limestone channels for treating acid mine drainage'. *In*: Paper presented at the 2000 National Meeting of the American Society for Surface Mining and Reclamation, Florida.

Rôsner, (1999) ' The environmental impact of seepage from gold mine tailings dams near Johannesburg, South Africa'. PhD Thesis, University of Pretoria.

Rosner, T., Van Schalkwyk, A. (2000) 'The environmental impact of gold mine tailings footprints in the Johannesburg region, South Africa'. *Bull Eng Geol Environ*, **Vol.** 59; pp.137–148.

Roux, F., Diedericks G, Hoffman AC, Scherman P and Selepe M. (2019) 'Ecstatus of the Komati River Catchment. Inkomati River System. Phase II (2018)'. Internal Inkomati Usuthu Catchment Management Agency Report.

Roux, F. *et al.* (2016) 'Ecstatus of te Sabie-Sand river catchment', *J. Chem Info & Model*, **Vol.** 53(9); pp. 1–30.

Rudnick, R. L. and Gao, S. (2003) Composition of the Continental Crust . *Treatise Geochem 3 : 1-64 Composition of the Continental Crust*. 2nd edn, *Treatise on Geochemistry*. Second Edition. Elsevier Ltd. doi: 10.1016/B978-0-08-095975-7.00301-6.

Sahuquillo, A., Rubio, R., Davidson, C. (1999) 'Improvement of the BCR Three Step Sequential Extraction Procedure Prior to the Certification of New Sediment and Soil Reference Materials'.

Sahuquillo, A., Rigol, A., Rauret, G. (2003) 'Overview of the use of leaching/extraction tests for risk assessment of trace metals in contaminated soils and sediments'. *Trends in Analytical Chemistry*, **Vol.** 22(3); pp. 152-159.

Sallowmn, M., Shugard, A.D., Kanouff, M.P., Gharagozloo, P.E. (2013) ' A Coupled Transport and Solid Mechanics Formulation with Improved Reaction Kinetics Parameters for Modeling Oxidation and Decomposition in a Uranium Hydride Bed'.

Salmati, M., Salim, M.R., Ijang, Z., Azman, S. (2012) ' Lightning the lode: a guide to responsible large-scale mining'. *2012 2nd International Conference on Environment and Industrial Innovation*. **Vol.** 35; pp. 66-70.

Salomons, W. (1995) 'Environmental impact of metals derived from mining activities: Processes, predictions, prevention': *J. Geochem Expl*, **Vol.** 52; pp. 5-23.

Salt, D.E., Blaylock, M., Kumar, P.B.A.N., Dushenkov, V., Ensley, B.D., Chet, I. & Rashikin, I. (1995) 'Phytoremediation: A novel strategy for the removal of toxic metals from the environment using plants'. *Biotechnol*, **Vol.** 13; pp. 468-475.

Salt, D. E., Smith, R.D. and Raskin, I. (1998) 'Phytoremediation'. *Annual review of Plant Physiology – Plant Molecular Biology*, **Vol.** 49; pp. 643 –688.

Samad, M.A. and Yanful, E.K. (2005) 'A design approach for selection the optimum water cover depth for subaqueous disposal of sulphidic mine tailings'.

Sánchez-España, J., López-Pamo, E., Santofima Pastor, E., Andrés, J.R., Antonio, J., and Rubi, M. (2005) 'The natural attenuation of two acidic effluents in Tharsis and La Zarza-Perrunal mines' (Iberian Pyrite Belt, Huelva, Spain). *J. Environ Geol*; pp. 253-266.

Sandy, T., & DiSante, C. (2010) '*Review of Available Technologies for the Removal of Selenium from Water*'. Charlotte, NC: CH2M HILL, Inc. 2.1.

SANS-241 (2015) 'South African National Standard (SANS). '*Drinking Water for SANS*', 241. 1–2. Available at: <https://vinlab.com/wp-content/uploads/2016/10/SANS-241-2015.pdf>.

Sapsford, D.J., Barnes, A., Dey, M., Williams, K.P., Jarvis, A., Younger, P. and Liang., L. (2006) 'Iron and manganese removal in a vertical flow reactor for passive treatment of mine water'. pp. 1831- 1843. In: Proceedings of the 7th International Conference on Acid Rock Drainage (ICARD). St. Louis, Missouri. 25-30 March.

- Santomartino, S. and Webb, J.A. (2007) 'Estimating the longevity of limestone drains in treating acid mine drainage containing high concentrations of iron'. *J. App Geochem*, **Vol.** 22; pp. 2344-2361.
- Sapsford, D., Santonastaso, M., Thorn, P., Kershaw, S. (2015) 'Conversion of coal mine drainage ochre to water treatment reagent: Production, characterization and application for P and Zn removal. *J. Environ Mgt*, **Vol.** 160; pp. 7-15.
- Sarmiento, A.M., Olíasb, M., Nietoa, M.J., Cánovasb, C.R., Delgado, J. (2009) 'Natural attenuation processes in two water reservoirs receiving acid mine drainage'. *J. Sci Tot Environ*, **Vol.** 407; pp. 2051-2062.
- Sauve´, S., McBride, M. and Hendershot, W. (1998) 'Lead phosphate solubility in water and soil suspensions'. *J. Environ. Sci. Technol*, **Vol.** 32(3); pp. 388–393.
- Sauvé, S., M.B. McBride, and W.H. Hendershot (1998) 'Soil solution speciation of Pb²⁺: effects of organic matter and pH'. *J. Soil Sci. Sco. Amer*, **Vol.** 62(3); pp. 618-621.
- Seervi, V. Yadav, H.L. Srivastav, S.K. and Jamal, A. 'Overview of Active and Passive Systems for Treating Acid Mine Drainage'. *IARJSET*, **Vol.** 4(5); pp. 131-137.
- Schutte, I. C. (1986) 'The General Geology of the Kruger National Park', *Geological Survey of South Africa*, **Vol.** 29; pp. 13–37.
- Scientific Software Group (2010) 'Aqueous Geochemical Analysis, Plotting and Modeling'. Accessed March 23, 2010. <http://www.scientificsoftwaregroup.com/pages/software.php>.
- Sibrell, P.L., Watten, B.J., Friedrich, A.E., Vinci, B.J. (2000) 'ARD remediation with limestone in a CO₂ pressurized reactor'. In: Proc., 5th Internat. Conf. Acid Rock Drainage. Denver, CO. *J. Soc Min, Met and Expl*; pp. 1017–1026.
- Singh, A. and Singh, R. (2005) 'Surface chemistry', Campus Books Int., New Delhi, 1, 199-209.
- Silva, M., Cabral, P.M., Carvalho, P. (2016) 'Major, trace and REE geochemistry of recent sediments from lower Catumbela River (Angola)'. *J. Afr Earth Sci*, **Vol.** 115; pp. 203-217.
- Simeonov, V., Stratis, J. A., Samara, C., Zachariadis, G., Voutsas, D., Anthemidis, A., Sofoniou, M., Kouimtzisc, T. (2003) 'Assessment of the Surface Water Quality in Northern Greece'. *Water Res*, **Vol.** 37; pp. 4119–4124.

Simon-Hettich, B., Wibbertmann, A., Wagner, D., Tomaska, L. and Malcolm, H. (2001) 'Environmental health criteria 221. Zinc'. WHO, Geneva.

Simmons et al., (2000) 'Small-Scale Chemical Changes Caused by In-stream Limestone Sand Additions to Streams'. *J. Mine Water and the Environ*, **Vol.** 25; pp. 241–245.

Singh, M.R. and Gupta, A. (2017) 'Water Pollution-Sources , Effects and Control Water Pollution-Sources, Effects and Control'. **Vol.** 5(3); pp. 1-17.

Singo, N.K. and Kramers, J.D. (2021) 'Feasibility of tailings retreatment to unlock value and create environmental sustainability of the Louis Moore tailings dump near Giyani, South Africa. *J. Southern Afr Ins of Min and Met*, **Vol.** 121(7); pp. 361–368.

Sirkiä, P. *et al.* (1999) 'Electric and electrochemical properties of surface films formed on copper in the presence of bicarbonate anions', (June).

Shackelford, C.D., Sevick, G.W., Eykholt, G.R. (2010) 'Hydraulic conductivity of geosynthetic clay liners to tailings impoundment solutions. *Geotext Geomembr*, **Vol.** 18; pp. 133-162.

Shackelford, C.D., Sevick, G.W., Eykholt, G.R. (2010) 'Hydraulic conductivity of geosynthetic clay liners to tailings impoundment solutions. *Geotext Geomembr*, **Vol.** 18; pp. 133-162.

Shao, J. and Yang, S. (2012) 'Does chemical index of alteration (CIA) reflect silicate weathering and monsoonal climate in the Changjiang River basin?'. *Chinese J. Sci*, **Vol.** 57; pp. 1178-1187.

Shao, J., Yang, S., Li, C. (2012) 'Chemical indices (CIA and WIP) as proxies for integrated chemical weathering in China: Inferences from analysis of fluvial sediments'. *J. Sed Geol*, **Vol.** 265-266; pp. 110-120.

Skousen, J., Sencindiver, J., Smith, R. (1987) 'A Review of Procedures for Surface Mining and Reclamation in Areas With Acid-producing Materials'. EWRC 871. West Virginia University, Morgantown, WV.

Skousen, J. and Ziemkiewicz, P. (1996) 'Acid Mine Drainage Control and Treatment. Second Edition. National Research Center for Coal and Energy, National Mine Land Reclamation Center, West Virginia University, Morgantown, WV.

Skousen, J., Rose A., Geidel, G., Foreman, J., Evans, R., Hellier, W. (1998) 'A handbook of technologies for avoidance and remediation of acid mine drainage'. Acid drainage technology

initiative, published by the National Mine Land Reclamation Center at West Virginia University. Morgantown, West Virginia, USA.

Skousen, J., Politan, K., Hilton, T., Meek, A. (1995) 'Acid mine drainage treatment systems: chemicals and costs'. In: Skousen, J.G., Ziemkiewicz, P.F., (Compilers), Acid Mine Drainage—Control and treatment. West Virginia University and the National Mine Land Reclamation Center, Morgantown, WV. 121-129.

Skousen, J. and Ziemkiewicz, P. (2005) 'Performance of 116 passive treatment systems for acid mine drainage'. Proceedings, National Meeting of the American Society for Surface Mining and Reclamation, Lexington, Kentucky, June 19-23; pp. 1100-1133.

Skousen, J.G. (2002) 'A Brief Overview of Control and Treatment Technologies for Acid Mine Drainage'. *J. Amer Soc Min & Recl*; pp. 879-889.

Skousen, J. (2017) 'A methodology for geologic testing for land disturbance: acid-base accounting for surface mines'. *Geoderma*, **Vol. 308**; pp. 302–311.

Skousen, J., Zipper, C.E., Rose, A., Ziemkiewicz, P.F., Nairn, R., McDonald, L.M., Kleinmann, R.L. (2017) 'Review of Passive Systems for Acid Mine Drainage Treatment'. *J. Mine Water and the Environ*, **Vol. 36**(1); pp. 133-153.

Skousen, J.G., Ziemkiewicz, P.F., McDonald, L.M. (2019) 'Acid mine drainage formation, control and treatment: Approaches and strategies'. *J. Extr Indus & Soc*, **Vol. 6**; pp. 241-249.

Slimani, R., Guendouz, A., Trolard, F., Moulla, A. S., Hamdi-Aïssa, B., and Bourrié, G. (2016) 'Geochemical inverse modeling of chemical and isotopic data from groundwaters in Sahara (Ouargla basin, Algeria)'. *Hydrol. Ear Syst. Sci.* doi:10.5194/hess-2015-385, 2016.

Smyth, D. J. A., Blowes, D. W., Ptacek, C. J. and Bain, J. G. (2003). 'Removal of Dissolved Metals from Groundwater Using Permeable Reactive Barriers – Applications'. Paper presented at the 6th ICARD, July 12-18, Cairns, Australia.

Šmuc, R. *et al* (2015) 'Mineralogical and geochemical study of Lake Dojran sediments (Republic of Macedonia)'. *J. Geochem Expl*, **Vol. 150**; pp. 73-83.

Sobek, A.A., Schuller, W.A., Freeman, J.R. Smith, R.M. (1978) 'Field and Laboratory Methods Applicable to Overburden and Minesoils'. EPA 600/2-78-054.

Sobelewski, A. (2010) 'Benefits of using liquid carbon sources for passive treatment systems'. *In: Wolkersdorfer & Freund (Editors), IMWA2010 Mine Water and Innovative Thinking, Sydney, Nova Scotia, Canada 5 – 9 September.*

Spellman, F.R. (2009) 'Handbook of Water and Wastewater Treatment Plant Operations. '

Sperling, M., Xu, S. and Welz, B. (1992) 'Determination of chromium(III) and chromium(VI) in water using flow injection on-line preconcentration with selective adsorption on activated alumina and flame atomic absorption spectrometric detection'. *Anal. Chem*, **Vol.** 64(24); pp. 3101–3108.

Spacek, O., Choquette, M., Gélinas, P., Lefebvre, R., Nicholson, R.V. (2004) 'Geochemical characterization of acid mine drainage from a waste rock pile, Mine Doyon, Québec, Canada'. *J. Contam. Hydrol*, **Vol.** 69; pp. 45–71.

Spacek, O., Mihaljević, M., Kržibek, B., Majer, Veselovsky, V.F. (2010) ' Geochemistry and mineralogy of Cu and Co in mine tailings at the Copperbelt, Zambia'. *J. Afr Ear Sci*, **Vol.** 57; pp. 14-30.

Spacek, O. *et al.* (2012) 'Mining-related contamination of surface water and sediments of the Kafue River drainage system in the Copperbelt district , Zambia : An example of a high neutralization capacity system'. *Geochem: Expl, Environ, Analysis*, **Vol.** 112; pp. 174–188.

Srouf, E., Hussien, R.A., Moustafa, W.M. (2022) 'Geochemical modeling and isotopic approach for delineating water resources evolution in El Fayoum depression, Egypt'. *Environl Earth Sci.* **81**, 105.

Stolz, M. (2018) 'Water quality assessment of the Sabie River catchment with respect to adjacent land use'. MSc Thesis, North West University.

Stumm, W., Morgan, J. (1996) 'Chemical Equilibria and Rates in Natural Waters'. Aquatic Chemistry, Third Edition, JOHN WILEY & SONS, INC.

Sudlow, B.E. (2008) 'Birds as bio-indicators of the ecological integrity of the Sabie River, Mpumalanga'. MSc Thesis, Johannesburg: University of Johannesburg.

Suie, C., Fatichi, S., Burlando, P., Weber, E., Battista, G., (2021) 'Modeling distributed metal pollution transport in a mine impacted catchment: short and long-term effects'. *J. Sci Tot Environ*, **Vol.** 812(22); pp 151473.

Sweeting, A.M. and Clark, A.P. 'Lightening the lode: a guide to responsible large-scale mining'. *Cons Intern.* 1-117.

Swiegers, J.U. (1948) 'The gold deposits of Pilgrim's Rest gold mining district: Transvaal: Transaction of Geological Society of South Africa'.

Sweeting, A.R. and Clark, A.P. (2000) 'Lightening the Lode- A Guide to Responsible Large-scale Mining. *Conservation International.*

Świetlik, R. (1998) 'Speciation analysis of chromium in waters', *Polish J. Environ Studies*, **Vol.** 7(5); pp. 257–266.

Szegedi, K. Vetterlein, D., Nietfield, H. Jahn, R., Neue, H.U. (2008) 'New tool RhizoMath for modeling coupled transport and speciation in the rhizosphere'. *J. Vadose Zone*, **Vol.** 7; pp. 712-720.

Taylor, S.R. and McLennan, S.M. (1985) 'The Continental Crust: Its Composition and Evolution: An Examination of the Geochemical Record Preserved in Sedimentary Rocks [M]'. Blackwell Science, Oxford.

Tokalio, S., Kartal, S., Birol, G. (2001) 'Application of a three-stage sequential extraction procedure for the determination of extractable metal contents in highway soils'. *Turk. J. Chem.* **Vol.** 27; pp. 333-346.

Torres, T.E, Ayora, C. Canovas, C.R., García-Robledo, E., Galván, L. and Sarmiento, A.M. (2013) 'Metal cycling during sediment early diagenesis in a water reservoir affected by acid mine drainage'. *J. Scie Tot Enviro*, **Vol.** 1; pp. 416-492.

Trumm, D. (2010) 'Selection of active and passive treatment systems for AMD - Flow charts for New Zealand conditions'. *New Zealand J. Geol and Geop*, **Vol.** 53; pp. 195-210.

Tukker, A., Buijst, H., van Oers, L. and van der Voet, E. (2001) 'Risks to health and the environment related to the use of lead in products', TNO report, STB-01-39 (Final), For: EU, DG ENTR.

Tutu, H., Cukrowska, E., McCarthy, T.S., Mphephu, N.F., Hart, R. (2003) 'Determination and modelling of geochemical speciation of uranium in gold mine polluted land in South Africa'. *8th International Congress on Mine Water & the Environment*, Johannesburg; pp. 137-155.

Tyler, R. and Tyler, N. (1991) 'Stratigraphic and structural controls on gold mineralization within Lower Proterozoic carbonate platform succession, Pilgrim's Rest goldfield, South Africa'. *Abstr Prog. Geol. Soc. Amer*, **Vol.** 23(5), A172.

Tyler, R. and Tyler, N. (1993a) 'Gold-quartz vein mineralization in hinterland-dipping duplex thrust systems within the Lower Proterozoic Malmani carbonate platform, Eastern Transvaal, South Africa'. *Abstr Prog. Geol. Soc. Amer*, **Vol.** 25(6): pp. A-164.

Tyler, R. and Tyler, N. (1996) 'Stratigraphic and structural controls on gold mineralization in the Pilgrim's Rest goldfield, eastern Transvaal, South Africa', *Precamb Res*, **Vol.** 79(1–2); pp. 141–169.

Tyler, J., Pepe, S. and Murphy, N. (2005) 'A Summary of Passive and Active Treatment Technologies for Acid and Metalliferous Drainage'. In: *Proceedings of the 5th Australian Workshop on Acid Drainage*, **Vol.** 29; pp. 1-49.

Udayabhanu, S.G. and Prasad, B. (2010) 'Studies on Environmental Impact of Acid Mine Drainage Generation and its Treatment: An Appraisal'. *Indian J. Environmental Protection*. **30**, 953-967.

Ullmann, F., Gerhartz, W. (1998) 'Ullman's encyclopedia of industrial chemistry, VCH'.

UNEP (2016) United Nations Environment Programme 'A snapshot of the world's water quality: towards a global assessment'. Nairobi. UNDESA.

U.S. EPA (1986) United States Environmental Protection Agency 'Test Methods for Evaluating Solid waste', Third Edition, Office of Solid Waste and Emergency Response, Report SW-846, **Vol** 1, November 1986 with revisions to January 1995.

U.S. EPA (1991) United States Environmental Protection Agency 'Comprehensive review of lead in the environment under TSCA', *Federal Register*. **Vol.** 56; pp. 22,096–22,098.

U.S. EPA (1996) United States Environmental Protection Agency 'Nonpoint Pointers, Nonpoint Source Pollution: The Nation's Largest Water Quality Problem'. EPA-841-F-96-004A.

U.S. EPA (1999) United States Environmental Protection Agency 'Introduction to Contaminated Sediments'. EPA-823-F-99-006.

U.S. EPA (2000) United States Environmental Protection Agency 'Wastewater technology fact sheet, Chemical Precipitation'. US EPA Washington, DC.

U.S. EPA (2006) United States Environmental Protection Agency 'Reference Guide to Non-combustion Technologies for Remediation of Persistent Organic Pollutants in Stockpiles and Soil', EPA-542-R-05-006.

Uster, B. (2013) 'Treating Acid Mine Drainage using Waste Mussel Shells in Sulfate-Reducing Bioreactors Operating at Different Hydraulic Retention Times'. AusIMM NZ Branch Annual Conference.

Van der Lee, J. and De Windt, L. (2002) 'Present state and future directions of modeling of geochemistry in hydrogeological systems'. *J. Cont Hydrol*, **Vol.** 47(2-4); pp. 265-282.

Vangronsveld, J., Herzig, R., Weyens, N., Boulet, J., Adriaensen, K. (2009) 'Phytoremediation of Contaminated Soils and Groundwater: Lessons from the Field'. *Environ Sci Pollut Res*. DOI 10.1007/s11356-009-0213-6.

van Niekerk, A. W. and Heritage, G.L. (1993) 'Geomorphology of the Sabie River: An overview and classification'. Report No. 2/93. Centre for Water in the Environment, University of the Witwatersrand, Johannesburg.

Vassilev, A., Schwitzguébel, J.P., Thewys, T., van der Lelie, D., Vangronsveld, J. (2004a) 'The use of plants for remediation of metal contaminated soils'. *J. Scientific World*, **Vol.** 4; pp. 9–34.

Vassilev, A., Lidon, F.C., Ramalho, J.C., Do Céu Matos, M., da Graca, M. (2004b) 'Cadmium accumulation and photosynthesis performance of cadmium-exposed barley plants. *J Plant Nutr*, **Vol.** 27; pp. 775–795.

Verplanck, P.L., Nordstrom, D.K., Tayler, H.E. and Kimball, B. (2004) 'Rare earth element partitioning between hydrous ferric oxides and acid mine water during iron oxidation'. *J. Applied Geochemistry*, **Vol.** 19(8); pp. 1339-1354.

Vermeulen, N.J. (2001) 'THE COMPOSITION AND STATE OF GOLD TAILINGS'. PhD Thesis, University of Pretoria.

Vicente-Martorell, J.J., Galindo-Riancho, M.D., García-Vargas, M. and Granado-Castro, M.D. (2009) 'Bioavailability of heavy metals monitoring water, sediments and fish species from a polluted estuary'. *J. Hazard. Mater*, **Vol.** 162; pp. 823–836.

Walker, C.H., Hopkin, S.P., Sibly, R.M. and Peakall, D.B. (2005) 'Principles of ecotoxicology', Third Edition. CRC Press, Boca Raton, Florida.

Walker, C.H., Hopkin, S.P., Sibly, R.M., Peakall, D.B. (2012) 'Principles of Ecotoxicology', Fourth Edition. CRC Press Taylor & Francis Group, London.

Wang, P., Anderko, A., Kosinski, J.J., Springer, R.D and Lencka, M.M. (2017) ' Modeling Speciation and Solubility in Aqueous Systems Containing U(IV, VI), Np(IV, V, VI), Pu(III, IV, V, VI), Am(III), and Cm(III)'. *J Solution Chem*, **Vol.** 46; pp. 521-588.

Wasay, S.A., Barrington, S., Tokunaga, S. (2001) 'Organic acids for the in situ remediation of soils polluted by heavy metals: soil flushing in columns'. *Water Air Soil Pollut*, **Vol.** 127; pp. 301–314.

Watzlaf, G.R. (1986) 'Control of Acid Drainage From Mine Wastes Using Bacterial Inhibitors'. *J. Amer Soc Min and Reclam.* 123-130.

White, S. (2000) 'Wetland Use in Acid Mine Drainage Remediation'.

WHO (1991) World Health Organization 'Environmental Health Criteria 108, Nickel (EHC 108)'. *INTERNATIONAL PROGRAMME ON CHEMICAL SAFETY.*

WHO (2011) World Health Organization 'Guidelines for Drinking-Water Quality', 4th ed.; WHO: Geneva, Switzerland. pp. 155–202.

WHO (2003) World Health Organization 'Aluminium in drinking-water. 2'.

Wissmeier, L. and Barry, D.A. (2010a) 'Implementation of variably saturated flow into PHREEQC for the simulation of biogeochemical reactions in the vadose zone'. *J. Enviro Model & Soft*, **Vol.** 25(4); pp. 526-538.

Wissmeier, L. and Barry, D.A. (2010b) 'Simulation tool for variably saturated flow with comprehensive geochemical reactions in two- and three-dimensional domains'. *J. Environl Model & Soft.* **Vol.** 26; pp. 210-218.

Wong, M.H. (2003) 'Ecological restoratin of mine degraded soils, with emphasis on metal contamintated soils'. *J. Chemosphere*, **Vol.** 50; pp. 775-780.

Wu, C. (2021) 'Acid Mine Drainage Prediction Techniques and Geochemical Modelling: Case Study on Gold Tailing Dams, West Rand, Witwatersrand Basin Area, South Africa'. PhD Thesis, Western Cape University.

WWAP (2017) '*The United Nations World Water Development Report 2017: Wastewater, the untapped resource*'. United Nations World Water Assessment Programme (WWAP). Paris, United Nations Educational, Scientific and Cultural Organization.

Yang, J. and Ni, J. (2007) 'Sediment-copper distributions in hyper-concentrated turbulent solid-liquid system'. *J. Environ. Sci*, **Vol**, 19(1); pp. 123–127.

Young, R.A. (1995) 'Toxicity Profiles'. Toxicity summary for nickel and nickel compounds. Web site: <http://risk.lsd.ornl.gov/tox/profiles/nickel>.

Younger, P.L., Banwart, S.A. and Hedin, R.S. (2002) 'Mine Water: Hydrology, Pollution, Remediation'. Kluwer Academic Publishers, Boston.

Younger, P.L. and Wolkersdorfer, C. (2004) 'Mining impacts on the freshwater environment: technical and managerial guidelines for catchment scale management'. *J. Mine Water Environ*, **Vol**. 23; pp. 2–80.

Younger, P.L. and Sapsford D.J. (2006) 'Acid Drainage Prevention Guidelines for Scottish Opencast Coal Mining: the Primacy of the Conceptual Model'. *Proceedings, International Conference of Acid Rock Drainage (ICARD)ICARD*. St. Louis. **Vol**. 7; pp. 2558-2570.

Yusupov, R.A., Abzalov, A.F., Smerdova, S.G. and Gafarov, M.R. (2000) 'Complex heterogeneous equilibrium states with violation of mass action law in "Pb(II)-water-KOH" system'. *Chemistry and Computational Simulation. Butlerov Commun*, **Vol**. 3; pp. 29–35.

Zamzow, K., Tsukamoto, T. and Miller, G. (2006) 'Waste from biodiesel manufacturing as an inexpensive carbon source for bioreactors treating acid mine drainage': *J. Mine Water and Environ*, **Vol**. 25(3); pp. 163-170.

Zietsman, A.L. (1964) 'The geology of the Sabie-Pilgrim's Rest Goldfield'. MSc thesis. Univ. Orange Free State (unpubl.).

Zietsman, A.L. (1967) 'The relationship between mineralization and structure in the Pilgrim's Rest-Sabie gold field'. Ph.D thesis, University of Orange Free State, Bloemfontein (unpubl.).

Zhang, W., Tsang, D.C.W., Chen, H., Huang, L. (2013) 'Remediation of an electroplating contaminated soil by EDTA flushing: chromium release and soil dissolution'. *J. Soils Sediments*, **Vol**. 13; pp. 354–363.

Zhu Y, Pilon-Smits E, Jouanin L, Terry N (1999) 'Overexpression of glutathione synthetase in Indian mustard enhances cadmium accumulation and tolerance'. *Plant Physiol*, **Vol.** 119; pp. 73–79.

Zhu, C., & Anderson, G. (2002) 'Environmental Applications of Geochemical Modelling'. Cambridge, United Kingdom: The Press Syndicate of the University of Cambridge.

APPENDICES

7. Annexure A: Stream sediment and surface water sampling sites along the Sabie River system



Figure 24 SB01: Sabie River headwaters wet (A) and dry (B) seasons (R. Lusunzi).

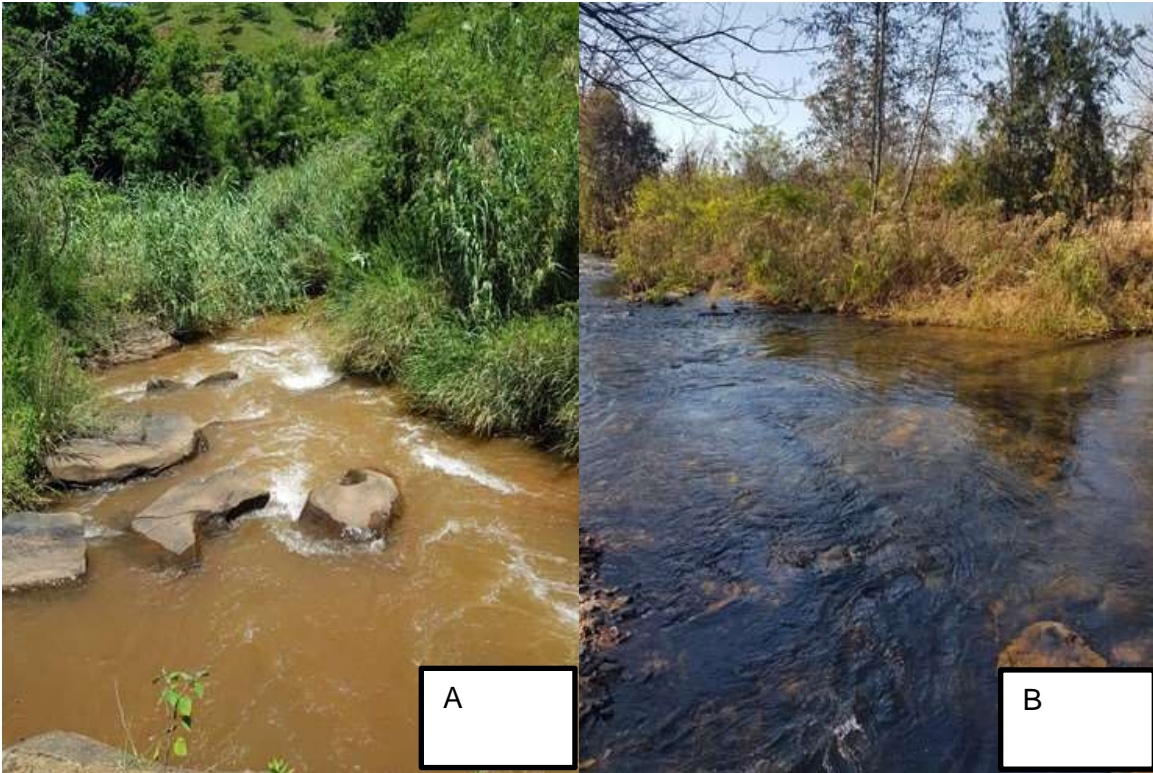


Figure 25 SB 02: Sabie River wet (A) and dry (B) seasons (R. Lusunzi).

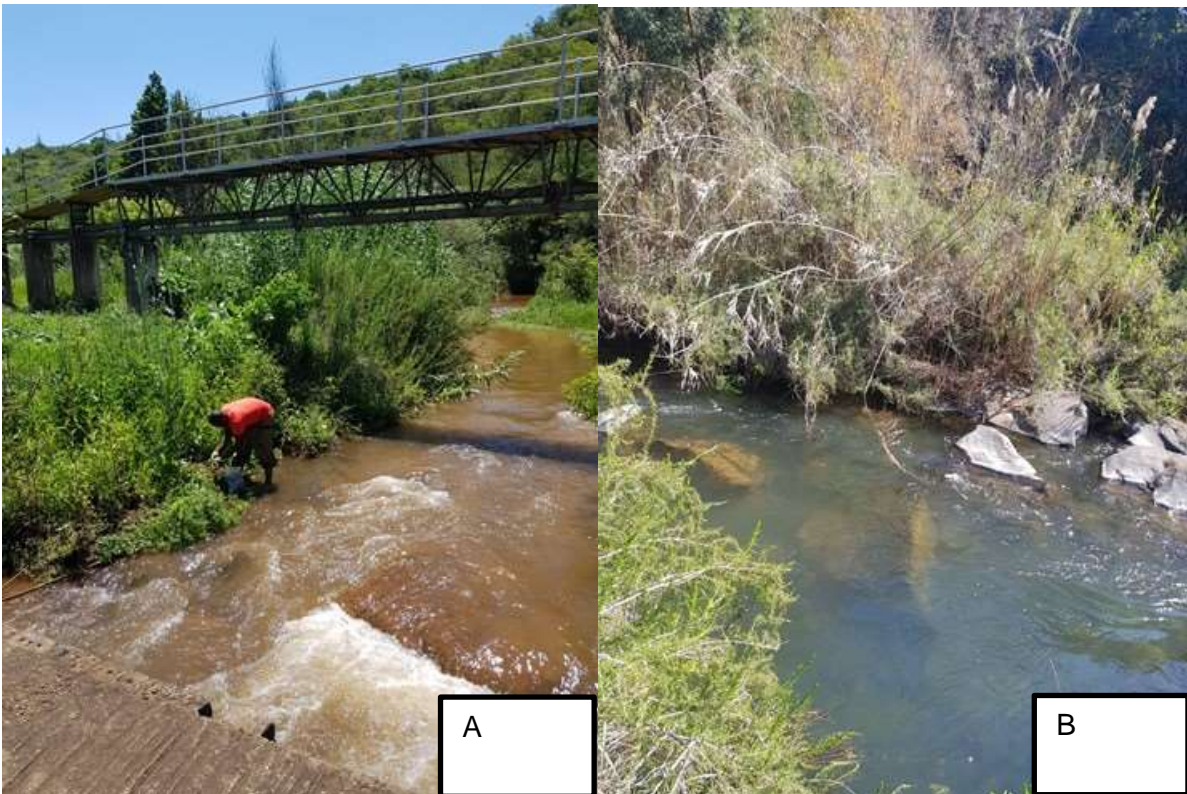


Figure 26 SB03: Sabie River wet (A) and dry (B) seasons (R. Lusunzi).



Figure 27 SB04: Sabie River wet (A) and dry (B) seasons (R. Lusunzi).



Figure 28 SB05: Sabie River wet (A) and dry (B) seasons (R. Lusunzi).



Figure 29 SB06: Sabie River wet (A) and dry (B) seasons (R. Lusunzi).

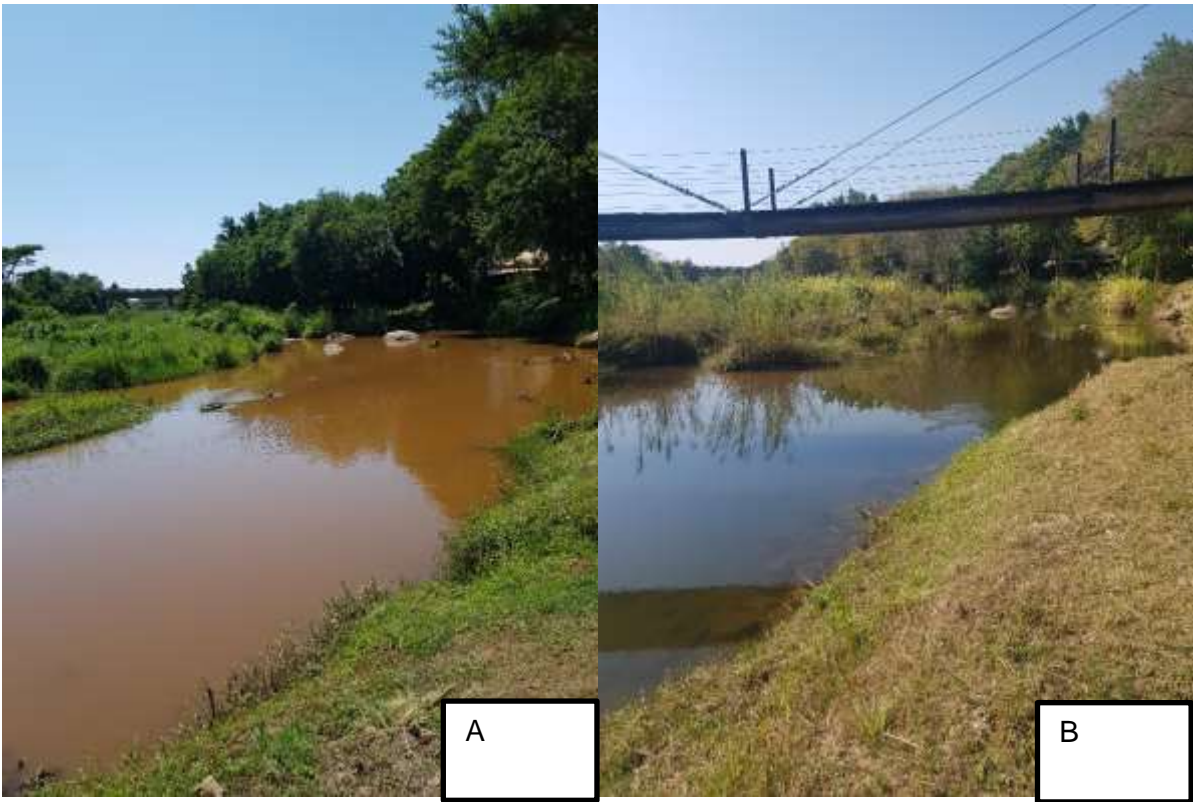


Figure 30 SB07: Sabie River wet (A) and dry (B) seasons (R. Lusunzi).

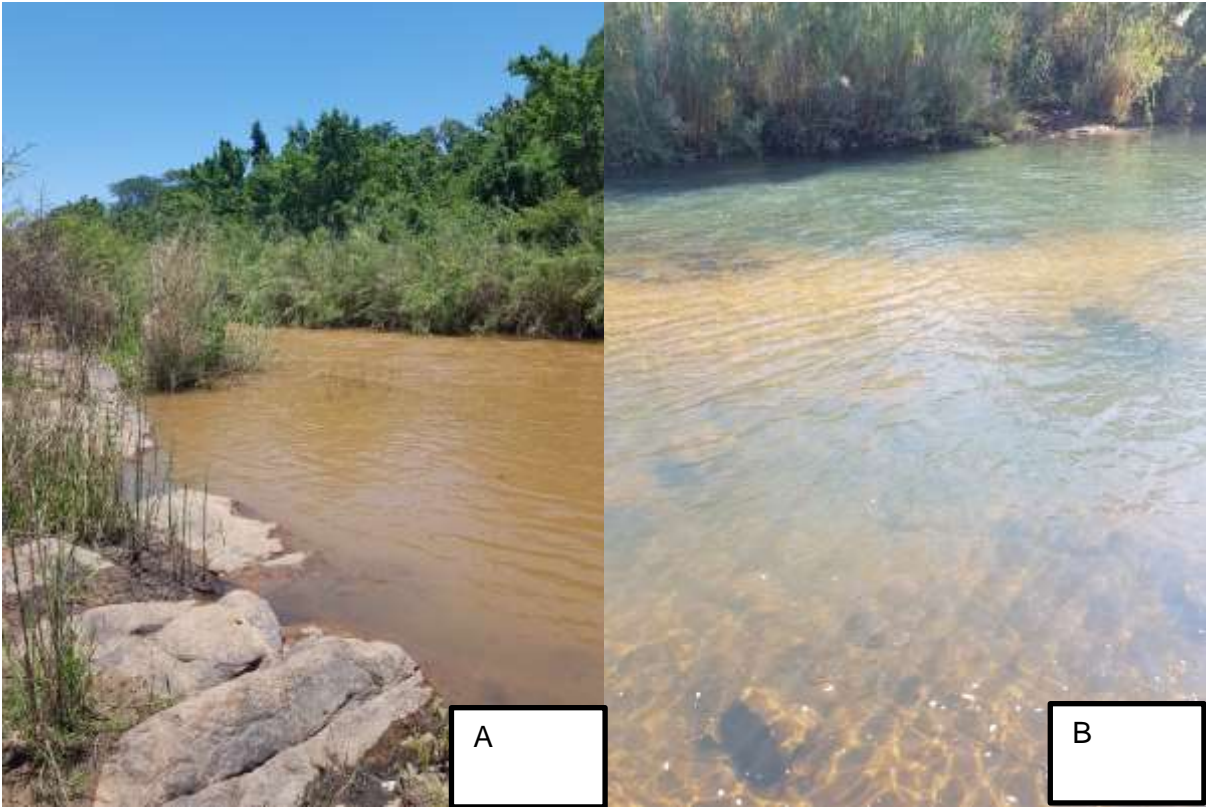


Figure 31 SB08: Sabie River wet (A) and dry (B) seasons (R. Lusunzi).

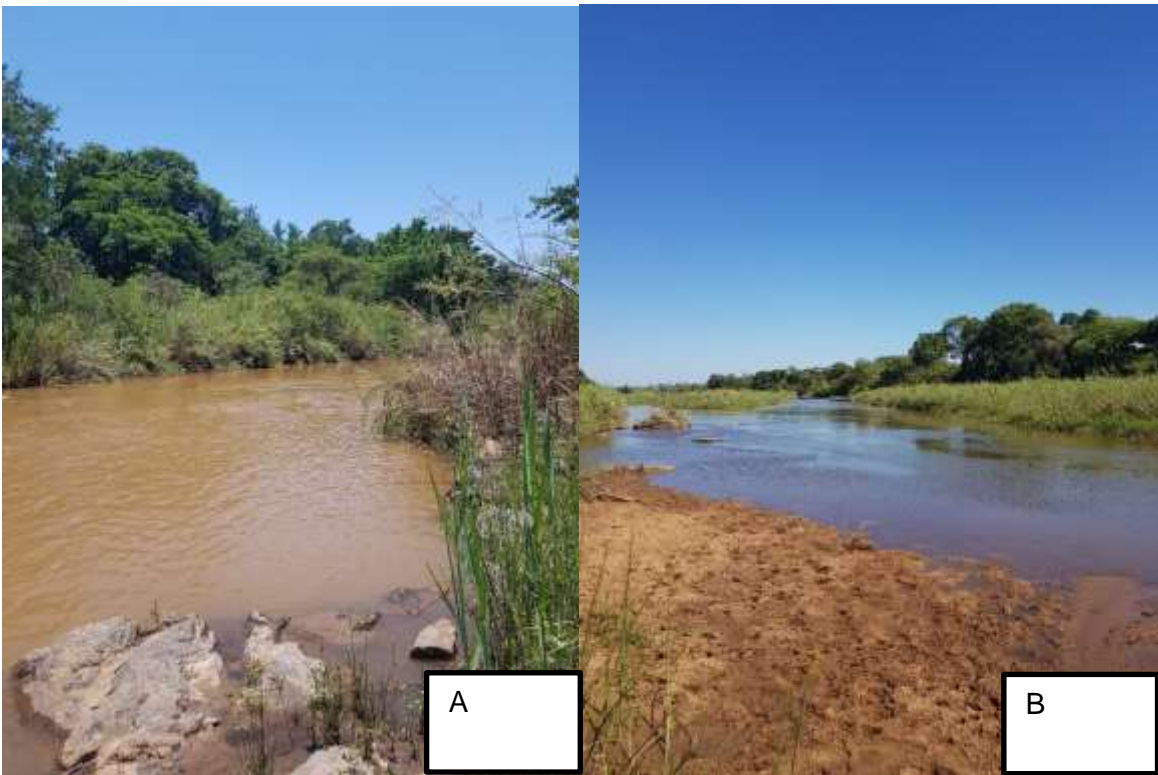


Figure 32 SB09: Sabie River inside Kruger National Park, wet (A) and dry (B) seasons (R. Lusunzi).



Figure 33 SB10: Lone Creek River, wet (A) and dry (B) seasons (R. Lusunzi).



Figure 34 SB11: Glynns Drainage/Malieveld, wet (A) and dry (B) seasons River (R. Lusunzi).



Figure 35 SB12 Klein Sabie River, wet (A) and dry (B) seasons (R. Lusunzi).

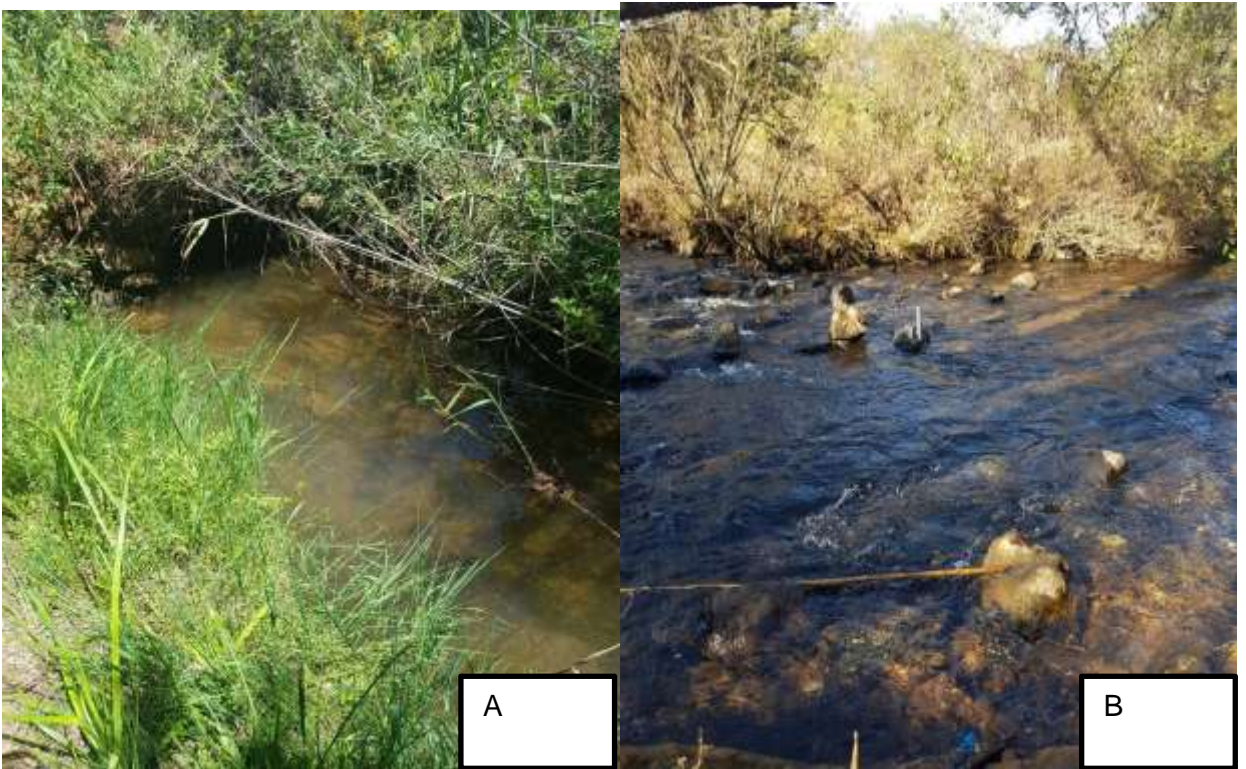


Figure 36 SB13: Klein Sabie River, wet (A) and dry (B) seasons (R. Lusunzi).



Figure 37 SB14: Spitskop River, wet (A) and dry (B) seasons (R. Lusunzi).

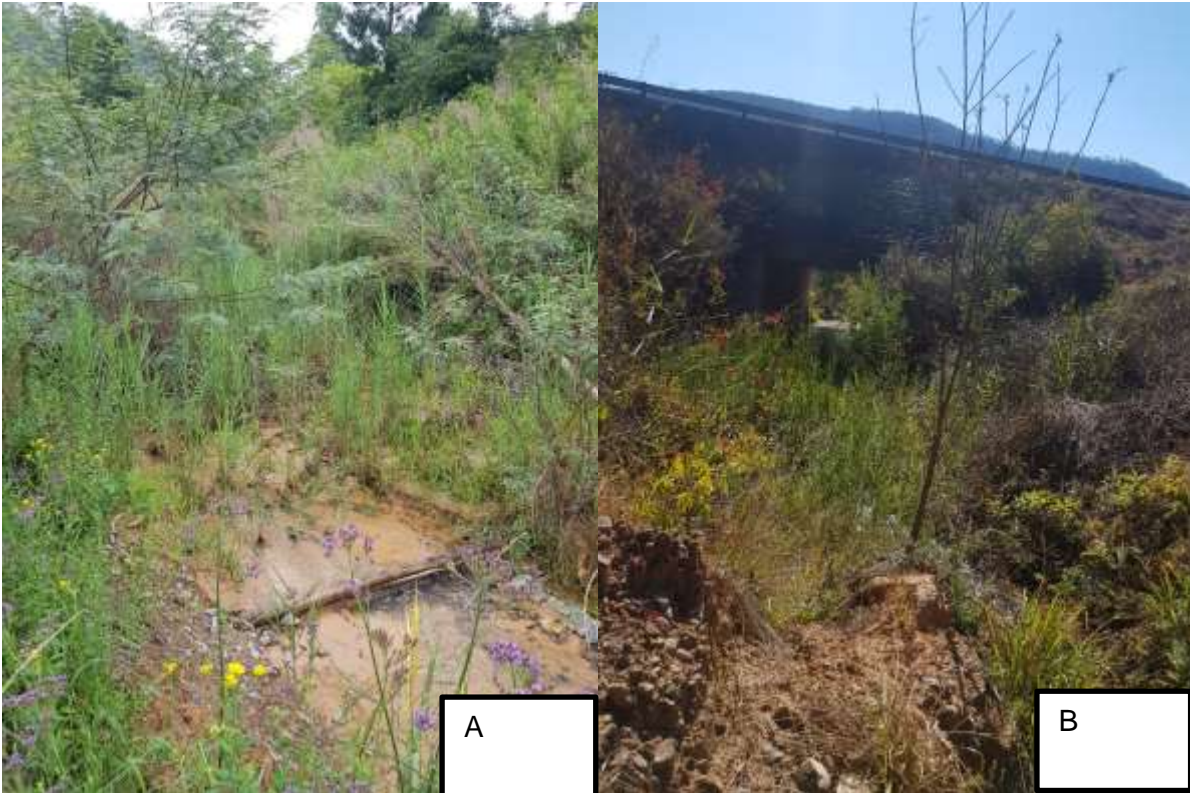


Figure 38 SB15: Rietfontein Mine drainage, wet (A) and dry (B) seasons (R. Lusunzi).



Figure 39 SB16: Goldstream, wet (A) and dry (B) seasons (R. Lusunzi).



Figure 40 SB17: Sabana River, wet (A) and dry (B) seasons (R. Lusunzi).



Figure 41 SB18: Mac-Mac River, wet (A) and dry (B) seasons (R. Lusunzi).

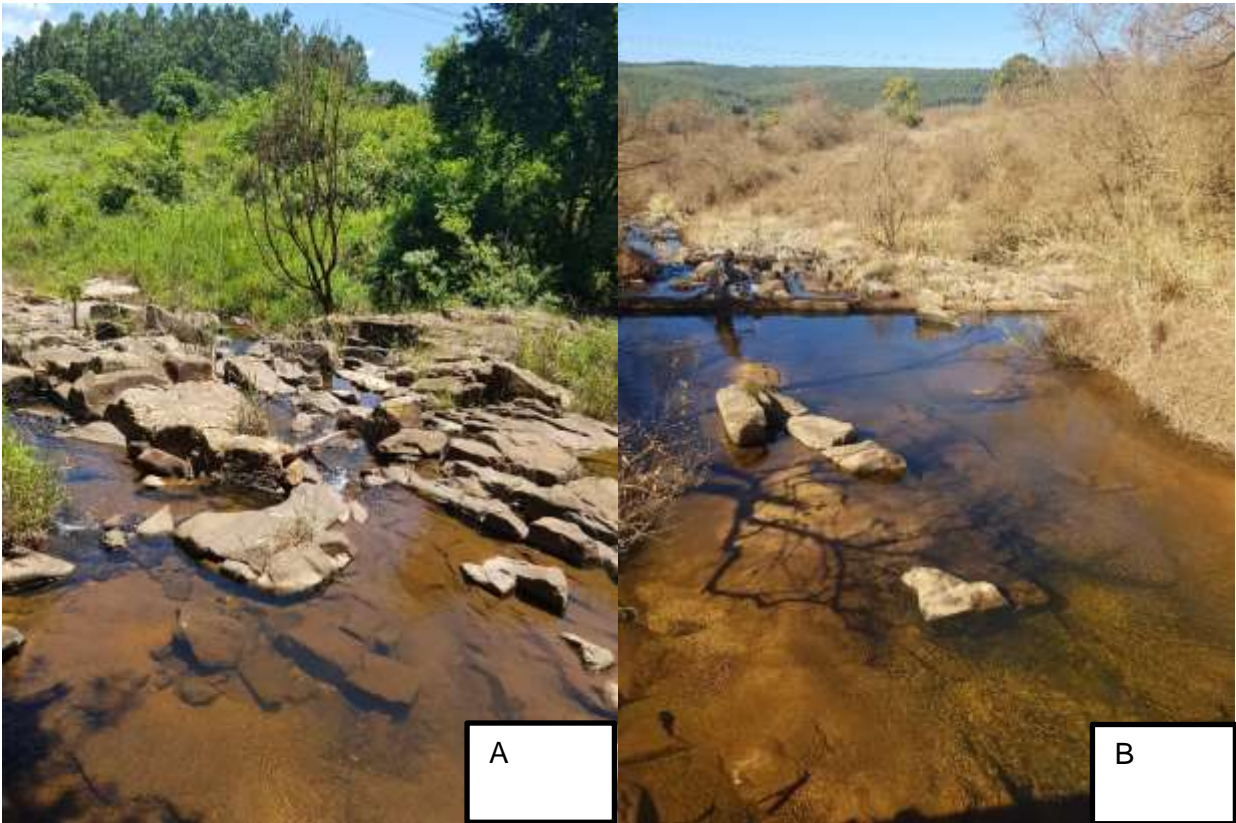


Figure 42 SB19: Sunlight River, wet (A) and dry (B) seasons (R. Lusunzi).



Figure 43 SB20: Nkambeni/ Noord Sand River, wet (A) and dry (B) seasons (R. Lusunzi).



Figure 44 SB21: Bega River, wet (A) and dry (B) seasons (R. Lusunzi).

8. Annexure B: speciation pattern for metals in the mine wastes of Nestor and Glynn's Lydenburg mines and surrounding soils

Sample ID	Fraction	Concentration (mg/L)									
		As	Al	Co	Cr	Cu	Fe	Mn	Ni	Pb	Zn
SB00	F1	2.52	422	0	0.7	11	623	27	4	0	7.5
	F2	0	22	0	0.1	0	1447	1.3	0	0	0
	F3	10.54	79	0	0.9	2.7	308	0.7	0	0.1	0.3
	F4	135.88	906	0	11	16	13779	48	12	14.4	52
NS01	F1	615.1	1951	22	38	167	67110	264	50	1	77
	F2	6.08	1.2	0	0	0	329	0.1	0.2	0.1	0
	F3	2.2	0	0	0	0.4	49	0.2	0	0.04	0.2
	F4	135.88	46	0	0.5	1.2	906	3.1	4.7	0.92	18
NS02	F1	1.08	113	0	0	0	195	11	1.8	0.02	0.2
	F2	0	13	0	0	0	1168	4.3	0	0	0
	F3	4.16	310	0.1	2.2	4.7	856	7.3	1.3	0.02	1.4
	F4	200.7	1931	0	19	23	19340	53	11	22.3	62
NS03	F1	0.14	146	0	0	0	25	289	3.3	0.04	1.5
	F2	0.04	104	6.6	0	0	577	1431	0.4	0.08	1.4
	F3	0.9	1237	1.3	6.1	7.3	548	76	1.8	2.32	1.5
	F4	32.94	6277	1.7	37	18	15500	207	15	3.84	64
GL00	F1	0.52	27	0	0	1	27	148	3.7	0.02	10
	F2	0.5	6.6	0	0	0	290	63	1.1	0.02	2

	F3	37.18	15	0.2	0.2	3.5	275	12	0.4	0.92	5.3
	F4	450.16	465	0	16	14	15718	72	14	5.92	89
	F1	0.04	39	0	0	0	39	183	2.8	0.1	4.1
	F2	0.02	29	0	0	0	1007	32	0.8	0.14	1.3
GL01	F3	0.2	480	0.3	2.2	1	387	10	0.7	1.52	1.8
	F4	0.96	6639	0	16	5.4	6828	46	11	2.44	58

9. Annexure C: speciation pattern for metals in the mine soil away from mining activities in the Sabie River system

Sample ID	Fraction	Concentration (mg/L)									
		As	Al	Co	Cr	Cu	Fe	Mn	Ni	Pb	Zn
SB26	F1	0.02	92	0	0	0	46	40	1.2	0.14	0.6
	F2	0	42	0	0	0	167	21	0	0	0
	F3	0.12	1301	0	1.5	0.4	106	7	0.2	1.64	0.8
	F4	0.62	9545	0	14	6.6	7070	41	8.1	2	53
NS27	F1	0	174	0	0	0	2.4	95	2.2	0	0
	F2	0.02	108	8.7	0	0	301	985	1.6	0.24	0.4
	F3	0.32	1406	1.4	7.4	3.4	243	146	3.7	2.62	0.6
	F4	5.84	14885	3.3	85	30	23883	196	41	3.9	77
NS28	F1	0.04	41	0	0	0	24	110	2.1	0.28	0
	F2	0.02	13	0	0	1.7	319	187	0.1	0.12	0.4
	F3	2.3	752	6.4	4.1	8.2	235	188	6.6	2.74	1.9
	F4	15.44	3595	5.1	21	10	7086	167	14	2.02	49
NS29	F1	0.02	97	0	0	0	109	10	1.2	0.36	0.1
	F2	0	44	0	0	0	115	1.6	0	0	0
	F3	0.04	1380	0	0.7	0	29	0.8	0.1	1.3	0.2
	F4	0.44	16225	0	5.6	2.3	6003	22	3.4	2.38	41

10. Annexure D: Speciation pattern for metals in the stream sediments of the Sabie River system

Sample ID	Fraction	Concentration (mg/L)									
		As	Al	Co	Cr	Cu	Fe	Mn	Ni	Pb	Zn
SB01	F1	0.02	131	0.1	0	0	40	143	1.8	0.06	1
	F2	0.02	110	0	0	0	654	57	0.3	0.08	2
	F3	0.38	1339	2.2	8.7	3.9	617	18	2.7	1.84	2.3
	F4	7.2	11313	5	56	21	22811	107	28	3.84	81
SB03	F1	0.5	110	2.1	0	7.6	33	349	4.1	0.14	7.5
	F2	0	46	0	0	0	822	26	0	0	0
	F3	6.76	826	2	6	6.4	544	26	4.1	2.22	5.5
	F4	165.68	4894	3.5	38	18	18458	85	21	3.6	67
SB04	F1	0.72	98	1.4	0	0.1	102	204	4.9	0.12	9.6
	F2	1.18	65	0	0	0	1183	46	0.3	0.18	5
	F3	8.44	925	1.3	5.9	31	585	18	3	2.72	3.8
	F4	151.4	8126	2.7	27	33	17596	72	17	5.16	67
SB05	F1	0.7	91	1.3	0.1	2.8	106	262	4.8	0.06	7.9
	F2	0.9	82	0	0	0	1425	37	0.8	0.1	2.9
	F3	9.92	977	1.6	6.2	27	1338	23	2.6	2.38	4
	F4	126.94	9722	1.2	23	20	14544	61	14	4.46	62
SB06	F1	1.08	84	0	0	0	99	48	2.9	0.06	1.5
	F2	1.1	27	0	0	1.8	771	9.1	0	0.04	0.5

	F3	7.62	518	0.6	2.9	2.9	349	8.4	1.2	0.72	1.6
	F4	115.72	4012	1.5	17	10	12578	56	10	2.28	59
SB08	F1	0.12	46	0	0	0	132	17	1.1	0.06	0.3
	F2	0.22	7.1	0	0	0	504	4.8	0.3	0.04	0.3
	F3	0.6	121	0	0.8	0	111	3.5	0.3	0.2	0.8
	F4	4.44	752	0	4.6	1.3	1728	14	3.1	0.48	36
SB09	F1	0	168	0	0	0	6.8	456	4	0.02	0.9
	F2	0	46	7.4	0	1.7	629	1712	2	0.06	1.2
	F3	0.16	1375	2.8	10	8.2	473	108	5.8	1.9	2.1
	F4	5.64	10519	7.8	51	10	20697	269	25	2.96	71
SB11	F1	0.12	89	0	0.9	0	234	251	1.9	0.4	3.8
	F2	0.1	21	0	0	0	336	184	0.1	0.3	0.4
	F3	1.34	285	1.8	5.8	0	210	43	2.4	1.66	1.3
	F4	6.42	1652	0.5	28	2.3	4510	90	11	1.58	53
SB12	F1	0.82	116	3.6	0	3.6	37	377	8.7	0.12	46
	F2	1.12	52	0	0	0	1282	61	2	0.18	16
	F3	6.72	1555	3.3	8.6	25	1066	37	10	4.74	18
	F4	90.94	7611	2.4	32	34	20269	171	22	9.18	97
SB13	F1	0.08	105	0	0	0	80	62	1.7	0.08	0.2
	F2	0.08	9	0	0	0	579	13	0.3	0.04	0
	F3	0.56	144	0	0.7	0	96	6.3	0.3	0.2	0.2
	F4	3.7	908	0	6.3	1.4	1927	18	3.7	0.6	30

	F1	0.22	52	2.3	0	9.3	15	246	3.4	0.46	2.5
	F2	0.18	20	8.8	0	1.6	447	301	2.3	0.42	1.1
SB14	F3	5.62	382	7.6	3	14	209	107	6.3	3.14	2.6
	F4	76.94	3449	8.8	39	27	11804	180	26	6.64	62
	F1	0.28	316	1.7	0	333	120	71	2.8	0.28	6.8
	F2	0.84	120	0	0	48.3	928	68	0.4	1.6	1.2
SB15	F3	7.3	683	0.1	0.4	29	120	5.8	0.3	1.08	1
	F4	25.88	5020	0	3.6	26	4535	25	2.9	3.88	46
	F1	0	73	0	0	0	52	30	2.8	0	0
	F2	0	23	0	0	0	410	160	1	0.6	0
SB18	F3	0.14	375	1.7	1.7	2.9	84	84	3.1	0.4	0.8
	F4	3.46	3373	0.9	15	6.2	4579	103	12	1.04	55
	F1	0	27	0	0	1.4	135	47	1.9	0.06	1
	F2	0	18	0	0.1	2.2	568	8.3	0.9	0.06	0
SB21	F3	0	244	0	2.5	0	181	2.1	21	0.48	0.8
	F4	0.32	2287	0	29	2.5	3260	22	8.9	0.86	34
